

UNSTABLE GROUND CONDITIONS ASSOCIATED
WITH KAROO OUTLIERS
IN THE DOLOMITIC ENVIRONMENT
OF THE FAR WEST RAND

By

DAVID HUW JONES

A thesis submitted in partial
fulfilment of the requirements
for the Degree of Doctor of Science
in the Department of Geology,
University of Pretoria.

JOHANNESBURG

4th May 1984

PART 1

1. INTRODUCTION

	<u>Page</u>
1.1 <u>GENERAL STATEMENT</u>	1
1.2 <u>AREAS OF INVESTIGATION</u>	2
1.3 <u>GEOLOGICAL HISTORY</u>	3
1.4 <u>LITHOSTRATIGRAPHY</u>	10
1.4.1 <u>MALMANI SUBGROUP</u>	10
1.4.2 <u>KAROO SUPERGROUP</u>	13
1.4.3 <u>PLEISTOCENE AND RECENT SOILS</u> ..	15
1.5 <u>GEOHYDROLOGY</u>	15
1.6 <u>HISTORY OF GROUND INSTABILITY</u> <u>IN THE FAR WEST RAND</u>	20

PART 2

2. FACTORS CONTRIBUTING TO GROUND INSTABILITY

2.1 <u>WEATHERING OF DOLOMITE</u>	30
2.2 <u>PRODUCTS OF DOLOMITE WEATHERING</u>	35
2.3 <u>CHANGES IN GROUNDWATER ELEVATIONS</u>	38
2.4 <u>MECHANISMS RESPONSIBLE FOR DOLINE AND SINKHOLE OCCURRENCES</u>	39

	<u>Page</u>
2.4.1	<u>THEORY OF DOLINE DEVELOPMENT...</u> 40
2.4.2	<u>THEORY OF SINKHOLE DEVELOPMENT</u> 46
 <u>PART 3.</u> 	
<u>3. CONVENTIONAL METHODS OF MONITORING GROUND INSTABILITY</u>	
3.1	<u>MEASUREMENT OF SURFACE MOVEMENTS</u> 53
3.1.1	<u>INSTRUMENTATION</u> 54
3.1.2	<u>INSTRUMENT FIELD PROCEDURES...</u> 58
3.1.3	<u>RECORDING OF OBSERVATIONS</u> 60
3.1.4	<u>ADJUSTMENT OF CIRCUITS</u> 62
3.1.5	<u>DISCUSSION ON PRECISE LEVELLING METHODS</u> 65
3.2	<u>MEASUREMENT OF SUBSURFACE MOVEMENTS</u> ... 66
3.2.1	<u>TELESCOPIC BENCH MARKS</u> 68
3.2.2	<u>THEORY OF TELESCOPIC BENCH MARK MEASUREMENTS</u> 71
3.2.3	<u>METHODOLOGY FOR CALCULATING SUBSURFACE MOVEMENTS</u> 79
3.3	<u>INTERPRETATION OF SURFACE AND SUBSURFACE MEASUREMENTS</u> 86
3.3.1	<u>DISPLACEMENT GRAPHS</u> 86
3.3.2	<u>ISOPLETH MAPS</u> 93

PART 4.

4. UNSTABLE GROUND CONDITIONS IN
KAROO OUTLIERS

	<u>Page</u>
4.1	
<u>FACTORS INFLUENCING GROUND INSTABILITY</u>	95
4.1.1 <u>GEOLOGICAL STRUCTURE</u>	95
4.1.1.1 <u>Re-activation of pre- Transvaal Tectonic Features</u> ...	99
4.1.1.2 <u>Post-Karoo Structural Features</u>	100
<i>Rietvlei Area</i>	102
<i>Henley/Lawley Area</i>	103
<i>Driefontein Area</i>	105
4.1.2 <u>LITHOLOGY</u>	109
4.1.3 <u>HYDROLOGY</u>	111
4.2	
<u>GROUND INSTABILITY IN THE DRIEFONTEIN OUTLIER</u>	123
4.2.1 <u>SEQUENCE OF EVENTS</u>	123
4.2.2 <u>INTERPRETATION OF SURFACE AND SUBSURFACE MEASUREMENTS</u>	129
4.2.2.1 <u>Malfunctioning of Telescopic Bench Marks</u>	130
4.2.2.2 <u>Effects of Subsurface Water Behaviour</u>	138
<i>Compound Area</i>	140
<i>Factory Area</i>	150

	Page
4.2.2.3 <u>Negative Movements</u>	156
4.2.2.4 <u>Positive Movements</u>	162
<i>Capillary Action</i>	167
<i>Mineralogy of Materials in the Vadose Zone</i>	168
<i>Air Entrapment and Atmospheric Pressure Effects</i>	170
4.2.2.5 <u>Conclusion</u>	175

PART 5.
=====

5. PREDICTION OF GROUND INSTABILITY
IN KAROO OUTLIERS

5.1	<u>PROPOSED INSTABILITY RISK POTENTIAL EVALUATION</u>	176
5.1.1	<u>METHOD FOR OBTAINING HYDROLOGICAL AND GEOLOGICAL DATA</u>	177
5.1.2	<u>INSTABILITY RANKING OF MATERIALS WITHIN A PROFILE</u>	187
5.1.2.1	<u>Parameters Affecting Stability</u>	183
5.1.2.2	<u>Evaluation of a Potential Risk Evaluation</u>	185
5.1.3	<u>INSTABILITY RANKING OF OTHER FACTORS</u>	188
5.1.3.1	<u>Lithological Succession</u>	189
5.1.3.2	<u>Subsurface Water</u>	189
5.1.3.3	<u>Configuration of the Domomitic Bedrock</u>	190
5.1.4	<u>INSTABILITY RISK EVALUATION</u>	191

/Part 6 ---

PART 6.
=====

6. SUMMARY AND CONCLUSIONS

<u>CONCLUSION</u>	227
<u>ACKNOWLEDGEMENTS</u>	236
<u>LIST OF REFERENCES</u>	237

APPENDICES

1. SINKHOLE AND DOLINE OCCURRENCES AT DRIEFONTEIN BRICKWORKS
2. GRAVIMETRIC SURVEY OF THE DRIEFONTEIN AREA AND ENVIRONS.....
3. ISOPLETHS SHOWING SURFACE (ΔH_s), UPPER SUBSURFACE MARKER (ΔH_u) AND LOWER SUBSURFACE MARKER (ΔH_l) ELEVATION CHANGES IN THE HOUSING AREA.....
4. ISOPLETHS SHOWING SURFACE (ΔH_s), UPPER SUBSURFACE MARKER (ΔH_u) AND LOWER SUBSURFACE (ΔH_l) ELEVATION CHANGES IN THE COMPOUND AREA
5. SLOT CONFIGURATIONS IN THE DOLOMITE AT DRIEFONTEIN BRICKWORKS.....
6. SLOT CONFIGURATIONS IN THE DOLOMITE AT HENLEY/LAWLEY OUTLIER.....
7. GEOLOGICAL PROFILES OF SLOTS IN THE VICINITY OF DRIEFONTEIN BRICKWORKS.....
8. STRUCTURAL FEATURES OF THE KAROO SEDIMENTARY ROCKS IN THE RIETVLEI OUTLIER.....
9. GEOLOGICAL PROFILES SHOWING STRUCTURAL FLEXURING OF THE KAROO SEDIMENTARY ROCKS IN THE RIETVLEI OUTLIER.....
10. GRAVIMETRIC SURVEY OVER PART OF THE LAWLEY OUTLIER.....
11. STRUCTURAL FEATURES OF THE KAROO SEDIMENTARY ROCKS IN A PORTION OF THE LAWLEY OUTLIER.....

APPENDICES CONTINUED

12. STRUCTURAL FEATURES IN THE KAROO
CARBONACEOUS SHALES IN THE DRIEFONTEIN
BRICKWORKS AREA.....
13. SUBSIDENCE CRACKS ON SURFACE AND BUILDINGS
OF DRIEFONTEIN BRICKWORKS.....
14. THICKNESS OF PLEISTOCENE AND RECENT SOILS
IN THE VICINITY OF THE DRIEFONTEIN BRICK-
WORKS.....
15. INTERSECTED DEPTHS OF SUBSURFACE WATER
IN THE RIETVLEI OUTLIER.....
16. PATTERN OF SURFACE RUN-OFF IN THE DRIE-
FONTEIN OUTLIER SHOWING DRAINAGE SYSTEMS
PRIOR AND SUBSEQUENT TO OCTOBER 1981.....
17. ACTUAL ΔH_s , ΔH_u , AND ΔH_θ MOVEMENTS IN
TBM 34 AND SUBSURFACE WATER MOVEMENTS
MEASURED IN PIEZOMETER CLUSTER NORTHWEST
OF DRIEFONTEIN BRICKWORKS COMPOUND.....
18. CORRELATION COEFFICIENT DATA OF ΔH_s AND
 ΔH_θ MOVEMENTS IN TBM 34 RELATIVE TO SUB-
SURFACE WATER MOVEMENTS IN PIEZOMETER
CLUSTER NORTHWEST OF COMPOUND.....
19. ACTUAL ΔH_s , ΔH_u AND ΔH_θ MOVEMENTS IN
TBM 10 AND SUBSURFACE WATER MOVEMENTS
MEASURED IN PIEZOMETER CLUSTER WEST OF
DRIEFONTEIN BRICKWORKS GAS PRODUCER.....
20. CORRELATION COEFFICIENT DATA OF ΔH_s AND
 ΔH_θ MOVEMENTS IN TBM 10 RELATIVE TO SUB-
SURFACE WATER MOVEMENTS IN PIEZOMETER
CLUSTER WEST OF GAS PRODUCER.....

/Page

APPENDICES CONTINUED

21. LOCALITIES OF 750mm DIAMETER
BOREHOLES DNWC, DNC, DH1
AND DH6
22. GEOLOGICAL PROFILE OF BOREHOLE
DNWC
23. GEOLOGICAL PROFILE OF BOREHOLE
DNC
24. GEOLOGICAL PROFILE OF BOREHOLE
DH1
25. GEOLOGICAL PROFILE OF BOREHOLE
DH6
26. RESULTS OF INDICATOR TESTS ON
SAMPLES FROM BOREHOLES DNWC
AND DNC
27. RESULTS OF CONSOLIDOMETER TESTS
ON SAMPLES FROM BOREHOLE DNWC
28. RESULTS OF INDICATOR TESTS ON
SAMPLES FROM BOREHOLE DH1
AND DH6

LIST OF FIGURES

	Page
Figure 1:- Locality plan of the Driefontein research area.	3
Figure 2:- Outline of the Witwatersrand Basin (after Brock and Pretorius, 1964).	4
Figure 3:- Cross-section during post-Ventersdorp Supergroup times (after Brink and Eriksson, 1970).	5
Figure 4:- Cross-section during Malmani Subgroup times (after Brink and Eriksson, 1970).	6
Figure 5:- Cross-section during post-Pretoria Group times (after Brink and Eriksoon 1970).	7
Figure 6:- Diagrammatic cross-section through the Far West Rand area showing the relationship between geology and surface topography (after Brink, 1979).	9
Figure 7:- Composite stratigraphic column through the Malmani Subgroup in the Far West Rand (after Eriksson, 1970).	11
Figure 8:- Vertical distribution of calcium/magnesium and of the soluble and total manganese content in dolomite of the Malmani Subgroup of the Far West Rand (Brink and Eriksson, 1970 after Eriksson, 1970).	12
Figure 9:- Generalised geological map of the Far West Rand. (From Brink, 1979 after de Kock, 1964).	16
Figure 10:- Strike frequency diagram of faults in the Far West Rand (Brink, 1979 from a compilation by Papendorf, 1971).	30
Figure 11:- Model of plunger on a spring demonstrating the subsidence caused by ground water lowering (from Jennings, 1971 a).	42

/ Figure 12 ---

	Page
Figure 12:- Doline and sinkhole development. (After Brink, 1979).	45
Figure 13:- Section through a small sinkhole at West Rand Garden Estates showing the collapse of the crown only (after Jennings, 1966).	50
Figure 14:- Sub-Transvaal geology of the Far West Rand (adapted from de Kock, 1964 by Brink, 1979).	51
Figure 15:- Precise levelling circuit used at Driefontein Brickworks (compiled from Watt, 1972).	55
Figure 16:- Procedure for obtaining precise elevation differences using a Zeiss Koni Level and Nedo Invar Staff.	57
Figure 17:- Field book procedure used for precise levelling.	61
Figure 18:- Diagram showing levelling circuit closures for the housing area at Driefontein Brickworks.	63
Figure 19:- Analogy of a bottom discharge bin with surface and subsurface movements (after Jennings, 1971 b).	67
Figure 20:- Assembly details of a Jennings type telescopic bench mark.	69
Figure 21:- Assembly of a "Sondex" type telescopic bench mark.	70
Figure 22:- Telescopic bench mark movements associated (a-b) with void development at depth.	73
Figure 23:- Telescopic bench mark movements associated (a-b) with void development at depth between asymmetrical dolomite abutments.	76
Figure 24:- Method of calculating subsurface movements using a Jennings type telescopic bench mark.	80

/ Figure 25 ---

	Page
Figure 25:-	Format used at Driefontein Brickworks for recording surface and subsurface movements. 84
Figure 26:-	Displacement graph showing surface and subsurface movements in monthly increments. 87
Figure 27:-	Movements of the surface (ΔH_s) upper subsurface (ΔB) and lower subsurface (ΔA) markers in TBM 34. Compound area, Driefontein Brickworks. 88
Figure 28:-	Elevation changes of surface (ΔH_s), upper (ΔH_u) and lower (ΔH_l) subsurface markers in TBM 34, Compound area, Driefontein Brickworks. 91
Figure 29:-	Geographical situations at the Driefontein Henley/Lawley and Rietvlei areas. 101
Figure 30:-	Stratigraphic successions in the Rietvlei, Henley/Lawley and Driefontein outliers. 108
Figure 31:-	Unconfined aquifer and its water table, confined aquifer and its piezometric level (after Freeze and Cherry, 1979). 113
Figure 32:-	Water fluctuations in a confined aquifer produced by earth tides (after Robinson, 1939). 117
Figure 33:-	Automatic water level recording in borehole GB16 in the Zuurbekom area illustrating tidal effects in parts of a confined aquifer (Fleische, 1979). 118
Figure 34:-	Showing perched water table ABC, inverted water table ADC, true water table EF and lowered water table GH (after Freeze and Cherry, 1979). 122

/ Figure 35 ---

Figure 35:-	Diagrammatic section showing assembly details of water conduit borehole in abandoned quarry "A" at Driefontein Brickworks.	127
Figure 36:-	Assembly details of a monitor, single point, telescopic bench mark.	136
Figure 37:-	Assembly details of single and multiple tipped piezometers used in the Driefontein area.	139
Figure 38:-	Showing poor correlation between rainfall and subsurface water behaviour.	143
Figure 39:- (a-b)	Showing the correlation between the upper (W2) and lower (W1) piezometric levels and ΔH_s , ΔH_u and ΔH_ℓ measurements in TBM 34.	146
Figure 40:- (a-b)	Showing the correlation between the upper (W2) and lower (W1) piezometric levels and ΔH_s and ΔH_ℓ measurements in TBM 10.	153
Figure 41:-	Total stress, effective stress and fluid pressure on an arbitrary plan through a saturated, porous medium. (Freeze and Cherry, 1979).	158
Figure 42:-	Hydraulic head (h), pressure head (ψ) and elevation head (z) in a field piezometer. (Freeze and Cherry, 1979).	160
Figure 43:-	Aquifer compaction caused by lowering of ground water. (Freeze and Cherry, 1979).	161
Figure 44:- (a-c)	Diagrammatic representation of succession of layers in kaolinite, illite and montmorillonite (adapted from Clews, 1969 after Brindley, 1951).	169
Figure 45:- (a-c)	Water fluctuations due to air entrapment during ground water recharge in an unconfined aquifer. (Freeze and Cherry, 1979).	171

/ Figure 46 ---

Figure 46:- (a-b)	Water level fluctuations due to atmospheric pressure effects in a confined aquifer. (Freeze and Cherry, 1979).	173
Figure 47:-	Idealised example of criteria obtainable from a borehole sunk with a percussion drill.	182
Figure 48:-	Showing rates of surface (ΔH_s) and sub-surface (ΔH_ℓ) movements during doline development.	194
Figure 49:-	Showing ΔH_s , ΔH_u and ΔH_ℓ displacements and $\Delta H_s/\Delta H_\ell$ velocity and acceleration/deceleration behaviour in TBM 10G situated near the epicentre of a developing doline.	196
Figure 50:- (a-c)	Showing ΔH_s , ΔH_u and ΔH_ℓ displacements and $\Delta H_s/\Delta H_u$ velocity, and acceleration/deceleration behaviour in TBM 10 prior and subsequent to the development of sinkhole No. 17.	199
Figure 51:-	Isopleths of progressive means and standard deviations for surface movements in the Driefontein housing area. (Cycles $\Delta 25-1$).	203
Figure 52:-	Isopleths of means and standard deviations for surface movements in the vicinity of the Down-draught Dryers at Driefontein Brickworks. (Cycles $\Delta 25-4$).	208

/Figure 53 ---

Figure 53:-	Isopleths of means and standard deviations for surface movements in the vicinity of the Down-draught Dryers at Driefontein Brickworks. (Cycles $\Delta 31-4$).	210
Figure 54:-	Schematic profile showing geotechnical requirements for the development of satellite sinkholes.	211
Figure 55:-	Predicted elevation changes of upper (ΔW_2), lower (ΔW_1) and combined upper/lower ($\geq WT$) subsurface water elevations and resulting surface movements ($P_d \Delta H_s$).	214
Figure 56:- (a-c)	Predicted surface ($P_d \Delta H_s$) movements associated with cyclic elevation changes of subsurface water systems ($P_d \geq \Delta WT$) in the Driefontein Brickworks area.	217
Figure 57:- (a-c)	Predicted lower subsurface marker ($P_d \Delta H_l$) movements associated with cyclic elevation changes of subsurface water systems ($P_d \geq \Delta WT$) in the Driefontein Brickworks area.	218
Figure 58:-	Predicted total subsidence in a developing doline (i.e. total doline subsidence plus cyclic movement fluctuations).	219
Figure 59:- (a-c)	Effect of seasonal surface movement on a structure (after Holland, 1982).	222
Figure 60:- (a-b)	Effects of cyclic elevation of the ground water at piezometric level on a surface structure.	224

LIST OF TABLES

			Page
Table	1:-	Identification of manganese wad, carbonaceous shale and dolomite (after Brink and Eriksson, 1970).	14
Table	2:-	Calculated daily replenishment of the Far West Rand Water compartments with maximum quantities pumped by certain mines.	19
Table	3:-	Summarised physical properties of manganese wad (Partridge, Harris and Diesel, 1981).	37
Table	4:-	Movements of surface (ΔH_s) as well as upper (ΔB) and lower (ΔA) subsurface markers in TBM 34.	89
Table	5:-	Elevation changes of surface (ΔH_s), upper (ΔH_u) and lower (ΔH_l) subsurface markers in TBM 34.	90
Table	6:-	Correlation between ΔH_u and ΔH_s movements in TBM 34, compound area.	132
Table	7:-	Mean movements and correlation coefficient analyses of ΔH_s , ΔH_u and ΔH_l movements (measurements in mm).	133
Table	8:-	Mean movements and correlation coefficient analyses of TBM 40 ^B , 41 ^B and TBM 41 ^A (measurements in mm).	137
Table	9:-	Depths of measuring tips below surface in piezometer cluster northwest of the Compound at Driefontein Brickworks.	140
Table	10:-	Recorded measurements (m) of subsurface water movements situated northwest of the Compound and rainfall figures (mm).	141
Table	11:-	Correlation coefficient analyses (r^2 (100)) of subsurface water in piezometer cluster N.W. of Compound, Driefontein Brickworks.	141

/ Table 12 ---

Table 12:-	Depths of measuring tips below surface in piezometer cluster west of Gas Producer at Driefontein Brickworks.	150
Table 13:-	The swelling potential of montmorillonite, hallosite and kaolinite clay minerals (after Mielenz and King, 1955).	163
Table 14:-	Subsurface water movements in the Driefontein Brickworks area.	166
Table 15:-	Chemical analyses of Karoo shales and mudstones.	168
Table 16:-	Evaluation of instability hazards to structures at Driefontein Brickworks	192
Table 17:-	Maximum ratios between subsurface water elevation changes and $\Delta H_s/\Delta H_\theta$ movements in the Driefontein area.	213

LIST OF PLATES

Page

Plate	1:-	Well developed sinkholes in the Bank Compartment at the Far West Rand.	23
Plate	2:-	Sinkhole on the Venterspost Golf Course, Venterspost Compartment, Far West Rand.	25
Plate	3:-	Sinkhole on the Venterspost Golf Course, Venterspost Compartment, Far West Rand.	26
Plate	4:-	The 5m diameter sinkhole (Sinkhole 17) which occurred at Driefontein Brickworks on 18 February, 1980.	29
Plate	5:-	Aerial view of a doline in the Bank Compartment of the Far West Rand.	40
Plate	6:-	The Zeiss Koni Automatic level and measuring staff.	56
Plate	7:-	Flexured Karoo shales in the Rietvlei outlier.	103
Plate	8:-	Showing cracking in the wall of the Down-draught dryers of Driefontein Brick Factory caused by differential subsidence.	207
Plate	9:-	Showing cracking along floor of the Down-draught dryers at Driefontein Brickworks caused by differential subsidence.	208
Plate	10:-	Details of cracking along floor at the Down-draught dryers at Driefontein Brick- works caused by differential subsidence.	207
Plate	11 and 12:-	Examples of satellite type sinkholes occurring immediately northeast of Driefontein Brickworks.	212

SUMMARY

Areas of the economically important Far West Rand, which are underlain by dolomite, have a latent potential for the development of unstable ground conditions ranging in intensity from catastrophic sinkhole occurrences to differential surface movements measureable only in millimetres.

Karoo outliers, occurring within the dolomitic environment, have special significance not only as a source of brick-making raw materials but also as areas which have been traditionally considered more stable and safer for development than their surrounds. The occurrences of major instability and the severe structural damage to the Driefontein Brickworks subsequent to dewatering has motivated this study, which specifically examines the causes of instability in Karoo outliers, so that the human and capital resources deployed in such areas can be protected.

The study shows that post-Transvaal weathering and erosion has caused not only the development of a harsh, karst-like topography in the Malmani Subgroup dolomitic bedrock, but also the creation of a covering layer of unstable residual soils. The subsequent deposition of Karoo sedimentary rocks, which may contain indiscriminately disseminated, expansive clay minerals, adds further complexities to the conditions which promote ground instability.

Almost invariably, it is evident that water is the major factor responsible for the development of unstable ground conditions. The majority of sinkhole occurrences are attributable to the downward percolation of water and erosion of residual materials, particularly down the flanks of subterranean slots weathered out of the dolomite. Analyses of telescopic bench mark and piezometer measurements show that all ground subsidences are attributable to either natural or artificial lowering of subsurface water through residual soils. Conversely, upward surface movements are caused by a rise of subsurface water levels and also the migration of moisture beyond the capillary fringe (by the mechanisms of air entrapment and atmospheric pressure changes) into the expansive clay bearing, sedimentary rocks present in the vadose zone.

In conclusion it is shown that by the application of statistical and other interpretive techniques to available lithostratigraphic, telescopic bench mark and piezometer data, predictions can be made regarding future ground instability in Karoo outliers. Four prediction techniques are proposed; namely the evaluation of a potential risk factor, the analysis of the rates of surface and subsurface movements, the interpretation of means and standard deviations of ground movements using isopleth maps and the prediction of differential ground movements induced by the cyclic recharging of aquifers.

OPSOMMING

Gebiede in die ekonomies belangrike Verre Wes-rand wat deur dolomiet beslaan word, is onderworpe aan die moontlike voorkomste van onstabiele grondtoestande wat kan wissel in intensiteit van katastrofiese sinkgatvorming tot differenssiële oppervlakkbewegings van so min as enkele millimeter.

Karooloslappe wat in die dolomietomgewing voorkom is van besondere belang, nie alleen as bron van die grondstowwe vir baksteenvervaardiging nie maar ook as gebiede wat tradisioneel meer stabiel en veiliger vir ontwikkeling as die omliggende gebiede bejeen is.

Die voorkoms van grootskaalse onstabiliteit en ernstige skade aan strukture by die Driefonteinsteinwerke na ontwatering het annleiding gegee tot hierdie studie om spesifiek die oorsake van onstabiliteit op Karooloslappe in oënskou te neem sodat die menslike - en kapitaal hulpbronne in sulke gebiede beskerm kan word.

Die studie toon dat na-Transvaalse verwering en erosie nie alleen gelei het tot die ontwikkeling van 'n ru, karsttopografie in die dolomietbodemrots nie, maar ook tot die skepping van 'n deklaag van onstabiele residuele grond. Die latere afsetting van Karoosedimente wat oneweredig verspreide uitsetbare kleiminerale mag bevat, dra verder by tot die toestand wat onstabiliteit van die grond bevorder.

Bykans sonder uitsondering blyk dit dat water die belangrikste faktor by die ontwikkeling van onstabiele grondtoestande is. Die meerderheid van sinkgatvoorkomste kan toegeskryf word aan die afwaartse sypeling van water en erosie van residuele materiale, veral langs die kante van verweringsplete in die dolomiet. Ontledings van metings met behulp van teleskopiese hoogtemerkerers en piësometers toon dat alle grondversakking toegeskryf kan word aan óf natuurlike óf kunsmatige verlaging van die grondwatervlak deur residuele gronde. Opwaartse grondbeweging, aan die ander kant, word veroorsaak deur 'n styging van grondwatervlakke en die opwaartse beweging van grondvog (deur die meganismes van luginperking en atmosferiese drukverandering) tot in die vadose sone bokant die kapillêre rand waar sedimente met uitsetbare kleiminerale voorkom.

Ten slotte word getoon dat met die toepassing van statistiese- en ander interpretasietegnieke op beskikbare data oor die litostratigrafie asook van teleskopiese hoogtemerkerers en piësometers, voorspellings gemaak kan word omtrent toekomstige onstabiliteit op Karooloslappe. Vier voorspellingstegnieke word voorgestel, naamlik die evaluering van 'n potensiële risikofaktor, die ontleding van gemiddeldes en standaardafwykings van grondbewegings met buhulp van isopleetkaarte en die voorspelling van differensiële grondbeweging wag deur die sikliese aanvulling van akwifers veroorsaak word.

UNSTABLE GROUND CONDITIONS ASSOCIATED WITH KAROO

OUTLIERS IN THE DOLOMITIC ENVIRONMENT

OF THE FAR WEST RAND

PART 1

1. INTRODUCTION

1.1 GENERAL STATEMENT

The following dissertation describes a detailed investigation of the unstable ground conditions associated with a Karoo outlier in the dewatered dolomitic environment of the Far West Rand. The investigation was undertaken with the objectives of:

- (i) Diagnosing the geological, geohydrological and environmental factors which contribute to unstable ground conditions which may range in intensity from differential movements of the surface at one end of the scale to severe doline and sinkhole development at the other.
- (ii) Evolving a system for monitoring and interpreting surface, as well as subsurface movements.
- (iii) Categorising areas of instability on a basis of their danger potential.
- (iv) Statistically analysing surface and subsurface movements to determine firstly, what is a

/significant ---

significant amount of movement, and secondly, what ratio between time and amount of subsidence is of critical proportion.

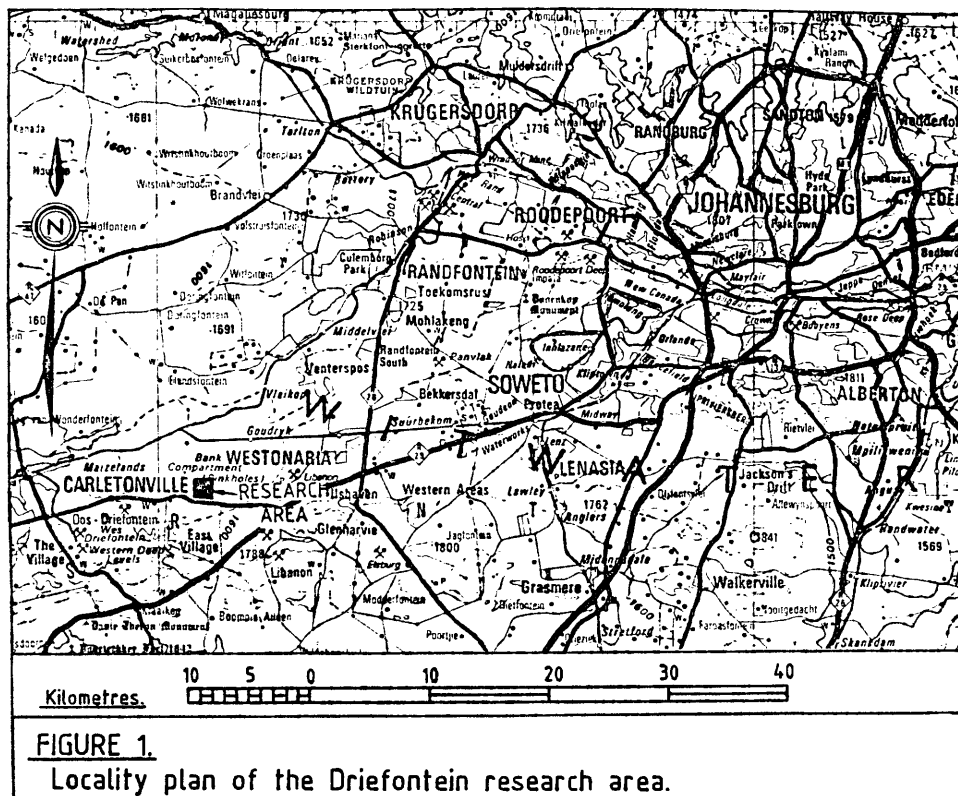
These research objectives involved analysing surface, subsurface and water table movements from late-1979 to mid-1983 some 11 years after the dewatering of the so called Bank Compartment was commenced. Although measurements were taken by the late Professor Jennings between 1971 and 1972, these earlier records have been excluded for three reasons. Firstly, many of the earlier installations used for monitoring surface and subsurface movements, namely telescopic bench marks, have become non-functional. Secondly, earlier measurement records are often incomplete and thirdly, surface subsidence had already commenced before telescopic bench marks were installed making it difficult to relate subsequent subsurface movements to such subsidence.

1.2 AREAS OF INVESTIGATION

The area chosen for the research investigation is the farm Driefontein No. 355IQ, currently owned and occupied by a Corobrik Transvaal brickworks, situated some 13km from Westonaria and 14km from Carletonville (Figure 1). Although occupying only 337,5ha, this area has been ideal for research as:-

- (i) It occupies part of the Far West Rand which has been the subject of geological, geohydrological and geophysical research for nearly three decades.

/Figure 1 ---



- (ii) Over 350 boreholes have been drilled by the Driefontein Brickworks company with the result that detailed knowledge of the local geology is available.
- (iii) It has 322 points at which surface and subsurface movements have been measured over a minimum period of 3 years to accuracies of 0,1mm and 0,01mm respectively.
- (iv) Its geological and geohydrological history has imprinted conditions conducive to ground instability which have been further palingene-tically accelerated by dewatering as a result of gold mining activities.

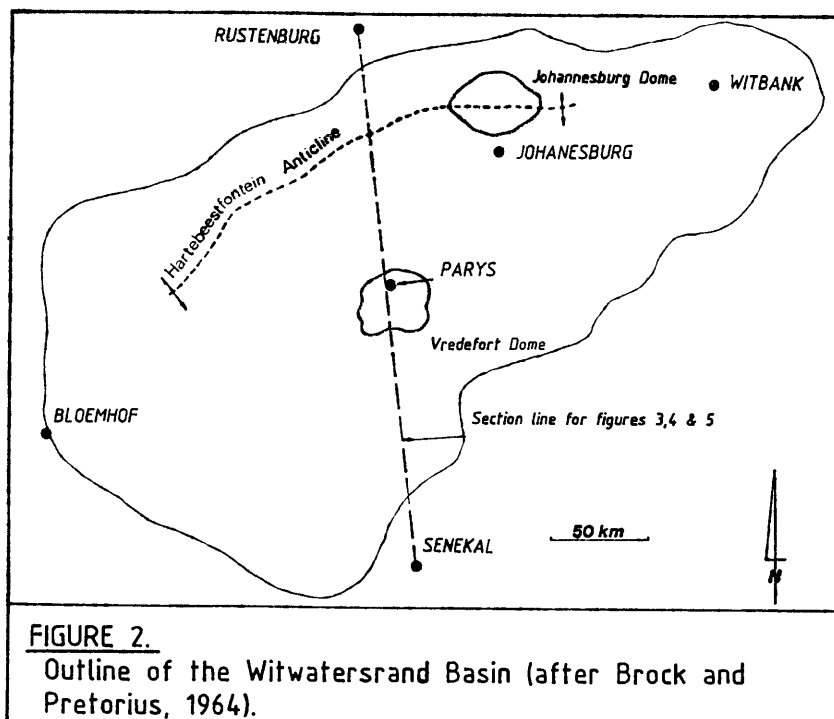
/In many ---

In many aspects of the study it was found appropriate to compare the Driefontein area with the Karoo outliers at Rietvlei and Henley-Lawley, situated 20km south-southeast of Pretoria and 30km southwest of Johannesburg respectively, which have equitable, but undewatered dolomitic environments.

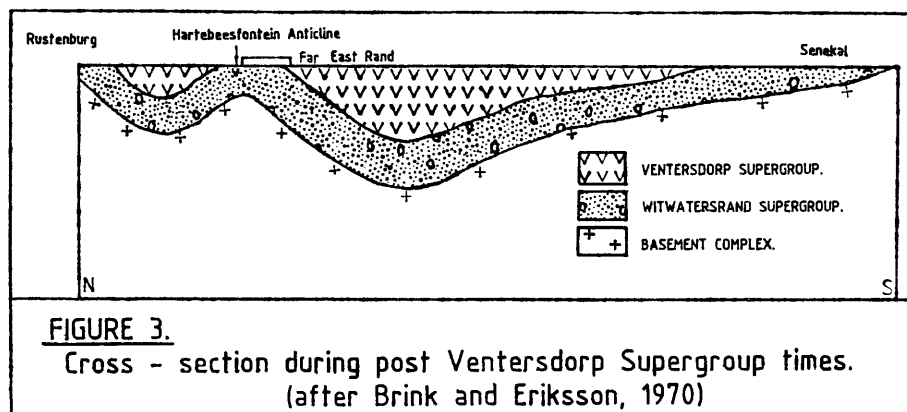
1.3 GEOLOGICAL HISTORY

The geological history of the Far West Rand, of which the Driefontein area is an integral part, has included a number of depositional, tectonic and erosional events each of which has had an influence on ground instability.

The oldest rocks present in the Far West Rand are those constituting the Basement Complex which formed the floor of a synclinal basin as described by Brock and Pretorius (1964) shown in Figure 2.



Into this Proterozoic basin was deposited the sedimentary sequence of the Witwatersrand Supergroup. At the conclusion of this depositional cycle, tectonic activity occurred in the form of tilting to be followed by partial planing of the sedimentary rocks. Thereafter followed the extrusion of the Ventersdorp Supergroup lavas and associated pyroclastics which culminated in another period of tectonism expressed by the uplifting of the Johannesburg Dome and the Hartbeestfontein Anticline. As described by Brink and Eriksson (1970), this post-Ventersdorp, tectonic impulse imposed local tilting and fracturing upon existing rocks (Figure 3).

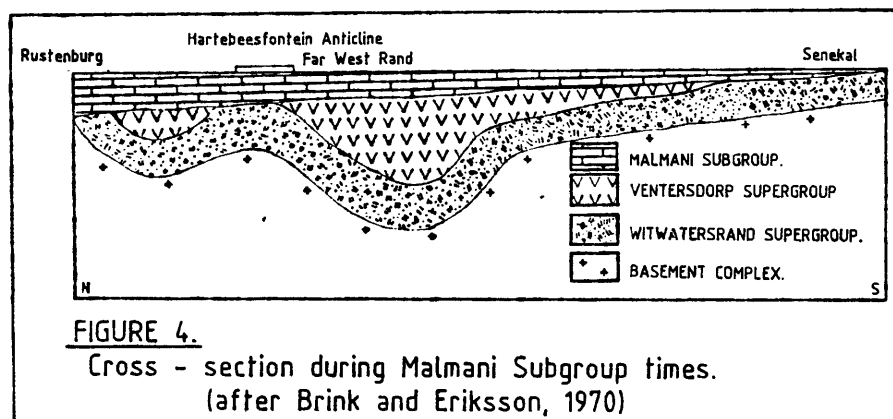


Subsequent to the post-Ventersdorp tectonism, there occurred a major cycle of erosion resulting in the formation of the large depository, extending at least from Pietersburg in the north to the Orange Free State in the south and from beyond Pilgrims Rest in the east to Botswana and the northern Cape

/in the ---

in the west. Into this depository were laid down the sedimentary rocks of the Transvaal Sequence.

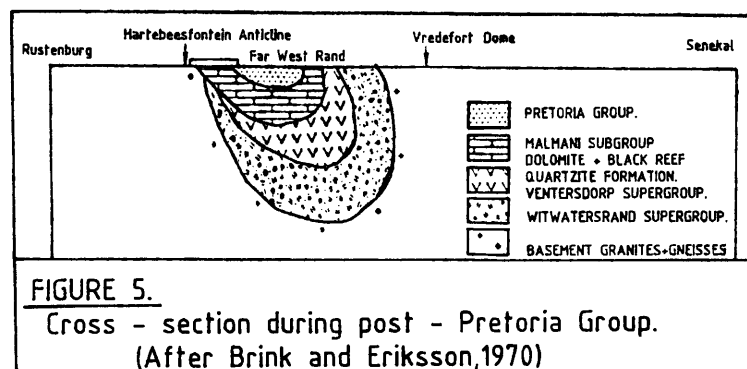
In the Far West Rand, the lowest member of the Transvaal Sequence is represented by the Black Reef Quartzite Formation followed by rocks of the Malmani Subgroup which constitute the dolomitic representatives of the Chuniespoort Group. (Figure 4).



The water during Malmani times was, as described by Brink (1979), rich in bicarbonates and silica leached from the acidic rocks of the Basement Complex and lavas of the Ventersdorp Supergroup. By chemical and organic processes, the latter by algae as evidenced by fossilised stromatalitic structures (Truswell and Eriksson, 1972), the deposition of the carbonate-rich rocks which characterise the Malmani Subgroup was accomplished. It is likely that the original precipitate was limestone but this is now represented by dolomite and chert as a

/result of ---

result of secondary replacement (Eriksson, McCarthy and Truswell, 1975). Subsequent to the deposition of these soluble rocks of the Malmani Subgroup, yet another tectonic event occurred causing renewed uplifting of the Johannesburg Dome and further activity along the Hartebeestfontein Anticline (De Kock, 1964; Brink, 1979). Thereafter there was a major period of erosion which saw vast amounts of the carbonate rocks of Malmani age being put into solution and insoluble substances, such as chert, being residually concentrated later to form the chert zone of the Rooihogte Formation. As described by Brink and Eriksson (1970), the deposition of the Pretoria Group was followed by further tectonism, which resulted in the re-activation of the Johannesburg Dome and the Hartebeestfontein anticline as well as the uplifting of the Vredefort Dome (Figure 5).



The intrusion of syenite and diabase dykes, trending slightly east of north, occurred at the close of the

/tectonic ---

tectonic activity. An ensuing 1600 million years of erosion resulted in the removal of great quantities of the rock material constituting the Transvaal Sequence, leaving its distribution very much as it exists at the present day. During this erosion period, the dolomitic limestones were severely weathered to considerable depths along near vertical aquifers constituted by faults, cleavage and fracture planes (Brink and Partridge 1965; Brink 1979). Consequently, a series of depressions and deeply incised valleys were created in the dolomitic rocks; the latter frequently choked with chert rubble and other insoluble residue derived from the weathering of the dolomite.

During the Carboniferous period, ice-sheet glaciation, with its characteristic scouring action, occurred over most of Southern Africa. In the Far West Rand, the chert rubble, lying on the floor of the deep valleys, which had been incised into the Malmani dolomitic rocks, were susceptible to removal by glacial scouring (Brink, 1979). When, finally, the glacial conditions were drawing to a close, the retreating ice sheets dropped glacial debris into the clean-scoured depressions and deep valleys created in the dolomite. Thus tillites, representing the basal members of the Karoo Supergroup, are frequently found occupying some of the deeper valleys in the dolomite (Jennings, Brink, Louw and Gowan, 1965; Brink and Partridge, 1965; Brink, 1979).

/At the ---

At the conclusion of the Carboniferous period, the bulk of the Karoo supergroup sedimentary rocks was laid down. The Far West Rand was situated along the northern flank of the depository with the result that the Karoo succession in this area is both sporadic and relatively thin. Such deposition was, however, sufficiently effective to fill the depressions and deeply incised valleys eroded into pre-existing rocks.

Various cycles of erosion followed in post-Karoo times, as described by Brink and Partridge (1965), leading to planation and the formation of an extensive pediment. In the Far West Rand, this planation cut uniformly across both the Malmani dolomites and the Karoo strata in the area flanking the Wonderfontein Spruit (Figure 6). As a result, sedimentary rocks of the Karoo Supergroup are now found only as outliers in the depressions and deep chasms weathered out of the Malmani dolomites. Finally, the Wonderfontein pediment was covered by a thin layer of naturally transported soils of Pleistocene and Recent ages.

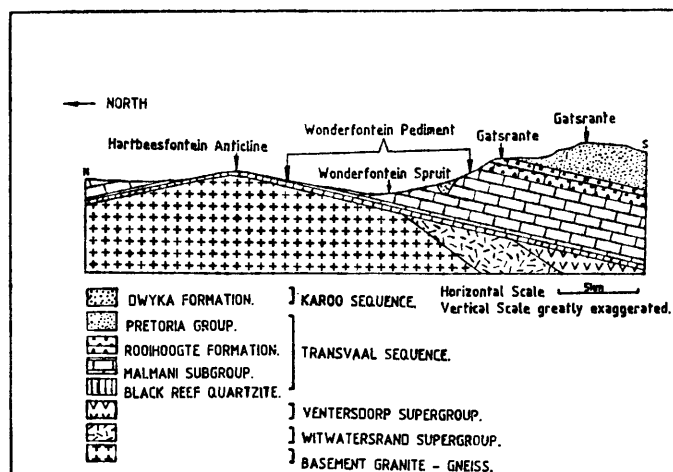


FIGURE 6.
 Diagrammatic cross - section through Far West Rand area showing the relationship between geology and surface topography.
 (after Brink, 1979)

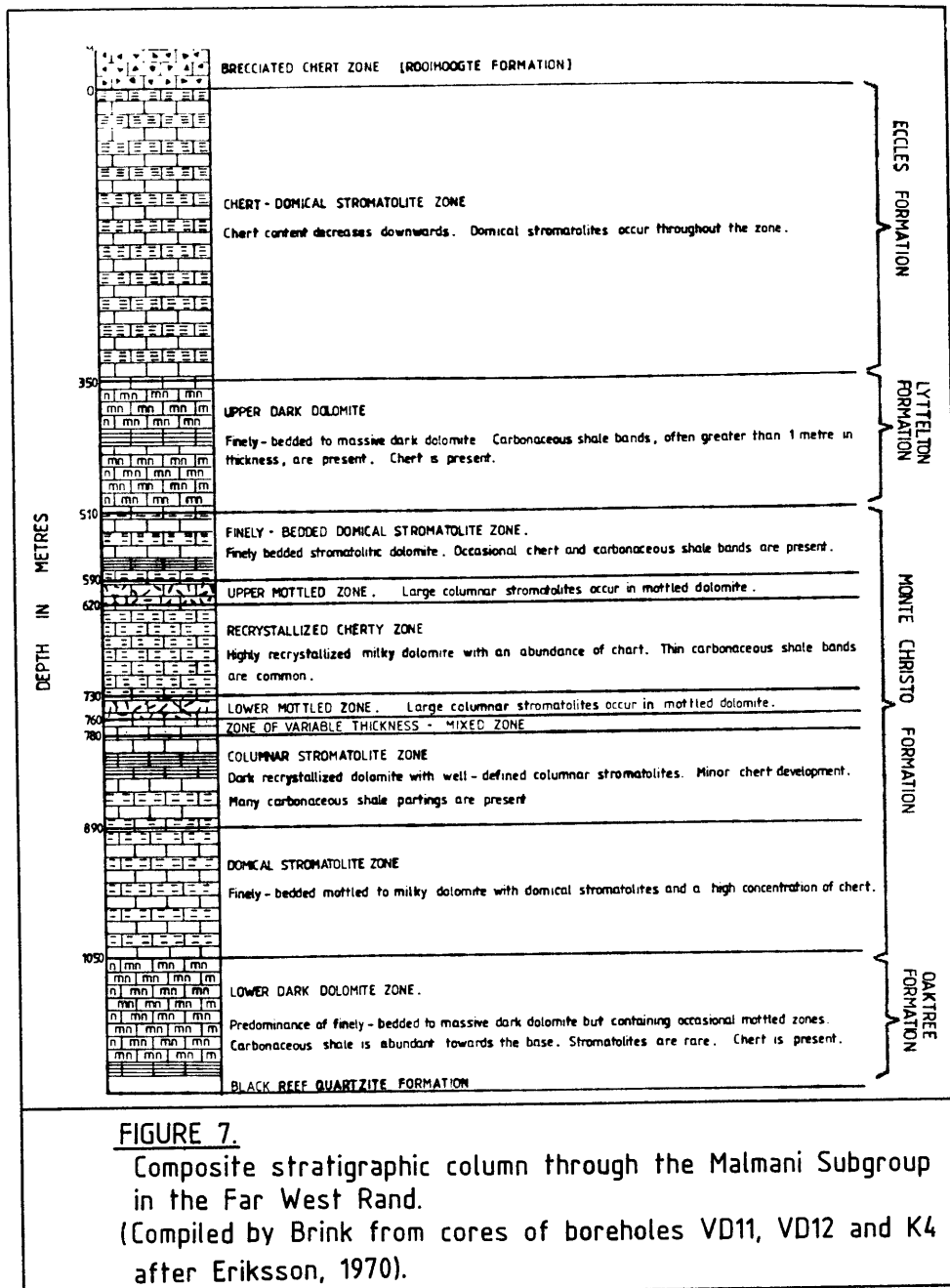
1.4 LITHOSTRATIGRAPHY

In considering the ground instability of the area in which research was undertaken, the lithostratigraphic features of the Malmani dolomites, the Karoo sedimentary rocks and the Pleistocene to Recent deposits are significant.

1.4.1 THE MALMANI SUBGROUP

Basically, the lithology of the Malmani Subgroup is relatively simple comprising alternating layers of dolomite and chert with a total thickness of some 1200m. A composite stratigraphic column of the succession, compiled by Brink and Eriksson (1970) from the logs of three boreholes within a 20km radius of the Driefontein area, is given in Figure 7. The chert bands vary from a few centimetres up to metres in thickness with a tendency to increase in respect of frequency towards the top of the succession where they constitute up to 20 per cent of the total volume. The composition of the Malmani Subgroup equates to that of pure mineral dolomite with the approximate ratio of CaO to MgO in the region of 1,00 to 0,67. In the lowermost fifty metres of the succession, however, a sharp increase in the calcium content of the rock occurs so that it approximates the composition of a dolomitic limestone, as determined by Eriksson (1970).

/ Figure 7 ---



In Figure 8, the vertical distribution of the Ca/Mg ratio is given for the whole of the Malmani Subgroup.

/Figure 8 ---

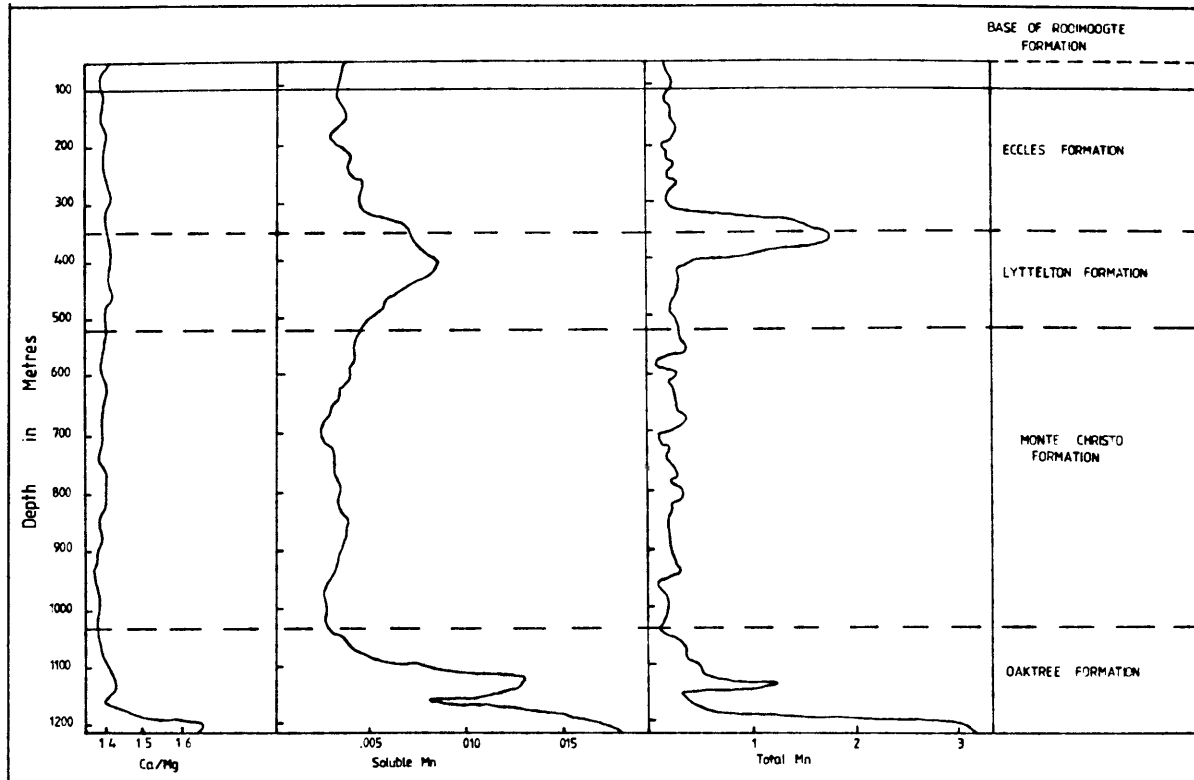


FIGURE 8.
Vertical distribution of calcium/magnesium and of the soluble and total manganese content in dolomite of the Malmani Subgroup of the Far West Rand. (Brink and Eriksson, 1970 and after Eriksson, 1970)

Included within the composition of the dolomite are small amounts of iron and manganese carbonates. As will be seen later, the composition of the dolomite, together with its minor mineral constituents,

/ have ---

has a direct bearing on the present day unstable conditions in the Driefontein area.

1.4.2 THE KAROO SEQUENCE

The lowest beds of the Karoo Sequence are found in the deeply incised valleys eroded out of the Malmani dolomites. They consist of sporadically distributed, unconsolidated gravels (Wolmarans, 1980), together with grey to olive silts, the latter frequently containing pebbles of quartzite and vein quartz. It is highly likely that the gravels represent glacial debris and Brink (1979) considers the pebbles in the overlying silts to be fluvio-glacial in origin having been deposited from the melt waters which moved along the U-shaped valleys in the dolomite. At the termination of glacial conditions, Brink (1979) considers that stagnant water in the valleys would have favoured the development of carbonaceous sediments. On the basis of their mode of deposition, Brink (1979) is of the opinion that these lowest members of the Karoo Sequence in the area should be classified as representatives of the Dwyka Formation. Initially, the carbonaceous sediments were erroneously identified as manganiferous wad, particularly where they were intersected in boreholes immediately overlying either

/ fresh ---

fresh or weathered dolomite. Confirmatory tests were, however, conducted on 33 samples by the Department of Geology of the University of Witwatersrand using X-ray fluorescence spectrometry techniques (Table 1). These tests proved that the material was in fact carbonaceous sediment, in many cases approximating low grade coal rather than wad (Brink and Eriksson, 1970).

BOREHOLE NUMBER	DEPTH IN METRES	DESCRIPTION OF SAMPLE	MANGANESE CONTENT
		Wad	32,6
45	56,39	Carbonaceous Shale	0,03
45	64,01	do.	0,05
45	70,10	do.	0,03
45	76,20	do.	0,06
19	46,63	do.	0,02
19	47,24	do.	0,02
19	59,44	do.	0,02
19	71,63	do.	0,02
19	83,82	do.	0,24
19	89,92	do.	0,34
60	64,01	do.	0,30
60	65,53	do.	0,46
60	82,30	do.	0,20
60	92,96	do.	0,96
62	48,77	do.	0,02
62	57,91	do.	0,13
62	76,20	do.	0,39
62	91,44	do.	0,09
62	97,54	do.	0,06
70	74,68	do.	0,19
70	79,25	do.	0,11
70	88,39	do.	0,07
71	44,20	do.	0,05
71	62,48	do.	0,06
71	80,77	do.	0,05
71	86,87	do.	0,63
83A	54,86	do.	0,03
83A	67,06	do.	0,03
83A	80,77	do.	0,03
83A	91,44	do.	0,04
158	47,24	do.	0,02
158	65,53	do.	0,04
158	77,72	do.	0,16
6	-	Solid dolomite	1,25
53	-	do.	1,23
10	-	do.	1,06
56	-	do.	1,58

After Brink and Eriksson (1970).

/ Overlying ---

Overlying the carbonaceous and tillitic sediments are pale grey, illitic and kaolinitic shales which are exploited by Corobrik Driefontein for brick manufacture.

1.4.3. PLEISTOCENE AND RECENT SOILS

It has been previously mentioned that transported soils of Pleistocene and Recent age form a thin mantle over the Transvaal and Karoo rocks. Primarily, these soils consist of brown peat and alluvial gravels deposited by the Wonderfontein Spruit, and red sands. The red sands were deposited mainly in the form of hillwash derived from the quartzites of the Pretoria Group which form the prominent Gatsrand range. A pebble marker, comprising chert, quartzite and syenite boulders is frequently present at the base of the transported soils.

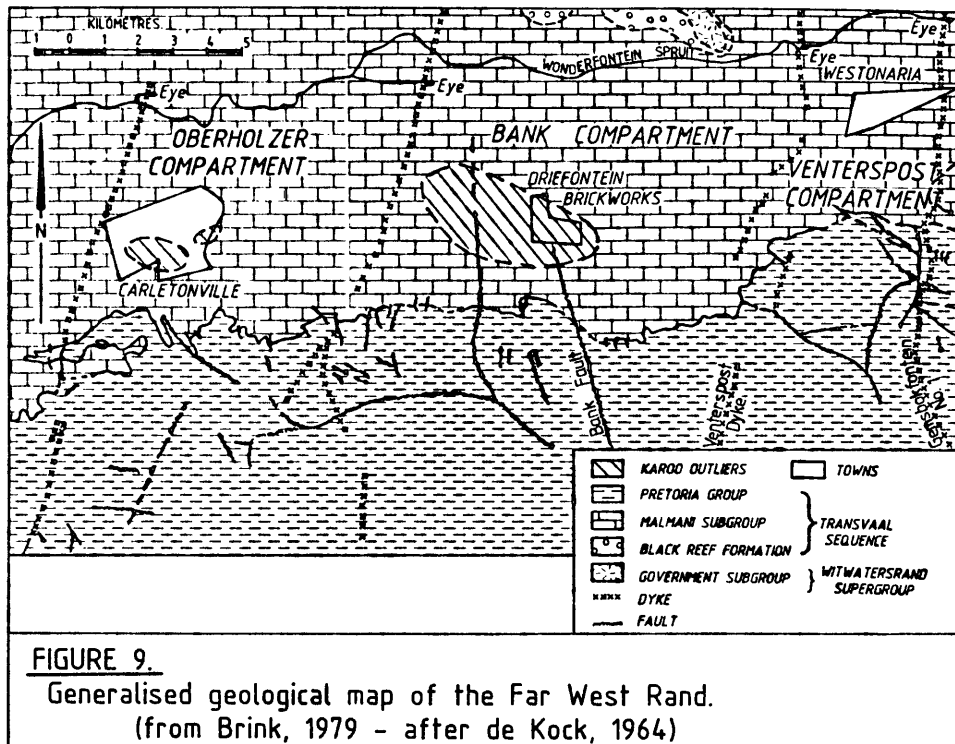
It has been suggested by Brink (1979), that some of the red sands may have been locally transported by wind action. The surface soils, together with the upper horizons of chert rubble formed as a residue from the most recent weathering of the dolomite, are extensively cemented into a sporadic blanket of hardpan ferricrete.

1.5 GEOHYDROLOGY

The post-Transvaal syenite and diabase dykes, which were intruded along a preferred direction slightly east of north, effectively divided the Malmani Subgroup beneath

/the---

the Wonderfontein pediment into a number of ground water compartments . (Figure 9).



Along the northern periphery of the pediment, the Basement Complex rocks in the core of the Hartebeestfontein anticline form a ground water barrier whereas, to the south, the Pretoria Group rocks act as an effective sealant. Ground water in each compartment is contained in a network of interconnected caverns in the dolomites as well as fault and joint planes widened by solution. Under natural conditions the level of the water table in each compartment would tend to be near-horizontal and controlled by the level of a spring or "eye" occurring at a surface point where the Wonderfontein

/ Spruit ---

Spruit crosses the dyke on the western side of each compartment. Schwartz and Midgley (1975) appropriately compared the situation to a "gigantic, freshly filled and tilted ice-tray". As can be seen by referring to Figure 9, the Driefontein area lies in the so called Bank Compartment; its westernmost and easternmost limits being confined by the Bank and Venterspost dykes respectively.

Throughout geological time the natural water table has occupied more than one position in the Far West Rand. Brink and Partridge (1965), originally considered that three distinct water table elevations could be recognised; namely those corresponding with the post-Gondwana, African and possible post-African erosion cycles. According to Partridge 1984 (verbal communication to the writer), however, the evidence for the presence of a post-Gondwana cycle of erosion is suspect. The African erosion cycle is encountered 152m from the surface at an approximate level of 1463m above mean sea level. Furthermore in the vicinity of the Wonderfontein Spruit, the African cycle water table position was lowered by about 30m. As a result of this cycle of erosion, caverns formed in the dolomite now occur in the vadose zone.

The advent of gold mining in the Far West Rand, which commenced in the early 1930's, heralded the artificial

/ lowering ---

lowering of the water table. Such a practice was necessitated by the fact that tension faults and fractures of post-Transvaal age, which transected both the Malmani dolomite and the Witwatersrand rocks, behaved as aquifers connecting water reservoirs in the dolomite to the mine workings below. According to Wolmarans (1976) dewatering can be considered to have commenced when the volume of water being pumped from underground exceeds the natural rate of replenishment. Thus, a dewatered compartment can be defined as one in which, subsequent to dewatering, the amount of water ingressing into underground workings is equal or less than the rate of replenishment.

The Venterspost Compartment was the first to be dewatered with pumping commencing in 1935/36. By the early 1960's, the maximum amount of 56,8 megalitres of water was being pumped daily. With the progressive lowering of the water table, the rate of pumping gradually diminished so that at present the amount is only about 30 megalitres a day. During the early 1960's, the dewatering of the Oberholzer Compartment commenced and by the 1970's, 340 megalitres a day were pumped from the Bank Compartment. In Table 2 details are given of the maximum pumping rates achieved in each compartment, which have been derived from the records of Cousens and Garrett (1969) as well as those of Taute and Tress (1971), compared with the calculated daily
/ replenishment ---

replenishment. The replenishment calculation is based on the assumptions that :

- (i) The average annual rainfall in the Far West Rand is 660mm.
- (ii) The estimation by Cousens and Garrett(1969) that only about 10 per cent of the annual rainfall percolates downwards to the water table, is valid.

COMPARTMENT	SURFACE AREA (km ²)	REPLENISHMENT (Mℓ/day)	PUMPING (Mℓ/day)	MINE	YEAR
Venterspost	54,4	9,8	56,8	Venterspost	1961
Bank	56,7	28,3	13,0	Libanon	1968
			340,0	East and West Driefontein	1970
Oberholzer	153,8	27,6	145,5	West Driefontein	1963
Calculated daily replenishment of the Far West Rand water compartments compared with maximum quantities pumped by certain mines.					

As at the present time, the original water table in the Driefontein area has been lowered to over a kilometer leaving behind complex subsurface water systems in the outlier of Karoo sedimentary rocks. Because of the dewatering of the compartment, these perched subsurface water systems have, as will be discussed later, assumed increased importance in influencing stability conditions at Driefontein.

/ 1.6 ---

1.6 HISTORY OF GROUND INSTABILITY IN THE FAR WEST RAND

Since late 1962 the Far West Rand has had a dramatic history of ground instability. Brink (1979) has comprehensively chronicled such events which are liberally repeated here as they provide a backdrop for the research which was undertaken for this dissertation. With the exception of sinkhole developments and surface subsidences in the vicinity of Carletonville town and the Driefontein Brickworks, the events described occurred where Karoo sedimentary rocks were either absent or else constituted only a thin mantle on top of highly weathered dolomitic bedrock.

At 6.10am on the 12th December 1962, a three-storey crusher plant at the West Driefontein Gold Mine, situated in the Oberholzer Compartment, was engulfed by a sinkhole 55m in diameter and at least 30m deep. The catastrophe, which occurred without any apparent warning, resulted in the death of 29 people. No trace of either the victims or the building was ever found. According to Jennings and others (1965), the time span of the disaster was not more than 30 minutes, most of which was taken up with the sides of the sinkhole falling in.

During 1963, extreme surface differential settlements, caused by the compaction of compressible materials

/ below ---

below the original water table, also occurred in the Oberholzer Compartment. One of these dolines occurred in a suburb of Carletonville, named Lupin Place, and involved about twenty houses. Those houses along the edge of the doline were completely destroyed by the effects of differential subsidence, whereas those in its centre subsided uniformly for about 5,0m without any apparent structural damage. Eventually, however, occupation of the latter houses became untenable because of malfunctioning sewers and other services. By 1967 all the houses were demolished and the depression was backfilled with slimes from the mines. A similar type of subsidence, measuring 180m in diameter and attaining a depth of 8m, occurred in the vicinity of a Mr. Schutte's house. It was aptly named "Schutte's Depression".

In August 1964, yet another sinkhole occurred in the Oberholzer Compartment, this time in a residential area of the Blyvooruitzicht Gold Mine. During the night, a house containing a family of five was engulfed and there were no survivors. Three houses on the periphery of the 30m deep sinkhole also collapsed as its sides fell in, but their occupants had time to escape.

A large sinkhole appeared in the Oberholzer Compartment in early 1964 underneath a slimes dam of the West Driefontein Gold Mine. By September of the same year,

/ the ---

1260295
1255997

the sinkhole accepted more than 2,5 million tonnes of waste slimes which had been pumped into it.

In October 1964, a 21m diameter sinkhole with a depth of 15m, appeared during heavy rain in a suburb of Westonaria situated in the Venterspost Compartment. Fortunately there were no casualties.

Between December 1962 and February 1966, eight very large sinkholes developed in the Oberholzer Compartment within the cone of depression formed in the water table as a result of pumping from the West Driefontein Gold Mine. All eight of these sinkholes had a diameter in excess of 45m and were more than 30m deep. The largest sinkhole, having a diameter and depth of 125m and 50m respectively, occurred in the open veld in the vicinity of Carltonville Extension No.8 during February 1966. In addition 122 smaller sinkholes opened up on the Far West Rand by 1966, of which 107 formed between 1961 and 1963. An aerial view of a well-developed sinkhole in the Bank Compartment is shown in Plate 1. The diameter of the sinkhole should be compared with the railway line transecting the right hand corner of the paragraph.

On 26th October 1968, some 360 megalitres of water a day flooded one of the underground stopes of the West Driefontein Mine. Access to the stope, which was situated below the Bank Compartment, was by means of a drive which penetrated the Bank Dyke

/separating ---

PLATE 1.



Well developed sinkhole in the Bank Compartment of the Far West Rand.

separating this un-dewatered compartment from the dewatered Oberholzer Compartment. The inrush of water, although largely associated with the so called Big Boy Fault, was also promoted by the settlement of the stope's hanging wall. Despite the fact that approximately 1200 men were in the mine section at the time, all of them escaped unharmed. After 23 days, two concrete plugs were installed successfully sealing that section of the mine from its western portion, thereby stopping the flow of water from the Bank

/ Compartment ---

Compartment to the Oberholzer Compartment. To enable re-entry into the flooded workings, it became apparent that the Bank Compartment would have to be dewatered. On 17th December 1968, permission was granted by the Department of Water Affairs and pumping operations commenced. By December 1969, ground instability had reached such proportions that the residents of Bank town were given one month's notice to evacuate the area. About thirty days later one of the two provincial roads traversing the area was closed to traffic.

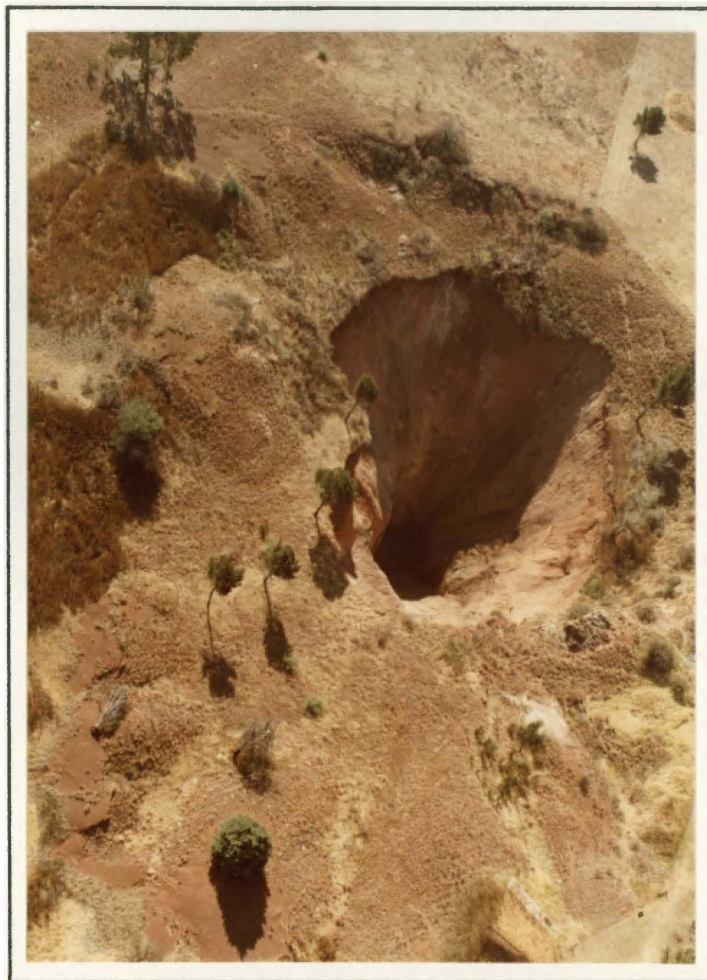
At Driefontein Brickworks, the first effects of dewatering the Bank Compartment became apparent in May 1970 when rails feeding kilns and dryers became so misaligned that kiln cars became jammed. All attempts at re-alignment and re-levelling proved abortive. Simultaneously, structural cracks appeared in the kilns as well as the clay-blending plant sited 60m to the south.

By July 1970, the amount of water being pumped by the West Driefontein and East Driefontein Gold mines reached a massive daily average of 340 megalitres a day. Corresponding with the above-mentioned rate of dewatering, serious subsidences in the form of dolines and sinkholes occurred, as well as the opening up of tension cracks in the ground.

/ The ---

The month of October 1970 was marked by the occurrence of a sinkhole at the Venterspost Gold Mine recreation centre which resulted in the engulfment of the clubhouse and one spectator watching a game of tennis. Six months later, yet another sinkhole developed in the vicinity of the same locality of Venterspost Gold Mine but this time on the bowling green some 60m from the tennis court sinkhole. Aerial views of a sinkhole on the Venterspost Golf Course are shown in Plates 2 and 3. The size of the sinkhole can be gauged relative to the trees and road at its periphery.

PLATE 2.



Sinkhole on the Venterspost Golf Course,
Venterspost Compartment, Far West Rand.

/Plate 3.....

PLATE 3.



Sinkhole on the Venterspost Golf Course, Venterspost Compartment, Far West Rand.

By 1972, the subsidence and structural cracking of the kilns and dryers at Driefontein brickworks had reached such dimensions that they could no longer be operated and their demolition was inevitable.

The 9th April 1975 was marked by yet another event of ground instability in the Bank Compartment. A 20m diameter and 7m deep sinkhole opened up under the railway line near the deserted town of Bank only eight days after a decision had been made to re-open the line to passengers. Although the driver of an approaching train saw the sinkhole, he was unable to stop in time and as a result three coaches were derailed and a further two left straddling the sinkhole. Fortuitously,

/ none ---

none of the passengers was hurt.

Late in December 1976 the first sinkhole occurred at Driefontein Brickworks on the floor of an abandoned water-filled quarry some 90m southeast of the so called Down-draught Making Section (Appendix I). Although this sinkhole had a diameter of only 5m, it was nevertheless able to drain 440 megalitres of water from the quarry within about 3 hours. Sinkhole No. 2, situated some 65m east of the first occurrence, also with about a 5m diameter, developed almost simultaneously. Two hours later, sinkholes Nos. 3 and 4 appeared along the southern rim of the quarry (Appendix I). Sinkhole No. 3, which had a diameter of about 18m, resulted in the engulfment of an electrical substation.

With the approach of summer rains in October/November 1977, prominent tension cracks started to develop on surface in the vicinity of the four sinkholes which had occurred up to that time at the Driefontein Brickworks. On the 17th November 1975, sinkhole No. 5 appeared near the south-eastern corner of the Down-draught Making Section. Sinkhole No. 6 occurred adjacent to the disused Making Workshop on the 23rd November 1977. This sinkhole was 12m deep and onion shaped in as far as it had a diameter of approximately 5m at the surface, but belled out to 9m diameter some 3m deeper and then narrowed to less than 4m for the bottom-most 8 metres. Another

/ distinguishing ---

distinguishing feature of sinkhole No. 6 was the fact that the "neck" of the sinkhole was not vertical but inclined at 60° from horizontal in a south-easterly direction. On the 9th December 1977, sinkhole No. 7 appeared below the conveyor belt, as shown in Appendix I and three days later, No. 8 sinkhole opened up in the backfill on the northern perimeter of the quarry. Sinkhole No. 9 opened up near the north-eastern edge of the abandoned quarry on 14th December 1977. The 27th December 1977 marked the occurrence of two sinkholes within hours of one another; sinkhole No. 10 being sited on the south-eastern corner of the Crushing and Grinding Plant and sinkhole No. 11 below the conveyor belt. The rapid development of sinkholes in the vicinity of the Down-draught Making Section continued and, on 11th January 1978, sinkhole No. 12 occurred immediately to the east of sinkhole No. 5. Although the water in the abandoned quarry had been completely drained out through sinkhole No. 1 in December 1976, it had accumulated yet again by early 1978. On the 18th April 1978, sinkhole Nos. 13, 14 and 15 developed almost simultaneously on the floor of the quarry and, once again, the accumulated water drained away, mostly down sinkhole No. 12. During June 1978, sinkhole No. 16 was noticed as a pool of water on the floor of the quarry some 55m south of sinkhole No. 13. The last recorded sinkhole, namely No. 17, occurred on 18th February 1980, on the eastern side of the disused dryers of the Down-draught Making Section. This sinkhole,

/ which ---

which has a diameter of 5m and is inclined at some 60° from horizontal in a southwesterly direction, is illustrated in Plate 4.

PLATE 4.



The 5m diameter Sinkhole (Sinkhole 17) which occurred at Driefontein Brickworks on 18th February, 1980.

- - - o0o - - -

/ PART 2 ---

PART 2

2. FACTORS RESPONSIBLE FOR GROUND INSTABILITY

The factors which have contributed to ground instability in an area underlain either by surface or subsurface outcropping dolomite rocks are both varied and complex.

2.1 WEATHERING OF THE DOLOMITE

Tectonic events prior and subsequent to the deposition of the Transvaal Sequence, the latter often being expressed in reactivation of the former, imprinted well-defined fracture and fault patterns on the dolomite rocks of the Malmani Subgroup. Three major fault and fracture directions were recognised by Papendorf (1971) as shown in the strike frequency diagram (Figure 10).

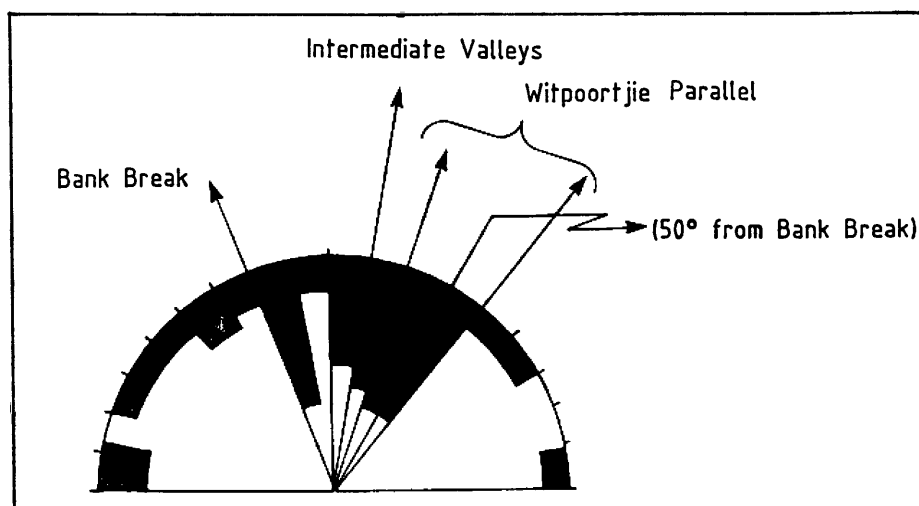


FIGURE 10.
Strike frequency diagram of faults in the Far West Rand.
(Brink, 1979 from compilation by Papendorf, 1971).

/ One ---

One set of faults and fracture trends in a direction between 10° and 20° west of north, the most prominent of which is the Bank Break. A second set of faults and fractures strikes between 20° and 40° east of north; the Witpoortjie Parallel being a prime example. A third, and intermediate set of faults and fractures, follows a direction of between 5° and 10° east of north. These last-mentioned faults and fractures are frequently occupied by dykes. It is noteworthy that the directions followed by faults and fractures tend to be arranged at approximately 60° to one another. Both Pienaar (1971) and Brink (1979), concluded that these fault and fracture directions are "consistent with the principle stress pattern involved at the margin of the dolomite basin at the Far West Rand and are compatible with a stress field in which the major principle stress acted in a direction 10° east of north" (Brink 1979). It was along these directions of structural weakness that preferential solution of the dolomite occurred with a pre-Karoo, karst type topography being developed. The delineation of the near-vertical avens, grikes or slots is clearly shown by the results of gravimetric surveys in the Driefontein area and its environs (Appendix 2), which are based on the work of Enslin and Smit (1955) as well as Bezuidenhout and Enslin (1969). The fact that dolomite has a specific gravity of 2,85 whereas for chert rubble and unconsolidated debris it ranges between 1,7 to 2,4, enables gravimetric anomalies to be recognised and

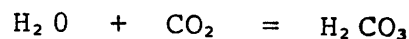
/ related ---

related to the mean depth of bedrock. As pointed out by Brink (1979), however, gravimetric observations do not permit a distinction to be drawn between "floaters" and bedrock, nor do they define the outline of dolomite pinnacles. Furthermore, the interpretation of gravimetric surveys does not enable the presence of voids in the residuum or caverns in the bedrock to be detected with any certainty. When, however, Bouguer values have been calculated and corrections, based on the depth of bedrock as observed in selected boreholes, have been applied to eliminate regional trends, gravimetric surveys can, in specific conditions, clearly indicate the presence of slots in the ground water compartments of the Far West Rand. Bezuidenhout and Enslin (1969) show that corrections can be applied to "... reduce the zero gravity contour to correspond to lines along which the subsurface of solid dolomite coincides with the original ground water table". Thus positive gravity contours indicate areas where the solid dolomite is above the original water table, and which will not, therefore, be affected by dewatering. Conversely, negative contours define where the original water table was above the solid dolomite and demarcate areas of potential subsidence, particularly where the contours are closely spaced indicating scarps to adjoining valleys.

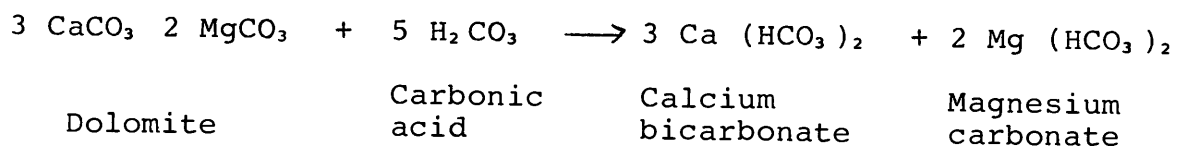
It must be borne in mind that, although dolomite rocks are impervious, the rock mass is accessible

/ to ---

to percolating water because of the intricate system of faults, fractures and joints. Erosion, by means of solution took place along these planes of weakness so that steep sided slots developed in the vadose zone. Whereas dolomite is almost insoluble in pure water, the presence of carbon dioxide in ground water promotes solubility. Rainwater already contains a small amount of carbon dioxide in solution when it falls onto the surface. As it percolates through the soil, however, the water becomes enriched with carbon dioxide so as to become much more acidic than previously, to form a weak carbonic acid:



It is believed that this weak, acidic ground water causes the dolomite to go into solution in the form of bicarbonate as follows:



Chemical analysis of water pumped from the dolomite, shows that the dissolved solids consists of nearly 90 per cent bicarbonates and 10 per cent silica, the latter indicating that partial solution of chert also occurs. At the Wonderfontein Eye it was calculated that, with a flow rate of 50 megalitres per day, some 9000 kilograms of dolomite were put into solution during the

/period---

period (Brink and Eriksson, 1970). Furthermore, at the Gerhardsminnebron Eye, A.L. du Toit (1954) arrived at a figure of 10 tonnes of bicarbonate for 57 mega-litres per day.

The writer subscribes to the hypothesis that the solution of the dolomite above the water table is significantly different from that occurring at or below this level. In the vadose zone, the ground water percolates in a downward direction causing the widening of any existing structural weaknesses in the dolomite. In the Far West Rand, the pattern of faults, fractures and joints imposed upon the dolomite of the Malmani Subgroup constitute aquifers along which preferential solution takes place. As will be shown later, a study of the sub-outcropping dolomite topography in the Driefontein area reveals that chasms up to 30m wide with near vertical sides, have been formed along such planes of structural weakness. The term "aven" was applied by Brain (1958) for such chasms, but like Brink and Eriksson (1970), the writer has adopted the term "slot" as being more appropriate for this type of dolomite weathering. The water table itself has been defined by Brink and Partridge (1965) as "... the level at which pore water pressure (ie. hydrostatic pressure due to gravity acting on water in the voids within soils and porous rock), equals atmospheric pressure." In areas of soluble rock, however, the water table may be flatter in some areas than in others, causing laminar flow from areas of high to low

/hydrostatic ---

hydrostatic pressure in the phreatic zone immediately below the water table. Observations in the Far West Rand indicate that the non-static water conditions in the phreatic zone have enabled preferential solution of the dolomite to occur along horizontal planes of weakness such as joints and bedding planes. The flow of carbonic acid-charged water was responsible for the development of cavities, "spongeworks and networks" as well as horizontal caverns as postulated by Davis (1930) and supported by Bretz (1942 and 1953).

2.2 PRODUCTS OF DOLOMITE WEATHERING

As previously mentioned, the dolomites of the Malmani Subgroup contain minor amounts of manganese and iron carbonate as well as more prominent chert horizons. Unlike the rock's main constituents of magnesium and calcium carbonates, which are put into solution by permeating, acidic water, the manganese, iron and chert are relatively insoluble and remain as residues.

Iron from thin, ferruginous shale partings as well as ferruginous dolomite occurring above the water table, oxidizes to form hematite. This hematite material, together with insoluble clays derived from the weathering of shaley partings, is easily transported downwards by moving groundwater and is frequently found in fissures

/ and ---

and caverns. As a result of the weathering of the dolomite, the rock's minor manganese constituent is represented by a manganiferous earth known as "wad". Chemical analyses have shown wad to consist mainly of manganese and iron oxide. Wad may be encountered in caves in the dolomite, in accumulations within chert rubble along the zone of weathering or at the contact between dolomite and a different rock type such as syenite in the form of sills or dykes. As pointed out by Brink (1979), however, concentrations of wad occur within certain horizons of the dolomite where inherent quantities of manganese and iron, which were originally present, have been exposed to weathering. Such occurrences apply to the Lyttleton Formation of the Malmani Subgroup underlying the outlier containing Karoo sedimentary rocks in the Driefontein Brickworks area where over 8m of earthy manganiferous wad are frequently encountered as a mantle on top of weathered dolomite.

The term "wad" is frequently misused to describe any black and brown coloured materials. In fact, a closer examination of such materials, especially in diamond drill cores and percussion drill cuttings, reveals them to be either carbonaceous sediments or else manganese or iron-stained clays. By comparison, manganiferous wad is characterized by its earthy appearance, low density, susceptibility to easy transportation by agents of erosion and high

/ compressibility ---

compressibility as shown in Table 3. It must be noted, however, that manganiferous wad frequently occurs together with clay or other materials. Consequently, the properties of such mixtures are dependant upon their constituents and degree of compaction.

PROPERTY	NO. OF DETERMINATIONS	MAXIMUM	MINIMUM	AVERAGE
Clay Content (%)	3	35	28	31
Alterberg Limits (less than 0,425mm material)				
(a) Liquid limit	4	96	47	63
(b) Plasticity index	4	29	5	18
(c) Linear shrinkage	4	14	4	10
Specific gravity	8	3,47	1,63(?)	3,01
Bulk density (kg/m ³)	8	1 462	858	1 246
Moisture content (%)	8	202	57	117
Dry density (kg/m ³)	8	722	285	607
Initial void ratio	9	9,6	2,7	4,5
Compression index	9	1,80	0,57	1,15
Recompression index	9	0,07	0,03	0,05
Over consolidation ratio	3	15,00	2,32	6,68
Summarized physical properties of manganese wad. (Partridge, Harris and Diesel, 1981)				

The chert horizons in the dolomite are relatively immune to the weathering processes described above, except that prolonged exposure may reduce chert to a friable white substance with a sugary or chalky texture. Selective removal of thin dolomite, ferruginous or manganiferous intercalations in chert horizons can, however, lead to mechanical collapse. Thus, chert residuum may be represented either by angular gravels or slabby

/ boulders ---

boulders. When overlain by iron-enriched Karoo sediments or Pleistocene soils, chert horizons which have suffered mechanical collapse may be cemented by the ferruginous matter derived from such sources.

2.3 CHANGES IN THE ELEVATION OF THE WATER TABLE

From what has been stated in the preceding section, it can be readily conjectured that the weathering of dolomite and the formation of by-products resulting from such weathering, would induce potentially unstable conditions even if the water table had remained constant. Such constancy of the water table seldom, if ever, occurs in fact. Thus, in the Far West Rand, various cycles of erosion and planations, such as the African and possible post-African cycles, reflect radical fluctuations in the water table elevations during geological times. Furthermore, a drastic, artificial lowering of the water table due to the pumping activities of various gold mines, has dramatically contributed to the development of unstable conditions. Fundamentally, any lowering of the water table results in horizontal caverns, previously in the phreatic zone being promoted into the vadose zone. Consequently, the whole process whereby vertical slots are eroded out of the dolomite in the vadose zone and horizontal caverns being created in the phreatic zone, together with the development of resultant weathered products, is repeated. In the Far

/ West ---

West Rand, the Malmani dolomite contains a complex system of vertical slots and horizontal caverns, each system having evolved when the water table was positioned at a particular elevation for a prolonged period.

When horizontal caverns, which were originally in the phreatic zone, are promoted into the vadose zone, the stability of any residual deposits they may contain is placed in jeopardy. Thus, manganiferous sand may become dehydrated and suffer consequent compactions whereas similar, easily erodable materials may be eroded out of promoted slots and caverns, because of an increased hydraulic gradient, to be re-deposited into newly formed receptacles below. As a result, the virtually dehydrated or denuded system of slots and caverns in the vadose zone sets up conditions of ground instability which are conducive to the development of dolines and sinkholes.

2.4 MECHANISMS RESPONSIBLE FOR DOLINE AND SINKHOLE OCCURRENCES

Terrain underlain by dolomite or other soluble rocks is prone to severe subsidences of the ground surface. These subsidences may be categorized into two types, namely dolines and sinkholes.

/ 2.4.1 ---

2.4.1 THEORY OF DOLINE DEVELOPMENT

A doline can be defined as a gradual surface subsidence caused either by the compaction or removal by erosion of unconsolidated materials close to the surface. The enclosed depression formed by a doline may be as much as 200m in diameter and attain 12m of subsidence at its centre as shown in Plate 5. By contrast, sinkholes are deep, crater-like subsidences which develop with the sudden collapse of the surface into underground slots or caverns. Some typical sinkholes which have occurred in the Bank and Ventersport compartments are illustrated in Plates 1 and 2.

PLATE 5.



Aerial view of a doline in the Bank Compartment of the Far West Rand. The diameter of the doline can be gauged from the railway track transecting the left hand corner of the photograph. Subsidence at it's centre amounts to 12m.

/ sinkholes ---

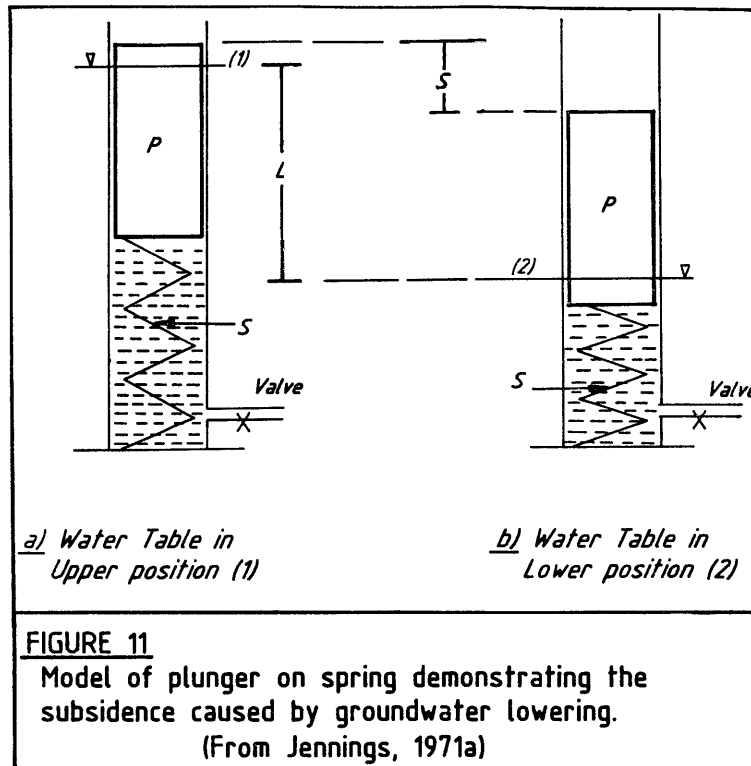
Sinkholes tend to be cylindrical in shape and may be as large as 125m wide and more than 30m deep. Both dolines and sinkholes can cause great damage to property but in the case of sinkholes there is also the possibility of lives being lost because of the rapidity at which they can develop. The theoretical mechanisms responsible for the development of dolines and sinkholes have been postulated by numerous past research workers including Brink, Partridge, Jennings, Gowan and Louw (Brink and Partridge 1965; Jennings, Brink, Louw and Gowan 1965; Jennings 1966; Brink and Eriksson 1970; Brink 1979).

When the level of the water table fluctuates, the surface of the ground may also change. Thus, under certain circumstances, if the water table rises the ground surface also rises and if it falls, the surface level drops. In a condition of equilibrium, surface level changes resulting from normal, seasonal fluctuations of the water are too small to be detected except by taking precise measurements. Should the water table, however, be lowered abnormally and the materials through which it has retreated are highly compressible, then the resulting changes in subsidence levels may be dramatic.

The mechanism of surface subsidence due to the lowering of a water table was considered by Jennings (1971a)

/ in ---

in terms of the Archimedes principle as illustrated in Figures 11a and 11b.



The plunger "P" in Figure 11a, which has a weight of 2,25 times that of water and approximately corresponds to a well-compacted soil, rests on a compressible spring "S". The spring and most of the plunger are in water which stands at level (1) in Figure 11a. In Figure 11a, plunger "P" represents an incompressible soil supported in a state of equilibrium by a compressible soil shown as the spring "S". When the water is drained out, a new level is achieved (2), which is still within the body of the plunger as shown in Figure 11b. The water level drops by an amount "L", which equates to the lowering of the

/ water ---

water table, and the piston drops by an equal amount "S" which corresponds to the degree of ground settlement. The "S" movement, or ground surface settlement, is due to the compression of the spring as a result of the additional load coming on to the spring being caused by the loss of buoyancy of the water on the plunger over the length of water drop within the plunger length, namely (L-S). It can be seen that if the length of the spring equates to the thickness of the compressible stratum and the stiffness of the spring corresponds to the compressibility of compactible soil, then the amount of surface movement (S) will also change. It is, therefore, logical to conclude that the amount of surface settlement is dependant upon :

- (i) the amount by which the water table is lowered;
- (ii) the thickness of compactible stratum;
- (iii) the compressibility of such compactible stratum.

The principles of the model shown in Figure 11a and 11b can be used for the calculation of surface subsidences under actual conditions by applying the theory of settlement due to the consolidation of soils as expounded by Terzaghi (1925). The Terzaghi theory introduced the concept of "effective" stress which is the difference, at any specific point in the subsoil

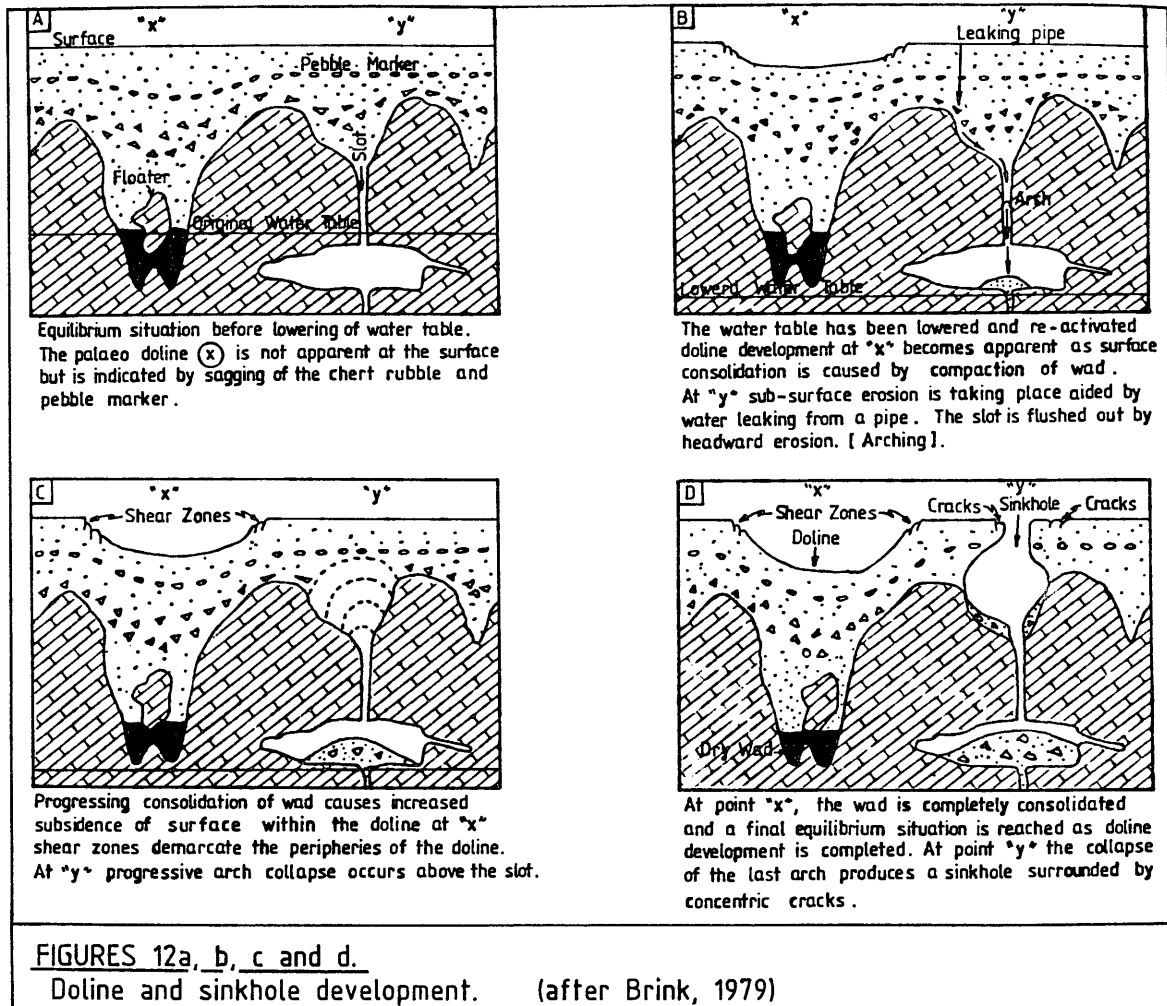
/ between ---

between total stress and the pore-water pressure. It follows that the compression of a soil or subsoil is exclusively due to increases in this effective stress. For example, if at a depth of 30m the total vertical stress amounts to 590 kPa, representing the total mass of overlying soil in a column with a 1m square cross-section, and should the water pressure at the same point be 245 kPa, then the effective stress will be 345 kPa. The water pressure quoted in the previous sentence corresponds to a static head at 25m above the level at a depth of 30m. Should this static head, above the same level, be reduced to 10m, the water pressure would be 98 kPa and the new effective stress would be 492 kPa which would equate to an increase in effective stress of 147 kPa (ie 492 kPa less 345 kPa). Thus, in accordance with the principles illustrated in Figures 11a and 11b, it can be seen that the lowering of the water table increases the effective stress which, in time, will cause the soil or the subsoil to be compressed. The application of such principles in an area such as the Far West Rand, where a karst-like topography exists in the sub-outcropping Malmani dolomite, has been described by Brink (1979).

Figure 12a shows a palaeo-doline which, being in a state of equilibrium, is not apparent on surface but is indicated by a sagging of chert residuum and a

/ pebble ---

pebble marker at the base of the Pleistocene to Recent soils. When the water level is lowered, as shown in Figure 12b, further compaction of compressible



material, such as manganiferous wad, occurs thereby causing surface subsidence. With this subsidence of the surface, a shear zone and tension cracks develop around the periphery of the doline as shown in Figure 12c. Finally, Figure 12d illustrates the conditions when the compactible material is

/ thoroughly ---

thoroughly consolidated and the growth of the doline is concluded.

2.4.2 THEORY OF SINKHOLE DEVELOPMENT

The basic factors responsible for the development of sinkholes are the same as those contributing to doline type subsidences. Firstly, the underlying dolomite must have been eroded into a rugged, karst topography comprising vertical slots above the water table and horizontal caverns immediately below it. Secondly, these vertical slots and horizontal caverns must be filled with erodible materials originating from the processes of weathering. Thirdly, a lowering of the water table must occur to promote a condition of instability. In contrast to the doline development, however, there are a number of unique conditions, defined by Jennings, Brink, Louw and Gowan (1965), which are essential for sinkhole development :

- (i) Ground water emanating from rain water seepage, a leaking pipe, soak pits or uncontrolled surface drainage, must percolate down convenient aquifers to that it can reach the surface of the dolomite. Convenient aquifers are constituted by tension cracks, shear zones and interfaces between
/ intrusive ---

intrusive dykes and older country rock. On reaching the surface of the dolomite the percolating water must flow down a convenient slope to the nearest slot;

- (ii) Residual materials choking the slot must be eroded away by the percolating water to a lower-lying cavern, leaving a void;
- (iii) The span between the dolomite abutments of the slot must be appropriate to the tensile strength of the "bridging" material above the void so that arching conditions can develop within it. Thus, the vertical load imposed upon the arch must be carried by arching thrusts to the abutments. Complete arching will develop when the vertical stress along the intrados of the arch is zero;
- (iv) The cavity beneath the arch must be of sufficient dimension to accept the materials from above;

/ (v) ---

- (v) The material forming the arch must lose its cohesion so that successive arch collapse can occur in the form of a "headward piping" type of erosion.

With specific conditions described above, the mechanical theory of sinkhole development is readily explained. In Figure 12a, a condition of equilibrium, prior to the lowering of the water table, is illustrated. The situation after the lowering of the water table is shown in Figure 12b when horizontal caverns have been promoted into the vadose zone and active erosion of residual materials, choking vertical slots, is being accomplished by percolating water. As a result of this erosion, a temporary arch is formed in the residual material. Figure 12c illustrates upward "piping" erosion caused by successive arch collapse, whereas Figure 12d shows the ultimate creation of a sinkhole when failure of the last arch causes the ground surface to collapse.

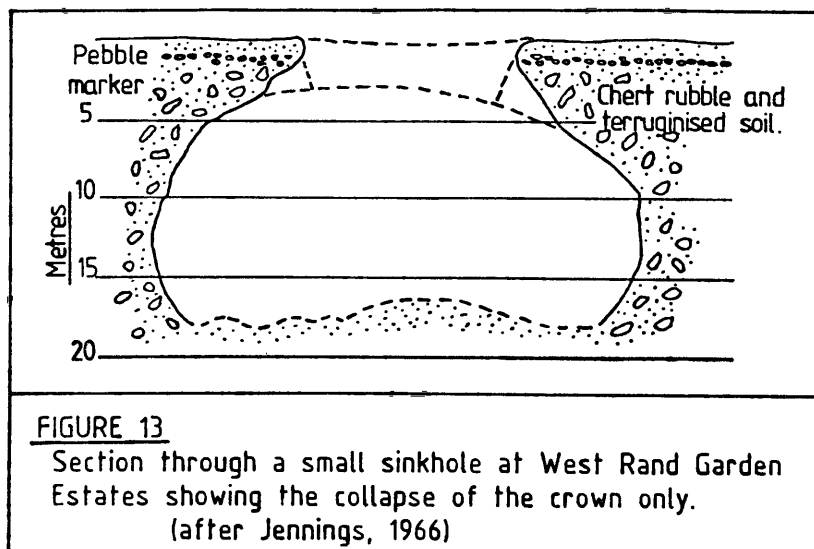
There are a number of reasons why successive arch collapse should occur. The most obvious reason is a continued seepage of percolating water down the flanks of the dolomite abutments, which are so frequently lined with readily erodable materials, causing a loss of cohesion. Another contributing factor to arch collapse is variability in the

/ residual ---

residual strengths of the individual layers of bridging materials. Such a factor results in upward "piping" erosion and successive arch collapse accelerating through a layer with poor residual strength and being retarded through stronger materials. The most obvious circumstances conducive to a differential in the rates of successive arch collapse would be when headward erosion is occurring through a layered succession of sedimentary rocks, such as those of Karoo age, where well-defined lithological units are present. Differential arch collapse has, however, also been observed in the Pleistocene "hillwash". Thus, even when the arching has reached an almost final stage very close to surface, it may remain stable for a considerable period of time if it is supported by a layer of ferricrete or a ferruginised pebble marker. When final collapse of the surface ultimately takes place, Jennings (1966) observed that the resulting sinkhole may be "onion" or "bottle"-shaped in cross section as shown in Figure 13. Small sinkholes may retain this onion-shaped profile for quite a long period of time before the overhanging "lips" fall in.

Successive arch collapse may also be stimulated by profiles of the solid dolomite abutments themselves. The erosion of the dolomite has resulted in the flanks

/ of ---

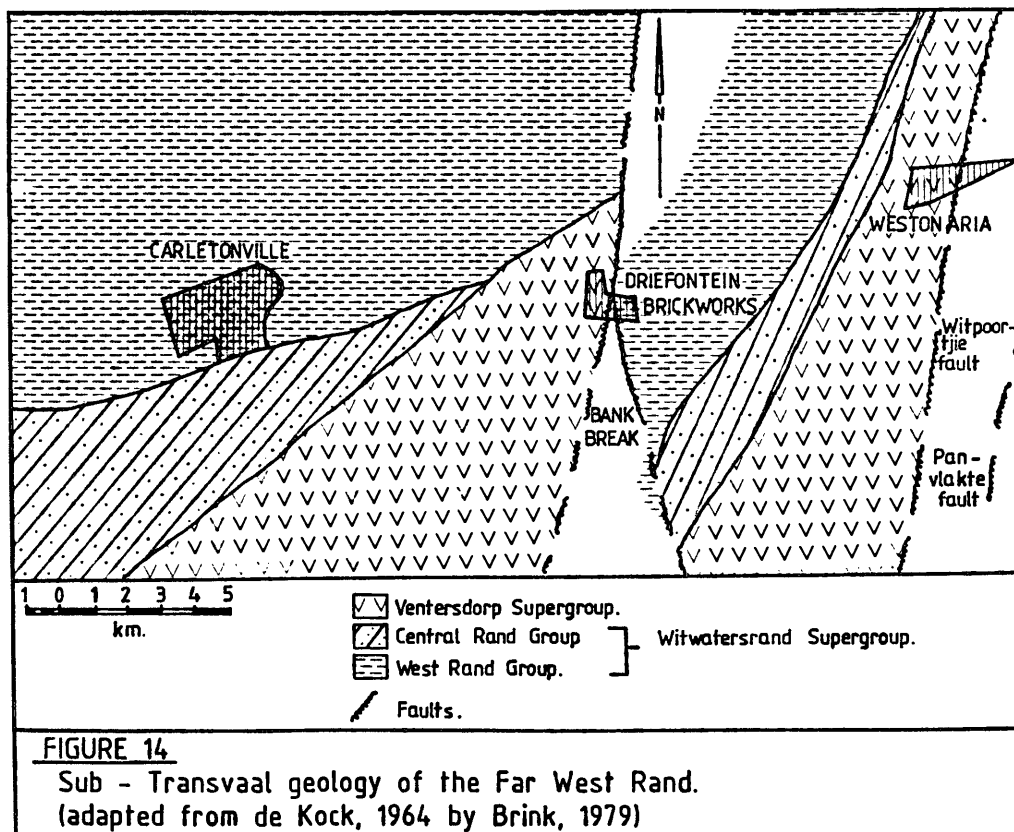


of the abutments being highly irregular. The span between the abutments which is so important to the formation of an arch must, therefore, vary in such circumstances with the result that arch stability is also effected. If the residual strengths of the bridging materials between the abutments are also variable, then the factors causing arch collapse become compounded.

Jennings (1966) suggested a further three causes for loss of cohesion and resulting arch collapse. One of these causes is attributed to ground movements resulting from subsidences associated with the collapse or settling of underground mine workings. Another reason for loss of cohesion in an arch could be due to surface loading of a vibratory nature, particularly where the energy of vibrations

/ is ---

is high and sustained. Finally, Jennings suggested that earth tremors, which are common occurrences over the whole of the Witwatersrand, cause vertical and lateral accelerations resulting in external forces being applied to the materials of the arch. Almost certainly the Driefontein area is sensitive to the effects of ground movements at depth resulting from gold mining operations, the "shock waves" of which may be transmitted and their effect amplified by planes of structural weakness both in the dolomitic bedrock and in younger, overlying materials. The Bank Fault, which traverses in a northeasterly direction, virtually beneath the Driefontein brickworks, constitutes such a structural feature (Figure 14).



/ As ---

As previously stated, the Bank Fault is a significant structural feature in the Far West Rand for not only has it displaced the strata of the Witwatersrand Supergroup for a horizontal distance of some 8km, but it has also manifested itself in post-Transvaal times. Thus, the Timeball Hill Quartzite on the Gatsrand as well as rocks of the Malmani Subgroup are displaced. In other words, this zone of structural weakness penetrates through the dolomite into the underlying gold-bearing rocks of the Witwatersrand Supergroup. Consequently, the seismic energy generated by the sudden collapse of abandoned old workings is absorbed or reflected by the plane of the Bank Fault giving rise to an increased release of such energy, thereby rendering Driefontein area particularly sensitive to arch collapse.

- - - o0o - - -

PART 3

3. CONVENTIONAL METHODS OF MONITORING GROUND INSTABILITY

Acceptance of the theories for surface and subsurface movements necessitated the evolving of logically sound procedures whereby meaningful interpretations of measured surface and subsurface movements could be made.

3.1 MEASUREMENT OF SURFACE MOVEMENTS

The method of measuring surface movements, based on a precise, differential levelling method of surveying, was first introduced at Driefontein by Watt (1972). Precise levelling work involves the determination of elevation differences between targets grouted into concrete blocks cast around strategically placed measuring points relative to at least three stable bench marks. Such stable bench marks termed Permanent Bench Marks (PBM's) are of the deep borehole variety with casing or piping, appropriately marked with measuring targets,

/ anchored ---

anchored to solid dolomite rock, sometimes as much as 60m below surface. Essentially, all the points to be measured are incorporated into inter-related and inter-dependant circuits which yield degrees of accuracy proportional to the number of closed loops and permanent bench marks forming the configuration. Obviously, the more loops in the configuration, the higher the accuracy obtainable. The initial differences levelling exercise undertaken at Driefontein, comprised 10 closed loops connecting various measuring points in the vicinity of the Factory Complex, Office Block and Compound as shown in Figure 15. As can be seen, measuring points common to two or more circuits, such as BM, AG, BI and so on, provided an inter-relationship between the various circuits.

3.1.1 INSTRUMENTATION

Prior to 1970, the instruments used comprised a Wild-Heerbrugg Automatic Level, Model NA2, and a standard Sopwith levelling staff graduated in feet, tenths and hundreds. It was decided by Professor Watt (1972), however, that such equipment was unsuitable for the required precision of levelling. Consequently, a Zeiss Koni Automatic Level (Model 007) is now used as illustrated in Plate 6. In addition to the obvious quality of this precision instrument, it has the advantage of having a permanent "built in" Pentaprism Micrometer which is an integral

/ part ---

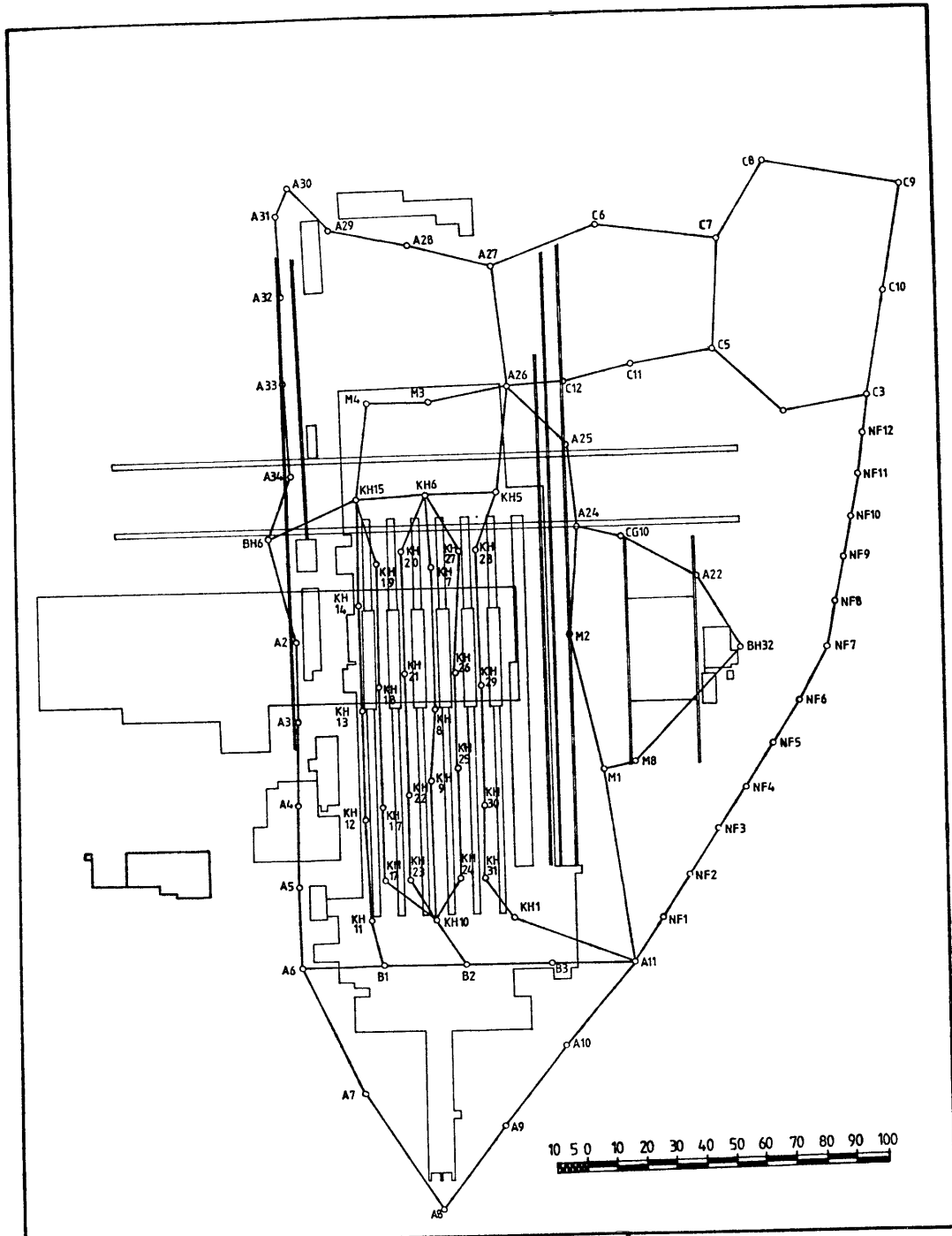
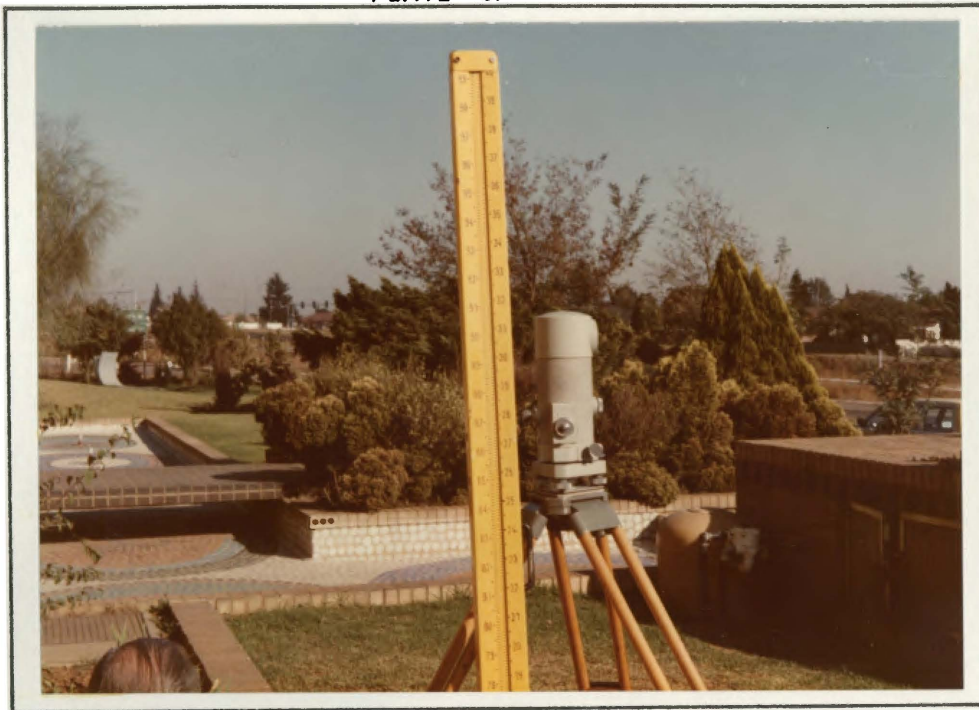


FIGURE 15.
Precise levelling closure circuit used at Driefontein Brickworks.
(Compiled from Watt, 1972.)

part of the sealed optical and micrometer system. The instrument's line of sight is elevated by an additional 140mm and, furthermore, it is not subject to the error defects over the range of distances measured at Driefontein.

PLATE 6.



The Zeiss Koni Automatic Level and measuring Staff.

In addition to the Koni level, a Nedo Invar precise levelling staff was purchased with circular bubbles to ensure verticality and, by means of steadying poles, is held stable during observation. A double set of independent gradations, at an interval of 5mm, is marked on the staff. The numbering of the staff units, that is 50mm, is displaced by 59,250 staff units for the two scales. Thus by adopting a / procedure ---

procedure of reading back sight left scale, fore sight left scale, fore sight right scale and back sight right scale, two completely independant determinations of the height difference between two bench marks are obtained as explained in Figure 16.

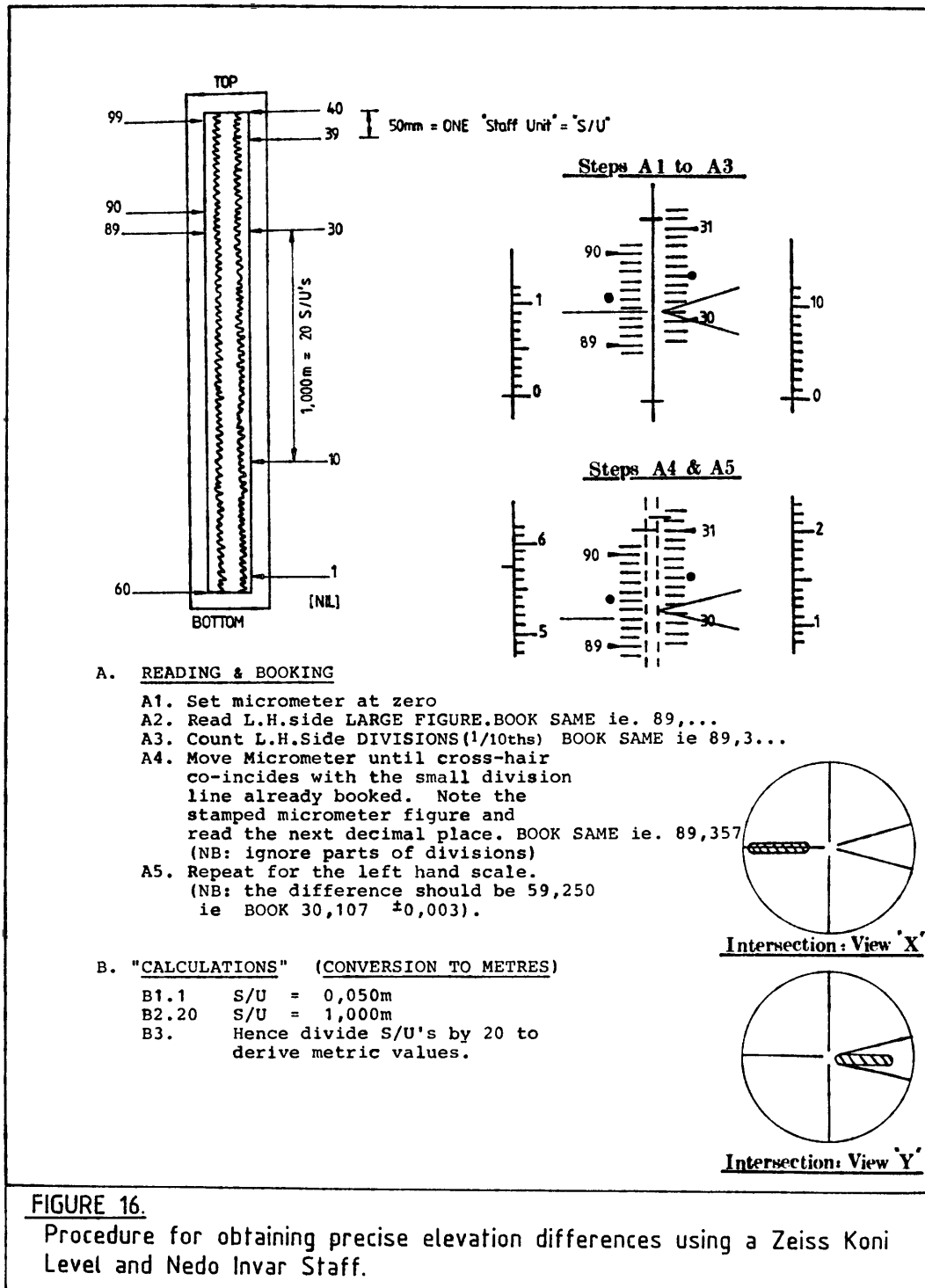


FIGURE 16.

Procedure for obtaining precise elevation differences using a Zeiss Koni Level and Nedo Invar Staff.

Such a procedure of measurement reading is ideally suited for the precise levelling undertaken at Driefontein, where turning points in the circuit loops are permanently marked. In addition, this method of measurement reading eliminates the need to duplicate either the levelling or the necessity to observe a second height difference, after having displaced the elevation of the instrument axis, to provide the necessary check.

3.1.2 INSTRUMENT FIELD PROCEDURES

In any specific loop, instrument points are sited midway, within limits of 0,25mm, between turning points. These instrument points are permanently marked by means of steel pegs encased in concrete whitewashed for easy relocation. All distances are recorded so that the relevant correct "weights" can be calculated when the adjustment of the circuits is undertaken. The observing and instrument reading procedures, which have been adopted, are described below :

If "IP" is the instrument position exactly midway between measuring points TP_n and TP_{n+1} and IS_i and IS_{i+1} are the intermediate sights to be observed from the set up, the routine is to :

- (i) Take a backsight reading (BS) to measuring point TP_n on the left hand scale (LHS).

/ (ii) ---

- (ii) Take a fore sight reading (FS) to measuring point TP_{n+1} on the left hand scale (LHS).
- (iii) Take a fore sight reading (FS) to measuring point TP_{n+1} on the right hand scale (RHS).
- (iv) Take a backsight reading to measuring TP_n on the right hand scale (RHS).
- (v) Calculate the height differences between measuring points TP_n and TP_{n+1} by subtracting the readings described in paragraph (ii) from paragraph (i) and paragraph (iii) from paragraph (iv) respectively.
- (vi) Sight the staff held on intermediate sight 1 (ISi). The instrument's micrometer is set individually for the two scales to be read, both the left hand and the right hand readings being taken. Therefore, the height differences with respect to measurements taken as described in paragraph (i) and (ii), in other words measuring point TP_n , can be calculated. The

/ two ---

two values thus obtained must agree with
0.003 staff units.

- (vii) Continue with readings to other intermediate sights (ie IS_{i+1} , IS_{i+2} etc.), using the procedure described in paragraph (vi) above.

- (viii) Complete the series of measurements taken from the particular instrument set up position with check observations to either measuring point TP_n or TP_{n+1} .

3.1.3 RECORDING OF OBSERVATIONS

It is important that the procedure adopted for recording field observations should be described.

It must be remembered that the height differences read in the field are in staff units of 50mm as previously mentioned. To convert these staff readings to differences of elevation between measured points in terms of metric values, the field readings must be divided by 20; such a division being performed in the field book. In the interests of clarity as well as minimizing any chance of arithmetic error, the field book is divided into a left hand side (LHS) and a right hand side (RHS)

/ as ---

as shown in Figure 17; the former-mentioned side being shaded red.

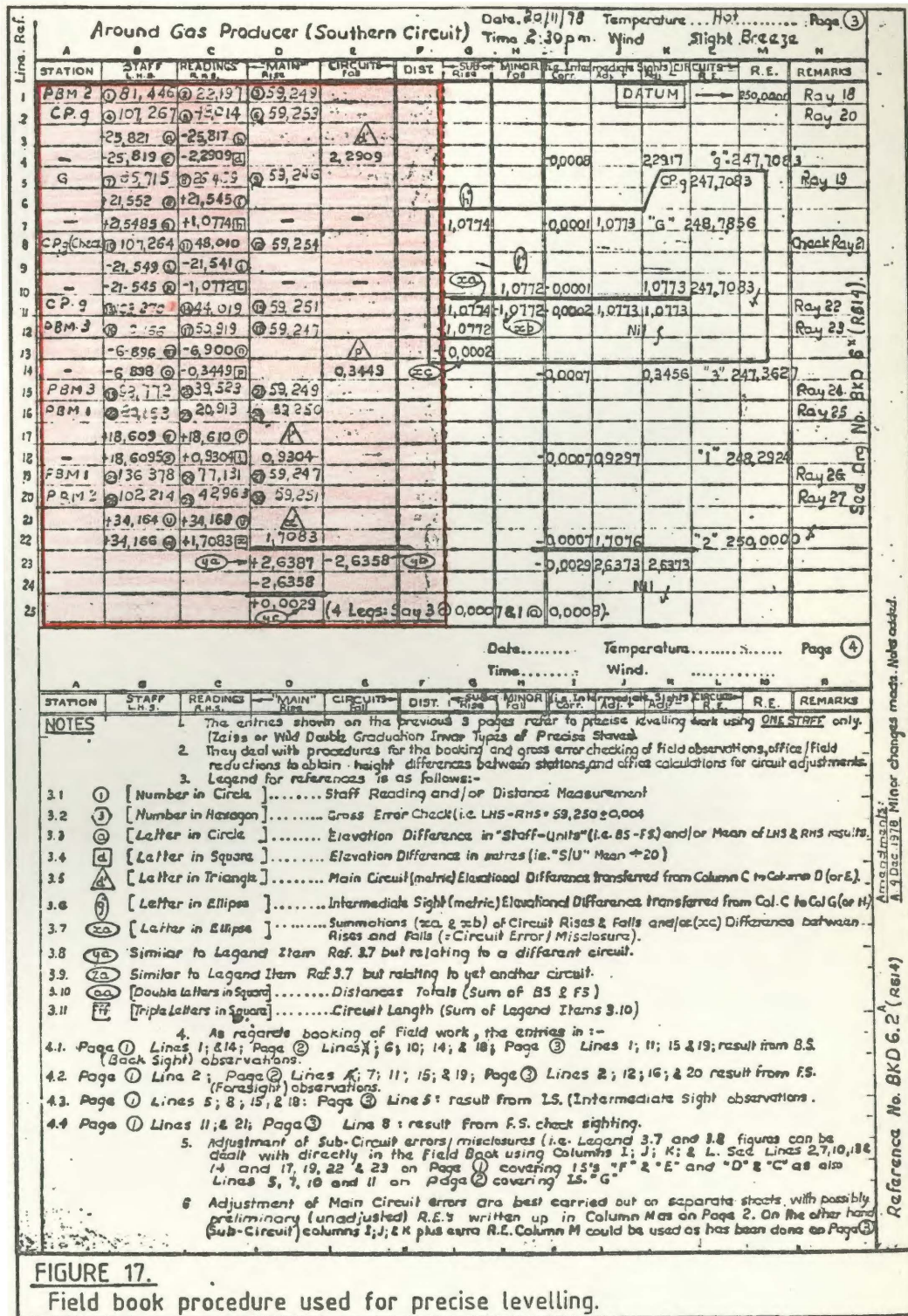


FIGURE 17.
Field book procedure used for precise levelling.

/ Generally ---

Generally, LHS entries represent direct observations made in the field, as shown by light coloured figures. By contrast, the thicker, heavier figures represent "hand" arithmetic carried out almost immediately after field observations have been taken in order to check for gross observational errors.

Entries on the RHS of the field book represent derived figures worked out "by hand" in accordance with simple adjustment principles for the reduction of observations.

3.1.4 ADJUSTMENT OF CIRCUITS

The complexity of a typical system of precise levelling circuits and loops is shown in Figure 18 and illustrates the need for the adjustment of closures between loops and, ultimately, the end of the circuit. The method used for reconciliation is that based on the "least squares conditional adjustment" principle whereby height differences between junction points are weighted inversely proportional to the length of the measured distance. The application of such an adjustment method yields:

/ Figure 18 ---

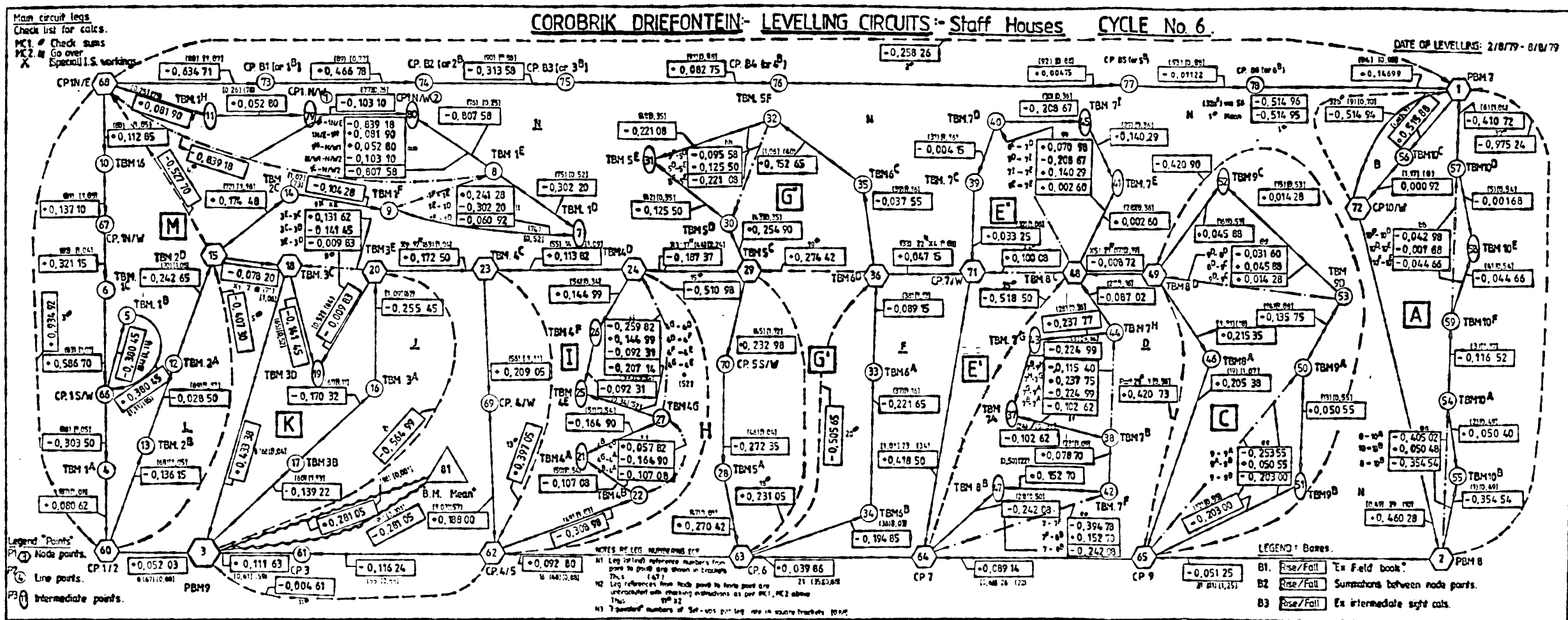


FIGURE 18.

Diagram showing levelling circuit closures for the housing area at Driefontein Brickworks.

- (a) A consistent network of height differences between junction points so that the circuit or loop closure errors are distributed according to the least squares principle.

/ (b) ---

- (b) Adjustment residuals (V), which are used to estimate the precision of the results in terms of the standard deviation for the statistical population ($\hat{\sigma}$). This standard deviation of an observed height difference of unit weight ($\hat{\sigma}_0$) is obtained from the equation below, in which "p" is the weighted, inversely proportioned length between two consecutive measuring points :

$$\hat{\sigma}_0 = \sqrt{\frac{\sum p v^2}{\sum p}}$$

The population standard deviation (σ) of an adjusted height difference (a) is then determined by :

$$\sigma_a = \hat{\sigma}_0 \sqrt{\frac{n - n_c}{n}}$$

In the above formula "n" represents the number of independent weight differences included in the adjustment of the network and "n_c" the total number of conditions.

/ 3.1.5 ---

3.1.5 DISCUSSION ON THE PRECISE LEVELLING METHOD

The choice of instrumentation, field procedures, the methods of observation and the adjustment of circuit closures based on a rigorous least squares principle enables a 95 per cent confidence limit of accuracy to be achieved. In theory, this implies that differences in elevations between points can be measured to within 0,001mm limits. In practice, however, a statistical analysis of measurement readings taken over a period of 3 cycles, shows that significant accuracy is limited to 1,00mm only. The main reasons for the differential between the theoretical and practical limitations are:

- (i) The fact that it is optically impossible to read staff measurements within the theoretical precision limits.
- (ii) That a network circuit may become extremely complicated as shown in Figure 18 and, even with the application of the "least squares" principle, discrepancies in closures must be expected and tolerated.

/ (iii) ---

(iii) That even permanent bench marks of the deep borehole variety apparently suffer minor amounts of movements relative to one another thereby even further complicating the closure adjustments of a circuit.

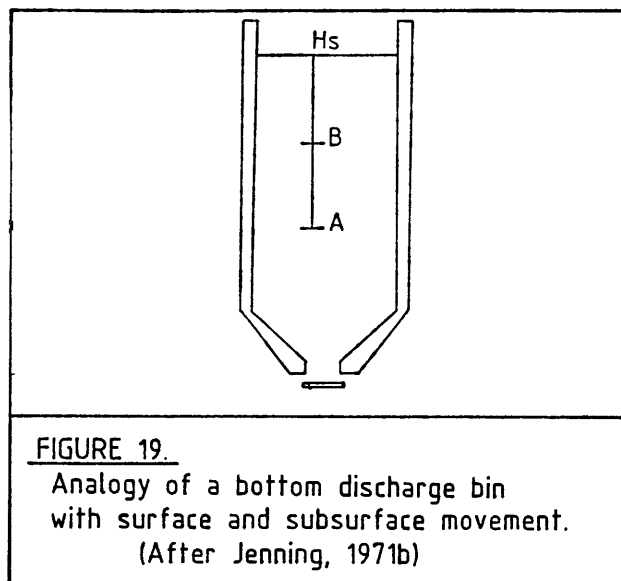
Because of the needs to minimise the above-mentioned problems and to achieve as much accuracy as is humanly possible, it is essential that a highly competent person undertakes the precise levelling field work. In this respect, Driefontein Brickworks is fortunate to have the services of Mr. S.L. Botes who is a self-employed and fully qualified surveyor. Furthermore, it is important that the field work data, calculations and adjustments of circuit closures are independently checked and the services of consultants Collings and Schaerer (Johannesburg) are retained for this purpose.

3.2 MEASUREMENT OF SUBSURFACE MOVEMENTS

The measurement of subsurface movements at Driefontein is undertaken by means of so-called telescopic bench marks (TBM's). The principle involved is basically simple, being based on observations by the late Professor Jennings and other research workers in the Far West Rand. These workers noted that when,

/ under ---

under certain circumstances, surface settlement occurred in areas with dolomitic environments, points situated at depth moved downward at a greater rate than points immediately above them and closer to surface. As Jennings (1971b) pointed out, such behaviour of subsurface points relative to surface could be compared with the behaviour during drawdown in a bottom discharge bin. (Figure 19).



As the material is withdrawn from the bottom of the bin, the point "Hs" will move downwards less than point "B", which, in turn, will move less than point "A". In comparison with the bin analogy, special circumstances apply when the removal of material below surface takes place by means of vertical transportation into a void in the dolomite ; the void

/replacing ---

replacing the discharge point at the bottom of the bin. The behaviour of subsurface points leads to the concept that the observation of elongations of vertical lines such as "Hs:A", "Hs:B" or "B:A" can indicate a withdrawal process even though the discharge point may be situated at a depth well below either points Hs, B or A.

3.2.1. TELESCOPIC BENCH MARKS

The telescopic bench mark (TBM) is a device designed to act as a vertical strain indicator for the detection of subsurface void development and to monitor its movement. A number of types of TBM are available; the main ones being the heavy pipe or Jennings TBM, the "piano wire" variety and the Sondex type.

At Driefontein, only Jennings type TBM's have been installed. Basically, the device consists of a rod and numerous pipes of different diameter which are grouted into concrete blocks at selected levels in a borehole. Each rod or pipe is sleeved, telescoped into the pipe established at the next level above, then extended up to surface. At surface, as shown in Figure 20, the pipes and rods pass through a 1.4m long stem-pipe grouted into a concrete block thereby allowing measurements to be made of the changes between the surface and the various rods and pipes. It should be noticed in Figure 20 that building sand is packed between the system of telescoped rods and pipes and the walls of

/the ---

the borehole so as to enable them relatively free movement.

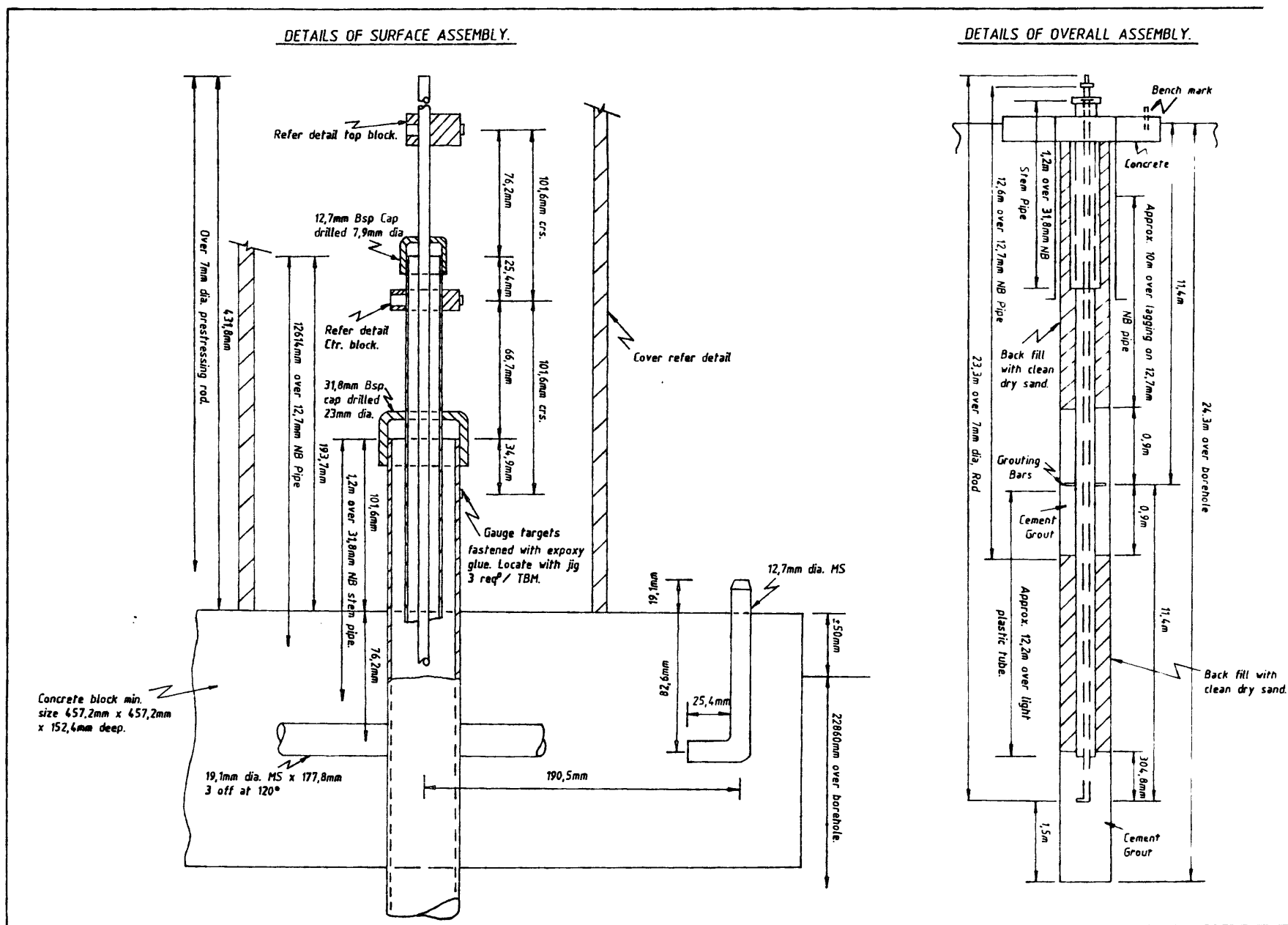


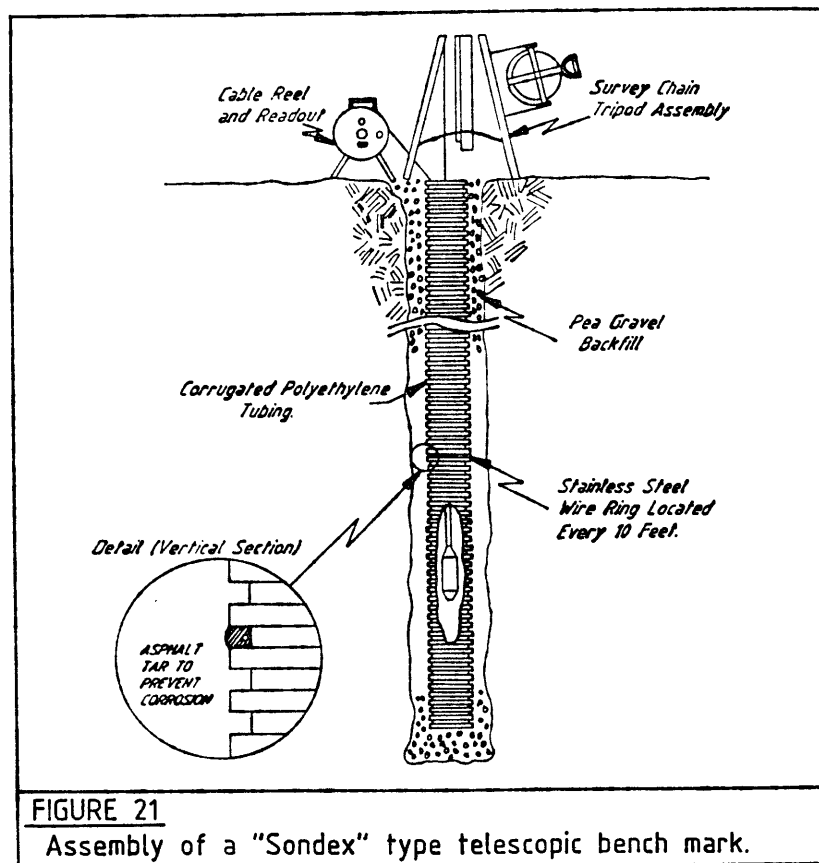
FIGURE 20.
Assembly details of a Jennings type telescopic bench mark.
(Not to Scale.)

The "piano wire" type TBM operates on the same basic principle as the Jennings variety except that steel wire instead of rods and piping is anchored to the concrete blocks in the borehole. The steel wire is tensioned on the top by a spring and a variety of

/arrangements ---

arrangements can be adopted for measuring changes in the lengths of the line relative to surface.

The Sondex TBM comprises a flexible plastic casing with metal rings fixed at specified intervals, as shown in Figure 21.



The measuring apparatus comprises a probe, electrical cable and a steel tape. Electronic circuitry within the probe detects the location of the metal rings by induction principle. A readout meter is peaked whenever the probe is centred on the cross-axis of

/ a ---

a detective ring. The depth of each ring is measured using a steel tape attached to the probe.

3.2.2. THEORY OF TELESCOPIC BENCH MARK MEASUREMENTS

The use of telescopic bench marks entails taking accurate measurements at their collar elevations as well as the amount of movements which have occurred between their various subsurface markers relative to each other and also to the surface elevations. Referring back to the analogy of a bottom discharge bin (Figure 19), three different measuring points were considered; namely "Hs", "B" and "A". Obviously, the collar elevations (HS) of TBM'S are the main objective of the precise levelling procedures described in the preceding section of this chapter. The subsurface markers "A" and "B" are normally anchored at depths where geological conditions are such that they will amplify any ground instability. In the Driefontein area it has become normal practice to locate the "B" marker in Karoo sedimentary rocks at a depth of 12m from surface and the "A" marker 22m from surface where compactable manganiferous wad is frequently present. The theory of TBM behaviour is founded on the principle that changes in the lengths between points "Hs", "A" and "B" provide important

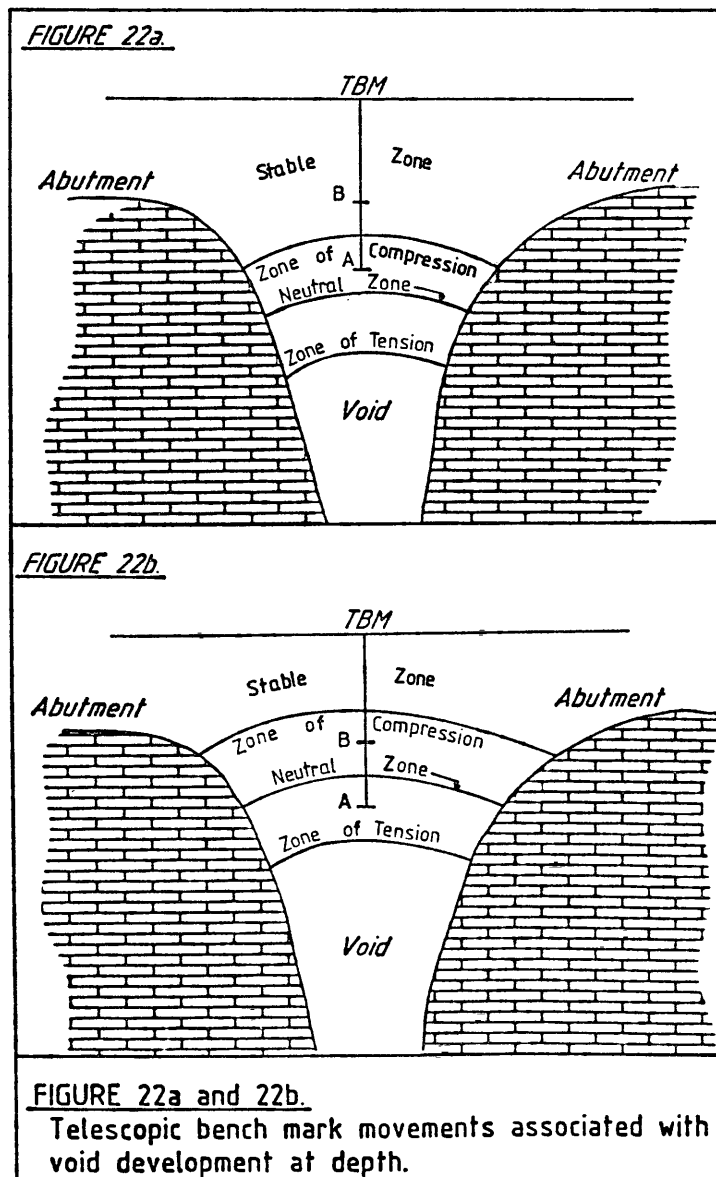
/information

information on the development and increasing size of a void being developed at depth. The analogy of a bottom discharge bin, as described by Jennings (1971b) does, however, require refinement when applied to void development because of the stress patterns occurring in the overlying subsoil.

Prior to the development of a void, the downward and upward vertical stresses in the subsoil will be equal and no movement will occur at any of the subsurface markers of a TBM. With the development of a void, however, the vertical upward stresses in the subsoil will diminish as the void is approached whilst the downward vertical stresses are balanced by shear stresses. Ultimately, an arch-shaped "roof" will be formed in the subsoil over the void as the downward vertical stress is transferred laterally to the abutments. From conventional arch theory, it becomes apparent that two distinct stress behaviour zones may develop in the subsoil above a void, the "thicknesses" or "depths" of which will be dependant upon the shape of the arch, the distance between the arch abutments and the properties of the subsoil material. Thus, some distance above the void there will exist a zone of tangential compression within which downward vertical stress will be supported by

/ the ---

the shear strength developed as a result of high tangential normal stresses. Within the tensile zone and also within the zone of low compressive stress, the cohesion ability of the soil arch may be sufficient to span the void and either a zone of equilibrium will exist or gradual movement directly above the void may occur. Figures 22a and 22b illustrate the behaviour of TBM subsurface markers when a void develops in a homogeneous soil between symmetrical abutments.



/ In

In Figure 22a, subsurface marker B, being located in the stable zone, will not display any movement. Subsurface marker A, however, falls within the compression zone and gradual downward or "negative" movement may occur resulting in an extension of the measurable distance between points B and A. The amount of this negative extension will increase the closer the void gets to the subsurface marker A.

The arch forming the roof of the void cannot exist indefinitely and it must ultimately collapse when the subsoil within the tension zone loses its cohesion for such reasons as a change of moisture or movement beyond the cohesive ability of the soil. This collapse need not necessarily be instantaneous but may occur gradually over several days or even weeks, and will result in a new arch being developed. Figure 22b illustrates the conditions which will be recorded by TBM subsurface markers during the collapse of an arched roof of a void, these being as follows :

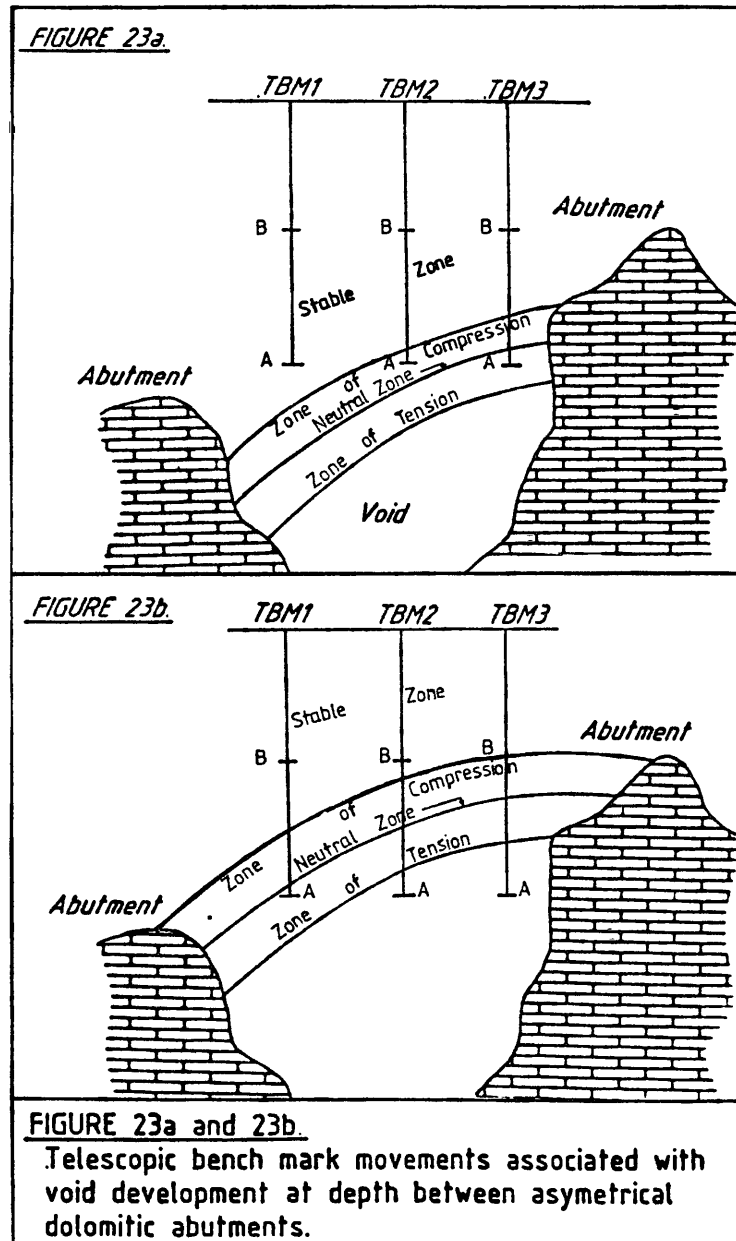
- (i) A collapse occurred in the subsoil at the intrados of the arch causing the arch to migrate upwards to a position where the subsoil material had cohesive strength appropriate to the span between the abutments. It can be seen that the subsurface
/marker ---

marker B is now positioned into the zone of compression and will begin showing negative movements as it is subjected to increased lateral and downward compressive stresses.

- (ii) Subsurface marker A is situated below the neutral zone in subsoil material which is no longer subjected to compressive stresses but which is dilating and in the process of collapsing into the void. Subsurface marker A will, therefore, show large amounts of negative movement with increasing acceleration until it ultimately falls into the void.

The TBM behaviour described above pre-supposes an homogenous soil and small variations in the geological profile. In practice, however, both lateral and vertical subsoil inhomogenities may be present and the abutment profiles may be irregular. Consequently, the behaviour of TBM subsurface markers become more complex. Figures 23a and 23b illustrate a condition where the subsoils are still homogeneous but where the abutments are asymmetrical and the movement behaviour in each TBM will be as follows :

/ Figure 23 ---



- (i) In Figure 23a, both the "A" and "B" subsurface markers of TBM 1, as well as the "B" subsurface markers of TBM 2 and TBM 3 will be situated in the stable zone and will not show any / movement ---

movement. Subsurface marker A in TBM 2 will, however, begin moving negatively because it is situated in the zone of compression. Subsurface marker "A" in TBM 3 is situated in the zone of tension and will display substantial downward movements as the subsoil is dilating and in the process of collapsing into the void.

- (ii) In Figure 23b, where a newly formed arch has been established at a higher elevation, the behaviour of the various telescopic bench marks will be different. Thus, in TBM 1, the "B" subsurface marker will still be in the zone of stability and show no movement but subsurface marker "A" will now be moving downward since it is situated in the zone of tension. In TBM 2, although subsurface marker B is still situated in the stable zone, subsurface marker A will have vanished into the void. As far as TBM 3 is concerned, subsurface marker B will have just found itself in the zone of compression so that it may show very small amounts of negative movement

/ but ---

but its "A" subsurface marker will also have disappeared.

Actual TBM readings in the Driefontein area, where both irregularly shaped abutments and inhomogeneous subsoils exist, indicate that upward or "positive" movements may also occur. These positive movements may be attributed to :

- (a) localised zones of compression or tension occurring in an inhomogeneous soil as it adjusts to progressive arch collapse. It is noteworthy that a TBM subsurface marker situated immediately above an arch may, in some circumstances, show positive movement immediately before collapse occurs. Possibly this movement can be attributed to a sudden release of downward vertical and shear stresses when the zone of tension moves upwards beyond the position of the subsurface marker.
- (b) the influence of subsurface water on TBM measuring points; a subject to be discussed in some detail later in this dissertation.

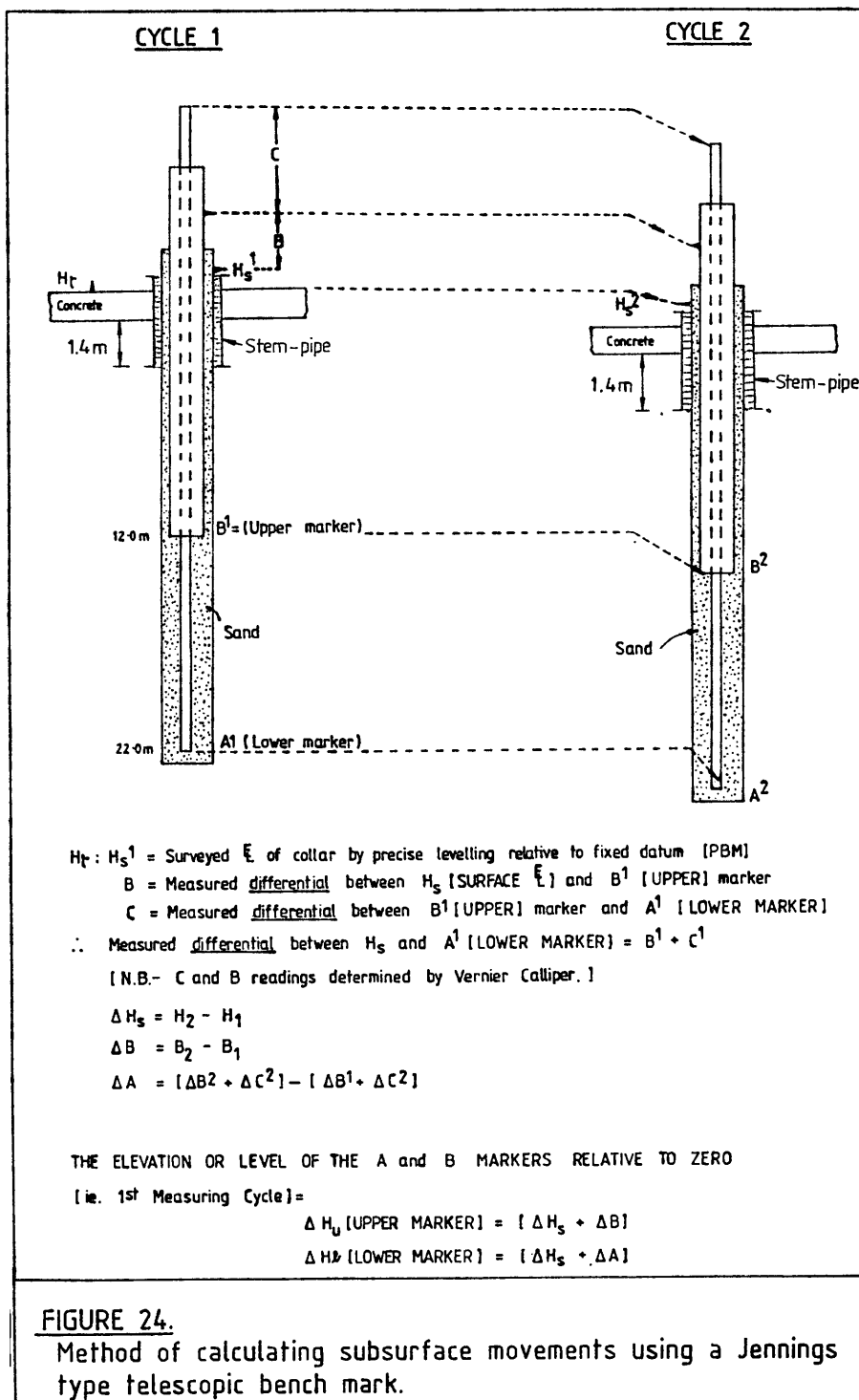
/ In ---

In conclusion, it must be stated that the development of a void at depth need not necessarily be reflected by subsidence of the ground surface. Theoretically, when the zone of compression intersects the surface, it should result in minor, but significant subsidence. In practice, however, such negative surface movements are frequently masked by influences to be later described.

3.2.3 METHODOLOGY FOR CALCULATING SUBSURFACE MOVEMENTS

The method of calculating subsurface movements is easily explained by reference to Figure 24 which is a diagrammatic representation of a Jennings type TBM. The stem pipe, which extends some 1,4m below the TBM collar, is fixed with a concrete slab. Set in the concrete slab is a target H_t , which is used for surveying the elevation of the TBM's collar relative to a permanent bench mark (PBM). Another target (H_s) is welded to the stem pipe at a constant height relative to the target set in the concrete slab. Thus, the H_s reading can be equated to the H_t reading by adding the constant between the two targets to obtain any difference in elevation between the TBM and a permanent bench mark. A smaller diameter pipe is lowered through the stem-pipe to a depth of 12m below surface where it is anchored into a block of concrete to form the so-called "B" marker. A target

/ Figure 24 ---



/ is ---

is also welded on to the outside of this smaller diameter pipe. Any movement of the "B" marker relative to surface can be detected by measuring with a vernier calliper, to a minimum accuracy of 0.1mm, the distance between the Hs target and the target set on the side of the small diameter pipe.

A length of reinforcing steel rod is lowered through the small diameter pipe to a depth of 22m where it is anchored into a block of concrete to constitute the so called "A" marker. A target is welded at the top of the steel rod. By measuring again with a vernier calliper the vertical distance between the target on the small diameter pipe and the steel rod, that is "C" measurement, the amount of relative movement between the B marker set at 12m and the A marker at 22m below surface, can be ascertained. To determine whether or not there has been any movement at the "A" marker relative to surface, can be ascertained by adding the A reading to the B reading. A summary of the significance of the various readings is given below :

Hs = Surface elevation at the TBM
collar relative to a fixed
datum (PBM) as ascertained
by precise levelling methods.

/ B ---

B = Distance between surface (Hs) and the upper subsurface marker (B) as measured with a vernier calliper.

C = Distance between the upper subsurface marker (B) and the lower subsurface marker (A) as measured with a vernier calliper.

B + C = Calculated distance between the surface elevation (Hs) and the lower subsurface marker (A).

Obviously, to evaluate whether the ground conditions in the vicinity of any specific telescopic bench mark are stable or deteriorating, the measurements taken must be evaluated relative to time. Thus, both surface and subsurface measurements are taken on a time cycle basis; the interval between each cycle at Driefontein being, on average, some 43 days. At Driefontein, although the monitoring of surface and subsurface movements were first commenced by the late Professor Jennings in early 1971, the movements evaluated in this dissertation are "zeroed" as from December 1979 for the following reasons :

- (i) Between 1973 and 1979, the Driefontein Brickworks fell under a management which
/ considered ---

considered precise surface levelling and subsurface measurements as superfluous. It was only in late 1979, when a merger of Primrose Holdings (Brickor) and Tongaat Corogroup (Corobrik) was finalised, that the importance of monitoring ground instability to protect human and capital assets, as advocated by the late Professor Jennings, was fully realised.

- (ii) Continuity of measurements as well as the refining of measurement techniques commenced as from December, 1979.

The format for recording movements is shown in Figure 25. It will be realised that changes in surface elevations as well as movements of the A, B and C readings are entered for each measuring cycle. The differences of the various movements between the first and subsequent measuring cycles is expressed by deducting the last recorded reading from the first entry thus :

$$\Delta H_s = H_2 - H_1$$

$$\Delta B = B_2 - B_1$$

$$\Delta A = (B_2 + C_2) - (B_1 + C_1)$$

/ In ---

In the above equations, H_2 , B_2 and $(B_2 + C_2)$ denote the latest measurement readings and H_1 , B_1 and $(B_1 + C_1)$ the readings of the very first measuring cycle.

COROBRIK DRIEFONTEIN
T.B.M. RECORD

PAGE NO. ... OF THIS T.B.M.

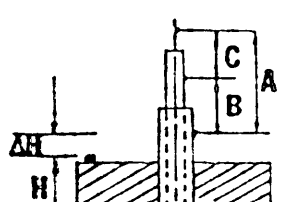
LOCATION: -----

TBM NO: -----

DEPTHS: L. -----

U. -----

POSITION OF T.B.M.



PROFILE

DATE									
DAY NO									
C									
Δ C									
B									
Δ B									
Δ A									
H_s (R.L.)									
Δ H_s									
$\Delta H_s = \Delta A + \Delta H_1$									
$\Delta H_s = \Delta B + \Delta H_1$									

ΔH_s = CHANGE IN LEVEL OF SURFACE
 ΔH_L = CHANGE IN LEVEL OF LOWER T.B.M. POINT
 ΔH_U = CHANGE IN LEVEL OF UPPER T.B.M. POINT

ALL CHANGES RECORDED +VE IF INCREASE IS SHOWN
 EG. ΔC ; ΔB ; $\Delta A = \Delta B + \Delta C$; ΔH = RISE IN PEG LEVEL

FIGURE 25.

Format used at Driefontein Brickworks for recording surface and subsurface movements.

/ Further ---

Further reference to the format in Figure 25 will show that besides the amount of movement of the B and A markers, their changes of elevation relative to the ground surface for each measuring cycle are also recorded. The equations to obtain the subsurface elevation changes are a simple arithmetic progression of the ΔB and ΔA measurement readings as shown below :

$$\Delta H_u \text{ (elevation change of the upper subsurface marker)} = \Delta H_s + \Delta B$$

$$\Delta H_\ell \text{ (elevation change of the lower subsurface marker)} = \Delta H_s + \Delta A$$

As will be described in the succeeding section, the ΔH_u and ΔH_ℓ readings are of prime importance for accurate evaluations to be made of prevailing ground conditions. Consequently, as is the case with precise surface levelling, the measurement of telescopic bench mark movements must be undertaken by a competent person such as the previously mentioned Mr. Botes of Driefontein Brickworks.

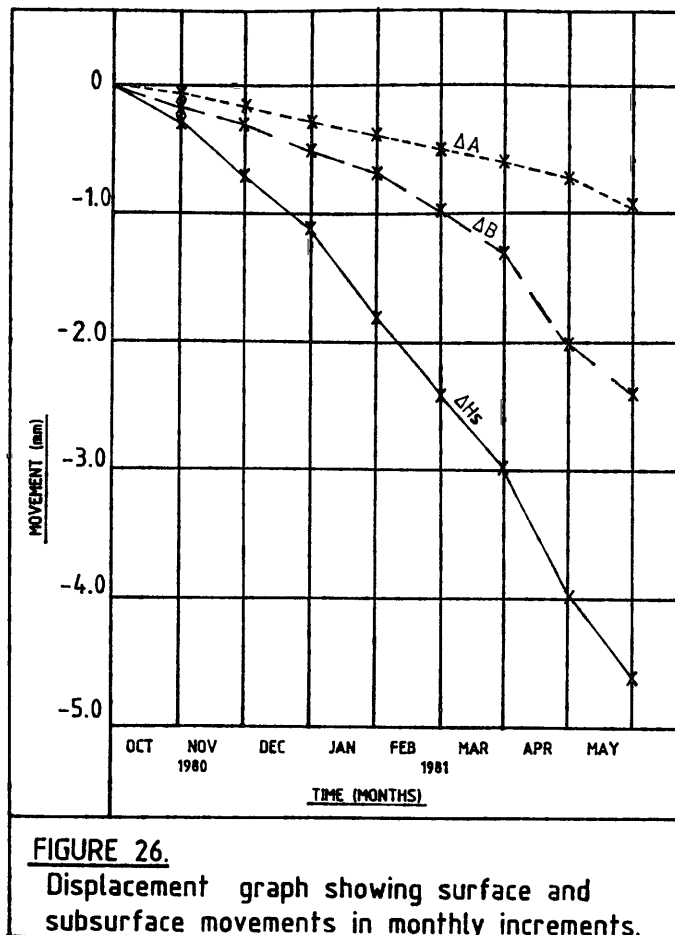
3.3 INTERPRETATION OF SURFACE AND SUBSURFACE MOVEMENTS

The movements between surface and subsurface markers during any specific measuring cycle give valuable information in respect of whether an area is undergoing either compaction or a condition of positive strain. Prior to January, 1979, the late Professor Jennings made extensive use of displacement graphs to interpret telescopic bench mark behaviour. Subsequent to the above-mentioned date, however, the writer introduced isopleth plans on which the amounts of surface and subsurface movements, recorded at any specific measuring cycle, are plotted.

3.3.1 DISPLACEMENT GRAPHS

Figure 26 illustrates how an interpretation of subsurface conditions may be made from a time/movement or "displacement" graph. It can be seen that accumulated surface movements (ΔH_s) over a period of eight months from October 1980 to May 1981 amounted to $-4,60\text{mm}$ whilst ΔB and ΔA measurements over the same time span were $-2,40\text{mm}$ and $-1,00\text{mm}$ respectively. It is apparent that if the distances between the surface and subsurface markers were regarded as a "layer", then there has been a "thinning" between $\Delta H_s:\Delta B$ by the amount of $2,20\text{mm}$ (ie. ΔH_s less $\Delta B = -4,50\text{mm}$ less $-2,40\text{mm}$).

/ Similarly ---



Similarly, between ΔH_s and ΔA the "thinning" is 3,60mm (ie. ΔH_s less $\Delta A = -4,60\text{mm}$ less $-1,00\text{mm}$) whilst between ΔB and ΔA it amounts to 1,4mm (ie. ΔB less $\Delta A = -2,40\text{mm}$ less $-1,00\text{mm}$). Such a "thinning" of the "layers" shows that the surface is subsiding at a greater rate than either the B or A markers and that the B marker, in turn, is subsiding by a greater amount than the A marker.

/ In ---

In other words, compaction or a doline type of settlement is occurring in the vicinity of the telescopic bench mark. Conversely, in Figure 27

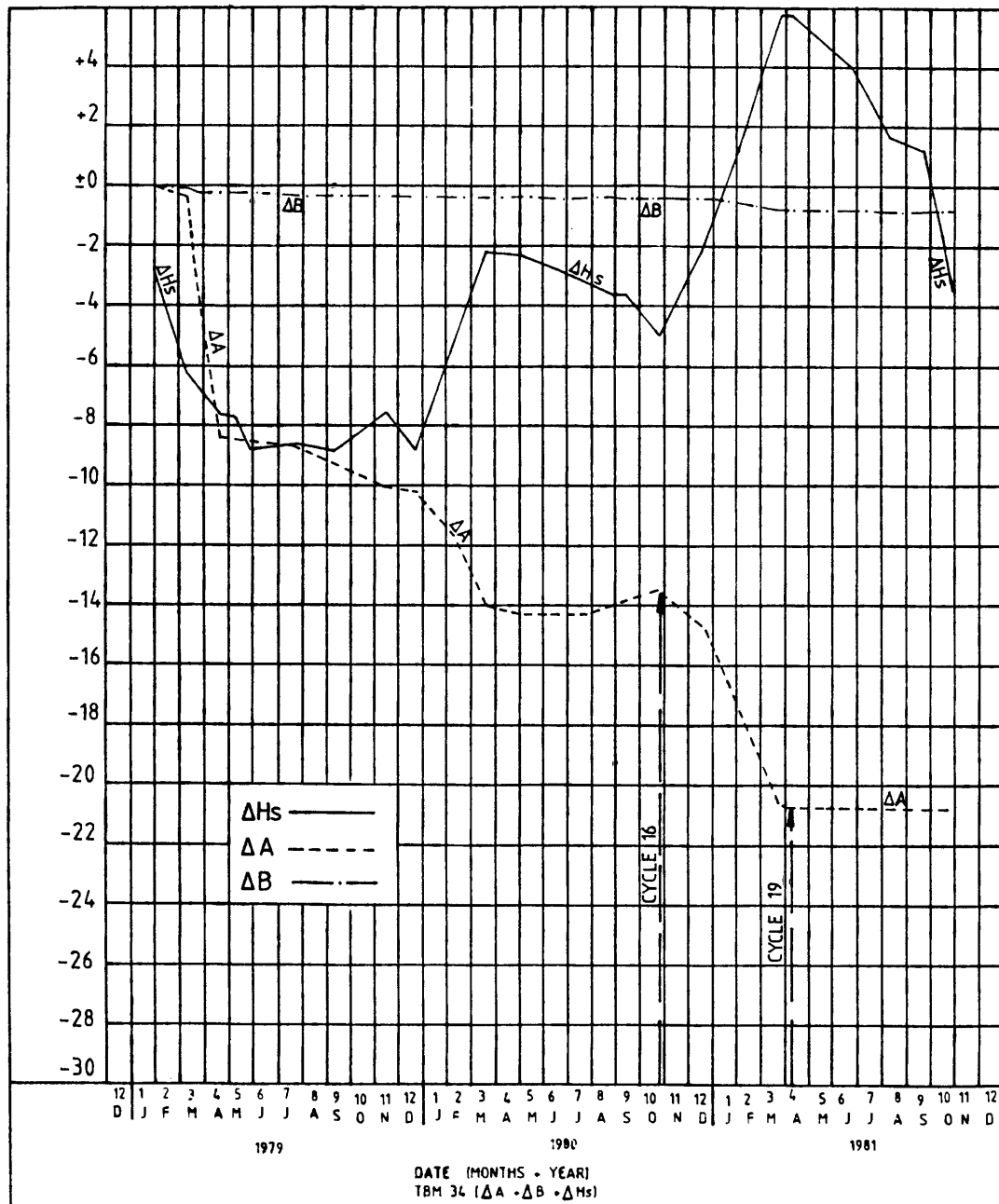


FIGURE 27.
Movements of the surface (ΔH_s), upper subsurface (ΔB) and lower sub-surface (ΔA) markers in TBM 34, Compound area, Driefontein Brickworks.

/ actual ---

actual movements of the surface, upper and lower subsurface markers in TBM No. 34 from December 1979 to July 1981, that is measurement cycles 1 to 21 ($\Delta 21:1$) are plotted. From October 1980, to May 1981, that is between measuring cycles Nos. 16 and 19 ($\Delta 16:1$ and $\Delta 19:1$), radical movements occurred as tabulated below:

CYCLE NO	MEASURED MOVEMENTS (mm)						RELATIVE MOVEMENTS (mm)					
	ΔH_s		ΔB		ΔA		$\Delta H_s : \Delta B$		$\Delta H_s : \Delta A$		$\Delta B : \Delta A$	
	THICKENING	THINNING	THICKENING	THINNING	THICKENING	THINNING	THICKENING	THINNING	THICKENING	THINNING	THICKENING	THINNING
$\Delta 16:1$	- 5,05	-	- 0,53	-	- 13,55	-	4,52	8,50	-	13,02	-	-
$\Delta 19:1$	+ 5,84	-	- 0,70	-	- 20,79	6,54	-	26,63	-	20,09	-	-
$\Delta 19:16$	THICK.	THIN.	THICK.	THIN.	THICK.	THIN.	THICKENING	THINNING	THICKENING	THINNING	THICKENING	THINNING
	10,89	-	-	0,17	7,24	-	11,06	-	18,13	-	7,07	-

Movements of surface (ΔH_s), as well as upper (ΔB) and lower (ΔA) subsurface markers in TBM 34.

Comparing the relative movements between measuring cycles Nos. 16 ($\Delta 16:1$) and 19 ($\Delta 19:1$) it can be seen that a progressive "thickening" of the various layers has occurred. The most significant thickening or "negative extension" applies between the surface (ΔH_s) and the lower subsurface marker (ΔA). Thus, it would be logical to conclude that TBM No. 34 is displaying conditions of dilation and that a potentially dangerous condition, such as progressive arch collapse over a void, is occurring at a depth below the subsurface marker.

/ The ---

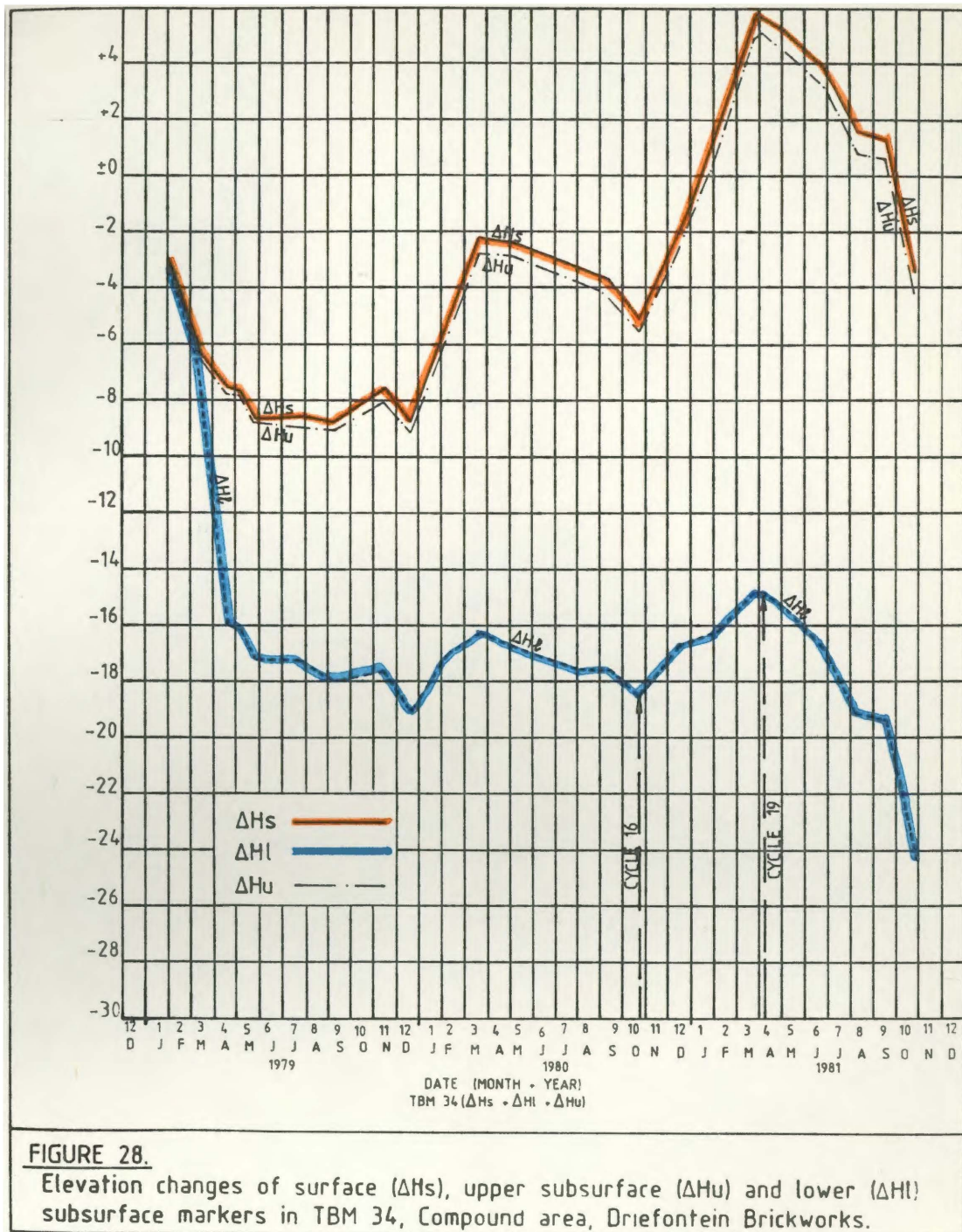
The ΔH_s , ΔB and ΔA measurements, on their own, can however, exaggerate prevailing conditions. Rather it is only by monitoring the changes of elevations attained by the subsurface markers relative to ground surface that a realistic geotechnical interpretation can be obtained.

In Figure 28 the same subsurface movements of TBM No. 34 as used in Figure 27 are re-plotted as ΔH_u and ΔH_l . The respective elevation changes are as follows :

TABLE 5.			
CYCLE NO.	ΔH_s	ΔH_u ($\Delta H_s + \Delta B$)	$\Delta H_l +$ ($\Delta H_s + \Delta A$)
$\Delta 16 : 1$	-5,05	-5,58	-18,60
$\Delta 19 : 1$	+5,84	+5,14	-14,95
$\Delta 19 : 16$	+10,89	+10,72	+3,65
Elevation changes of surface (ΔH_s), upper (ΔH_u) and the lower (ΔH_l) subsurface markers in TBM34.			

As can be seen, ΔH_s , ΔH_u and ΔH_l measurements all indicate corresponding movements rather than the alarming differential negative extensions between the ΔB and ΔA readings of Table 4.

/ Figure 28 ---



The significance of the ΔH_u and ΔH_l readings and more meaningful methods of interpreting them will be discussed in Part 5 of this dissertation.

3.3.2 ISOPLETH MAPS

Whereas displacement graphs can show the ΔH_s , ΔH_u and ΔH_ℓ relationships in individual telescopic bench marks, isopleth plans are ideal for indicating the ground conditions prevailing over a whole area. A separate plan is produced for the ΔH_s , the ΔH_u and the ΔH_ℓ measurements of every telescopic bench mark in the locality at the end of each measuring cycle. Ideally, such maps for successive cycles should be drawn up on transparent paper so that one can be overlain on the other. In this manner, an interpretation can be readily made of the ΔH_s , ΔH_u and ΔH_ℓ measurements. Typical examples of isopleth plans are given in Appendices 3 a, b, c and 4 a, b, c, d in which the isopleths are drawn at 1,0mm intervals. Positive and negative isopleths are coloured red and green respectively.

In Appendices 3 a, b and c, the excessive negative movements of the surface (ΔH_s), relative to the sub-surface markers (ΔH_u and ΔH_ℓ) clearly indicate the development of a doline immediately north of House No.10 with small localised subsidences immediately east of House No.9 and south of House No.7. The positive movements epicentered immediately south of House No.5, are inflated because the surface measuring point CP5S is being lifted by tree roots.

/ Appendices

Appendices 4 a, b, c and d show the unstable conditions associated with a "palaeo-sinkhole" situated immediately northwest of the Compound. The negative isopleths define the extent of instability associated with subsurface movement occurring at a depth in excess of 22m from surface. It is interesting to compare the configuration of the $\Delta H\theta$ isopleths (Appendix 4a) with contours showing the thickness of Pleistocene to Recent "hillwash" material (Appendix 4d).

As can be seen, TBM 34^A is situated in the 3,95m diameter "throat" of the palaeo-sinkhole, having only intersected the interface between "hillwash" and Karoo-aged materials at a depth of 39,50m, as well as being in the epicentre of ground instability. Unfortunately, because subsurface water in the area has saturated the hillwash, it is doubtful whether the subsurface bench marks in TBM 34^A were successfully grouted into position. Consequently, the movements recorded by TBM 34, as shown in Figure 27, are regarded as representing the ground stability conditions existing in the epicentre of the palaeo-sinkhole.

Possibly the greatest value of isopleth maps is that they clearly indicate the epicentres of unstable areas and, consequently, the movement measurements of specific telescopic bench marks which should be carefully

/scrutinized ---

scrutinized. This scrutiny should not only include the preparation of displacement graphs but also other methods of interpretation which will be described later in Part 5 when discussing the prediction of ground instability.

- - - 0o0 - - -

PART 4

4. UNSTABLE GROUND CONDITIONS IN KAROO OUTLIERS

4.1 FACTORS INFLUENCING GROUND INSTABILITY

Field and research work at the Driefontein outlier, as well as in other areas with similar geological and hydrological environments, confirms existing theories and also enables new proposals to be made as to the mechanisms influencing ground instability. It can be shown that past geological events as well as current subsurface water behaviour can assert considerable influence on the instability of Karoo outliers. Furthermore, analyses of surface and subsurface movements over a period exceeding three years has refined the techniques for interpreting measurements. Thus, it is postulated that once a sufficiently long historical data bank of measurements is available, it becomes possible to predict with reasonable credibility when an area will become geotechnically untenable.

4.1.1 GEOLOGICAL STRUCTURE

The information derived from some 384 boreholes at Driefontein as well as from the results of numerous gravimetric surveys, makes it possible to delineate

/ the ---

the trends of slots which have developed along lines of preferential solution as shown in Appendix 2. It can be seen that the slots follow directions of either 10° to 20° west of north; 5° to 10° east of north or 20° to 40° east of north, thereby confirming the findings of Papendorf (1971). Even so, the configuration of each slot is intricate and tortuous as shown by Appendices 5 and 6 for the Driefontein and Henley/Lawley areas respectively.

Because of the intensity of drilling undertaken within the environs of the Driefontein factory, considerable information is available of typical slot profiles. Thus, as can be seen from Appendix 5, there are five slots, namely Slots A, B, C, E and F spaced between 15m and 74m apart. The configuration of the slots is defined by contours showing the depth of chert residue and dolomite from surface. Since the phreatic level of the ground water prior to dewatering was situated some 58m from surface, the chert/dolomite configuration above a depth of 60m from surface is shaded yellow. For contrast, those parts of the slots extending below a depth of 60m below surface, are left unshaded. It is interesting to note that in the area between the easternmost extremity of the New Factory building and the Coal Crane Gantry, slots B and C transect one another. Furthermore, between the New Factory building and the Sub-Station,

/ an ---

an easterly trending "spur" branches off Slot A to connect up with intersection point between Slots E and C. According to Jennings (1971 b), areas underlain by intersecting slots should be regarded as highly dangerous as far as sinkhole development is concerned. The writer will, however, elaborate more fully on the danger potential presented by various geological profiles later in this dissertation.

Geological profiles across Slots A, B, C and D are shown in Appendix 7. The most striking feature of these profiles is the intensity of weathering suffered by the Malmani dolomite. Thus, pinnacles rising to within 20m or less of surface and near vertical slots plunging to depths in excess of 100m are characteristic of the dolomite configuration. Relatively gentle, undulating plateaux of dolomite occur, however, in the area underlying the westernmost portion of the Clay Storage building, in the vicinity of the Dolomite Store, and also between Slots D and E as well as Slots E and F in the areas north-northeast and northeast respectively of the Down-draught Making Section. Residuum, in the form of brecciated chert with varying amounts of manganiferous wad, may attain thicknesses of up to 14m on top of plateaux, 9m at the crest of pinnacles but thinning off rapidly to less than 2,5m down the flanks of the slots. In some instances,
/ particularly ---

particularly where the span of the slot is very narrow, it becomes choked with residual rubble comprising chert, ferruginous clay and manganiferous wad. Theoretically, areas underlain by plateaux of dolomite existing above the phreatic level of the original water table, should constitute geotechnically stable ground. Again, however, the writer would like to reserve comment on this assumption until later.

Obviously, such subsurface configurations as those shown in Appendix 5, must be prone to varying degrees of instability if subjected to dewatering and subsequent abuses such as the uncontrolled flow of surface water. However, detailed investigation at Driefontein as well as the Rietvlei and Henley/Lawley outliers, where the highly eroded Malmani dolomite subsurface is infilled with and overlain by Karoo and Pleistocene materials, indicates that :

- (a) Post-Transvaal erosion of the dolomite occurred along lines of pre-existing weaknesses.
- (b) The materials infilling the slots formed along the lines of preferential solution, may suffer compaction over a time span ranging from when the Karoo sedimentary rocks were deposited to the present day.

/ From ---

From the above observations, it can be inferred that the majority of Karoo outliers occupy areas of instability in terms of both geological history and at the present time. To substantiate this statement, it is necessary to describe the rejuvenation of pre-Transvaal structural features both prior and subsequent to the deposition of the Karoo sedimentary rocks.

4.1.1.1 Re-activation of pre-Transvaal Tectonic Features

Further reference to Figure 9 shows that the Far West Rand is transected by a number of major, north-south trending faults such as the Panvlakte, Witpoortjie and Bank faults. De Kock (1964) recognised that some of these pre-Transvaal faults have "... manifested themselves in post-Transvaal times". A noteworthy example of such reactivation is displayed by the Bank Fault which, as can be seen in Figure 14, displaced strata of the Witwatersrand Supergroup for a horizontal distance of about 8 kilometres. It is apparent, however, that subsequent movements along this same plane of structural weakness have resulted in the dislocation of Malmani Subgroup rocks as well as the Timeball Hill Quartzites forming the Gatsrand Range.

/ 4.1.1.2 ---

4.1.1.2 Post-Karoo Structural Features

There is no evidence to support the possibility that renewed activity occurred in post-Karoo times along already existing faults and fracture planes. Even so, there can be little doubt that the slots and depressions eroded out of the Malmani dolomite along such planes have continued to constitute zones of ground instability. Thus, the Karoo sediments infilling these slots and depressions can be seen, quite frequently, to be distorted and flexured into typical slump structures because of up to several meters of subsurface settlement. It is considered that these settlements are attributable to the compaction of subsurface materials, such as manganiferous wad, rather than renewed "microtectonic" activity as suggested by Wiid (1981). Characteristically, the axes of the slump structures in the Karoo sedimentary rocks appear, at first glance, to be haphazard in their orientation. However, a more careful study of the Rietvlei, Henley/Lawley and Driefontein outliers, the localities of which are indicated in Figure 29, shows that these fold axes are generally aligned parallel to the pre-Karoo planes of structural weakness in the underlying dolomite.

/ Figure 29 ---

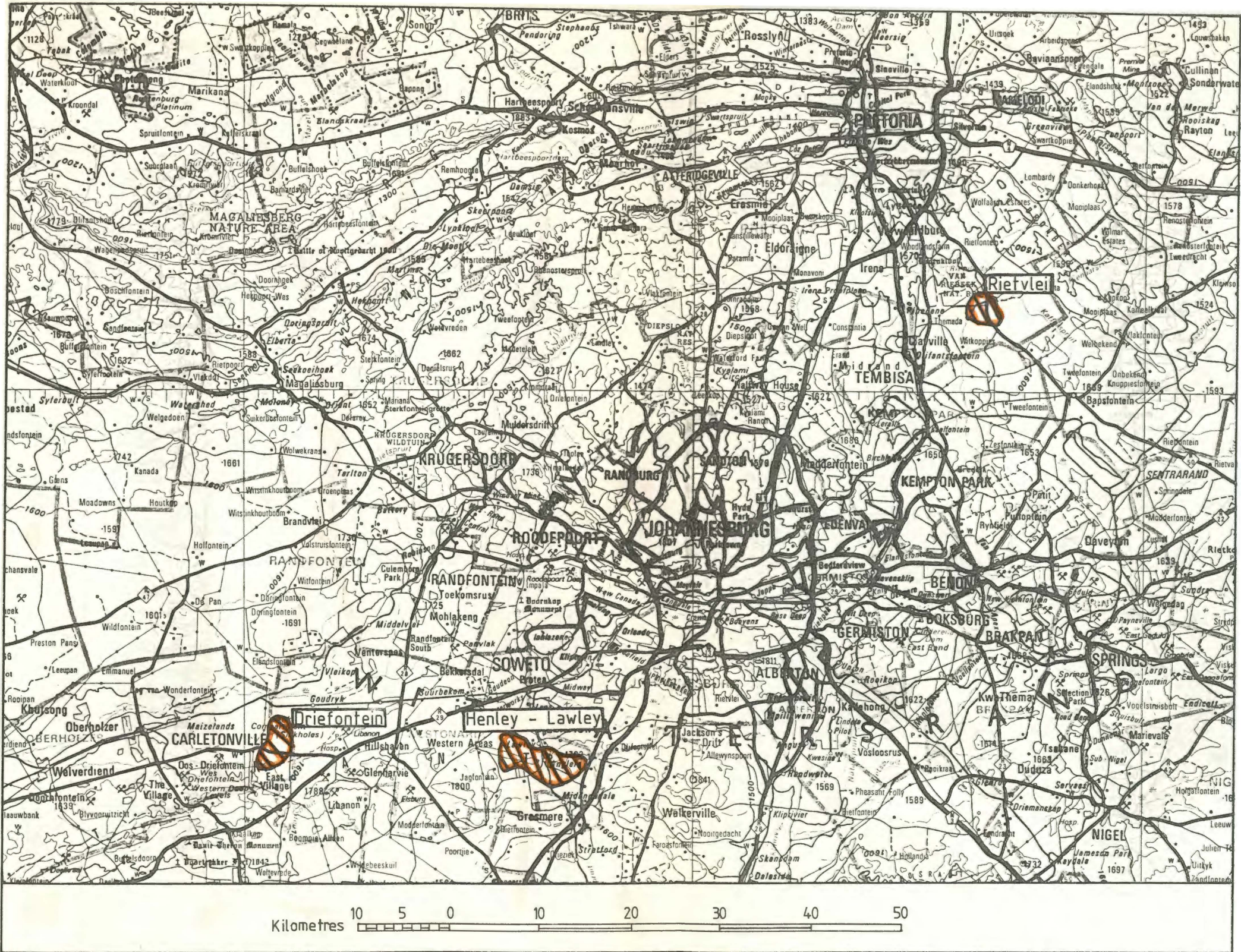


FIGURE 29.
Geographical situations of the Driefontein, Henley/Lawley and Rietvlei outliers.

/ The Rietvlei area ---

The Rietvlei Area

Information derived from some 107 boreholes drilled in the Rietvlei area shows the stratigraphical sequence of the Karoo sedimentary rocks, from top to bottom, to be as follows :

<u>Description</u>	<u>Thickness (m)</u>
Medium to coarse grained grit with thin, silty mudstone intercalations (YG)	12,0m +
Yellow, slightly sandy, micaceous mudstones and shales (YS)	20,0m
Off-white silstones, hard grit bands with thin intercalations of yellow mudstone and brown chocolate coloured clay. (TZ)	9,0m
Shaley sandstone comprising intercalated thin bands of fine grained buff sandstones and white, cream and purple coloured shales (SS)	8,0m
Pale grey/off-white coloured kaolinitic shale (CG)	6,0m
Chocolate and black coloured carbonaceous mudstone (CHOC=	3,5m
Fissile, carbonaceous shales with thin seams of low rank coal (CL)	14,5m
Grey sandy shales and mudstones with intercalated silstones, grits and unconsolidated gravels (GS)	25,0m +

Reference to Appendices 8 and 9 as well as Plate 7 shows that the above sequence is flexured rather than horizontally disposed. The axes of these gentle folds are, however, sinuous and without any apparent sympathetic alignment to regional geological structures. Consequently, the

/Karoo

Karoo beds occur in a series of haphazard domes and basins which, along the eastern margin of the outlier, are disrupted by a fault striking east of northeast.

PLATE 7.



Flexured Karoo shales in the Rietvlei area.
Note the slumping of strata into a small, laterite filled sinkhole (P).

According to Sheet 2528 CD (Rietvleidam) prepared by the Geological Survey, a magnetic anomaly, corresponding with the Rietvlei Fault, which dislocates the rocks of the Transvaal Sequence, occurs down the centre of the Rietvlei outlier. It is suggested, therefore, that the Karoo rocks of the Rietvlei outlier were deposited in a depression or "bogaz" weathered out of the dolomite, along the line of the Rietvlei Fault. As previously discussed, magnaniferous wad may form a weathered mantle on the surface of

/the bedrock

the bedrock. Such wad material may well have undergone compaction under the weight of soft accumulating sediments resulting in the development of slump structures.

The Henley/Lawley Area

Reference to Appendix 6 will show that the outliers of Karoo sediments in the Henley/Lawley area are irregularly shaped. These outliers are confined to slots eroded out of the Malmani Subgroup rocks, as illustrated by the gravimetric survey configuration shown in Appendix 10. The Karoo sequence, from top to bottom, in the Henley/Lawley area is as follows :

<u>Description</u>	<u>Thickness (m)</u>
Highly weathered, red mudstones with sporadic and intermittent chert pebble bands.	25,0m +
Pale cream and off-white coloured kaolinitic shales.	8,0m
Dark grey, brown and black carbonaceous mudstone.	9,5m
Dark grey carbonaceous shales.	0,0 - 2,0m
Grey and off-white coloured grits silstones and tillite.	3,0m +

It should be noted that the Karoo outliers in the Henley/Lawley area are elongated generally in a north-northwesterly direction; one of the directions

/favoured for

favoured for preferred solution of the dolomite in the Driefontein area. The northernmost outlier in the Lawley area is an exception, however, having a crude cruciform shape with one arm being north-northwesterly aligned and the other following a west-southwesterly direction. In this northernmost cruciform-shaped outlier, the Karoo Sequence comprises 15m of red mudstones overlying 8m of pale cream and off-white shales and some 2m of carbonaceous clay. By contrast, boreholes in the southernmost outlier confirm that the red mudstone has a thickness in excess of 35m. It is unlikely that the sequential differences between the northern and southern outliers represents a facies change because they are less than 300m apart. A more feasible explanation is that the uppermost members of the Karoo Sequence are preserved in the southernmost outlier because it has suffered more re-adjustment settlement or slumping than that to the north. Evidence that slumping has occurred within the outliers is provided by the steep dips achieved by the strata as illustrated by contours to the interface between the pale cream shale and carbonaceous mudstone in a portion of the Lawley quarry as shown in Appendix 11.

The Henley outlier is contained within a sinuously shaped, northwest-striking slot as also shown in

/Appendix 6 ---

Appendix 6. Once again post-Karoo slumping has occurred with dips, in excess of 50° , occurring at the interface with the dolomitic abutments.

The Driefontein Area

The generalised Karoo sequence, from top to bottom, in the Driefontein outlier is as follows :

<u>Description</u>	<u>Thickness (m)</u>
Pale cream to off-white coloured kaolinitic shale with occasional scattered, sub-angular chert pebbles.	15,0m
Pale grey and off-white coloured shale with abundant chert pebbles and occasional silstone horizons.	12,5m
Yellow, red and brown coloured silty mudstones.	3,0m
Black carbonaceous shales with thin seams of low grade coal.	27,0m
Pale grey, shales with sporadic silstone bands.	15,0m
Hard, olive green tillite and unconsolidated gravels.	24,0m

As with the Rietvlei, Henley and Lawley outliers, the Karoo Sequence at Driefontein is flexured rather than horizontally disposed. These flexures may have dips in excess of 45° .

The severity of these flexures or slump structures is apparent in the brick factory area where close-grid drilling provides detailed information. Thus, the depth below surface of the carbonaceous shales can be accurately profiled and contoured as can be seen by

/referring

referring to Appendices 7 and 12. In some cases, as in Slot C some 40m west-southwest of the Coal Crane Gantry, dips of up to 73° in the carbonaceous shales indicate the severity of post-Karoo readjustment slumping.

Strata of the Karoo Sequence in the Rietvlei, Henley/Lawley and Driefontein outliers display a remarkable similarity, in their lithological characteristics and, hence, depositional conditions. As far as the carbonaceous members at each locality are concerned, it is conceivable that their deposition was controlled purely by local environmental conditions. Thus, Brink (1979) suggests that the lowermost members of the Karoo Sequence "... represent deposition from the melt waters of the glaciers along the U-shaped slots in the dolomite. At the end of glacial activity, bodies of stagnant water in the slots would have favoured the development of carbonaceous sediments." It is contended, however, that the carbonaceous beds in the Karoo Sequence are not due to localised depositional conditions but rather they are an integral part of the Karoo Sequence which has remarkable similarities over a distance of 90km between the Rietvlei outlier and those at Henley/Lawley and Driefontein as shown in Figure 30.

/ Figure 30 ---

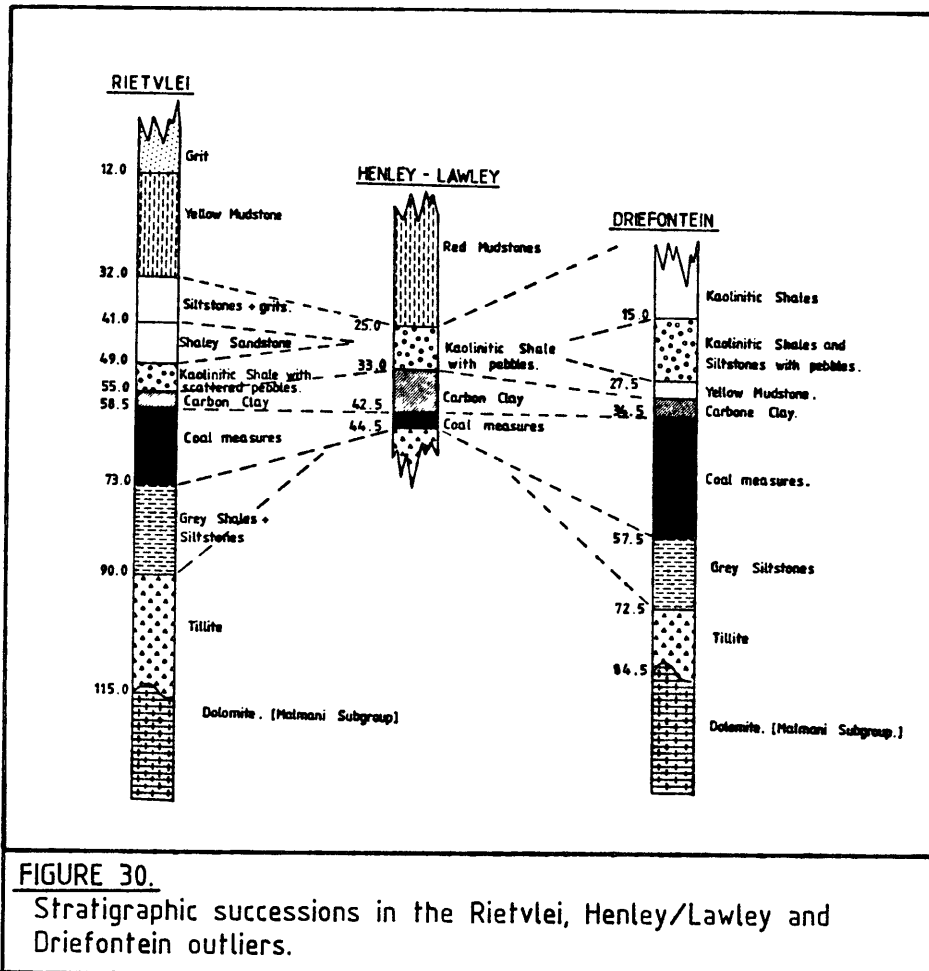


FIGURE 30.

Stratigraphic successions in the Rietvlei, Henley/Lawley and Driefontein outliers.

Thus, the presence or apparent absence of carbonaceous shales in a slot or depression eroded out of the dolomite may be due to the degree of readjustment slumping which has taken place. The potential instability of a slot or depression is not, however, solely dependant upon the amount of post-Karoo slumping that has occurred because the lithological characteristics of the infilling material in such zones exerts

/ even ---

even greater influence.

4.1.2 LITHOLOGY

As previously mentioned, the main lithological units infilling the palaeo-karst topography in the dolomite, are the residual materials such as manganese wad, the Karoo sedimentary rocks and also the Pleistocene to Recent soils. Each of these lithological units has its own physical or engineering characteristics such as compressibility, density, permeability, erodibility and cohesion and may, therefore, assert considerable influence on ground stability. Logically, therefore, the stability of any area may become a function of the following conditions :

- (i) The thickness ratios between the various lithological units, as well as the complete absence of one or more of them, which may often be determined by the amount of slumping which occurred prior to pre-Pleistocene planation. At Driefontein, for example, the relationship between pre-Pleistocene slumping and the thickness ratios of the lithological units becomes apparent from studying the behaviour of the carbonaceous shales. Reference to Appendices 5 and 7 shows that the slots "A", "B" and "C" are filled with at least 35m of kaolinitic shales, mudstones and siltstones at their rims increasing

/ locally ---

locally to exceed 48m at the centres of the slots. In contradistinction, the upper contact of the carbonaceous shales lies more than 40m from the surface at the flanks of slot "D". In all the slots there is evidence of acute slumping. It could be concluded from the distribution and disposition of the carbonaceous shales that the central positions of a slot should have higher instability potential than its sides. In fact, the converse may apply except where a void exists, because the greater thickness of shales, mudstones and siltstones in the centres of a slot, which possess sufficiently high tensile strengths and low compressibility potentials compared to residual material such as manganiferous wad, promote greater present day stability.

- (ii) The severity of the palaeo-karst development in the dolomitic bedrock.

The contributions made by each of the above-mentioned parameters to ground stability are intimately related. For example, the tensile strength or cohesiveness of a material is tested by the horizontal distance

/which ---

which must be spanned between two abutments. This span distance, in turn, is dictated by the severity of palaeo-karst development. Likewise, the vertical thickness of an infilling material may be controlled not only by its history of deposition, but also be relative to the depths of slots and depressions, whilst its apparent thickness will be dependent upon the amount of settlement deformation it has undergone. However, the degree of slumping will be a reflection of the amount of compaction or void development which has occurred beneath the material and the material's inherent physical capabilities, such as its tensile strength relative to the span distance between abutments. It is proposed that the inter-relationship between the physical characteristics of a material and its apparent thickness in a specific geological profile constitutes a basis for evaluating the "instability risk potential" of an area as will be discussed in Section 5 of this dissertation.

4.1.3 HYDROLOGY

When describing, in Part 3, the methods used for interpreting surface and subsurface movements, it will be recalled that positive (upward) movements as well as negative (downward) movements may occur. Jennings (1971 a) observed that "... when the level of the groundwater in the soil changes, the level

/ of ---

of the ground also changes. If the groundwater rises the ground surface also rises and if it falls, the ground surface level drops". It is considered necessary, however, to describe :

- (i) why subsurface water systems may change elevation; and
- (ii) the mechanisms responsible for negative and positive movements of subsoils as well as the ground surface.

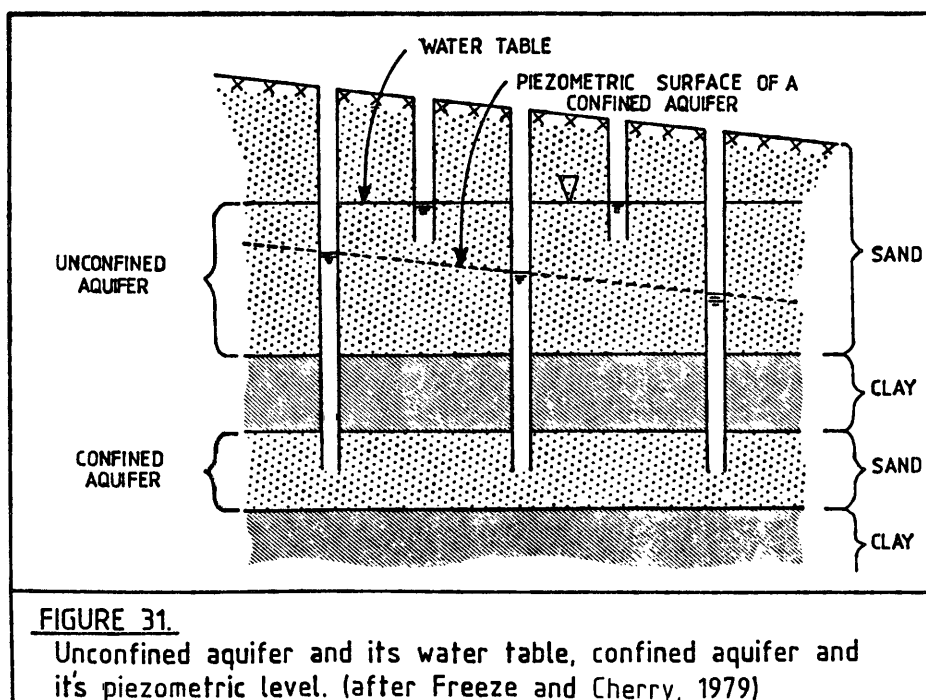
Hydrological conditions in the outliers of Karoo sedimentary rocks are far more complex than those occurring in the dolomitic bedrock. This hydrological complexity is influenced by both the lithological character and structural disposition of the Karoo beds.

As previously described, these successions are typified in the Rietvlei, Henley/Lawley and Driefontein outliers where they consist of shales and mudstones with thin, intermittent, coalescing arenaceous as well as rudaceous intercalations.

As would be expected, the arenaceous and rudaceous strata behave as aquifers whereas the argillaceous

/members ---

members of the succession constitute relatively impermeable layers. Consequently, complex regimes of unconfined and confined aquifers are prevalent in Karoo outliers. As defined by Todd (1959), an unconfined aquifer is regarded as one in which a water table serves as the upper zone of saturation and may, therefore, be also described either as free, phreatic or non-artesian. The form and slope of the water table may vary depending upon the areas of recharge and discharge. Confined aquifers, also known as artesian or pressure aquifers, occur where the groundwater is subjected to pressure greater than atmospheric by overlying, relatively impermeable strata. When any borehole, well or excavation penetrates a confined aquifer, the water level rises well above the bottom of the confining bed, as shown in Figure 31, until the piezometric level is attained.



/ In ---

In Karoo outliers, such as that at Driefontein, it may be presumed that stable conditions will be re-established once the main water table has retreated through compactible materials and their dehydration is complete. In practice, such lowering of the main water table instigates even further complexities in the hydrological regimes within the Karoo succession. Thus, consolidation of compactible strata causes stresses to be imposed on overlying aquifers, aquitards and aquicludes to the extent that ruptures may occur and so-called "leaky aquifers" may be created. Such "leaky aquifers", which in reality are aquifers leaking through aquicludes and aquitards, become a source of additional water over and above that which can be supplied by the aquifer itself. Consequently, the whole pattern of hydraulic pressures and gradients of the hydrological regimes within the Karoo succession is changed and the resulting imposed stresses, become intensified and self-propagating.

A simple example of how lithological and structural characteristics of the Karoo beds complicate the hydrology, is typified in the Rietvlei area. Thus, as can be seen by reference to Appendices 8 and 9, the so called "Transition Zone" (TZ), which comprises essentially grits and siltstones, as well as the carbonaceous shales with associated thin seams

/ of ---

of low grade coal (CL), behave as aquifers. By contrast, the yellow mudstones and shales (Ys), shaley sandstones (SS), kaolinitic shales (CG) and "chocolate" clays (CHOC) constitute aquicludes. Because of the slump structures, the aquifers exhibit confined conditions so that, regardless of the depth at which any aquifer is intercepted, which may be in the range of 11,5m \pm 5,5, the piezometric surface achieves a level of 6,1m \pm 3,5. Contours of the intercepted depths of subsurface water are shown in Appendix 15 and, as would be expected, show a crude relationship with the slump structures assumed by the Karoo sedimentary succession (Appendix 8).

Fluctuations in subsurface water levels, whether they be the water table of an unconfined aquifer or the piezometric surface of a confined aquifer, indicate changes of hydraulic pressure. Numerous phenomena may produce such pressure changes, these being :

- (i) Evapotranspiration
- (ii) Meteorological changes
- (iii) External loading
- (iv) Earth tides
- (v) Water recharge and discharge

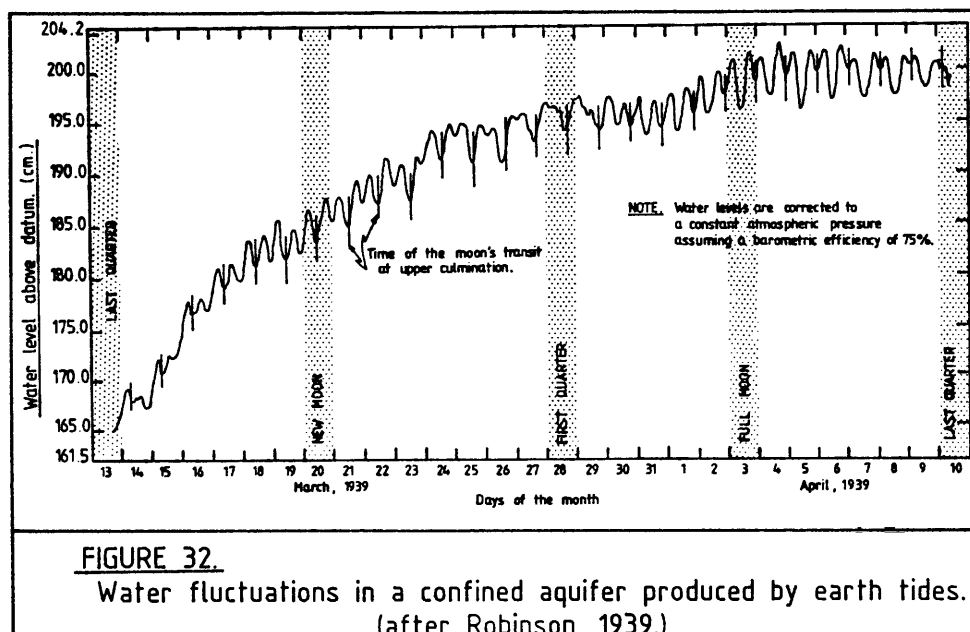
Evapotranspiration does not assert an influence on groundwater behaviour either at the Rietvlei, Henley/Lawley

/ or ---

or Driefontein outliers because, at these localities, the uppermost aquifer is never less than 2,7m from surface. As far as meteorological phenomena are concerned, the frequency of measurements taken at Driefontein is insufficient for comment to be made. Differences of barometric pressure are, however, known to exist. Thus, many open boreholes and piezometers, such as BH 8DD near the Down-draught Making Section and PBM 6 west of the Compound are known to "breathe" in the early morning and again at late evening. Undoubtedly, this flatulence is caused by dramatic barometric differentials between air-filled subsurface voids and ambient pressure at surface.

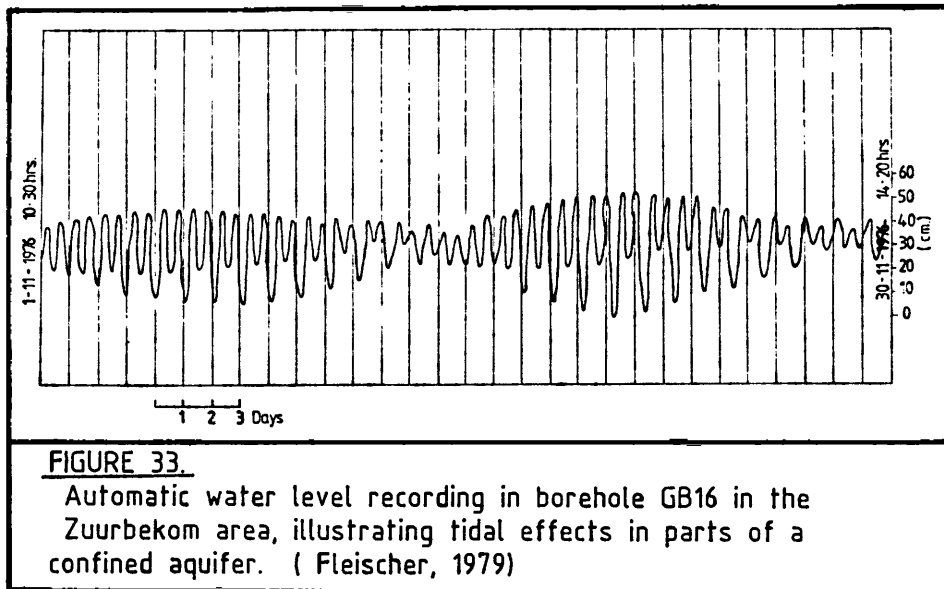
No testimony can be given as to the influence of external loads or earth tides, again because of the measurement frequency. It is unlikely, in either the Rietvlei, Henley/Lawley or Driefontein outliers, that the application of external loads, such as accumulation of water in abandoned quarries, would produce the kind of groundwater movements described by Jacob (1940). There is, however, a possibility concerning the effects of earth tides on confined aquifers. A statement made at the public enquiry after the tragic engulfment of the West Driefontein Gold Mine reduction works in 1962, for example, postulated that "... the water table in a dolomitic area fluctuates several inches twice daily due to solar attraction in the same way as tides
/ occur ---

occur in the sea. It seems likely that the effect on a large mass of ground, such as that forming the roof of the sinkhole in question, could precipitate a collapse when the combined effect is at its greatest or least. It might be coincidence that it was full moon the day prior to the accident and that the moon and sun were diametrically opposed, one settling and one rising, at the time of the accident resulting in a minimum of vertical attraction by these heavenly bodies". Robinson (1939) recognised that regular, semi-diurnal fluctuations of water levels in wells penetrating confined aquifers in New Mexico and Iowa, were attributable to earth tides. (Figure 32).



/ Similarly ---

Similarly, by means of automatic water level recorders installed in selected boreholes in the Gembokfontein Compartment, in which is situated the Lawley outlier, Fleischer (1979) was able to prove cyclic tidal effects as depicted in Figure 33.



The water level fluctuations caused by earth tides are, however, relatively small. Thus, although they may be sufficient to effect loss of cohesion along the abutments of an arch at a critical time, it is unlikely that earth tides are capable of significantly influencing either surface or subsurface behaviour.

Because of the structural and lithological characteristics of Karoo outliers, water recharge and discharge plays

/ the ---

the most important role in water level changes. It should be remembered that rainfall alone is not necessarily an accurate indicator of such level changes. Rather, the governing factor is recharge which, assuming annual discharges are constant, depends on rainfall intensity and distribution as well as the amount of surface run off.

At Driefontein, recharge is accomplished by rainfall and surface run off; the latter from the south across the pediment to the Wonderfontein Spruit as shown in Appendix 16. As is commonly the case, the erection of surface structures such as buildings, paved areas and surface drains, can alter the aerial extent and distribution of recharge areas. Consequently, the replenishment of aquifers, and hence the natural hydrological system, can be dramatically altered. In the Driefontein area, the erection of a brick factory with its buildings, concreted floors, surface drainage systems and quarrying activities to extract Karoo "clays" as a raw material for brick manufacture, has proved to be no exception. It is apparent that the last-mentioned activity has made a significant contribution to modifying the hydrological system of the Driefontein area. With the initiation of quarrying, overburden was first stripped from the proposed "clay pit" area and dumped at a convenient locality. In this

/ instance ---

instance, the locality selected for overburden dumps lay parallel to the road from Venterspost to Carletonville, as shown in Appendix 16, where they still form an obstruction to natural surface run off. Secondly, shallow drains were excavated around the peripheries of the quarry to keep it as dry as possible, so that the surface run off pattern suffered interference. Thus, selected areas were artificially kept dry at the expense of others, thereby altering the local pattern of water recharge. The third factor contributing to the creation of artificial recharge was the policy of allowing worked-out quarries to fill with water. Besides altering the hydrological balance of the area, quarrying operations have also reduced the thickness of Karoo bridging materials overlying compactible residuum derived from the weathering of the Malmani dolomite. It can be seen, therefore, that the artificial reduction in the thickness of bridging materials and modifications to surface run off patterns brought about by clay mining activities, promote ground instability. The abandoned quarry "A" (Appendix 16) immediately south of the Down-draught Making Section, is a typical example. A generalised geological profile of this locality originally comprised 3,3m of Pleistocene to Recent soils, 27m of kaolinitic shales and >9,9m of manganiferous wad overlying weathered dolomite. Quarrying extracted 20m

/ of ---

of the kaolinitic shales thereby reducing the thickness of "bridging" material to 7m. On completion of mining operations, the quarry was allowed to fill with water. Undoubtedly, seepage occurred through the thin veneer of Karoo shales, eroding away the underlying wad. On 31st December 1976, as previously related, some 440 megalitres of the accumulated water drained out within a period of three hours, through a 5m diameter sinkhole which had breached through the Karoo bridging material. A further eleven sympathetic sinkholes occurred thereafter, during a space of just over four weeks.

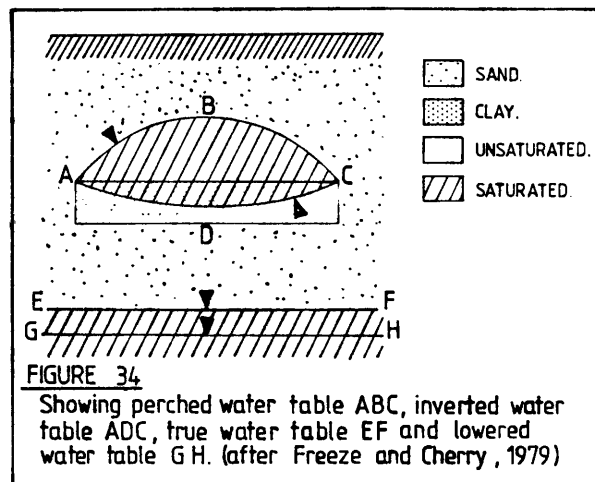
In many aspects, the Down-draught Making Section area typifies the ground instability of the Driefontein outlier.

Theoretically, the dewatering of the Bank COmpartment, which commenced in late December 1968, should not have induced instability where compactible or erodable materials were situated above the dolomitic water table prior to its retreat. In practice, dewatering triggered off a series of events each of which contributed to subsurface instability.

Firstly, the artificial lowering of the main water table promoted caverns, present in the phreatic zone, up into the vadose zone where they become receptacles to receive the products of erosion and arch collapse.

/ Secondly ---

Secondly, the retreat of the main water table tended to increase the hydraulic head between it and any "perched" water systems or aquifers at a higher elevation. Perched aquifers, as shown in Figure 34 occur where, as Todd (1959) describes, "... a ground-water body is separated from the main water table by a relatively impermeable stratum of small aerial extent and by the zone of aeration above the main body of groundwater." Obviously, the above definition implies that perched water tables are unconfined.



With the increase of the hydraulic head, it is possible for the hydraulic gradient between a perched aquifer and the main water table to be steepened, thereby / promoting ---

promoting the rate of seepage and degree of erosion in the vadose zone. Thus, the artificial lowering of the dolomitic water table in the Driefontein area not only caused instability as it retreated through compactible materials but also in such materials originally situated above it. Thirdly, the slump structures which occur in Karoo sedimentary rocks add further complications. In the case of confined aquifers, the resulting steeply inclined impermeable layers induce a steepening of hydraulic gradients and an increase of hydraulic pressures. Thus, relatively insignificant changes in recharge or discharge rates may be reflected as substantial fluctuations of hydraulic pressure within the aquifers. In addition, the complexity of structural and lithological features in Karoo outliers is conducive to the development of perched aquifers.

4.2 GROUND INSTABILITY IN THE DRIEFONTEIN OUTLIER

4.2.1 SEQUENCE OF EVENTS

The mechanisms which resulted in a history of instability at Driefontein are postulated to have been as follows :

MAY 1970 - OCTOBER 1972 : The effects of dewatering the Bank Compartment are expressed by excessive surface subsidence, structural cracking and ultimate
/abandonment ---

abandonment of dryers and kilns due to the lowering of the water table through compactible materials either mantling dolomite pinnacles or lining the flanks of slots. The increased intensity of movements which occurred in late 1972, can, possibly, be attributed to a sympathetic drop of perched water tables via newly created leaky aquifers causing consolidation or erosion of compactible residuum situated above the original water table.

OCTOBER 1972 - DECEMBER 1976 : The consolidation of residual materials, both above and below the original water table elevation in the vicinity of the kilns and dryers, is completed. In the vicinity of the Down-draught Making Section and an adjacent abandoned quarry "A", damage to original perched aquifers promotes accelerated infiltration of surface water which causes further consolidation and erosion of compactible materials less than 20m below surface.

DECEMBER 1976 - FEBRUARY 1977 : The extraction of the brickmaking materials from the quarry immediately south of the Down-draught Making Section is completed and surface run-off water allowed to accumulate in

/the

the abandoned workings. The rate of seepage through the reduced thickness of Karoo cover into the underlying erodable material increases, thereby causing the bridging material to collapse, and the water pours down the 5m diameter throat of a newly formed sinkhole. The rapid erosion of manganiferous wad and other residuum in the immediate vicinity results in four, closely spaced sinkholes, occurring in rapid succession.

FEBRUARY 1977 - JULY 1978 : A period of quiescence prevails up to November 1977 as the area becomes stabilised. Unfortunately, water has again been allowed to accumulate in the abandoned quarry and twelve more closely spaced sinkholes occur. The accumulated water drains away again, this time down sinkhole No. 13. Between April and July 1978, sinkhole No. 13 becomes blocked whereas sinkhole Nos. 14 and 15 are backfilled. As a result, water again accumulates in the quarry and in June 1978 yet another sinkhole (No. 16) develops near the southern periphery of the abandoned workings.

JULY 1978 - FEBRUARY 1980 : An attempt is made to control the flow of surface run-off water within the environs of the factory. Firstly, a system of fibreglass lined drains is constructed to lead all
/ run-off ---

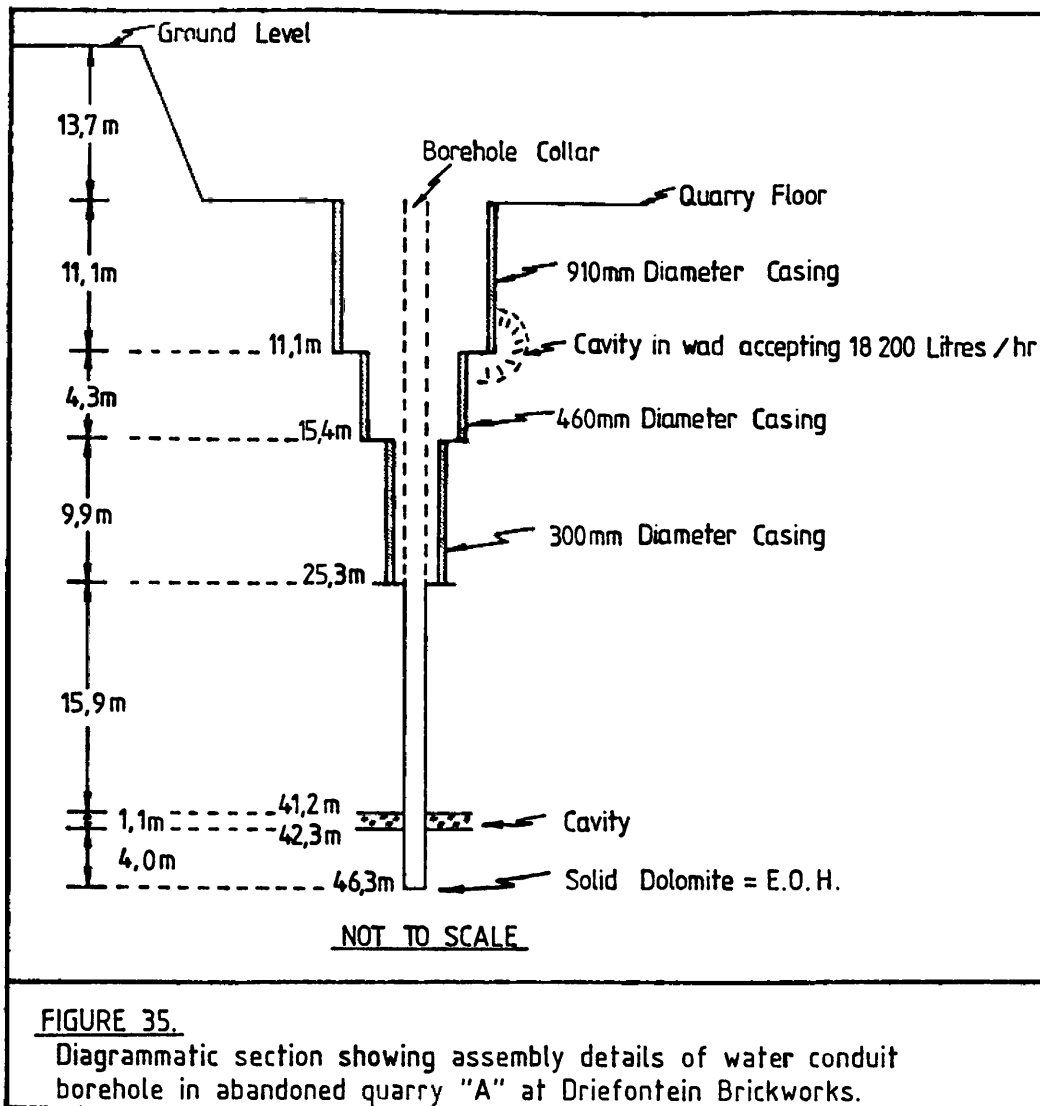
run-off water to the abandoned quarry. Secondly, the late Professor Jennings establishes a conduit on the quarry floor in the form of a borehole, drilled down the centre of sinkhole No. 13, to a depth of 46,3m where either solid dolomite or else a large floater is encountered. During the drilling of the borehole, a cavity is intersected between 41,2m and 42,3m from the borehole collar; that is 54,9m to 56,1m from ground level proper.

The borehole is lined with 910mm diameter casing to a depth of 11,1m from the collar (ie. 24,8m from surface level). For the next 4,3m of the borehole, the size of the casing is reduced from 910mm to 460mm diameter. Thereafter, 300mm diameter casing is used to line the remainder of the borehole to a depth of 25,3m from its collar. The details of the conduit assembly are shown in Figure 35.

On completion of the conduit, a cavity develops where the casing size has been reduced from 910mm to 460mm diameter, that is at a depth of 11,1m from the collar or 24,9m from the surface. It is determined that this cavity can accept 18 200 litres per hour.

Jennings, is convinced that water discharge from the quarry into the cavity 11,1m from surface will ultimately reach the lower cavity located at

/ 41,2m ---



41,2m to to 42,3m from collar elevation, without causing subsurface erosion. The uppermost cavity is, however, present in compactible residuum,
/ comprising ---

comprising manganiferous wad and manganiferous chert breccia. Within weeks, differential subsidence of the surface as well as the appearance of cracks in buildings, indicates that subsurface erosion is occurring. After 6 months, the 300mm diameter casing subsides 760mm and by late January 1980, the entire assembly not only subsides in excess of 4m but also slants over to an angle of 30° from the vertical. As a consequence of excessive subsidence and distortion, dislocation of the conduit occurs at a depth 11,1m from its collar, and it refuses to accept water, despite several attempts to unblock it.

On the 18th February 1980, yet another sinkhole appears adjacent to the Down-draught Dryers.

FEBRUARY 1980 - OCTOBER 1981 : Because of the abandoned quarry's sensitivity, it is decided that no further water accumulation be allowed. Consequently, any accumulated water is pumped to another shallower quarry "C" some 450m to the west. Within a few weeks of adopting this policy, it is noted that the sub-surface water levels rise, particularly in the vicinity of the Compound. It is later postulated that the water accumulated in the second quarry constituted a localised, artificially induced recharge area.

/ OCTOBER 1981 ---

OCTOBER 1981 - PRESENT : A detailed study is initiated of the surface run-off pattern across the Driefontein area to achieve two major objectives. Firstly, to divert water away from, and thus prevent it accumulating in, either working or abandoned quarries "A" and "C" as shown in Appendix 16. Secondly, to redesign the drainage system in the factory area so that surface water can be discharged into natural water courses flowing northwards. As a consequence of the above strategies, perched water table and piezometric surface elevations return to normal. Since October 1981, no new sinkholes develop and neither drastic subsidence nor cracking occurs on surface.

The sequence of events outlined above clearly indicates a strong correlation between the "movements" of either groundwater or piezometric levels and the behaviour of the surface. The mechanisms which are responsible for this correlation will be discussed in the succeeding sections dealing with surface and subsurface behaviour.

4.2.2 INTERPRETATION OF SURFACE AND SUBSURFACE MEASUREMENTS

Routine, precise levelling measurements of the surface indicates that both negative (downward) and positive

/(upward) ---

(upward) movements of the surface occur.

Similar movements have also been noted in the upper subsurface marker, situated 12m below ground level in telescopic bench marks and also, but to a lesser extent, in the subsurface marker set 22m from surface.

In fact, as was shown in Figure 28, a strong correlation exists between the surface (ΔH_s) and the upper subsurface marker (ΔH_u) elevation changes. Two explanations can be offered for this correlation :

- (i) That the ΔH_u movements reflect ΔH_s movements because of a malfunction in the telescopic bench mark assembly.
- (ii) Mechanisms exist which influence the behaviour of both the surface and the subsurface materials to a depth of 12m or more; that is, the relationship between ΔH_s and ΔH_u .

4.2.2.1 Malfunctioning of Telescopic Bench Marks

A major weakness in the design of the Jennings type telescopic bench mark is the possible inhibition of the movement between the rods and pipes making up / the

the assembly. Reference to Figure 20 shows that dry sand is used in the assembly as a packing to allow free movement. Experience at Driefontein shows, however, that unless the sand is thoroughly washed free of any contaminating material, the combined effects of compaction and permeating rain water causes it to solidify, thereby prohibiting any movement. Furthermore, if the telescopic bench mark has been installed in Karoo shales or mudstones, then infiltrating rainwater or movement of immediately adjacent subsurface water may cause the packing sand to be washed out and replaced by clay material. In some instances, such clay material may have sufficient expansive capacity to constrain the various rods and pipes of the TBM assembly by a "crimping action".

To determine whether mechanical malfunctions exist, the mean and standard deviations of surface and subsurface movements were taken and also a correlation coefficient analysis conducted in respect of a number of contentious as well as apparently "normal" telescopic bench marks. The correlation coefficients (r) are expressed as percentages ($r^2(100)$) by using the equation :

$$r^2(100) = \frac{\Sigma xy}{\sqrt{(\Sigma x^2) (\Sigma y^2)}}$$

/ In - - -

In the aforementioned equation :

- (i) X and Y denote movement measurements
(e.g. X = an ΔH_u measurement and Y = an ΔH_s measurement).
- (ii) \bar{X} and \bar{Y} represent the means of the sums of X and Y respectively (e.g. \bar{X} may be the mean of ten ΔH_u measurements and \bar{Y} the mean of ten ΔH_s measurements).
- (iii) x and y are the values obtained by respectively subtracting \bar{X} from X and \bar{Y} from Y.

An example of an analysis of movements in one telescopic bench mark, namely TBM 34, over ten measuring cycles, each covering 43 days, is given in Table 6 in which X = ΔH_u and Y = ΔH_s .

Cycle No.	X = ΔH_u	Y = ΔH_s	x = X - \bar{X}	y = Y - \bar{Y}	x ²	xy	y ²
1	00	00	+6,79	+6,51	46,10	44,20	42,38
2	-2,82	-2,70	+3,97	+3,81	15,76	15,13	14,52
3	-6,90	-6,70	-0,11	-0,20	0,01	0,02	0,04
4	-7,96	-7,70	-1,17	-1,20	1,37	1,40	1,44
5	-8,95	-8,70	-2,16	-2,20	4,67	4,75	4,84
6	-9,02	-8,06	-2,21	-2,10	4,88	4,64	4,41
7	-9,10	-8,82	-2,31	-2,32	5,34	5,36	5,38
8	-8,14	-7,67	-1,35	-1,17	1,82	1,58	1,37
9	-9,23	-8,83	-2,44	-2,33	5,95	5,69	5,43
10	-5,77	-5,33	-1,02	1,18	1,04	1,20	1,39
	$\Sigma X = -67,89$ $\bar{X} = -6,789$	$\Sigma Y = -65,05$ $\bar{Y} = -6,505$			$\Sigma x^2 = 86,94$	$\Sigma xy = 83,97$	$\Sigma y^2 = 81,20$
$r = \frac{\Sigma xy}{\sqrt{(\Sigma x^2) (\Sigma y^2)}} = \frac{83,97}{\sqrt{86,94 \cdot 81,20}} = 0,999 \quad - \quad r^2(100) = 99,80$							
Correlation between ΔH_u and ΔH_s movements in TBM 34, Compound area.							

/ The ---

The correlation coefficient analyses of the relationships $\Delta H_u : \Delta H_s : \Delta H_\ell : \Delta H_s$ and $\Delta H_\ell : \Delta H_u$ from twelve telescopic bench marks over 15 measuring cycles, are listed in Table 7.

TBM No.	LOCALITY	NUMBER OF MEASUREMENTS	MEAN MOVEMENTS			CORRELATION COEFFICIENT		
			ΔH_s	ΔH_u	ΔH_ℓ	$\Delta H_s : \Delta H_u$	$\Delta H_s : \Delta H_\ell$	$\Delta H_u : \Delta H_\ell$
34	Compound	15	-0,90 ^{+3,97}	-1,49 ^{+3,91}	-18,38 ^{+3,56}	99,98	39,02	40,29
32	Compound	15	+0,61 ^{+5,28}	-0,05 ^{+5,05}	+ 0,40 ^{+2,54}	99,84	47,08	44,99
25	Compound	15	+2,47 ^{+2,26}	+2,04 ^{+2,35}	+ 1,29 ^{+1,51}	96,79	58,32	50,34
22	Compound	15	+0,75 ^{+5,19}	-1,78 ^{+2,54}	- 0,49 ^{+2,71}	84,67	80,85	96,97
14	D.D. Dryers	13	-5,06 ^{+1,93}	-3,51 ^{+1,10}	- 4,02 ^{+1,70}	84,04	88,06	79,21
1/	D.D. Dryers	15	-7,05 ^{+2,13}	-7,10 ^{+2,10}	- 1,94 ^{+0,38}	99,84	0,22	0,46
8	D.D. Dryers	15	-1,06 ^{+0,44}	-1,40 ^{+0,49}	- 1,82 ^{+0,57}	92,95	70,82	84,06
10G	Houses	10	-22,83 ^{+4,71}	-8,39 ^{+1,40}	- 0,07 ^{+0,43}	86,88	2,49	0,99
9A	Houses	15	-7,47 ^{+2,06}	-2,04 ^{+0,46}	- 1,59 ^{+0,63}	1,51	38,75	69,80
7G	Houses	15	-5,99 ^{+5,48}	-3,36 ^{+0,66}	- 3,81 ^{+0,70}	0,41	9,16	91,79
1B	Houses	15	-3,12 ^{+1,15}	-3,12 ^{+1,07}	- 3,71 ^{+0,93}	99,82	97,27	97,38
10JA	Houses	8	-8,21 ^{+4,58}	N/A	- 5,18 ^{+2,65}	N/A	96,16) 99,53
10JB	Houses	8	-8,34 ^{+4,84}	-5,20 ^{+2,66}	N/A	96,46	N/A	

Mean movements and correlation coefficient analyses of ΔH_s , ΔH_u and ΔH_ℓ movements (measurements in mm.)

With the exception of TBM Nos. 9A and 7G, the correlation between ΔH_s and ΔH_u movements is in excess of 80 per cent thereby suggesting that there is mechanical malfunctioning of the upper subsurface marker in most of the telescopic bench marks. From the mean movements and standard deviations of the ΔH_s , ΔH_u and ΔH_ℓ movements it can be seen, however, that other than TBM Nos. 34, 22 and 8, all the prevailing

/conditions ---

conditions relate to compaction. While such compaction is associated with subsurface water elevation changes, at a point between 12m and 22m from surface, as is the case with TBM 32, 25 and 1B in the table above, then it could be expected that :

- (i) a genuinely high correlation would exist between ΔH_s and ΔH_u ;
- (ii) the relationship between ΔH_s and ΔH_ℓ as well as ΔH_u and ΔH_ℓ would be less strongly defined to the extent of almost being non-existent, the latter condition being well illustrated by the behaviour of TBM Nos. 10 and 10G.

Where compaction is associated with subsurface water movements below the lower subsurface marker, that is beyond a depth of 22m, then a well-defined correlation will exist between $\Delta H_s : \Delta H_u$, $\Delta H_s : \Delta H_\ell$ and also $\Delta H_u : \Delta H_\ell$. Such a condition is illustrated by the behaviour of TBM Nos. 22, 14, 8, 10^{JA} and 10^{JB}. The validity of these observations is verified by the surface and subsurface movements of the last two mentioned telescopic bench marks.

Both TBM 10^{JA} and TBM 10^{JB} were installed for the purpose of monitoring the relationships between

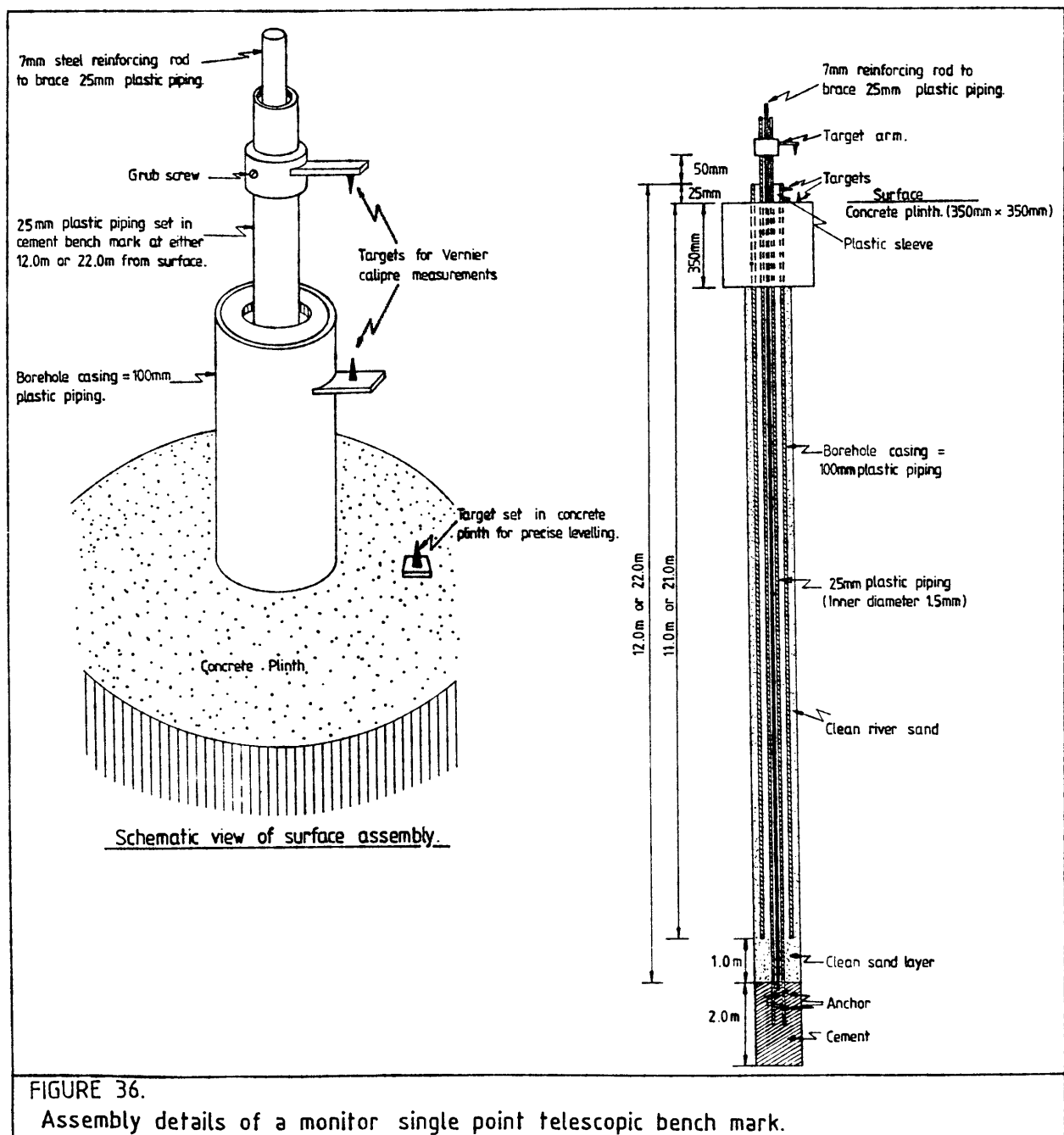
/ ΔH_s ---

ΔH_s : ΔH_u in TBM 10^{JB} (96,46 per cent) and ΔH_s : ΔH_ℓ (96,16 per cent) in TBM 10^{JA} whilst the relationship between ΔH_u and ΔH_ℓ equates to 99,53 per cent. It is highly probable, therefore, that in areas where compaction conditions are prevalent, almost equitable amounts of ΔH_s and ΔH_u movements occur which should not be misconstrued as mechanical malfunctions of the telescopic bench mark installation.

In cases where instability, promoted by possible void development, is occurring at a point below the lowermost subsurface marker, the differential between ΔH_s ΔH_u and ΔH_ℓ should become progressively greater. Reference to Table 7 shows that no such differential occurs in the relationship between ΔH_s and ΔH_u in TBM No. 34, although the H_ℓ behaviour is as one would anticipate. To resolve whether or not the subsurface measurements were artificial, monitoring telescopic bench marks, namely TBM Nos. 40^B, 41^A and 41^B were installed within the vicinity of TBM 34. The construction of the monitoring telescopic bench marks was the same as shown in Figure 36 and allows for unrestricted movement of the subsurface marker relative to surface. It should be noted that unlike the conventional telescopic bench mark assembly, there is no stem-pipe and that the 100mm diameter borehole casing extends to within 1m of the subsurface marker (i.e. to either 11m or 12m below surface). Because the 100mm diameter casing is packed in clean, washed river sand and has no contact with the sides of the

/borehole ---

borehole, the surface movement of the concrete plinth into which it is set, is not influenced by any subsurface movements. Even so, it must be emphasised that the design of this telescopic bench mark should only be used for temporary monitoring rather than for long-term measuring.



The fact that the ΔH_s movements are uninhibited is confirmed by correlation coefficient analyses between the monitoring telescopic bench marks, and conventional installations as well as surface measuring points, with 75,76 per cent (= absolute movements in the range of - 0,98mm) and 95,60 per cent (= absolute movements in the range of - 1,41mm) relationships being achieved in the Housing and Compound areas respectively. The subsurface markers in TBM No. 40^B and 41^B are situated 12m from the surface and in the case of TBM 41^A, at a depth of 22m. The analyses of the measurements from these telescopic bench marks, as from Measuring Cycle 29 when the subsurface movements first became available, are given in Table 8.

CYCLE NO.	TBM 40 ^B		TBM 41 ^B		MEAN OF TBM 40 ^B /41 ^B		TBM 41 ^A	
	ΔH_s	ΔH_u	ΔH_s	ΔH_u	ΔH_s	ΔH_u	ΔH_s	ΔH_L
29	-0,45	-1,91	-	-	-	-	-	-
30	+0,35	+0,48	-1,15	-0,68	-0,40	-0,10	-2,45	-2,64
31	+1,09	+1,04	-0,26	+1,01	+0,42	+1,03	-1,54	-1,60
32	+0,55	-0,11	-	-	-	-	-1,91	-0,45
33	+/.41	-1,21	-1,02	-2,62	-0,31	-1,92	-1,86	-1,81
34	-3,12	-4,79	-4,20	-3,21	-3,61	-4,00	-5,37	-2,83
35	-3,96	-5,98	-4,91	-3,96	-4,44	-4,97	-6,60	-3,85
\bar{x}	-0,73 ±1,98	-1,78 ±2,67	-2,31 ±2,09	-1,89 ±2,03	-1,67 ±2,19	-1,27 ±2,32	-3,29 ±2,14	-2,20 ±2,20
	r^2 (100) ΔH_s : ΔH_u 95,29		r^2 (100) ΔH_s : ΔH_u 59,38		r^2 (100) ΔH_s : ΔH_u 89,02		r^2 (100) ΔH_s : ΔH_L 68,61	
Mean movements and correlation coefficient analyses of TBM 40 ^B , TBM 41 ^B and TBM 41 ^A (measurements in mm.)								

It is interesting that the correlation coefficient between ΔH_s and ΔH_u in the free-moving monitor telescopic bench marks ranges from 95,29 per cent in TBM 40^B to 59,38 per cent in TBM 41^B with a combined correlation equating to 89,02 per cent.

/Thus ---

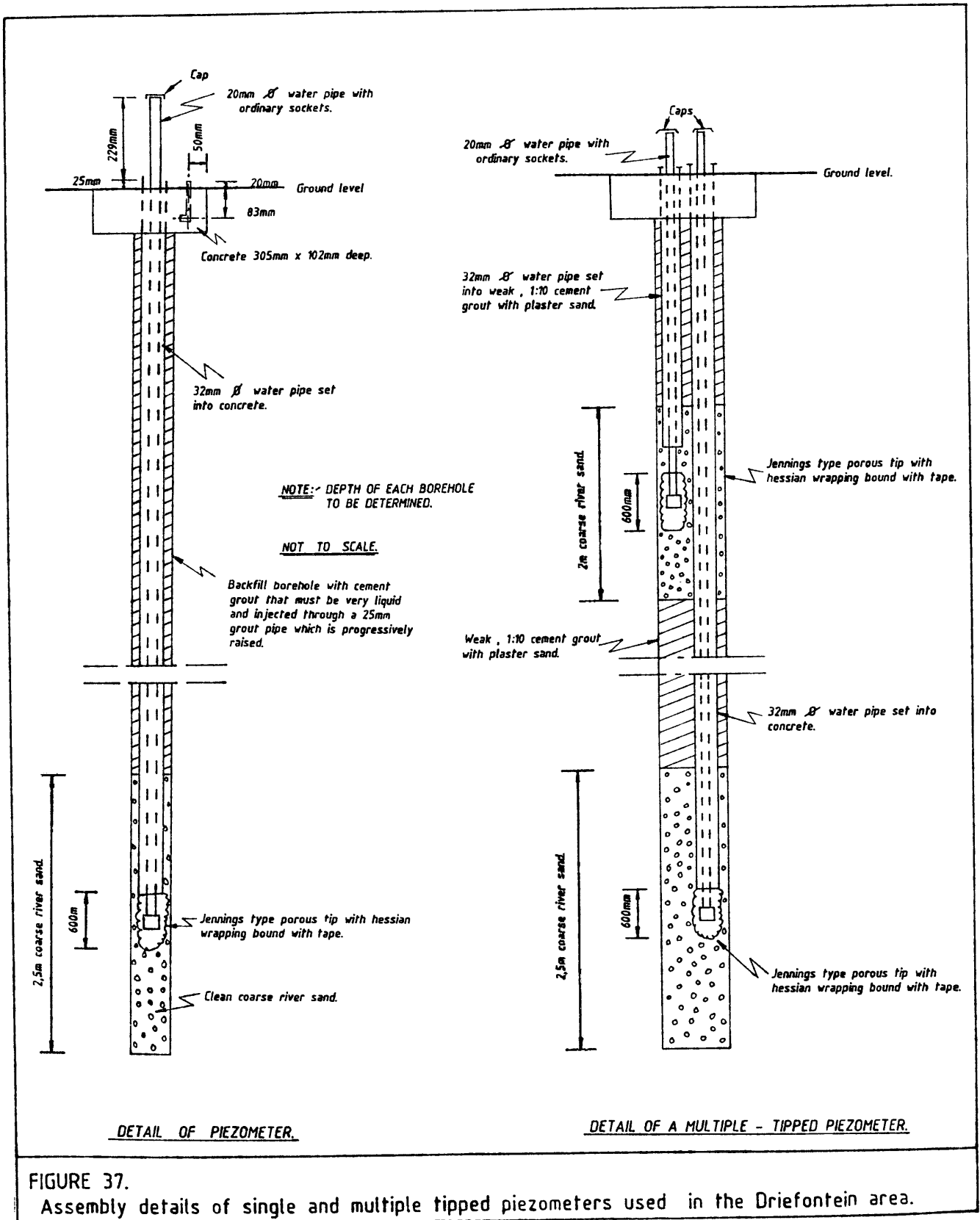
Thus, it would appear from the above analysis, albeit on an inadequately short statistical base, that the ΔH_u movements in TBM 34 are genuine rather than reflecting a mechanical malfunction. A fact which must be borne in mind, however, is that all telescopic bench marks in the Driefontein area which display contentious correlations between ΔH_s and ΔH_u are located in Karoo beds containing multiple, subsurface water systems. By contrast, where a telescopic bench mark is installed in dry Karoo rocks such as TBM 10^C in the European housing area, the relationship between ΔH_s and ΔH_u movements may be as low as 2,49 per cent. The conclusion that must be drawn, therefore, is that changes in elevation achieved by subsurface water regimes provides mechanisms for surface and immediate subsurface movements.

4.2.2.2 Effects of Subsurface Water Behaviour

To establish the relationship between the ΔH_s , ΔH_u and ΔH_ℓ movements measured in telescopic bench marks, it was first necessary to analyse statistically the behaviour of subsurface water as measured in piezometers situated at strategic localities in the Driefontein area. Two multiple piezometers were selected, namely the cluster northwest of the Compound near TBM Nos. 34 and 22 and another in the vicinity of the Gas Producer in the factory area.

/ Assembly ---

Assembly details of a typical multiple piezometer are illustrated in Figure 37.



Compound Area

The cluster northwest of the Compound comprises six piezometer tips set at the following depths below surface:

TABLE 9.	
TIP NO.	DEPTH BELOW SURFACE (m)
1	- 24,50
2	- 11,16
3	- 21,01
4	- 16,08
5	- 30,67
6	- 26,87

Depths of measuring tips below surface in piezometer cluster northwest of the Compound at Driefontein Brickworks.

Details of subsurface water movements obtained from each of these piezometer tips as well as rainfall over thirty two measuring cycles, that is from 18th December 1978 to 14th October 1982, are given in Table 10.

| Table 10 ---

TABLE 10.								
DATE	CYCLE NO.	TIP NO. (Elevation changes in metres)						RAINFALL (mm)
		Tip 1	Tip 2	Tip 3	Tip 4	Tip 5	Tip 6	
18-12-78	1	-0,02	-0,07	-0,04	0,00	+0,01	-0,01	68
5-02-79	2	-0,13	-0,39	-0,01	0,00	-0,07	-0,36	140
19-03-79	3	-0,23	↑ Blocked ↓	-0,09	0,00	-0,14	-0,51	52
10-04-79	4	-0,30		-0,37	-0,01	-0,20	-0,65	53
25-05-79	5	-0,38		-0,47	0,00	-0,26	-0,78	28
20-07-79	6	-0,50		-0,65	-0,65	-0,36	-1,04	9
3-09-79	7	-0,61		-0,70	+0,01	-0,43	-1,25	64
16-11-79	8	-0,77		-0,74	+0,01	-0,57	-1,26	201
20-12-79	9	-0,85		-0,42	+0,01	-0,69	-0,93	49
12-02-80	10	-0,91		+0,57	+0,01	-0,90	+0,14	192
25-03-80	11	-0,86		+1,95	+0,01	-0,99	+1,54	278
9-05-80	12	-0,83		+1,45	+0,01	-1,03	+1,08	41
20-06-80	13	-0,80	+0,65	+0,01	-1,05	+0,03	0	
30-07-80	14	-0,86	+0,25	+0,02	-1,08	-1,10	0	
12-09-80	15	-0,87	-0,19	+0,04	-1,09	-0,50	4	
7-10-90	16	-0,93	-0,69	+0,01	-1,15	-0,94	45	
1-12-80	17	-0,96	+0,73	+0,02	-1,17	+0,20	224	
26-01-81	18	-0,98	+2,24	+0,02	-1,18	+1,85	269	
17-03-81	19	+0,01	-0,36	+3,84	+0,03	-1,18	+3,44	201
28-04-81	20	+0,41	-0,12	+2,82	+0,02	-1,22	+2,47	72
11-06-81	21	+0,46	+0,03	+1,52	+0,03	-1,24	+1,18	4
27-07-81	22	+0,41	+0,06	+0,65	+0,03	-1,25	+0,30	0
11-09-81	23	+0,32	-0,02	+0,33	+0,00	-1,28	-0,01	38
12-10-81	24	+0,19	-0,14	-0,06	+0,01	-1,29	-0,36	53
8-12-81	25	-0,11	↓ Damaged ↑	+0,05	+0,03	-1,35	-0,58	85
1-02-82	26	-0,03		-0,25	+0,03	-1,37	-0,63	123
10-03-82	27	-0,07		-0,21	+0,02	-1,37	-0,65	184
14-04-82	28	-0,11		-0,21	+0,03	-1,39	-0,81	45
3-06-82	29	-0,15		+0,39	-0,18	-1,41	-0,81	85
13-07-82	30	-0,23		+0,27	-0,36	-1,43	-1,11	13
23-08-82	31	-0,28		+0,02	-0,37	-1,45	-1,29	9
14-10-82	32	-0,35		-0,21	-0,41	-1,48	-1,54	31

Recorded measurements (m) of subsurface water movements situated northwest of the Compound and rainfall figures (mm).

By means of correlation coefficient analyses, the following relationships were established as shown in Table 11 :

TABLE 11.	
MEASUREMENT	r ² (100)
Tip 3 (ξ = -21,01) : Tip 1 (ξ = -24,50)	0,56
Tip 3 (ξ = -21,97) : Tip 4 (ξ = -16,08)	6,88
Tip 3 (ξ = -21,07) : Tip 5 (ξ = -30,67)	27,56
Tip 3 (ξ = -21,97) : Tip 6 (ξ = -26,87)	94,09
Tip 1 (ξ = -24,50) : Tip 5 (ξ = -30,67)	55,62
Tip 1 (ξ = -24,50) : Tip 4 (ξ = -18,08)	0,02

Correlation coefficient analysis, (r²(100)) of subsurface water measurements in piezometer cluster N.W. of Compound, Driefontein Brickworks.

It is apparent from the above results that:-

- (i) The measurements recorded by Tip 3 and Tip 6, with absolute mean movements over 20 measuring cycles of $0,71\text{m} \pm 1,08$ and $0,72\text{m} \pm 1,17$ respectively, indicate that these tips monitor the same subsurface water systems.
- (ii) The measurements recorded by Tips 5 and 1, with absolute mean movements over 32 measuring cycles of $0,46\text{m} \pm 0,39$ and $0,20\text{m} \pm 0,17$ respectively, indicate that both these tips monitor another subsurface water systems.
- (iii) A poor correlation exists between the subsurface water movements measured by Tips 3 and 6 and those measured by Tips 5 and 1.
- (iv) There is a very poor correlation between the behaviour of the subsurface water movements recorded by Tip 4, situated 16m from surface, and any of the movements taken from Tips 1, 2, 5 and 6. It must be concluded, therefore, that the Tip 4 measurements are erroneous either because of blockage or else because it is situated in an aquiclude.
- (v) Measurements from Tip2, some 11m from surface must be disregarded because of damage to the installation.

/It ---

It appears, therefore, that in the vicinity of the Compound, two separate subsurface water systems exist each with its own aquifer and piezometric level. Furthermore, the two aquifers are apparently confined as their changes of piezometric levels are induced by recharge rather than by infiltration of rain and, as will be shown, these changes occur at different times. Confirmation of the poor relationships between subsurface water fluctuations and rainfall as well as between rainfall and surface elevation changes are shown in Figure 38. To determine the degree of correlation, the time lag between rainfall and changes of surface and subsurface water elevations per cycle, were taken into account. The time lags in Figure 38 are expressed in increments of 43 days which equates to the time interval between taking piezometer readings (i.e. a measuring cycle).

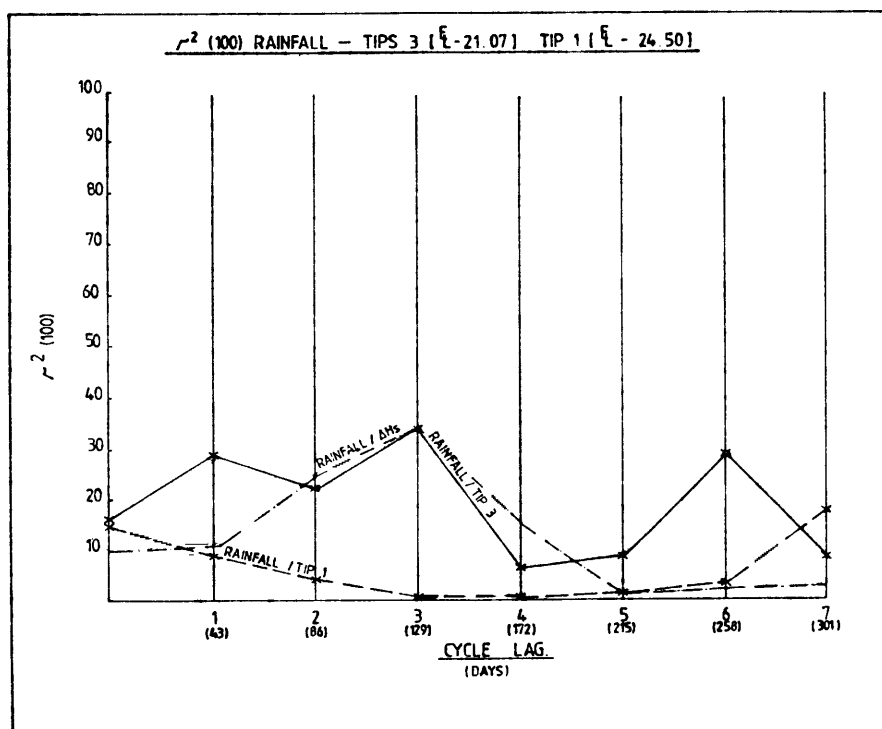


FIGURE 38.
Showing poor correlation between rainfall surface (Hs) and sub - surface water movements.

As can be seen, there is only a 13,87 per cent correlation between rainfall and a change in level of the piezometric level (Tip 3), at a zero time lag. After 43 days have elapsed (i.e. one cycle lag) the correlation coefficient increases to 28,60 per cent and remains at the 20,06 per cent to 33,32 per cent level for up to 129 days (i.e. 2 and 3 cycles lag). Thereafter, the correlation between rainfall and changes of the piezometric level is less than 10 per cent; the 28,75 per cent relationship existing 258 days (i.e. 6 cycles lag) after the occurrence of rain, being regarded as anomalous and attributable to a later rainfall. An even poorer relationship exists between rainfall and the water behaviour in the aquifer (Tip 1). Except for a 13,87 per cent correlation immediately after rainfall (i.e. zero time lag), there is a less than 5 per cent relationship thereafter. Again, the 17,88 per cent correlation recorded after 7 cycles lag (i.e. 301 days) is associated with a different rainfall occurrence and must be regarded as anomalous. Further reference to Figure 38 shows an equitable poor relationship exists between ground surface behaviour and rainfall.

The correlation between changes of elevation adopted by subsurface water and ΔH_s , ΔH_u and ΔH_l movements are, however, more definite. In Figures 39a and 39b the correlation coefficients are given to indicate the relationship between the subsurface water

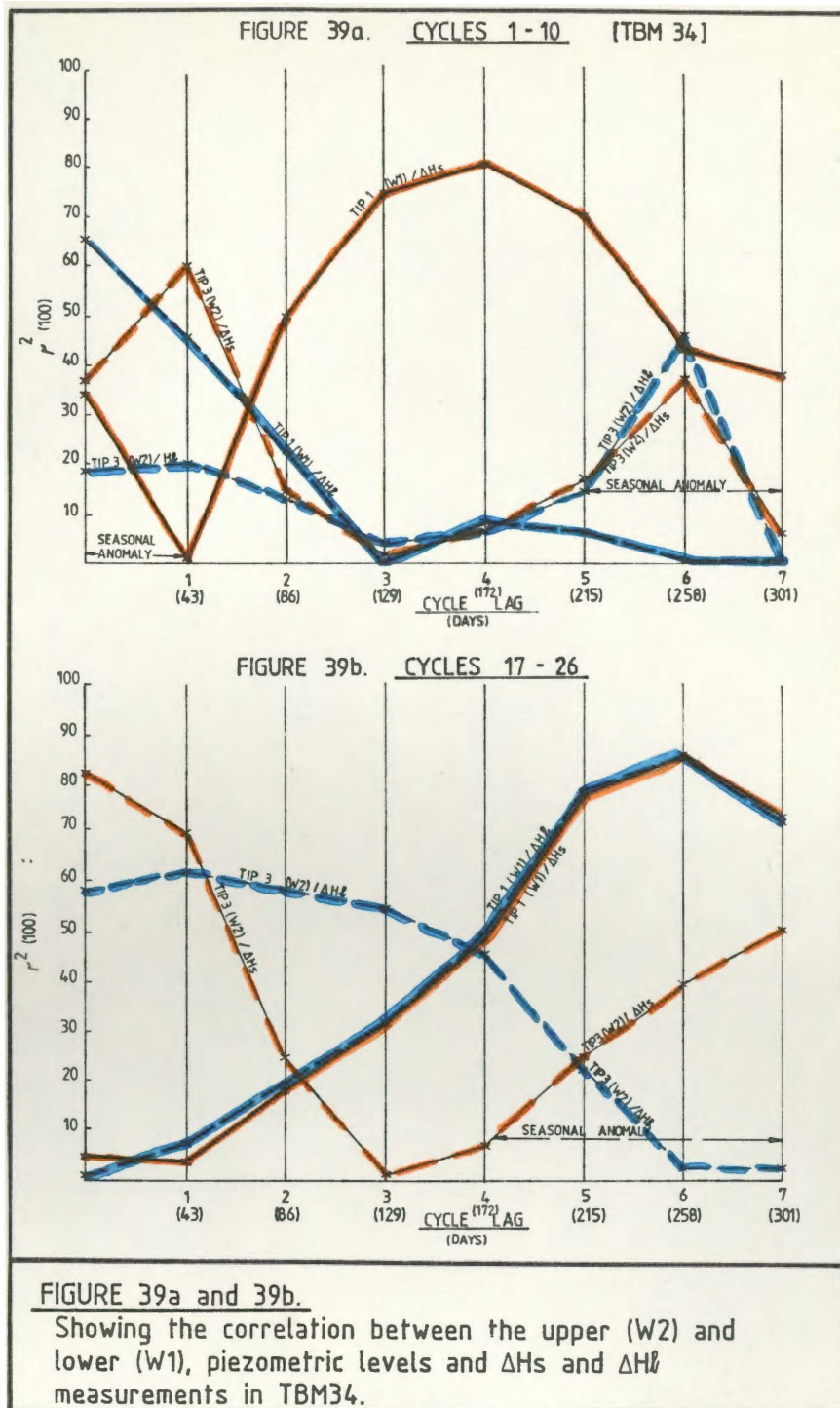
/movements ---

movements measured in piezometer Tip 3 (W2) and Tip 1 (W1) and the ΔH_s and ΔH_θ movements in TBM 34, over measuring cycles 1 to 10 and 17 to 26. In both instances, the ΔH_u relationship is omitted in the interests of clarity since it corresponds almost identically with the ΔH_s and subsurface water correlations.

The reason for the segregation of these two periods of measurement is to take cognisance of the change in the recharge pattern which occurred subsequently to February 1980 (Cycle 10) as previously described in pages 128 and 129 of this text. Although the changed recharge pattern prevailed from measuring cycles Nos. 11 to 25, the correlation coefficient analysis is confined to measuring cycles Nos. 17 to 26 so as to have the same statistical population as measuring cycles Nos. 1 to 10 as well as comparative climatic conditions.

The actual ΔH_s , ΔH_θ and piezometer tip measurements are tabulated in Appendix 17 while the data derived from correlation coefficient analyses undertaken from these respective measurements are given in Appendix 18.

/ Table 39a ---



Between measuring cycles 1 to 10, the uppermost subsurface water system, as measured by Tip 3 (W2) 21,01m from surface, asserts a 60,13 per cent and 19,5 per cent influence on ΔH_s and ΔH_l movements / respectively ---

respectively after a one cycle lag which amounted to 43 days as shown in Figure 39a.

By the end of 3 cycles, or a time lag of a further 86 days, the influence of the W2 subsurface water was reduced to 1,83 per cent and 3,35 per cent for ΔH_s and ΔH_l respectively. The renewal of W2 influence on ΔH_s and ΔH_l after 6 cycles lag must be regarded as false as it coincides with a subsequent seasonal fluctuation of recharge similar to that at measuring cycle "0" resulting in equitable W2 elevation and associated ground movements.

The behaviour of the lower subsurface water system (W1) is also of interest. Between the 1 and 4 lag intervals, amounting to 129 days, it asserts an ever-increasing influence on surface behaviour until a correlation coefficient of 80,73 per cent is attained in respect of ΔH_s measurements. After the 4 cycle lag interval, the influence of the W1 water system rapidly diminishes. During the same time lag intervals it is noteworthy that the ΔH_l movements are unaffected by elevation changes in the piezometric surface of the W1 water system. Attention must be drawn, however, to the correlation between the W1 water movements and the ΔH_s and ΔH_l behaviour at the zero lag interval in Figure 39a. It is apparent that these correlations are anomalous, being the "tail-end" of a previous period of seasonal movements.

/ The ---

The relationship between subsurface water behaviour and ΔH_s and ΔH_ℓ movements in measuring cycles 17 and 26 show the influence of the strong, local and artificially induced recharge as from February 1980. Thus, the uppermost water regime (W2), asserts an 82,67 per cent influence on ΔH_s behaviour at a zero lag interval compared with 37,37 per cent during cycles 1 to 10 as can be seen when comparing Figure 39a and Figure 39b. More significantly, however, is the greater influence asserted by the W2 water regime on ΔH_ℓ behaviour. Whereas in measuring cycles 1 to 10, the piezometric surface elevation changes of the W2 water system had a mere 19,5 per cent correlation with ΔH_ℓ movements, this correlation averages 58,9 per cent over four cycle lag periods, or 172 days, in measuring cycles 17 to 26. The intensified recharge of aquifers from February 1980 is also reflected in the influence of the lower water regime (W1) on ΔH_s and ΔH_ℓ measurements. Besides beginning to assert itself only after the influence of the W2 water system is diminishing, that is after 172 days or a 4 cycle lag period, the fluctuating piezometric surface of the lower subsurface water has equal control of ΔH_s and ΔH_ℓ behaviour for a time period in excess of 215 days. Attention must be drawn to the apparent re-assertion of the W2 water regime on ΔH_s and from 4 cycle lag period onwards as

/ shown ---

shown in Figure 39b. As was previously the case in Figure 39a, this renewed influence of W2 must be regarded as representing the beginning of a different seasonal recharge cycle.

Correlation coefficient analyses between W1 and W2 water system movements and the ΔH_s , ΔH_u and ΔH_ℓ behaviour was also conducted on measurements from TBM No. 32 and 22. In each case the results obtained were identical with those described in respect of TBM No. 34. It can be concluded, therefore, that in the Compound area :

- (i) surface and subsurface movements recorded in telescopic bench marks are controlled or affected by seasonal fluctuations of subsurface water and their associated piezometric levels.
- (ii) The fluctuations of piezometric levels are only indirectly associated with rainfall.
- (iii) Each subsurface water system asserts independant influences on the ΔH_s , ΔH_u and ΔH_ℓ movements occurring in telescopic bench marks. In the case of the uppermost
/ water ---

water regime (W2), maximum influence is affected on the surface and subsurface some 43 days after it changes elevations. By contrast, an elevation change of the lower water regime (W1) is only reflected by ΔH_s , ΔH_u and ΔH_l behaviour after a time interval of between 86 days and 129 days has elapsed during measuring cycles 1 to 10 and 17 to 26 respectively.

Factory Area

To determine the influence of subsurface water in the factory area, correlation coefficient analyses were undertaken between subsurface water movements, as recorded in a piezometer cluster situated immediately west of the Gas Producer relative to ΔH_s , ΔH_u and ΔH_l changes in TBM 10. The Gas Producer piezometer comprises five tips set at the following depths below surface:

TABLE 12.	
TIP NO.	DEPTH BELOW SURFACE (m)
1	- 24,51
3	- 21,08
4	- 18,08
5	- 30,67
6	- 26,87

Depths of measuring tips below surface in piezometer cluster west of Gas Producer at Driefontein Brickworks.

By means of correlation coefficient analyses, of subsurface water movements it was established that two distinct subsurface water systems, as was the case in the Compound area, also are present in the environs of the Factory. This conclusion is reached from the strong correlation of 81,13 per cent which exists between the measurements (absolute mean movement over 20 cycles of $0,39\text{m} \pm 0,24$ and $0,03\text{m} \pm 0,05$) recorded by Tips 3 and 1, situated 21,08m and 24,51m below surface respectively, indicating that these tips monitor the same subsurface water regime. Similarly, a $\geq 64,67$ per cent correlation between the subsurface water movements measured by piezometer Tips 4, 6 and 5, situated 19,08m, 26,87m and 30,67m below surface respectively, (absolute mean movements over 20 cycles of $0,06\text{m} \pm 0,28$, $0,04\text{m} \pm 0,26$ and $0,09\text{m} \pm 0,52$) indicate these tips are within a hydrological system distinct from that monitored by Tips 3 and 1.

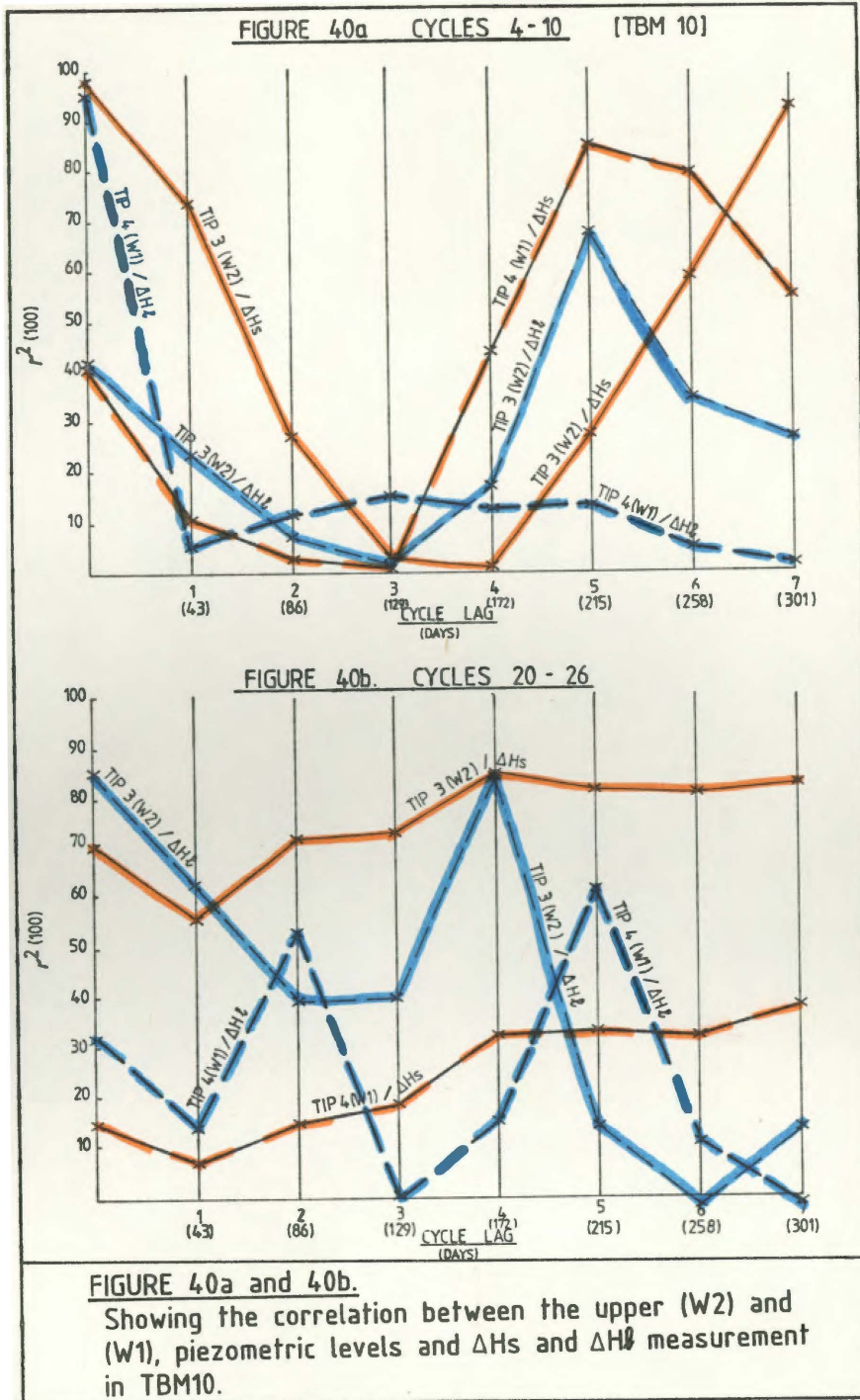
To determine the influence asserted by these two distinct subsurface water regimes, their changes of elevation were compared with the ΔH_s , ΔH_u and ΔH_θ measurements obtained from TBM 10. This particular telescopic bench mark was selected because of its proximity to sinkhole No. 17 which occurred during measuring cycle 10 in February 1980, as previously described. Once again, correlation coefficient analyses were undertaken prior and subsequent to

/measuring ---

measuring cycle 10, that is February 1980, when the recharge pattern changed at Driefontein. Because TBM 10 was only installed in late April 1979, only seven sets of measurements, that is Measuring Cycles 4 to 10 are available prior to February 1980. For statistical reasons, these readings are compared with those for Measuring Cycles 20 to 26 subsequent to the change of recharge pattern. The actual ΔH_s ΔH_ℓ and piezometer tip measurements are tabulated in Appendix 19 whilst the data obtained from correlation analyses conducted on these respective movements are given in Appendix 20. In Figure 40a and 40b, these correlation coefficient analyses are graphically illustrated. In both instances, the ΔH_u relationship is excluded in the interests of clarity since it corresponds almost identically with the ΔH_s and subsurface water correlation.

Between Measuring Cycles 4 to 10, it is apparent that the subsurface water movements recorded by Tip 3, which is the piezometric level of the upper water regime (W2), asserts considerable influence on ΔH_s measurements. This influence lasts from a zero lag interval to a 3 cycle lag interval equating to 129 days.

/ The ---



| The ---

The upper subsurface water system only commences affecting $\Delta H\ell$ behaviour after a 4 cycle lag interval (ie. 172 days) until a peak correlation of 67,01 per cent is achieved after a time lapse of 215 days. This cyclic influence of the W2 subsurface water regime on ΔHs and $\Delta H\ell$ behaviour would suggest that the W2 aquifer is a leaky one so that downward seepage is taking place. It should be noted that the influence of the W2 water system on ΔHs behaviour from the 4 cycle lag onwards is artificial, being a seasonal anomaly which occurred prior to Measuring Cycles 4 to 10.

As was the case of hydrological behaviour in the Compound area, so also the lower water regime in the Factory area only begins asserting itself upon ΔHs measurements after a delay of about 4 cycles (ie. 172 days). Thereafter, a maximum correlation of 84,76 per cent on ΔHs is attained at the 5 cycle lag interval which amounts to a lapse of 215 days from the time that an elevation fluctuation occurred in the W1 water regime. No significant influence is, however, asserted by this lower subsurface water regime on $\Delta H\ell$ behaviour.

Subsequent to February 1980, which was marked by a sinkhole occurrence in close proximity to TBM 10, dramatic changes occurred in the hydrological pattern

/ as ---

as can be seen by the correlation coefficients for Measuring Cycles 20 to 26. These dramatic changes can be summarised as follows :

- (i) The influence of the W2 water regime on surface behaviour is continuous for a 7 cycle lag period (ie. 301 days) with a mean correlation coefficient of 77,12 per cent.
- (ii) Little or no influence is asserted by the lower water regime W1 on ΔH_s measurements.
- (iii) The lower subsurface water system (W1) has a cyclic influence on ΔH_ℓ behaviour; maximum correlations of 55,27 per cent and 64,10 per cent being attained after 2 and 5 cycle lag intervals respectively. By contrast, the upper subsurface water (W2) achieves maximum influence of 86,86 per cent at the 4 cycle or 172 days lag interval.

It is apparent from the above changes that the occurrence of the sinkhole close to TBM 10 ruptured the W1 aquifer. As a result, subsurface water from the W1

/ aquifer ---

aquifer now replenishes the W2 piezometric level so that the cyclic influence on ΔH_s behaviour no longer exists. Substantiation that the lower water regime now feeds the upper water regime is afforded by the cyclic pattern of ΔH_l behaviour relative to W1 and W2 water movements at cycle lag intervals 1 and 4 respectively as soon in Figure 40b.

In conclusion, it becomes apparent that elevation changes in subsurface water as a result of seasonal recharge asserts considerable control on surface and subsurface movements in telescopic bench marks. Such fluctuations of subsurface water on their own, however, cannot motivate movements in either subsoils or ground surface. Consequently, it is now proposed to describe in some detail the factors that contribute to the occurrence of positive (upward) and negative (downward) movements.

4.2.3.1 Negative Movements

Negative movements or subsidence must be regarded as a function of compressibility and effective stress occurring in the subsoils. Freeze and Cherry (1979) define compressibility as a "... material property that describes the change in volume, or strain, induced in a material under an applied stress." If, for

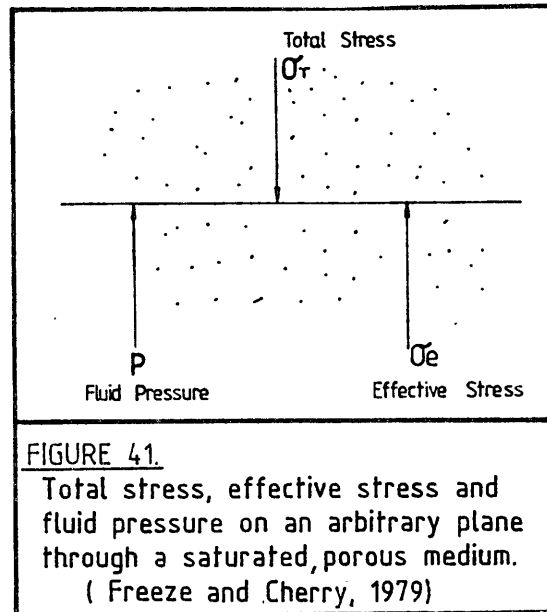
/ example ---

example, stress is applied to a porous medium such as sand or a compactible one like manganiferous wad, a reduction of volume can be affected by the following mechanisms :

- (i) Compression of any water and air in the pores of the material.
- (ii) Compression of the material's individual particles or grains.
- (iii) Re-arrangement of the particles or grains in the material.

Normally, the first of the above mechanisms is a function of fluid compressibility whereas the effects of the second mechanism are virtually negligible. The third mechanism involves the concept of effective stress first proposed by Terzaghi (1927). As Freeze and Cherry (1979) point out, a stress equilibrium is achieved on an arbitrary plane through a saturated geological formation of depth as shown in Figure 41.

/ Figure 41 ---



The total stress ' σ_T ', acting downward on the plane, is due to the weight of overlying subsoil or rock and water. This stress is partly borne by the granular skeleton of the porous medium and also by the fluid pressure 'P' of water in the pores. The portion of total stress which is not borne by the fluid may be defined as effective stress ' σ_e '. It is the effective stress which is applied to the particles or grains of the porous medium. Thus, re-arrangement of the grains or particles occurs, with resulting compression of the granular skeleton, which is induced by changes in the effective stress rather than by total changes of total stress. The relationship of the two stresses can be expressed by the equation :

$$\sigma_T = \sigma_e + P$$

$$\sigma_T = \sigma_e + P$$

or, in terms of the changes:

$$\Delta\sigma_T = \Delta\sigma_e + \Delta P$$

In many instances, there is no change of total stress and the weight of subsoil or rock and water overlying any specific point in the system remains constant through time so that :

$$\Delta\sigma_T = 0 \text{ and } \Delta\sigma_e = -\Delta P$$

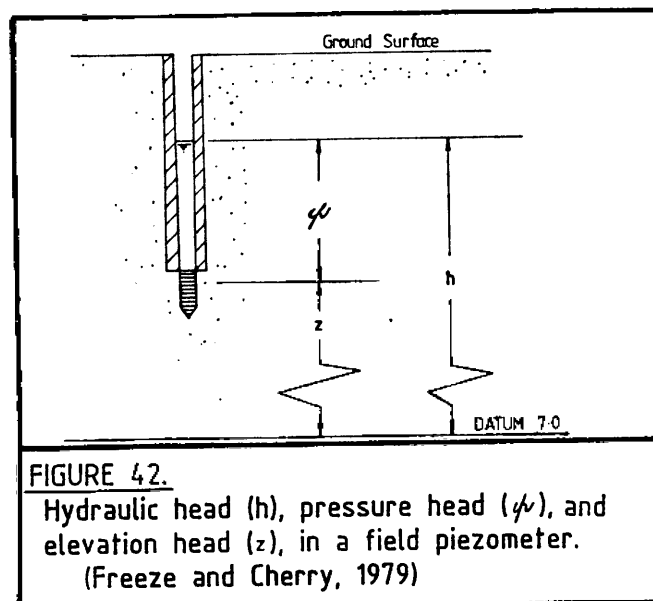
Under these conditions, should the fluid pressure increase, then the effective stress will decrease by an equal amount. Conversely, if the fluid pressure decreases then the effective stress will increase correspondingly. Where the total stress does not change with time, however, the effective stress at any point in the system together with the resulting volumetric deformations, are controlled by changes of fluid pressure. Because fluid pressure 'P' = $Pg\phi$ and $\phi = h-z$, where z, the elevation at the point of measurement, is constant whilst g, ϕ and h represent gravity, pressure head and hydraulic head respectively, then changes in the effective stress are governed by changes in the hydraulic head as

/ explained ---

explained in the equation :

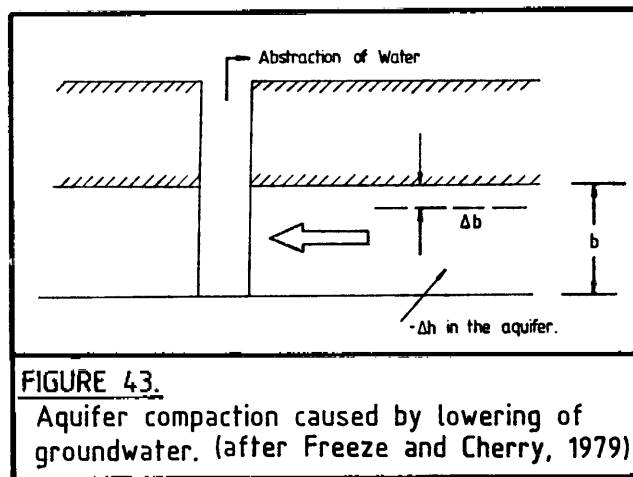
$$\Delta\sigma_e = -Pg\Delta\phi = -Pg\Delta h$$

It follows, therefore, that the hydraulic head is a function of the pressure head which, in turn, is dependent upon the elevation head. This inter-relationship is diagrammed in Figure 42.



Consequently, changes in either groundwater or piezometric levels must exert considerable influence on subsurface stress behaviour. The validity of this conclusion is substantiated by correlation coefficient analyses conducted in the Compound and Factory areas at Driefontein. Although the resulting subsurface stress field will have both vertical and horizontal expressions, the former will be the most / dominant ---

dominant factor influencing compressibility of an aquifer or porous medium with resulting subsidence. The nature of deformation which can occur in a compressed aquifer or saturated porous medium is illustrated in Figure 43.



Should the weight of overlying material remain constant and the hydraulic head in the aquifer or saturated porous layer be decreased by an amount of $-\Delta h$, then compaction can be expressed as follows :

$$\Delta b = -\alpha b \Delta \sigma_e = \alpha b P_g \Delta h$$

/ In - - -

The above equation, 'b' represents the thickness of the aquifer or saturated porous layer, ' α ' the aquifer's compressibility, 'P' the fluid pressure and 'h' the hydraulic head. The minus sign indicates that the decrease in hydraulic head produces a reduction in the thickness of the aquifer or porous layer. Thus, in the Driefontein area, the main water table was lowered because of dewatering the Bank Compartment. In response, effective pressure increased resulting in the compaction of saturated porous layers and aquifers. Such compaction of compressible horizons in the geological succession was propagated to the ground surface so that subsidence, doline and sinkhole, developments were inevitable.

4.2.2.4. Positive Movements.

Unlike incidences of subsidence, the reasons for positive or upward movements of the surface and subsurface require explanation. Obviously, the changes of elevation adopted by subsurface water systems could not on their own be responsible for the positive ΔH_s , ΔH_u and ΔH_l movements recorded in telescopic bench mark installations.

/Thus,

Thus, in the same way as subsidence is promoted by consolidation of a porous material, positive movements are a result of subsurface water saturating material with expansive potential. From X-ray diffraction tests conducted on the Karoo argillaceous rocks at Driefontein, it was established that the main clay minerals present are kaolin and illite. Even so, it was suspected that a swelling clay mineral, such as montmorillonite, may also be present in small quantities. The ability of a clay mineral, particularly montmorillonite, to absorb water and then expand depends upon such factors as the amount of clay mineral present, the exchangeable ions, electrolyte content of the aqueous phase, particle size distribution, void size, void distribution, internal structure and water content. The swelling potential of clays diminishes in the order montmorillonite, illite, halloysite and kaolinite as shown below in Table 13 :

TABLE 13.	
CLAY MINERAL	% FREE SWELLING
Na Montmorillonite	1400 - 1600
Ca Montmorillonite	45 - 145
Illite	15 - 120
Halloysite	70
Kaolinite	5 - 20
The swelling potential of montmorillonite, hallosite and kaolinite clay minerals. (after Mielenz and King, 1955)	

/It

It was decided, therefore, to determine the expansive-ness potential of the subsurface materials at localities in Driefontein where positive movements of ΔH_s , ΔH_u and ΔH_ℓ were either occurring or had taken place in the past. Two 750mm diameter boreholes were drilled to the northwest of the Compound in the vicinity of the palaeo-sinkhole and a further two in the European housing area so that undisturbed clay samples could be taken. The localities of the four boreholes are given in Appendix 21. Dr. A.B.A. Brink was commissioned to collect the undisturbed samples for laboratory testing by messrs. Kantey and Templer and also prepare geological profiles. Details of the profiles and the results of laboratory tests are given in Appendices 22 - 23 and 24 - 25 respectively. It is apparent from the indicator tests that the subsurface materials have an expansiveness potential ranging from low to high. The results of the swell under load tests are, however, less clearly defined. Nevertheless, the overall impression is one of a comparatively low expanding subsurface materials profile, the reactions of which are dependent upon movements of subsurface water. This impression is further confirmed by the correlation coefficient analyses between the ΔH_s , ΔH_u and ΔH_ℓ behaviour and elevation changes adopted by the various water regimes which have previously been discussed in some / detail ---

detail. Even so, the following discrepancies exist which require explanation :

- (i) The montmorillonite clay mineral is indiscriminately disseminated in the Karoo mudstones, siltstones and shales rather than being concentrated in any specific stratigraphical unit.
- (ii) The amounts of elevation fluctuations adopted by subsurface water are comparatively small, seldom exceeding a total movement of more than 0,4m to 0,6m as shown in Table 14.
- (iii) As can be seen by reference to Appendices 26 and 27, the clay-bearing materials situated above the subsurface water level have a moderately high moisture content. Immediately above the subsurface water level, the average moisture content is 22,79 per cent which drops to 18,16 per cent some 5,50m above it. Even immediately below the topsoil, the Karoo clay-bearing materials have a moisture content in excess of 12 per cent.

| Table 14 ---

TABLE 14.					
PIEZOMETER CLUSTER NW OF COMPOUND					
TIP NO.	DEPTH FROM SURFACE (m)	TOTAL POSITIVE AND NEGATIVE WATER MOVEMENTS (m)		WATER REGIME	MEAN POSITIVE/NEGATIVE WATER MOVEMENT (m)
		CYCLES 1 - 10	CYCLES 17 - 26		
3	-21,07	0,82	2,76	W ²	1,79
6	-26,87	0,98	2,80	W ²	1,89
MEAN		0,90	2,78	W ²	1,84
1	-24,50	0,62	1,08	W ¹	0,85
5	-30,67	0,58	0,16	W ¹	0,37
MEAN		0,60	0,62	W ¹	0,61
PIEZOMETER CLUSTER W OF GAS PRODUCER					
TIP NO.	DEPTH FROM SURFACE (m)	TOTAL POSITIVE AND NEGATIVE WATER MOVEMENTS (m)		WATER REGIME	MEAN POSITIVE/NEGATIVE WATER MOVEMENT (m)
		CYCLES 4 - 10	CYCLES 20 - 26		
3	-21,08	0,70	0,76	W ²	0,73
1	-24,51	0,12	0,04	W ²	0,08
MEAN		0,41	0,40	W ²	0,41
4	-18,00	0,30	0,38	W ¹	0,34
6	-26,87	0,34	0,42	W ¹	0,38
5	-30,67	0,50	0,72	W ¹	0,61
MEAN		0,38	0,51	W ¹	0,44
Subsurface water movements in the Driefontein Brickworks area.					

It is apparent that the concentration of the montmorillonite clay mineral, within the vicinity of the subsurface water elevation changes, is too low to influence the positive ΔH_s , ΔH_u and ΔH_θ measurements reflected in telescopic bench marks. Furthermore, the saturation for at least 12m above the highest subsurface water level of materials bearing clay minerals cannot be attributed to downward seepage as was proven by the poor correlation between rainfall and ΔH_s , ΔH_u and ΔH_θ behaviour. Consequently, upward moisture migration must occur sympathetically with positive, subsurface water elevation changes.

There are three mechanisms for such upward migration that should be considered, namely capillary action, absorption by clay minerals and the concepts of

/ air ---

air entrapment and atmospheric pressure.

Capillary Action

Capillary action can only occur in the unsaturated or vadose zone which, as defined by Freeze and Cherry (1979), has the following properties :

- (i) It occurs above both the water table and the capillary fringe.
- (ii) The pores are only partially filled with water and the moisture content ' θ ' is less than the porosity ' n '.
- (iii) The fluid pressure ' P ' is less than atmospheric and the pressure head ' ψ ' is less than zero.
- (iv) The hydraulic head can only be measured by using tensiometers because the pressure head is negative.
- (v) The hydraulic conductivity ' K ' and the moisture content ' θ ' are both functions of the pressure head ' ψ '.

In short, for unsaturated flow $\psi = <0$, $\theta = \theta(\psi)$ and $K = K(\psi)$ whereas for saturated flow $\psi = >0$, $\theta = n$ and $K = K_0$. Thus, in the capillary fringe, the pores are saturated but the pressure heads are less than atmospheric. Freeze and Cherry (1979) maintain that because fluid pressures are less than atmospheric, no flow can occur from the capillary fringe or "tension saturated zone". Consequently, this mechanism must be disregarded.

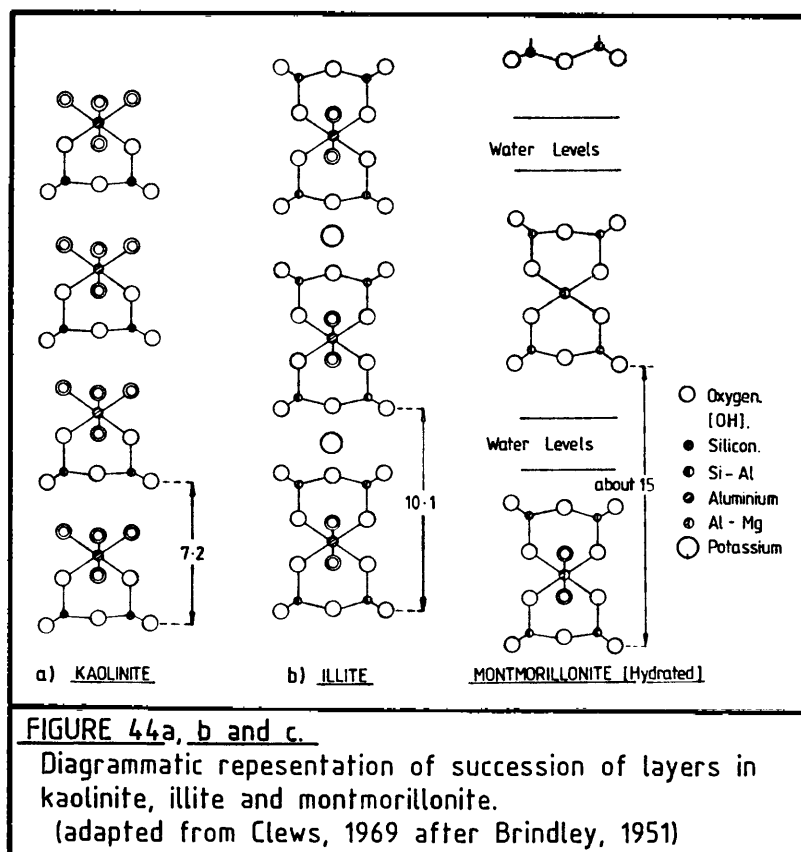
*Mineralogy of Materials in the
Vadose Zone*

The shales, siltstones and mudstones which, in the Driefontein area, invariably lie within the vadose zone consist mainly of quartz, illite and kaolinite with less dominant quantities of montmorillonite. Some typical analyses of these sedimentary rocks, in which the clay constituents are expressed as alumina, are given in Table 15.

TABLE 15.					
Constituent	Sample A	Sample B	Sample C	Sample D	Mean
SiO ₂	52,76	50,99	52,92	52,57	52,31
Al ₂ O ₃	30,19	32,21	31,26	30,90	31,14
MgO	0,34	0,51	0,56	0,67	0,52
CaO	0,31	0,39	0,16	0,16	0,26
Na ₂ O	0,18	0,18	0,13	0,13	0,16
K ₂ O	1,30	1,30	1,15	1,10	1,21
Fe ₂ O ₃	3,36	2,66	3,08	2,94	3,01
TiO ₂	1,30	1,40	1,30	1,30	1,33
Loss	10,90	11,32	10,15	11,01	10,85
TOTAL	100,64	100,96	100,71	100,78	100,79
Chemical analyses of Karoo shales and mudstones.					

/ The ---

The clay minerals in these sedimentary rocks are crystalline in character with a well-ordered spatial pattern. Thus, well-defined layers comprising sheets of oxygen and hydroxyl cores surround the cations Si, Al, Mg, Fe and so on. The layer structures of kaolinite, illite and montmorillonite are illustrated in Figures 44a, b and c. When water molecules are placed within the environs of clay particles, ions are attracted to the surface site, and then a structure of water molecules is built around the particle. Thus, $(OH)^-$ ions are absorbed onto the cationic sites so that a structure of water molecules is built around the particle and $(OH_3)^+$ ions absorbed onto the anionic sites. The ability of clay to absorb water, even against gravitational forces and differences in hydraulic pressures, is displayed by montmorillonite.



Although montmorillonite present above the capillary fringe could, therefore, absorb some moisture from below, it is unlikely that it will transmit moisture to overlying clays.

*Air-Entrapment and Atmospheric
Pressure Effects*

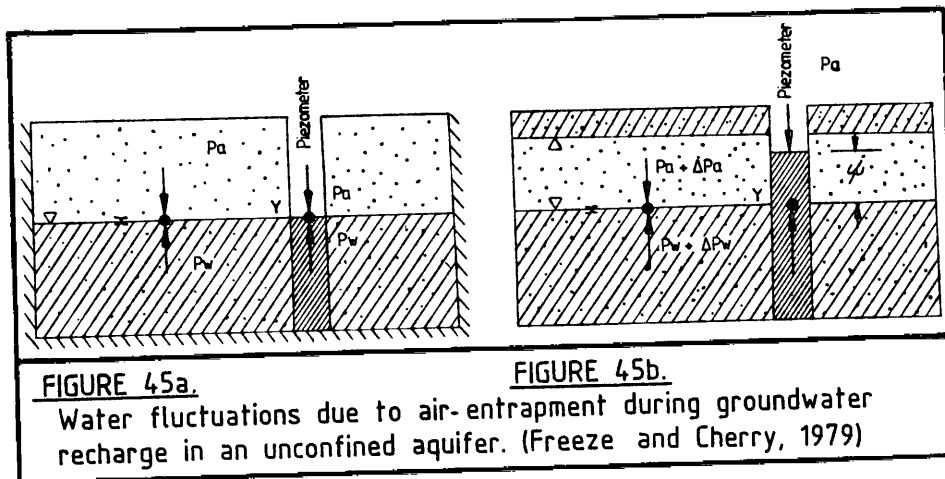
Many researchers, such as McWhorter (1971) as well as Bianchi and Haskell (1976) have observed that anomalously large rises of water levels occur in wells, boreholes and piezometers penetrating aquifers. It is becoming increasingly recognised that these anomalous levels can be attributed to the concepts of air-entrapment in the case of unconfined aquifers and atmospheric pressure influences in confined aquifers. It is proposed that the slump structures, so frequently developed in outliers infilled with Karoo rocks, have been accompanied by the development of sympathetic stress planes, axial planes and tension cracking in these materials. These planes of structural weakness will, if penetrating an aquifer, behave like small-scale wells, boreholes or piezometers and promote the upward migration of moisture to abnormal levels beyond the capillary fringe.

The principle of air-entrapment is as follows. After a heavy rainfall, an inverted zone of saturation is created at ground surface. The advancing wet front traps air between itself and the water table with the result that air pressure in this zone builds up to greater than atmospheric. A schematic

/ illustration,---

illustration, after Freeze and Cherry (1979) is given in Figures 45a and b.

In Figure 46a, the air pressure ' P_a ' in the subsoil material is at equilibrium with both the atmospheric and fluid pressure ' P_w '. Such a state of equilibrium will prevail at every point 'x' on the water table within the permeable medium and also at point 'Y' in the well.



However, the advancing wet front caused by infiltration, as shown in Figure 45b, will cause an increase in the pressure of the entrapped air ' ΔP_a '. Thus, the build up of fluid pressure on the water table at point 'x' must increase by an equivalent amount ' ΔP_w '. The pressure

/ equilibrium ---

equilibrium at point 'Y' can be expressed by the following equation in which ' γ ' represents the specific weight of water.

$$P_a + \gamma h = P_w + \Delta P_w \quad (\text{Freeze and Cherry, 1979}).$$

Since ' P_a ' equals ' P_w ' and ' ΔP_a ' equals ' ΔP_w ', the above equation logically becomes :

$$\gamma h = \Delta P_a$$

With ' P_a ' being greater than zero, it can be proved that an increase in the pressure of entrapped air leads to a rise in the water level of any well, borehole or piezometer.

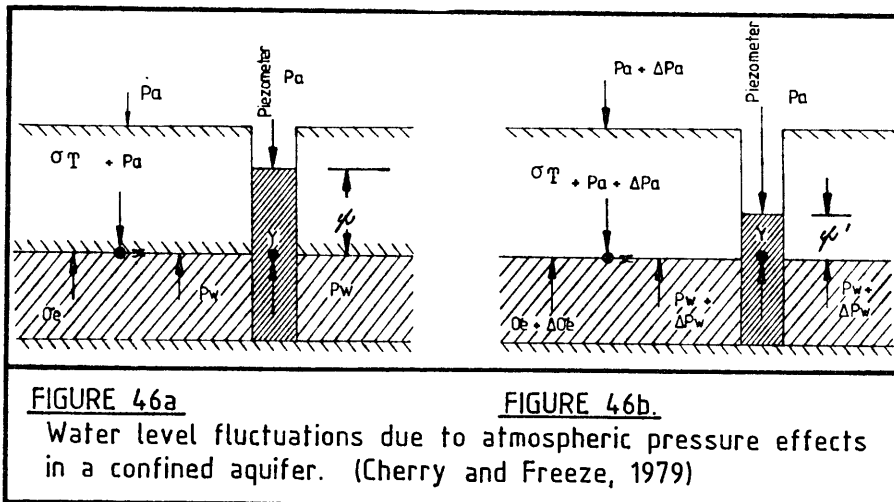
In the case of wells, boreholes, or piezometers penetrating a confined aquifer, increases of atmospheric pressure can produce large fluctuations of piezometric levels. The relationship is an inverse one to that described for air-entrapment since increases in atmospheric pressure lead to declines in observed water levels. To explain the influence of atmospheric pressure, the principle of effective stress can be applied. Thus, in Figure 46a, the stress equilibrium at point 'x' can be expressed by :

$$\sigma_T + P_a = \sigma_e + P_w \quad (\text{Freeze and Cherry 1979}).$$

/ In ---

In the above equation, 'Pa' represents air pressure 'σ_T' the total stress created by the overlying pressure caused by the weight of overlying rock and subsoil, 'σ_e' the effective stress acting upon the granular skeleton of the aquifer and 'P_w' the fluid pressure of the aquifer. The fluid pressure 'P_w' gives rise to the pressure head 'h' which can be measured in a piezometer tapping the aquifer. At point 'Y' in Figure 46a, the condition will be:

$$P_a = \gamma h = P_w$$



When the atmospheric pressure is increased by an amount of ΔPa, as shown in Figure 46b, the change

/ of ---

of stress equilibrium at point 'x' will be given by :

$$\Delta P_a = \Delta \sigma_e + \Delta P_w \quad (\text{Freeze and Cherry, 1979}).$$

From the above equation it is apparent that ΔP_a is greater than ΔP_w so that at point 'Y' the condition will be :

$$P_a + \Delta P_a + \gamma h' = P_w + \Delta P_w \quad (\text{Freeze and Cherry, 1979})$$

By substitution, the above equation can be resolved to :

$$\Delta P_a - \Delta P_w = \gamma(h - h')$$

Since $\Delta P_a - \Delta P_w$ is greater than zero, so also must $h - h'$ be greater than zero thereby proving that an increase in atmospheric pressure leads to subsurface water levels being depressed. Conversely, a decrease in this air pressure will cause water levels in wells, boreholes and piezometers to rise.

Freeze and Cherry (1979) also observe that changes in atmospheric pressure may induce small fluctuations in the water level of unconfined aquifers. Thus,

/ as

as the air pressure increases, water tables fall. Peck (1960) attributes such elevation changes to the effects of changing air pressures on air bubbles entrapped in the soil moisture zone. As the pressure increases, so the entrapped air is considered to occupy less space and it is replaced by soil moisture, thereby inducing an upward or positive migration of moisture from the water table.

4.2.2.5 Conclusion

The correlation coefficient analyses conducted in the Driefontein outlier indicate a strong relationship between elevation changes of subsurface water and subsurface as well as surface movements. Conversely, only a weak correlation exists between surface and subsurface movements and rainfall. It becomes apparent, therefore, that the upward migration of moisture through montmorillonite-bearing clays in the vadose zone, must be occurring. Since neither capillary action nor the absorption ability of montmorillonitic materials is capable of promoting sufficient upward moisture migration, it must be concluded that the principle mechanism responsible for positive movements, both at subsurface and surface levels, are those of air entrapment and atmospheric pressure effects.

- - - o O o - - -

PART 5

5. PREDICTION OF GROUND INSTABILITY IN KAROO OUTLIERS

So far in this dissertation, the analyses and interpretations of surface and subsurface movements have been retrospective. It is considered, however, that by the application of further interpretive and statistical techniques to existing data, predictions can be made as to the degree and intensity of future ground instability in Karoo outliers, particularly if they have been dewatered.

5.1 PROPOSED INSTABILITY RISK POTENTIAL EVALUATION

Besides the slump structures present in most Karoo outliers, the thicknesses and lithological characteristics of the materials infilling the palaeo-karst topography developed in the dolomite, has a direct bearing on current ground instability. It is considered possible to formulate a method whereby the potential instability of a specific area may be evaluated by using the above mentioned influences. Although it is beyond the scope of this current research to compile an authoritative formula it is intended, nevertheless, to outline the concept of such an evaluation and describe the necessary data inputs. The basic information required for the proposed evaluation includes:-

/i) The ---

- i) The physical or engineering characteristics of individual lithological units constituting a geological profile, ranked according to their potentials for instability.
- ii) The instability potential of a specific geological profile is compiled by weighting the engineering or physical characteristics of each lithological unit in the succession according to its thickness or apparent thickness and position as will be explained later in the text.
- iii) An appreciation of the impact that subsurface water movements may have in promoting instability on a specific geological profile.
- iv) Detailed knowledge of the dolomitic bedrock profile and presence of cavities within the rock.

5.1.1 METHODS FOR OBTAINING HYDROLOGICAL AND GEOLOGICAL DATA

Because of the major influence that subsurface water movements may have on promoting instability, it is essential that some boreholes are drilled for the purpose of determining the depths and complexities of hydrological systems in an area. Either single or multi-tipped piezometers should be installed at sites regarded as strategic and routine measurements

/both of ---

both of the subsurface water levels as well as the collar elevation of each installation, should be undertaken on a routine basis.

Numerous techniques are available for obtaining geological information including aerial photography, radar and thermal imagery as well as geophysical methods, acoustical methods and exploratory drilling. Each of these techniques has its own advantages and limitations. Thus, thermal imagery cannot be used in areas where shallow groundwater or deep ground cover exist. Exploratory drilling, whilst capable of giving accurate structural and stratigraphical information, is both costly and time consuming. Of the geophysical methods available, which include seismic refraction, magnetometer, electrical resistivity, multi-frequency electromagnetic, and gravimetric traverses, only the last two mentioned have comprehensive potential. Even so, the multi-frequency electromagnetic method, currently being investigated by the Geological Survey, is incapable of detecting shallow, wad-choked slots. The gravimetric method enables subsurface valleys to be detected particularly when Bouguer values have been calculated and corrections, based on selected borehole information, have been applied to eliminate regional trends. Providing the gravimetric stations are set out on a close grid, the gradients of slot sides

/ can ---

can be deduced, thereby enabling reasonable predictions to be made in respect of doline-prone areas.

Even so, the gravimetric method has the disadvantage of being unable to delineate areas where sinkholes may occur, define the outlines of dolomitic pinnacles or distinguish between dolomitic bedrock and "floaters".

The major limitations of remote sensing and geophysical methods are that they are unable to locate subsurface voids and can provide no lithostratigraphical information. As far as locating voids is concerned, either accoustical methods, such as variable frequency or subsurface radar techniques, may be tried but in most cases one has to make use of exploratory boreholes drilled at very close centres. The importance of the lithological characteristics of materials infilling depressions and slots in the dolomitic bedrock, has been given particular emphasis in this dissertation. It has become apparent, for example, that an area underlain by dolomitic bedrock with a severe palaeo-karst configuration may be geotechnically stable because the infilling material has sufficient tensile strength and is neither readily erodable nor compactible. By contrast, a profile comprising gently profiled bedrock with a mantle of unstable materials within which a fluctuating water table may be present, may have a higher instability potential. Ultimately, therefore, the drilling of boreholes is a prerequisite

/ for ---

for compiling a risk analysis of a specific area, although remote and geophysical methods may assist in determining the required drilling grid density. Ideally core drilling should be used rather than percussion drilling because the former provides a higher yield of information. Core drilling is, however, both expensive and slow whereas percussion drilling is fast and cheap. The fact that percussion drilling results are very largely dependant upon the operator's skills is obviously a disadvantage. Both the operator's skill and the capacity of the drilling machine can, however, be quantified by measuring the following parameters :

- (i) Fluctuations in the rate of penetration which is relative to the resistance of the formation being drilled. Such fluctuations may be indicative of such rock properties as hardness or strength.

- (ii) The percussion "wave" or amount of vibration reflected from the subsurface soil or rock to the drill rod stem. In percussion drilling, part of the energy conveyed by the drill to the hammer is absorbed by the rock being penetrated whereas the remainder is reflected back to surface. This quantity of unused energy, expressed as vibration, is greatest if the rock or subsoil being penetrated is

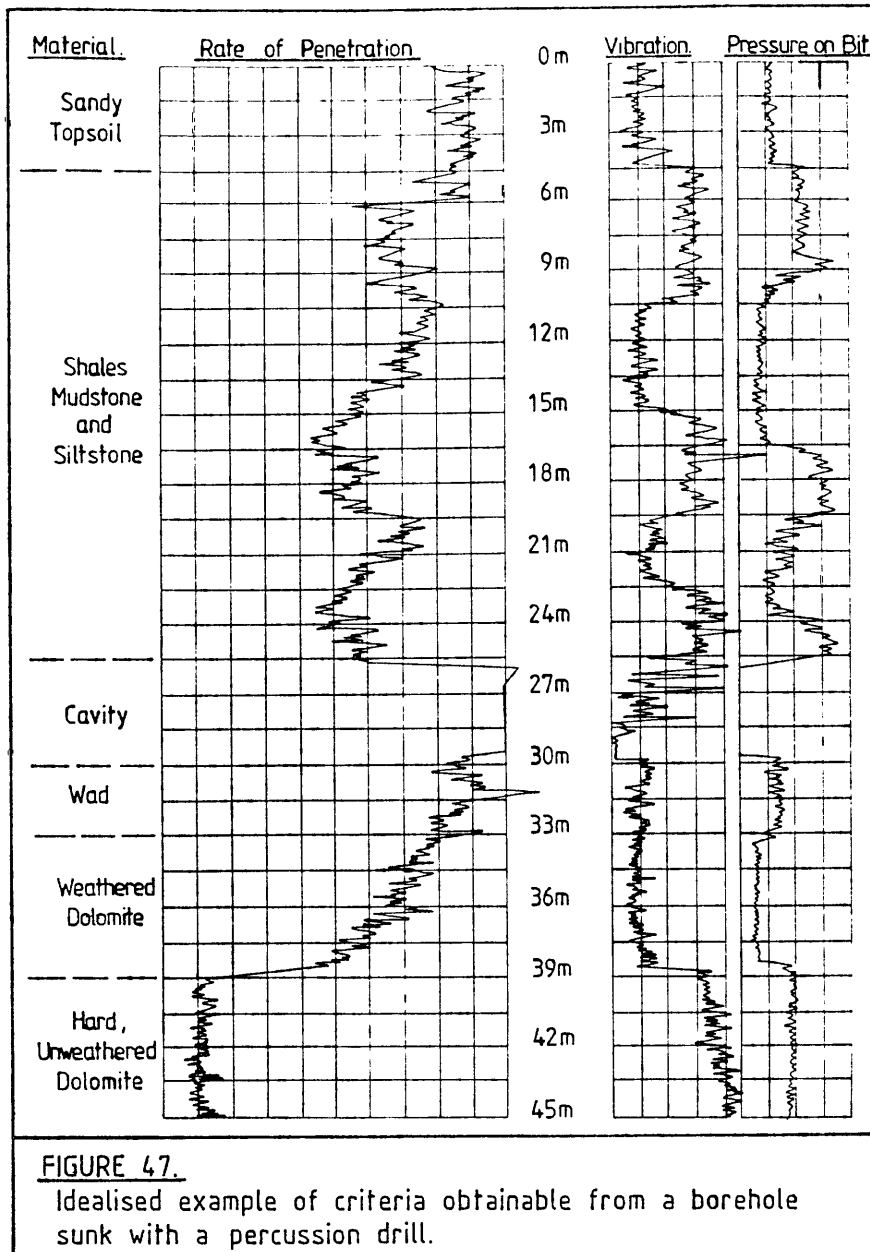
/hard. ---

hard. The so called Vibralog, patented by the Simescol Group, is a typical device used for measuring the quantity of wasted energy when penetrating a subsoil or rock (See Fig.47)

- (iii) The thrust or pressure applied to the drilling bit which verifies the regularity of the drilling operation. Furthermore a decrease in pressure on the bit, is a useful indication when a leached zone or cavity is being intersected (Fig. 47).
- (iv) The rotating torque of the drill stem, providing the drilling machine is fixed with torque meters. Some rocks or subsoils require more torque to penetrate than others. Hard rock for example, is penetrated by the punching effect of the drill bit. By contrast, soft material penetration is accomplished by the scraping action of the drill bit which causes a correlative increase of rotating torque.

The quality of information that can be obtained from measuring the above listed drilling criteria is typified in Figure 47.

/ Figure 47 ---



It is suggested that the cost time factor involved in evaluating the stability of outliers infilled with Karoo sedimentary rocks by means of exploratory drilling, can be considerably reduced if either trenching with a back-actor or shallow boreholes set on a close grid pattern are drilled merely to determine the thickness of topsoil. As was illustrated in Appendix 14, the thickness of topsoil may frequently

/have ---

have a strong correlation with the palaeo-karst configuration of the dolomitic bedrock. Consequently, deep drilling may then be concentrated in areas where the presence of slots or dolines is suspected.

5.1.2 INSTABILITY RANKING OF MATERIALS WITHIN A PROFILE

5.1.2.1 Parameters Affecting Stability

It is considered that the instability potential of an area is promoted by the compressibility, erodability and inverse of tensile strength or cohesion of the geological materials infilling the slots and depressions present in the dolomitic bedrock.

As far as unconsolidated soils, such as manganimiferous wad, are concerned, it is considered that their compressibility may be quantified by their compression index (C_c) and coefficient of consolidation (C_v) values obtained from laboratory tests. In the case of chert gravels and Karoo sedimentary rocks, however, the above-mentioned tests are ineffectual. Wrench (1983) has suggested that plate tests on pedogenic gravels, dolomitic rubble and terrace gravels show relationships between Young's modulus 'E', plate bearing capacity and consistency and that these relationships provide "initial estimates of compressibility and bearing capacity during foundation investigations in gravels.." As far as intact rocks are concerned, Hobbs (1974) also suggests that Young's modulus may also be applied to determine potential instability. In the case of rock masses,

/however ---

however, cognisance must be made of joints and fractures which contribute to potential instability. Coon and Merritt (1970) advocate the use of fracture frequency (i.e. number of fractures per metre) to quantify rock quality in terms of mass factor 'j'. The writer suggests, therefore, that the application of a j-factor to the modulus of elasticity of the rock material gives as meaningful a measure of compressibility potential of the rock mass as any.

The erodibility of infilling materials is a more difficult parameter to quantify. In an attempt to evaluate the potential erodibility of a soil, subsoil or rock mass, however, it is suggested that permeability and grain size (i.e. grading - percentage passing 0,075mm) could be considered as the effective parameters.

As far as the tensile strength of infilling materials is concerned, the cohesion value 'C' is considered a meaningful measure in the case of unconsolidated material. For sedimentary rock, however, the tensile strength ' σ ' of rock material adjusted by its j-factor can be used as an evaluating parameter for the rock mass.

Although insufficient testing has been undertaken on individual materials in the Rietvlei, Henley/Lawley and Driefontein outliers, it is proposed that the parameters of compressibility, erodibility and tensile strength, be given numerical index values for their contribution to promoting instability. Low index

/value ---

values would indicate low compressibility, low erodability and high tensile strength characteristics whereas the converse would apply to high index values. The instability ranking of a specific material (ind/L) could be derived from the following formula:-

$$\text{ind/L} = f(a, b, c)$$

In the above formula, 'a', 'b' and 'c' represent the instability index values given to compressibility, erodability and tensile strength/weakness. Because no explicit information is available, the instability promoting status of the three controlling parameters cannot be related in the above formula. It is essential, therefore, that if meaningful ranking values are to be obtained, detailed analyses should be made of each physical characteristic for every individual material in a large number of instability occurrences. Such a study is beyond the scope of this dissertation and could well be the subject of a further research project.

5.1.2.2 Evaluation of a Potential Risk Evaluation

Having established instability values for individual materials (ind/L), the instability potential of a geological profile (Rf) made up of a number of lithological units can be evaluated by an equation of the following type:-

$$R_f = \sum_{j=1}^n \left\{ \frac{(t_1 \times \text{ind}/L_1) + (t_2 \times \text{ind}/L_2) + (t_3 \times \text{ind}/L_3) \dots}{T} \right\}$$

/In the ---

In the above equation $\ln d/L$ and t represent the instability ranking index value of an individual material and its thickness respectively, whereas T represents the total thickness of all the materials in a specific geological succession. It must be emphasised that the thickness attained by the lithological units constituting a geological profile may be influenced by the degree of slumping to which they have been subjected as well as by the dolomite bedrock configuration. Reference to Appendix 7 showing geological profiles at Driefontein, for example, will show that where pre-Pleistocene planation has occurred, the thickness of relatively stable Karoo sedimentary rocks will be greater in the "root" or centre of a slot than towards its flanks. Verification of this statement can be obtained by comparing the profile of BH No. 29 with those at BH Nos. 90 and 117 in Profile 1 (Appendix 7). It is important to note by reference to Appendices 7 and 14 that in the Driefontein area, increasing thicknesses of Pleistocene to Recent materials frequently correspond with the positions of slots weathered out of the dolomite. Such increased thicknesses of "hill-wash" should not be construed as indicating areas where the slots are infilled with relatively stable materials as seen, for example, between BH Nos. 120 and 125 in Profile 2 (Appendix 7). In fact, rapid increases of the Pleistocene to Recent material may indicate the presence of a so called palaeo-sinkhole. In all probability, palaeo-sinkholes developed on the Far West Rand during the early period of subsurface erosion related to the natural lowering of the pre-existing water table at

/the ---

the time of post-African incisions of the Wonderfontein Spruit. Most of the major sinkhole occurrences can be attributed to the re-activation of these palaeo-sinkholes by the artificial lowering of the ground water level during pumping operations. At Driefontein, the geological profile in the area immediately northwest of the Compound has all the characteristics for compliance with the definition of a palaeo-sinkhole. As shown in Appendix 4, by contours showing the thickness of Pleistocene to Recent materials, the epicentre of a potential sinkhole is situated at TBM 34A. It should be noted that some 39,5m of "hillwash" occurs in this "throat" despite the fact that it has a diameter of only 3,95m. It is fortuitous that the potentially dangerous palaeo-sinkholes can be readily located either by trenching or probing with shallow boreholes drilled at very close centres. Variances in the thickness of "hillwash" relative to known slots at Driefontein are shown in Appendix 14. It should be noted that besides the palaeo-sinkhole existing northwest of the Compound, similar such conditions are indicated by excessive thicknesses of transported soil in the vicinity of the Tunnel Kiln overlying slots B and C. Some indication can be derived as to whether excessive thicknesses of "hillwash" occupy either a palaeo-sinkhole or a doline. In the case of a palaeo-sinkhole being present, there is a complete absence of a pebble band at the base of the soils or ferricrete (Wolmarans 1979, verbal communication). In the case of a

/doline, ---

doline, however, not only will the pebble marker be present but it may also show evidence of being affected by post-Pleistocene slumping re-adjustment. It is of interest that post-Pleistocene slumping, sometimes evident in the ferricrete gravels may also be indicative of palaeo-doline conditions. The presence of ferricrete or "hardpan" or even grass roots within the "hillwash" enhances its bridging strengths. Brink (1979), for example, quotes instances where 150mm to 100mm of "hillwash" overlying a void prevented surface collapse for several months. Similarly Pike (1971) subjected a soil capping, with a thickness of 200mm, to plate-loading tests so that its bridging capacity could be determined. Using a loading plate 250mm in diameter, progressive loadings were applied by means of a water tank and it was observed that failure occurred when the plate punched through the capping at the pressure of 215kPa. Ominously, however, the collapse of a "hillwash crown" over a void is abrupt and without warning.

5.1.3 INSTABILITY RANKING OF OTHER FACTORS

It must be realised that an Rf value applies only to a particular geological profile at a single point (e.g. a borehole). Consequently, Rf values cannot be used on their own to evaluate the potential instability risk hazard (RH) of a specific area as they do not take into account adjacent hydrological and geological influences.

5.1.3.1 Lithological Succession

It should be noted that the instability potential value (Rf) so far described, based on thickness and engineering or physical characteristics, does not take into account the lithological succession in a geological profile. Thus, as a simple example, a geological profile in which 15m of uncompacted wad overlies, 30m of Karoo mudstone would, unrealistically, have the same value as a succession where 30m of Karoo mudstone rested upon 15m of wad. It is important, therefore, that Rf values should be carefully scrutinized and modified where necessary by discerning engineering geologists or geologists.

5.1.3.2 Subsurface Water

Probably the most important influence for promoting instability in a geological profile is the movement of subsurface water. Thus, for example, the movement of subsurface water through a profile containing a considerable thickness of uncompacted wad would be more hazardous than that through Karoo shales, mudstones and tillites. Consequently, in the compilation of an instability risk hazard evaluation for a specific area or site, a hydrological factor, rated with numerical values, to indicate its contribution to instability, must be applied to the 'Rf' value. In the Compound area at Driefontein, for example, the lowering of the uppermost subsurface water (W2) level from 21m below surface down the throat of the palaeo-sinkhole to a depth in excess of 39,5m, would induce erosion of the Pleistocene

/to Recent ---

to Recent sandy infilling soils and culminate in a sinkhole collapse. Consequently a high hydrological influence rating is considered appropriate to the Compound area. Conversely in the vicinity of the Tunnel Kiln and Dryers, there is an absence of either compactible materials (refer to Appendix 7, profile between BH G3 and BH G1), or any apparent expansive clay minerals, and a low hydrological influence rating is considered applicable by the writer. The effects of ground water movements on the instability potential of material fabrics warrants further research to that undertaken in this dissertation.

5.1.3.3 Configuration of the Dolomitic Bedrock

Another factor which contributes to potential instability and which must be taken into account is the configuration of the dolomitic bedrock. A harsh, palaeo-karst topography with short spans between steep-sided pinnacles is conducive to potential sinkhole development if infilled with materials of high erodability and poor tensile strength characteristics. Conversely, a gently undulating bedrock configuration, with the span between shallow sloped abutments being too great to permit the formation of an arch in unstable infilling materials, will produce conditions suitable for differential surface settlement or doline development.

Probably the most practical method of classifying bedrock configuration would be that proposed by Venter (1981) whereby the configuration of abutments and pinnacles

/is regarded ---

is regarded as a function of their slope gradient, height and width. Venter (1981) also suggests that a percentage factor should also be applied for the presence of cavities in the dolomitic bedrock and the writer considers that such a factor also be used for voids located within the infilling materials.

5.1.4 INSTABILITY RISK EVALUTION

As can be seen, the compilation of a potential instability risk evaluation (RH) at any given point or locality involves consideration of many influences as shown by a formula of the following type:-

$$RH = f(R_f, R_h, R_d, R_v)$$

In the above equation R_f represents the instability potential of a specific geological profile as already discussed and R_h , R_d and R_v refer to the impact of hydrological influences, the severity of dolomitic bedrock configuration and the frequency of voids/cavities present respectively, each given numerical values with increasing instability potential.

Providing sufficient geological profile points, such as boreholes, are available, an isopleth map can be prepared of RH values which may then be applied to areas where surface structures are either proposed or in existence. It is recommended, however that confidence limits be applied to RH values relative to the density of profile points or boreholes using geostatistical

/techniques ---

techniques, particularly kriging, as advocated by Clark (1979). As far as surface structures are concerned, they also may be quantified with numerical values according to their ability to withstand stress. Steffen Robertson and Kirsten (1984) give a timber frame structure a low risk rating of 2, steel frame and brick infilling 6, concrete frame and brick 8 and load bearing brick 9. The results of a tentative attempt, by the author, to classify the hazard rating of structures at Driefontein brickworks is given in Table 16 below. To compile the RH values in this evaluation, geological and hydrological information was derived from boreholes and piezometers, whereas the physical or engineering parameters of lithological units were quantified using data from Hobbs (1974), Brink (1979), Douch and Wiid (1982), Steffen Robertson and Kirsten (1983), Brink (1983), Wrench (1983) as well as personal intuitive evaluations.

TABLE 16.			
Building	Structural Rating (a)	RH Value (b)	Hazard Rating = $\sqrt{a \times b}$
Intake hopper	6	3,0	4,2
Crusher/grinding	6	5,0	5,5
Clay storage	7	3,5	4,9
Tunnel Kiln and Dryers	4	2,0	2,8
Offices	8	2,5	4,5
Compound	9	8,0	8,5

/In conclusion ---

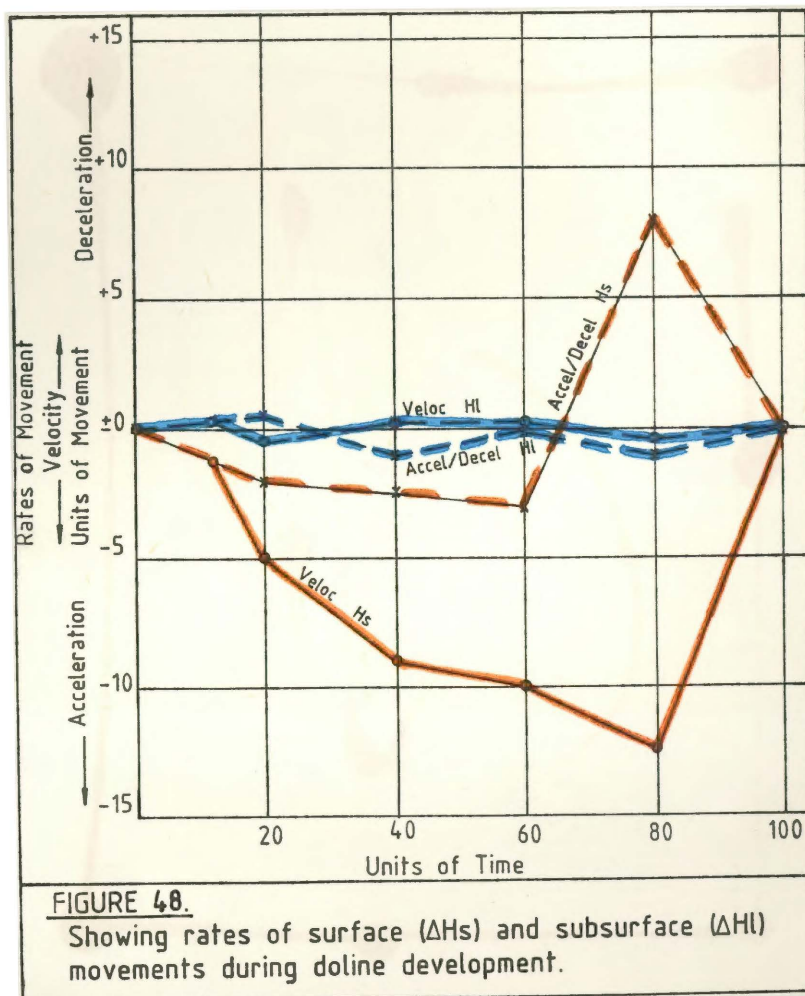
In conclusion, it must be emphasised that the compilation of a meaningful potential instability risk rating necessitates that detailed geological, hydrological and lithological data be collected, scrutinized and carefully evaluated by scientists or engineers with experience of dolomitic environments.

Even then, the proposed concept for quantifying instability as presented in this dissertation requires further research and refinement and should not be regarded as authorised on its own. Rather the concept must be used in conjunction with other established geotechnical evaluation techniques.

5.2 VELOCITY AND ACCELERATION/DECELERATION OF SURFACE AND SUBSURFACE MOVEMENTS

After interpreting and evaluating the surface and subsurface movements from several hundred telescopic bench marks, it becomes apparent that the rates of movements are more useful than the amounts of movement for diagnosing potential instability. The above statement can be simplified by comparing the respective movements for doline and sinkhole development. In the case of doline development, movements may be substantial, being measurable in terms of centimetres or even metres. By contrast, only a few millimetres of subsurface movement may

precede the occurrence of a catastrophic sinkhole. Regardless of the amounts of surface and subsurface movements which may be occurring, dolines and sinkholes display distinct velocity and acceleration/deceleration patterns. Velocity is calculated on the basis $\frac{\Delta d}{\Delta t}$ where Δt is a unit of time (eg. a measurement cycle every 43 days) and Δd is the difference of linear distance which has occurred between a current and a preceding measurement. Acceleration/deceleration, that $\frac{\Delta d}{\Delta t^2}$ is the change of velocity which has occurred between a current and a preceding measurement.



/Reference - - -

Reference to Figure 48 will show that in the case of a developing doline, the subsidence of surface is characterised by a gradual, but steady, increase of velocity ($v\Delta Hs$) without any erratic changes of either acceleration or deceleration ($a\Delta Hs$). When the process of consolidation is nearing completion, however, velocity of surface movement rapidly reduces and deceleration takes place.

As would be expected, no significant velocity, acceleration or deceleration of the subsurface occurs either at the development or post-consolidation stages of a doline. The actual ΔHs , $\Delta H\ell$ movements as well as the velocities, accelerations and decelerations in a telescopic bench mark situated near the epicentre of a doline are illustrated in Figures 49 a, b and c.

As can be seen in Figures 49a, b and c rates of movement when plotted every 43 days, that is on the conclusion of each measuring cycle, display an indiscriminate pattern. By plotting the moving average trends of these rates of movement, however, it can be seen that they correspond with the pattern expected in a doline development. The moving average trends plotted in Figures 49b and c are based on the arithmetic means of the rates of movement for four consecutive measuring cycles, using the equation :

/ Figure 49 ---

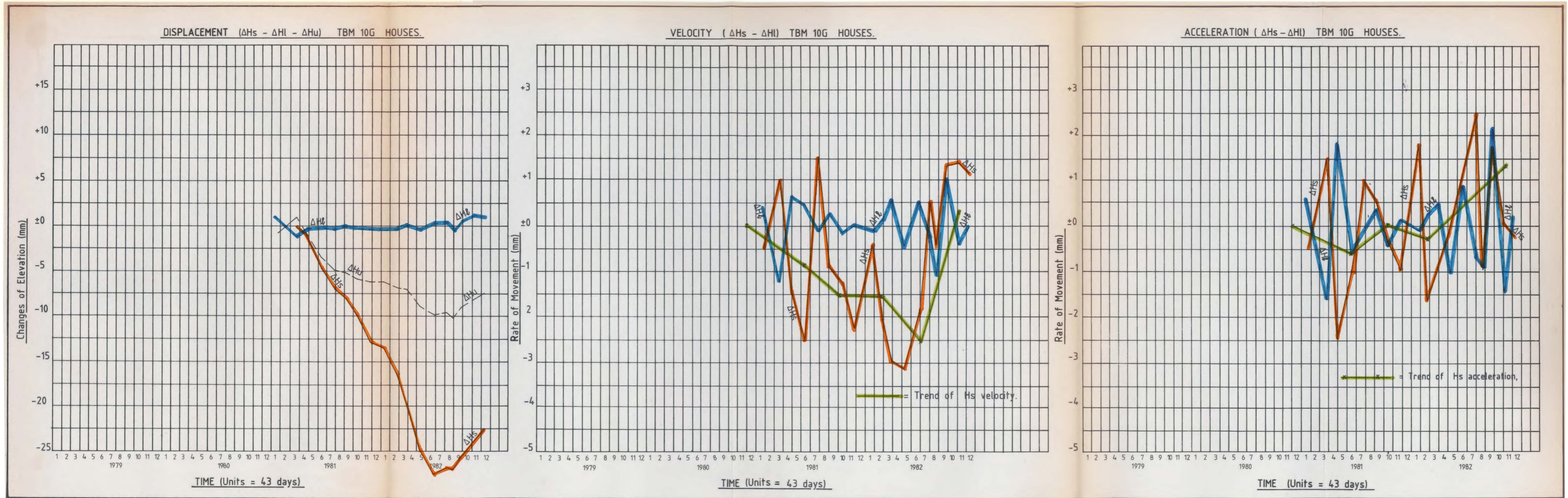


FIGURE 49.
Showing ΔH_s , ΔH_u and ΔH_l displacements and $\Delta H_s / \Delta H_l$ velocity and acceleration/deceleration behaviour in TBM 10G situated near the epicentre of a developing doline.

/ ε ---

$$\frac{\Sigma(y^1 + y^2 + y^3 + y^4)}{n}, \quad \frac{\Sigma(y^3 + y^4 + y^5 + y^6)}{n}, \dots\dots\dots$$

In this equation, 'y' represents either the velocity, acceleration or deceleration at the end of a specific measuring cycle and 'n' the number of cycles (ie. 4).

The velocity and acceleration/deceleration patterns for an area being subjected to sinkhole development show a marked difference to those previously described. Firstly, significant changes in the rates of movement are confined to the subsurface ($\pm\Delta H\ell$ or $\alpha\Delta H\ell$) rather than to the surface ($\pm\Delta Hs$ or $\alpha\Delta Hs$). Secondly, the frequency of changes in either velocity, acceleration or deceleration are so rapid, that no meaningful trend can be determined from plotting their moving, arithmetic means. In such a case, the significance of movement rates can be ascertained by determining the confidence limits from the equation :

$$\text{Confidence limit} = \pm \left(\frac{\hat{\sigma}}{\sqrt{n}} \right) \times t_{.025}$$

In the above equation $\hat{\sigma}$ represents the standard deviation of the mean, $t_{.025}$ the Student -t distribution for a 95 per cent confidence limit and n the number of "units" or readings constituting the statistical population.

/ Figures 50a, b and c ---

Figures 50 a, b and c illustrate the case history of a telescopic bench mark (TBM 10) situated some 30m from sinkhole No. 27 which developed on 18th February 1980. From Figure 50 a, it is apparent that the surface (ΔH_s) and upper subsurface marker (ΔH_u) elevation changes were closely related. Between April 1979 and mid-November 1979, they both showed negative movements of -7,84mm and -7,83mm respectively, but remained steady from mid-November to mid-February 1980. In mid-February, at the time of the sinkhole occurrence, both ΔH_s and ΔH_u showed positive trends so as to reach -6,61mm and -6,51mm respectively. Thereafter, negative movements were renewed attaining maximums of -10,73mm in the case of ΔH_s and -10,74mm for ΔH_u by mid-October 1980. Between October 1980 and May and May 1981, ΔH_s had risen to -4,04mm and ΔH_u -4,18mm but subsequently, they have both shown a downward trend in the order of -17mm. In contrast to the fluctuating behaviour of both ΔH_s and ΔH_u , the lower subsurface marker (ΔH_l) remained constant at $-1,97 \pm 0,24$ mm except between mid-December 1979 and early February 1980 when it dropped to -6,66mm. From the period 2nd February to 18th February 1980, when the sinkhole developed, there was virtually no change in the ΔH_l elevation. Immediately after the occurrence of the sinkhole, however, the lower subsurface marker rose rapidly to -1,43mm by the beginning of March.

/ Figure 50 a, b and c ---

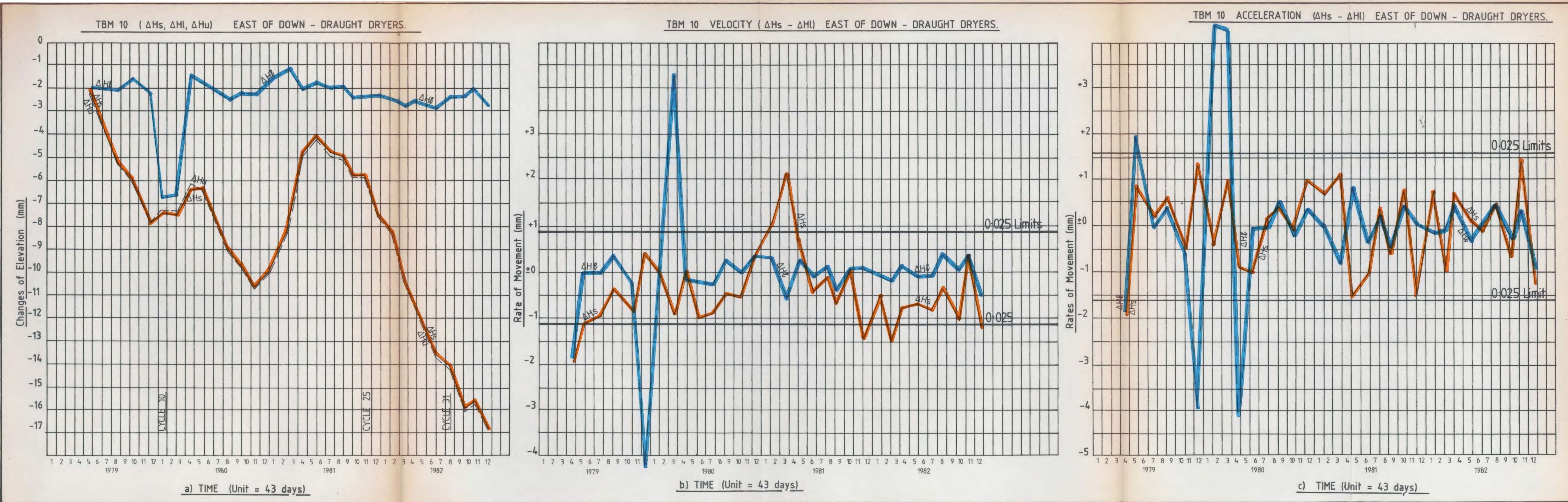


FIGURE 50a,b and c.
Showing ΔH_s , ΔH_u and ΔH_l displacements and $\Delta H_s / \Delta H_l$ velocity and acceleration/deceleration behaviour in TBM10 prior and subsequent to the development of sinkhole No. 17.

/Subsequently ---

Subsequently, $\Delta H\ell$ measurements have remained virtually constant at $-2,38 \pm 1,44$ mm. The overall interpretation of the ΔH_s , ΔH_u and $\Delta H\ell$ behaviour pattern is that of consolidation despite an apparently minor excursion beyond the 0,025 confidence limit immediately prior to the sinkhole development. By contrast the velocity and acceleration/deceleration patterns of ΔH_s and $\Delta H\ell$ movements are sufficiently sensitive to indicate an abnormal geotechnical event. This sensitivity is particularly apparent when 0,025 confidence limits are applied as can be seen in Figures 50 b and c. It is noteworthy that at the time of a measuring cycle, 16 days prior to the occurrence of sinkhole No. 17, the negative movements of the lower subsurface marker ($\Delta H\ell$) showed an increase of velocity from $-0,28$ mm/43 days to $-4,29$ mm/43 days. At the same time acceleration increased from $-0,62$ mm/(43)² days to $-4,01$ mm/(43)² days. Sixteen days before the sinkhole collapse, the movements of the lower subsurface marker showed a total slowing down of velocity by $4,34$ mm/43 days (ie. from $-4,29/43$ days to $+0,05$ mm/43 days) and a total deceleration of $9,36$ mm/(43)² days (ie. from $-4,02$ mm/(43)² days to $+4,34$ mm/(43)² days). Immediately after the sinkhole collapse, the movement of the lower subsurface marker showed an increased total velocity and acceleration extending over a period of 67 days

/ after ---

after the occurrence of the sinkhole. Thereafter, they displayed insignificant fluctuations well within the 0,025 confidence limit.

The $x\Delta H\ell$ and $\alpha\Delta H\ell$ behaviour in TBM 10 is not as unpredictable as appears at first glance. Had this telescopic bench mark been situated at the arch crown above the void, then the velocity and acceleration patterns of the lower subsurface marker would have shown dramatic increases until ultimate arch collapse took place. The erratic changes of velocity, acceleration and deceleration of $\Delta H\ell$ occurring in TBM 10 are compatible with the observations of Jennings (1971b) in respect of a telescopic bench mark situated immediately adjacent to the void position. Thus, the fluctuations in the rates of movement are associated with the lateral transfer of stresses by arching away from the crown of the void prior to its collapse. There is, therefore, an obvious need to locate with some precision, the position of the void.

5.3 MEANS AND STANDARD DEVIATIONS OF SURFACE AND SUBSURFACE MOVEMENTS

The preparation and diagnostic value of isopleth plans of ΔH_s , ΔH_u and $\Delta H\ell$ measurements has already been described in pages 92 to 94 of this dissertation.

Although such plans delineate areas of ground

/ instability ---

instability by the negative or positive values of the isopleths as well as their gradients, they do not accurately indicate either the epicentre of the extent of sensitivity of such areas. Both of the above objectives can, however, be obtained by plotting the means and standard deviations of the surface and subsurface movements recorded from telescopic bench marks. The mean isopleths are compiled by averaging the positive and negative measurement values obtained from each telescopic bench mark in a particular area. In Figure 51 for example, the mean values of ΔH_s movements in the Housing area represent the average value of movements which have occurred in a telescopic bench mark over 25 measuring cycles (Cycle 1 - 25). The standard deviation isopleths, in turn, are derived by the standard deviation of the average movement which has occurred in a telescopic bench mark.

/ Figure 51 ---

As can be seen, the mean movement isopleths ($\bar{\Delta Hs}$) indicate five distinct areas of subsidence with their epicentres being 10mm east-northeast of TBM 1B, 4m northeast of TBM 2D, at TBM7G, some 2m southeast of TBM9A and an undetermined distance north of PBM7 respectively. However, standard deviation isopleths ($\hat{\sigma}^{\Delta Hs}$), which have neither positive nor negative values, show that :

- (i) TBM 1B and TBM 2D are on the fringe of a zone of instability common to both. Furthermore, this zone of instability can be regarded as insignificant as far as Houses 1 and 2 are concerned because only a single standard deviation isopleth, with a value of 1mm encompasses them.
- (ii) The subsidence near TBM 7G is a concentrated and localised area of subsidence. An investigation into the cause of this instability showed it to be artificial having been induced by the growth of a privet hedge in the immediate vicinity of TBM 7G.

/(iii) ---

- (iii) The subsidence in the vicinity of TBM 9A is not an individual zone of instability but an integral part of a major doline development with its epicentres situated north of PBM 7.

The pattern assumed by crack development, both on ground surface and in the housing structures, as illustrated in Plates 8, 9 and 10, corresponds very closely with the standard deviation isopleths as seen in Figure 51.

In Figure 52, the isopleths of mean ΔH_s movements for Measuring Cycles $\Delta 25$ to 4 in the vicinity of the Down-draught Dryers have been plotted together with the standard deviation values. The mean ΔH_s isopleths ($\bar{\Delta H}_s$) indicate that the northern portion of the area is characterised by positive movements whereas negative movements occurred to the south. Two local points of negative movements exist; a major one situated at least 10m south of the dryer buildings probably in the vicinity of sinkhole No. 3 and a minor one 11m south-southwest of TBM 10. The standard deviation isopleths ($\hat{\sigma}\Delta H_s$), however, indicate that:

- (i) The two epicentres are of equal intensity both being encompassed by $\hat{\sigma}\Delta H_s$ values greater than 3mm.

(ii) The epicentre in the vicinity of TBM 10 is the more sensitive of the two because of the steeper gradients between the $\delta\Delta H$ isopleths.

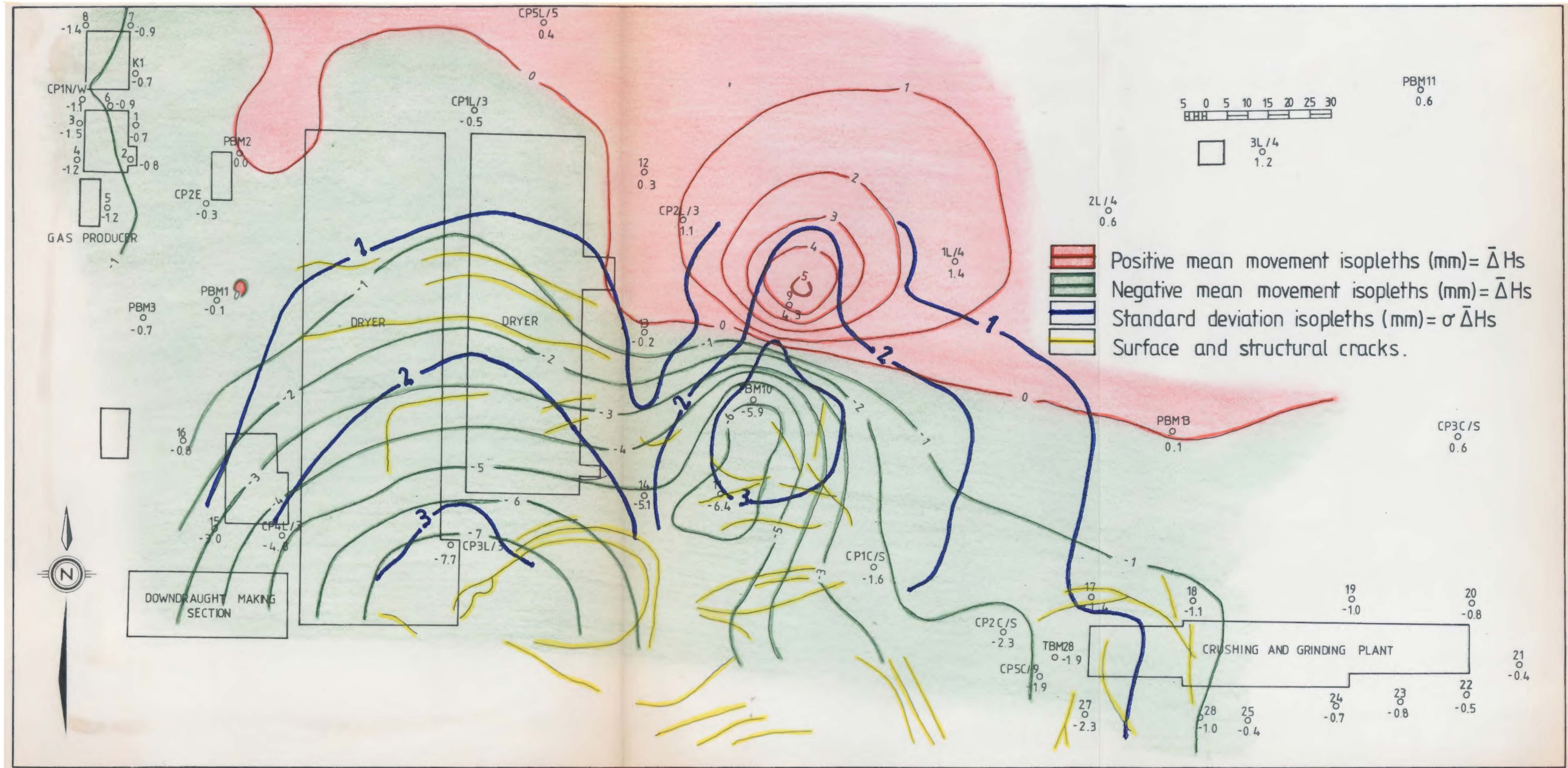
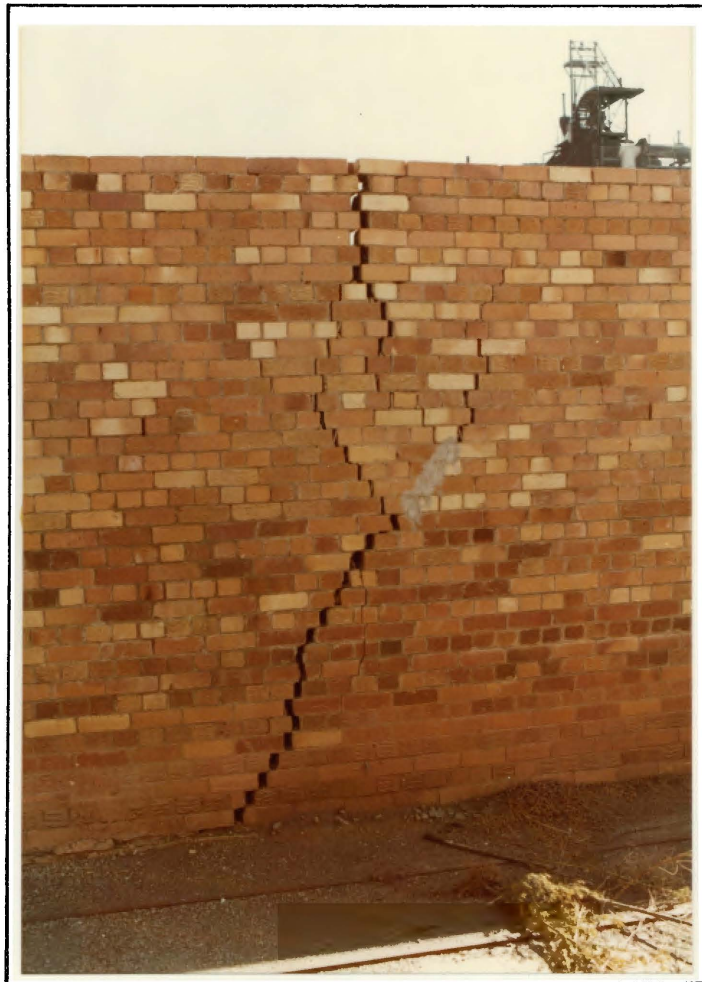


FIGURE 52.
Isopleths of means and standard deviations for surface movements in the vicinity of the Down - draught Dryers at Driefontein Brickworks (Cycles $\Delta 25 - 4$).

The authenticity of the $\delta\Delta H$ s isopleths as a means of delineating areas of instability is once again confirmed by the close relationship between them and crack development, such as those illustrated in Plates 8 to 10.

/Plates 8 to 10 ---

PLATE 8.



Showing cracking in the wall of the Down - draught
dryers at Driefontein Brickworks caused by
differential subsidence.

/ Plate 9 ---

PLATE 9.



Showing cracking along floor of the Down - draught dryers at Driefontein Brickworks caused by differential subsidence.

PLATE 10.



Detail of cracking along floor of the Down - draught dryers at Driefontein Brickworks caused by differential subsidence. Note the dislocation of the rail.

/the ---

The $\hat{\sigma}\Delta H_s$ isopleth map may, in conjunction with normal "displacement" isopleth maps, also be used to assess whether or not the unstable condition in a specified area is deteriorating. By comparing Figure 52 with Figure 53, the latter showing the $\bar{\Delta H}_s$ and $\hat{\sigma}\Delta H_s$ isopleths for Measuring cycles 4 to 31, it can be seen that between 1st December 1981 and 16th August 1982, instability worsened by a minor degree. This minor worsening is indicated by the migration and steepening of both the $\bar{\Delta H}_s$ and $\hat{\sigma}\Delta H_s$ isopleths towards the two centres of instability. Further applications for $\hat{\sigma}\Delta H_s$ isopleths are that they may be used to delineate areas where maximum distress may be imposed either on existing or proposed structures and also to predict ground developments. Reference to Figures 52 and 53 for example, shows that all the major sinkholes occurred within areas where the $\hat{\sigma}\Delta H_s$ isopleths had values greater than 1mm. This distribution is of considerable significance as it indicates that sinkhole development need not necessarily be confined to the epicentres of instability but also to their peripheries. These peripheral or satellite type sinkholes may occur where tension cracks have developed either along the shear zone demarcating the perimeter of a doline or else have radiated upwards from a deep-seated void to surface as illustrated in Figure 54. These cracks act as aquifers down which surface water may percolate downwards to

/Figure 53 ---

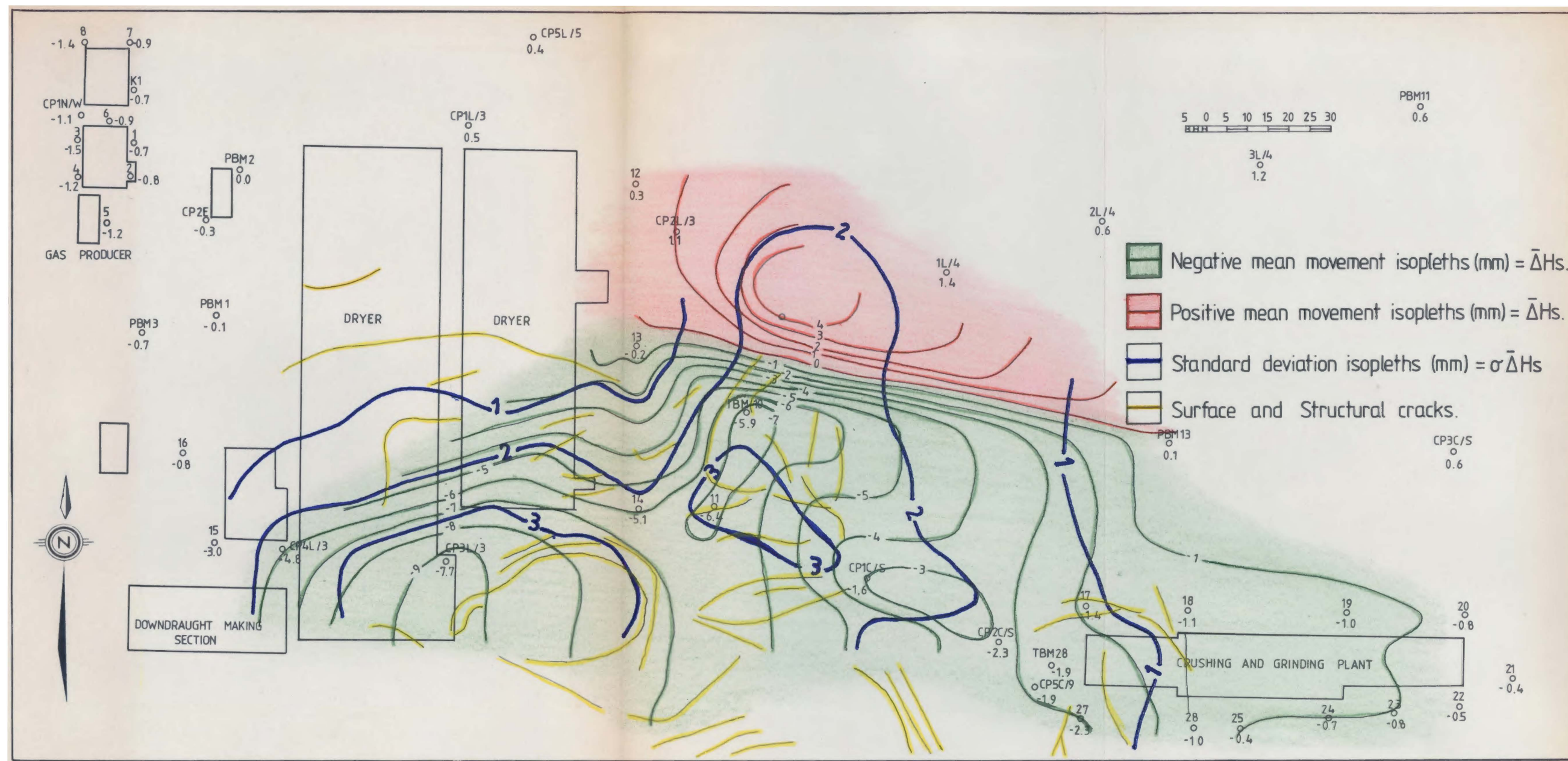


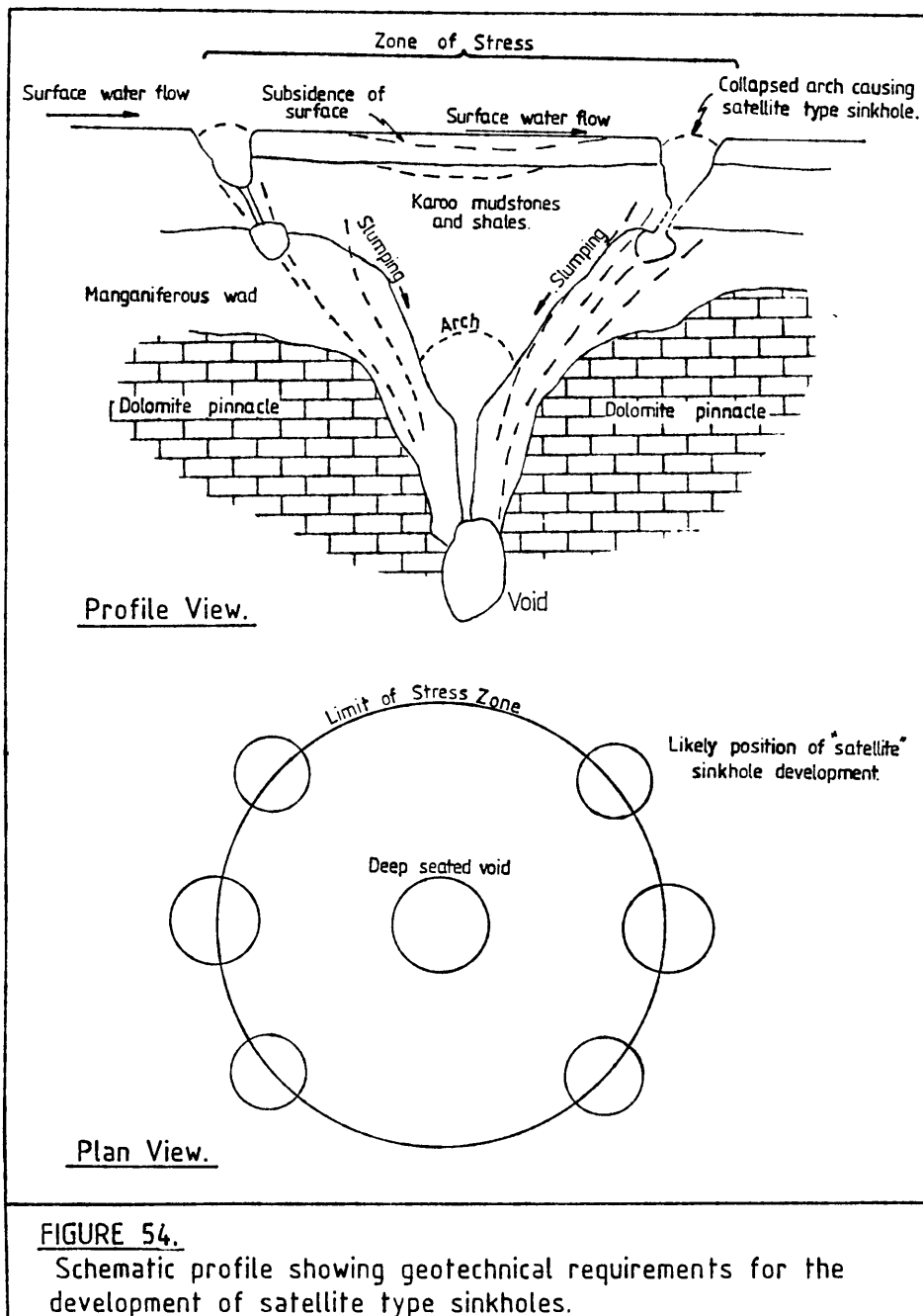
FIGURE 53.
Isopleths of means and standard deviation for surface movements in the vicinity of the Down - draught Dryers at Driefontein Brickworks. (Cycles Δ31 - 4).

erode soft materials, such as sandy soils or manganiferous wad. The subsequent sinkholes which occur because of the resulting arch collapse of voids

/ developed ---

developed in these erodable materials, will be characterised by :

- (i) a small diameter of between 7m to 10m;
- (ii) the "throat" of the sinkhole being inclined towards the epicentre of instability.



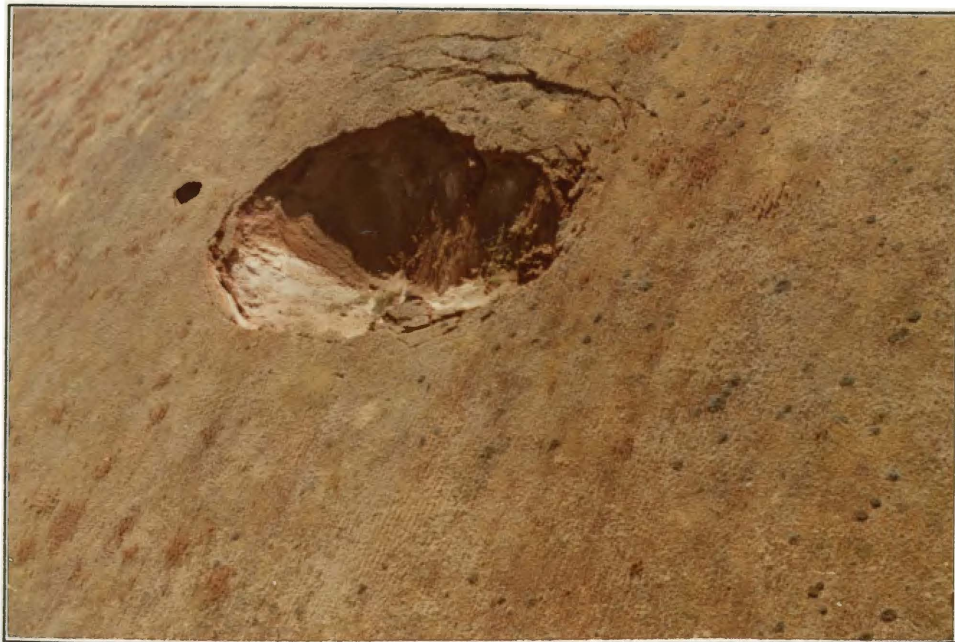
/ Sinkhole ---

Sinkhole Nos. 10 and 17 typify these satellite type sinkholes whilst further examples occurring in the vicinity of the Driefontein area are illustrated in Plates 11 and 12.

PLATE 11.



PLATE 12.



Examples of satellite type sinkholes occurring immediately northeast of Driefontein brickworks.

/ Secondary ---

Secondary type sinkholes may also develop at the crest of dolomitic bedrock pinnacles. It would appear that slumping of infilling sediments down the flanks of pinnacles results in the development of tension cracks along its crest. These tension cracks permit surface water to infiltrate downwards and possibly induce subsurface erosion and ultimate surface collapse.

5.4 CYCLIC RECHARGING OF AQUIFERS

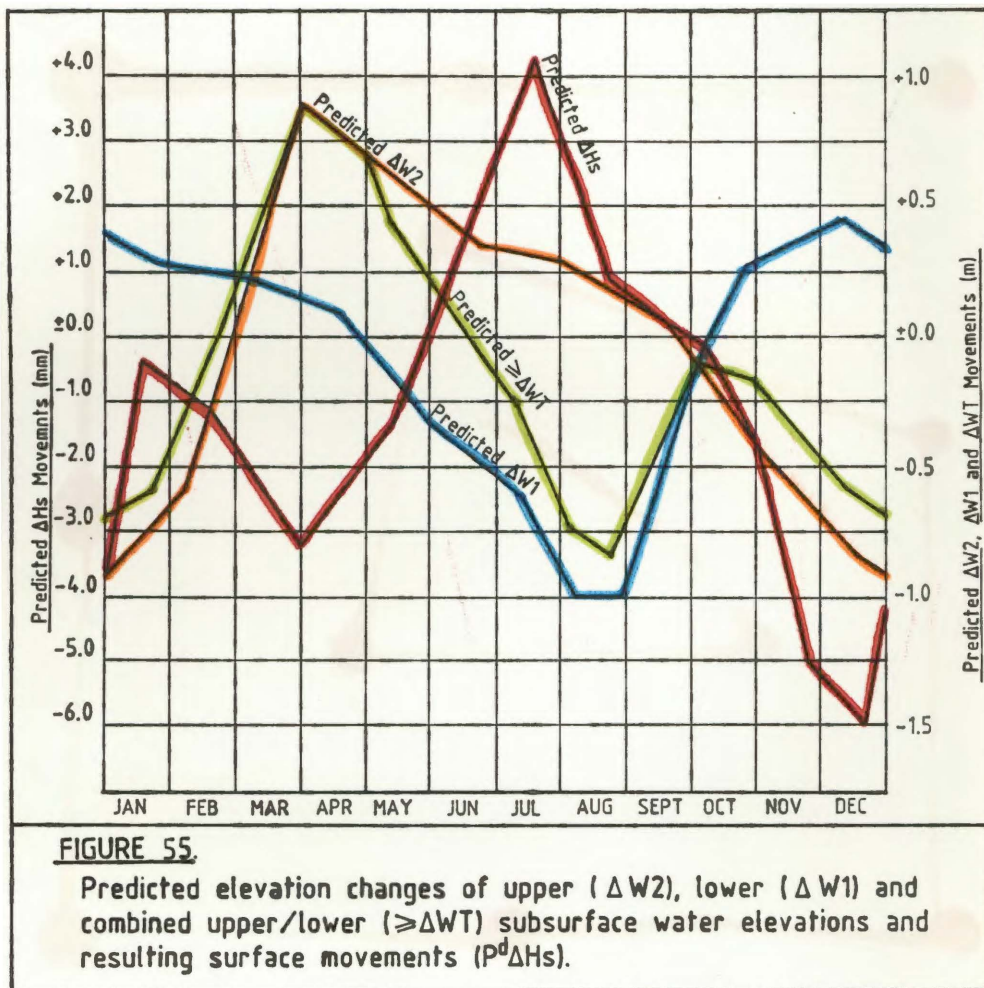
The influence asserted by the cyclic migration of subsurface water, through either compactible or swelling subsoils both on ΔH_s and ΔH_l behaviour has already been discussed in pages 138 to 175. Readings from piezometers and telescopic bench marks in the Driefontein area show that the ratio between subsurface water movements and $\Delta H_s/\Delta H_l$ behaviour to be as shown in Table 17.

RATIO	COMPOUND AREA	FACTORY AREA	HOUSING AREA
W2 : ΔH_s	216,35 : 1	94,25 : 1	308,10 : 1
W1 : ΔH_s	67,91 : 1	101,06 : 1	109,15 : 1
MEAN	142,13 : 1	97,66 : 1	208,63 : 1
W2 : ΔH_l	335,82 : 1	131,83 : 1	1250,10 : 1
W1 : ΔH_l	64,85 : 1	527,21 : 1	442,86 : 1
MEAN	200,34 : 1	329,52 : 1	846,48 : 1

Maximum ratios between subsurface water elevation changes and $\Delta H_s/\Delta H_l$ movements in the Driefontein area.

/ The ---

The amounts of movements occurring as a result of such subsurface water migrations will be relative to the compaction and expansion capacities of the subsoils. Furthermore, because the subsurface water elevation changes are associated with seasonal recharge of aquifers, these changes are cyclic. A prediction of



| the ---

the cyclic behaviour of subsurface water under normal climatic conditions can, therefore, be made by postulating from historical information. The predicted elevation changes of the upper (W2) and lower (W1) subsurface water systems in the Compound area are shown in Figure 55.

It should be noted that where more than one subsurface water system exists, as is the case in the vicinity of the Compound, their elevation changes may be at different frequencies. To predict the maximum amount of ΔH_s or ΔH_ℓ movements which may occur, the maximum positive or negative amounts of subsurface water movements are taken into account. Thus, from further reference to Figure 55, it can be seen that in April the W2 would show a positive elevation of +0,94m compared with +0,17m for W1 and, therefore, only the former reading is regarded as significant. Where, however, one subsurface water system may be showing a positive change of elevation and another system simultaneously has migrated negatively, then the mean of the two elevations is taken as significant. Thus, in August, the W2 subsurface water system would show a positive movement of +0,27m and the W1 system a -0,65m movement, the mean subsurface water is taken to be -0,38m. The prediction of ΔH_s or ΔH_ℓ movements ($P^d_{\Delta H_s}$ or $P^d_{\Delta H_\ell}$) may be obtained from the equation :

$$/ p^d \quad \text{---}$$

$$P^d \Delta H_s \quad \text{or} \quad \Delta H_\ell = \left(\frac{>\Delta WT}{R} \right) 10^{-3} + L$$

In the above equation $>\Delta WT$ represents either the maximum or mean subsurface water elevation change, as explained above, R is the ratio between surface (ΔH_s) or subsoil (ΔH_ℓ) movement and a change of subsurface water elevation as given in Table 17 and L the average time lag interval. Thus in April $>\Delta WT$ amounted to $+0,94\text{m}$ and the predicted ΔH_s movement would be :-

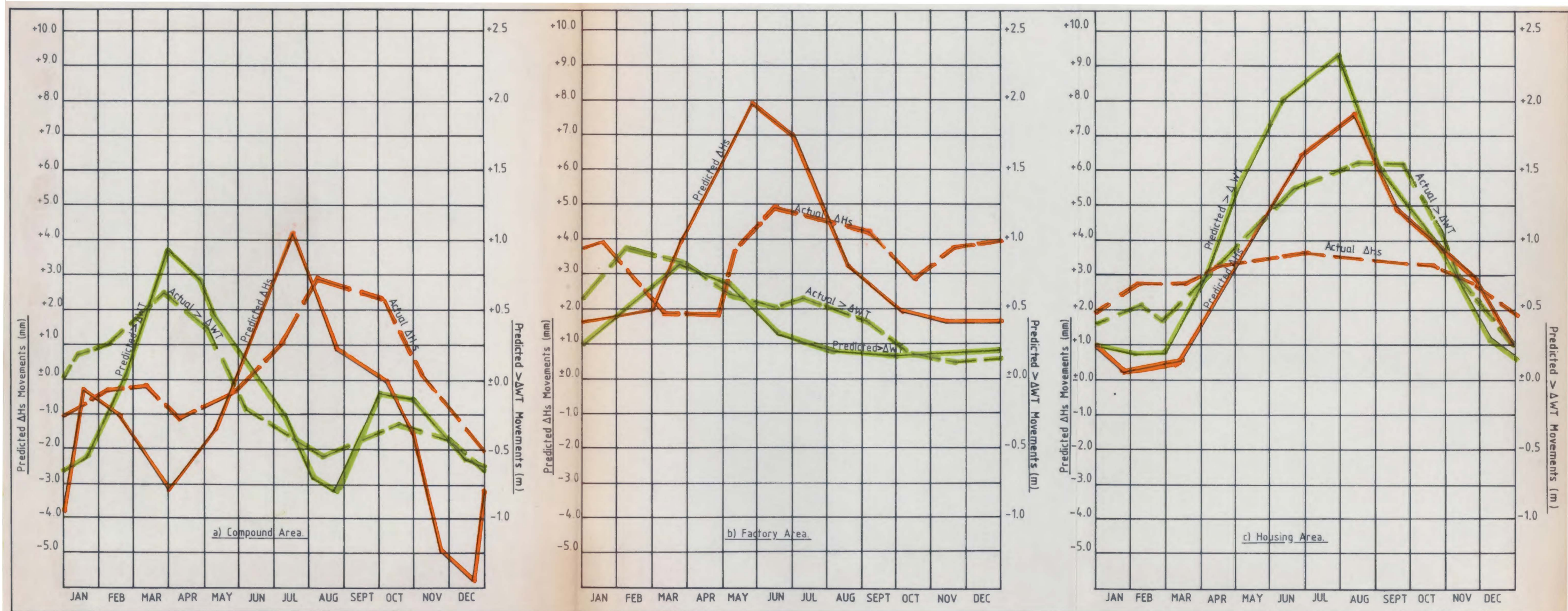
$$P^d \Delta H_s = \left(\frac{+0,94\text{m (W2 Movement)}}{216,35 \text{ (W2 : } \Delta H_s \text{ Ratio)}} \right) 10^{-3} = +4,34\text{mm} + L$$

Since the average lag interval, from the time of a subsurface water elevation change to when surface movement occurs is 107,5 days, in the Compound area, as can be seen by reference to Figure 56 a, b and c this $+4,34\text{mm}$ predicted ΔH_s movement will only occur in mid-July. Similarly, in August, the predicted $>\Delta WT$ amounted to $+0,94\text{m}$ and the predicted ΔH_s for mid-November would be :

$$P^d \Delta H_s = \left(\frac{-0,38\text{m (mean of W2/W2)}}{142,13 \text{ (Mean W2/W2 : } \Delta H_s \text{ ratio)}} \right) 10^{-3} = -2,67\text{mm}$$

Predictions of ΔH_s and ΔH_ℓ movements, made in 1981 at different localities in the Driefontein area as well as the actual movements which occurred one year later, are illustrated in Figures 56 a, b, c and Figures 57 a, b, c respectively.

/Figure 56a, b and c ---



Actual $> \Delta WT$ movements for cycles 25 - 34.
Actual ΔH_s movements for cycles 25 - 34 compiled
from measurements of TBM No's 3, 9, 14 and 18.

Actual $> \Delta WT$ movements for cycles 25 - 34.
Actual ΔH_s movements for cycles 25 - 34 compiled
from measurements of TBM No's 9 to 13.

Actual $> \Delta WT$ movements for cycles 25 - 34.
Actual H_s movements for cycles 25 - 34 compiled
from TBM No's 1^A, 1^B, 2^B and 7H.

FIGURE 56a, b and c.

Predicted surface ($P^d \Delta H_s$) movements associated with cyclic elevation changes of subsurface water systems ($P^d > \Delta WT$) in Driefontein Brickworks area.

/Figure 57a, b and c ---

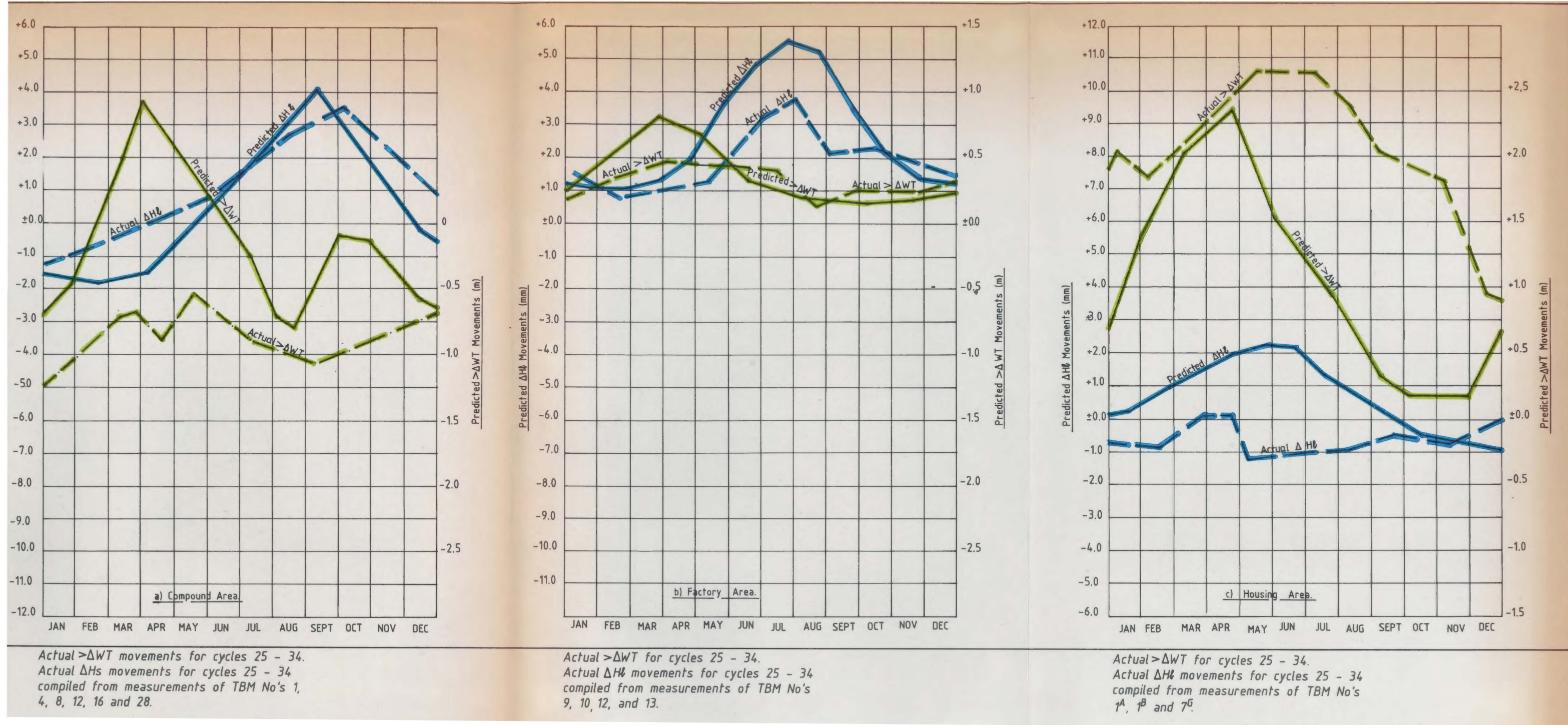


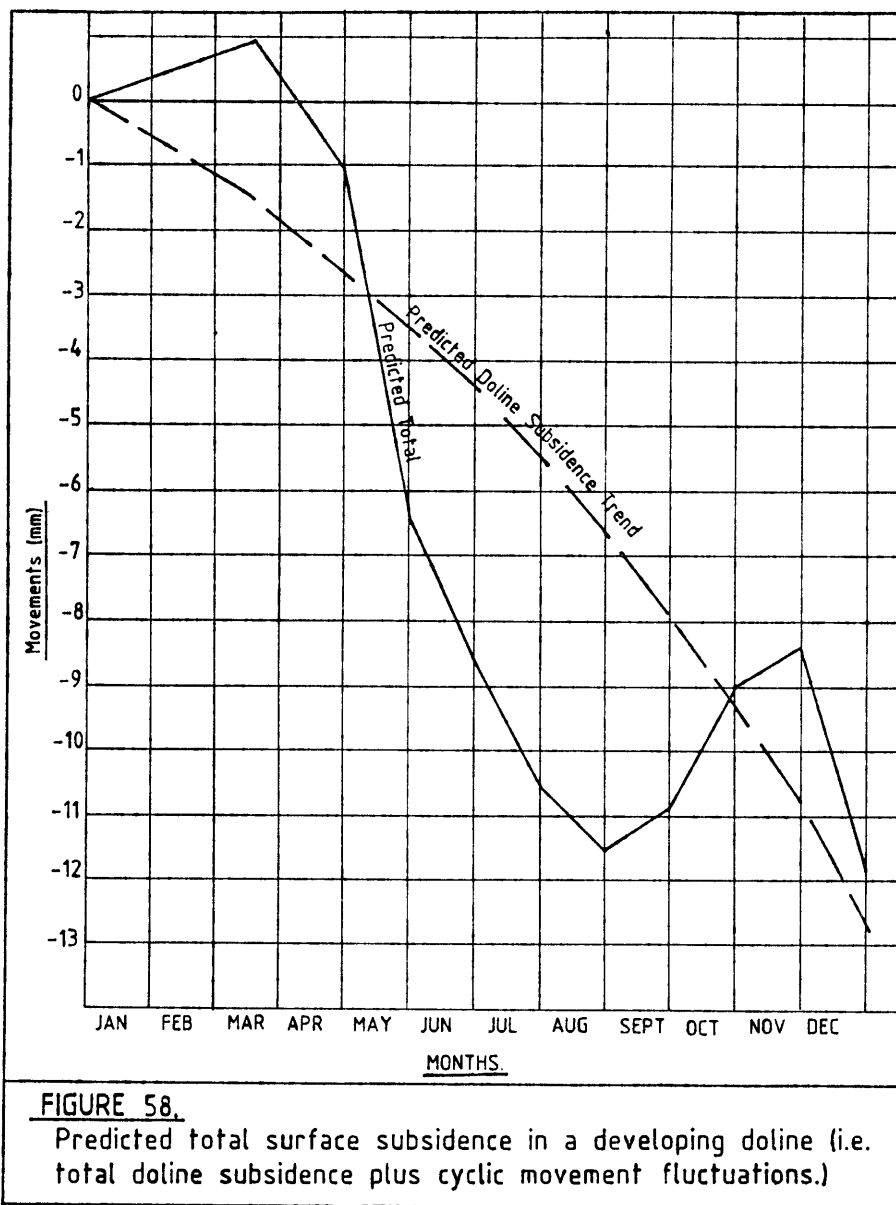
FIGURE 57a, b and c.

Predicted lower subsurface marker ($P^d \Delta H_i$) movements associated with cyclic elevation changes of subsurface water systems ($P^d \geq \Delta WT$) in the Driefontein Brickworks area.

can be seen, the amounts of movement resulting
m subsurface water elevation changes are relatively

/ small ---

small being measurable only in terms of millimetres
Even so, it must be emphasised that these cyclic
movements are over and above the movements associated
with deep-seated ground instability.



/ In ---

In Figure 58, for example, the predicted surface subsidence trend associated with doline development in the Driefontein housing area is shown together with the total subsidence, which is also affected by cyclic variations from this trend induced by subsurface water behaviour.

It is believed, however, that the cyclic fluctuations from the doline subsidence trend at different localities, is one of the main factors responsible for differential movement. As MacLeod and Abu-El-Magd (1980) have emphasised, differential movements, even though measurable only in millimetres are a major cause of cracking and structural damage.

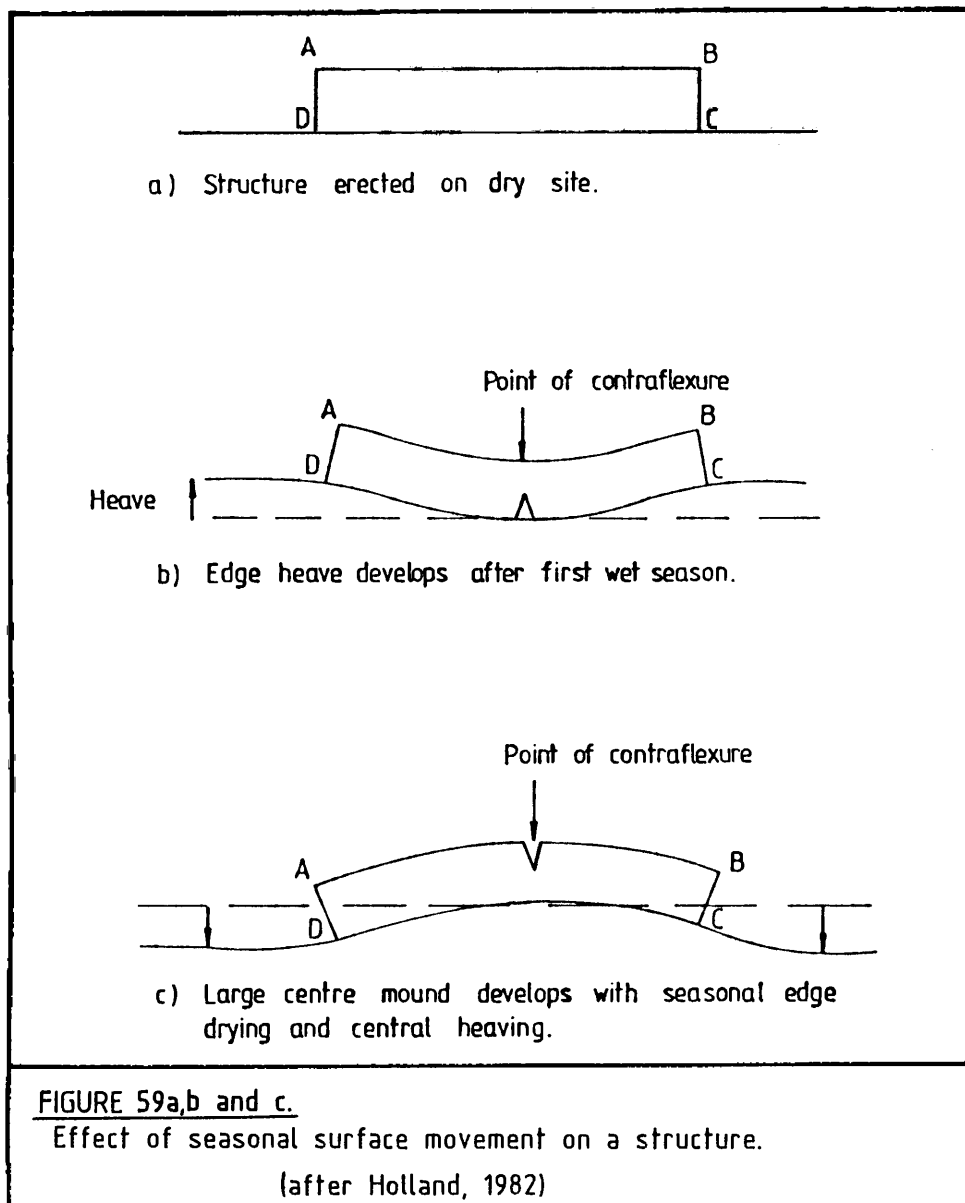
In a structure some 60m long, for example, a mere 1,5mm of vertical differential movement is sufficient to cause significant cracking patterns. It is interesting to note that contributions to a research paper presented by MacLeod and Abu-El-Magd (1980) were unanimous in their conviction that :

- (i) Although the amounts of total movement are predictable, no accurate prediction can be made in respect of differential movements.
- (ii) Differential movements may occur despite apparent soil uniformity.

/ It ---

It appears, therefore, that there is not a complete awareness that changes of elevation of either ground-water or piezometric levels can significantly influence surface movements. Furthermore, considerable emphasis has been given in the past as to how much differential movement is required to cause structural distress. The research at Driefontein, however, indicates that not only the amounts of movement but also the frequency at which they occur is important. Thus, any structure which is being subjected to cyclic contraflexuring can be subjected to alternating conditions of either tensile or compressive stresses. The cyclic imposition of alternating stresses can be illustrated in a condition where a structure has been erected on top of a heaving soil. In Figure 59 a is shown a structure, ABCD, erected upon a site underlain by dry heaving soil. After the first wet season, Figure 59 b, surface heave occurs, particularly towards the edges of the structure. It should be noted that at the point of contraflexure, the structure is suffering similar distress as if it had been subjected to settlement. Diagnostically, maximum crack width will develop towards the base of the structure.

/ Figure 59 a, b and c



In Figure 59c it can be seen that seasonal drying has occurred at the edges of the structure ABCD. A central mound is prevelant, however, since the structure has effectively retarded the drying out of the clay immediately beneath it. At the point

/ of ---

of contraflexure, it should be noted that conditions are now similar to those of hogging and, diagnostically maximum crack width development will occur at the top of the structure. Should a structure have been initially erected on a wet site, the pattern of surface movements remains the same but the amounts of movement are reduced.

At Driefontein, research has shown that cyclic differential movements can be caused by cyclic migration of subsurface water through subsoils with either heaving or compacting potential rather than seasonal rainfall directly saturating a heaving soil. The effects of such subsurface water migrations on a surface structure are illustrated in Figures 60a and b. In Figure 60a, it can be seen that the groundwater or piezometric level has, due to a positive migration, completely saturated a layer of "heaving clay", EFGH, beneath the centre of a structure ABCD and maximum upward vertical stress is asserted. Because of the disposition of the clay layer, however, only partial saturation has occurred at points immediately below the edges of the structure and the amount of upward vertical stress is correspondingly reduced. Because of the differential stress pattern, hogging occurs at the point of contraflexure.

/ Figure 60a, b, c ---

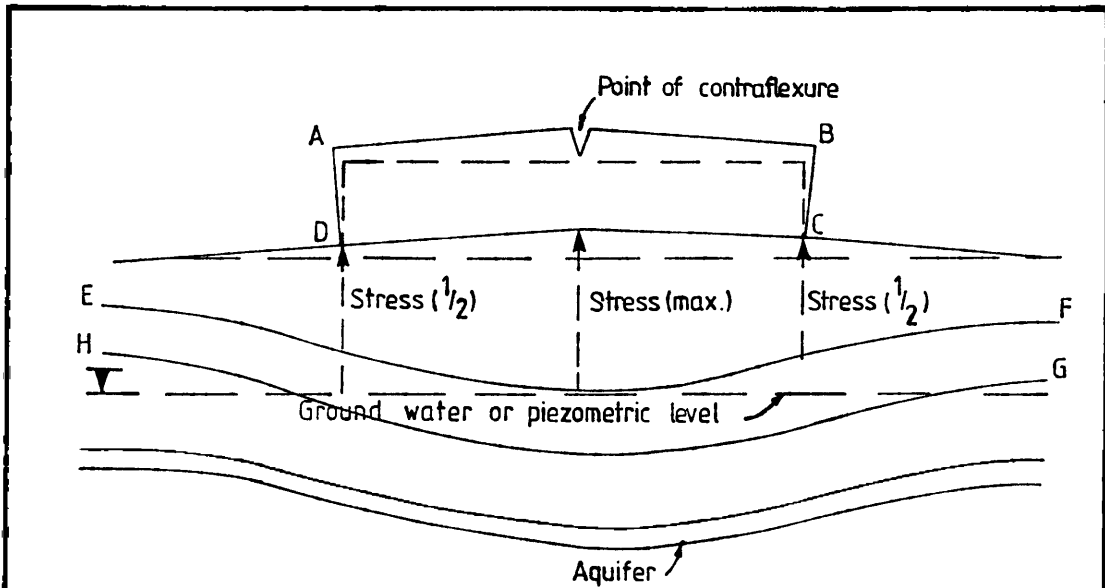


Figure 60a.

Stress pattern with a positive elevation change of the ground water or piezometric level.

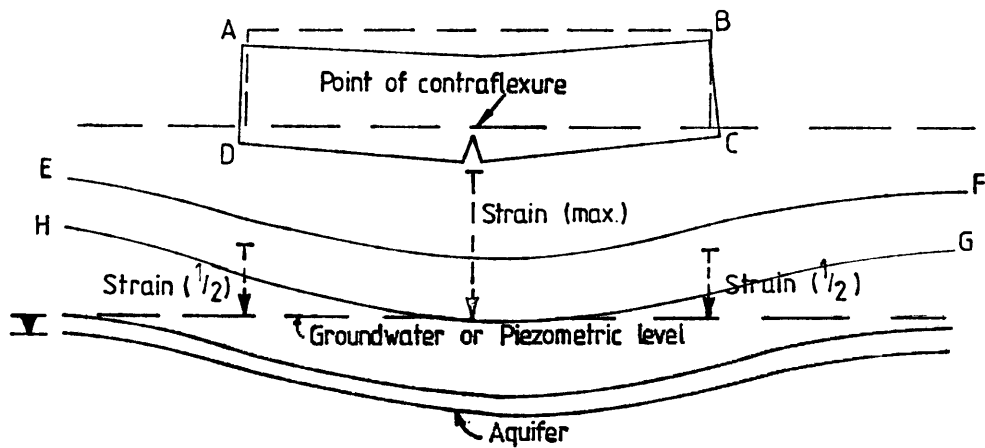


Figure 60b.

Strain pattern with a negative elevation change of the ground water or piezometric level.

FIGURE 60 a and 60b.

Effects of cyclic elevation changes of the ground water or piezometric level on a surface structure.

/ In ---

In Figure 60b, a negative cyclic movement of the groundwater or piezometric level has occurred so that drying out of the "heaving clay" layer has been effected. Immediately beneath the centre of the structure, the groundwater or piezometric level has retreated downwards through the complete thickness of the clay layer so that maximum possible shrinkage, with accompanying downward vertical strain, has occurred. Below the edges of the structure, however, only reduced strain is prevalent since the clay layer was only partially saturated prior to the negative retreat of the groundwater or piezometric level. Because of the strain pattern, maximum settlement will occur at the point of contraflexure accompanied by maximum crack width development along the floor and in the foundations of the structure.

It becomes apparent that the pattern of cyclic stress and strain is controlled by the inhomogeneity of the subsoil. Thus, for example, should "heaving clay" layer in Figure 60 a and b, been anticlinal rather than synclinal in its disposition, then the stress-strain pattern would have been reversed. Furthermore, should the distribution of smectitic clay minerals be haphazard as in the case in the Driefontein area, rather than confined to a well-defined layer or layers, then more complex differential movement patterns will result. In areas where the subsoil

/ inhomogeneity ----

inhomogeneity is characterised by the presence of materials only capable of compaction rather than heave, cyclic stress/strain patterns will still develop. With the presence of compactible subsoils, however, the total movement will always be one of settlement.

- - - o O o - - -

PART 6

=====

6. SUMMARY AND CONCLUSION

=====

The so-called Pretoria-Witwatersrand-Vereeniging triangle is not only an area of prime urban, commercial and industrial importance at the present time, but is also one growing with startling rapidity. A considerable portion of this area is underlain by dolomitic rocks and, if not currently characterised by unstable ground conditions as described in this disseration, has the latent potential for so doing. The research in the Driefontein and Henley/Lawley areas of the Far West Rand as well as in the Rietvlei area southeast of Pretoria has, therefore, appropriately examined many facets of ground instability which may occur within Karoo outliers associated with dolomitic bedrock, particularly at Driefontein where dewatering has taken place. It has shown how geological structure, lithology and geohydrology constitute major contributing factors to the development of unstable conditions.

The influence of geological structure is reflected in the erosion of the dolomitic bedrock along pre-Transvaal planes of weakness, particularly if they have suffered reactivation. That such post-Transvaal reactivation has occurred is clearly indicated in the

/Far West Rand ---

Far West Rand by the Bank Fault which not only displaced strata of the Witwatersrand Supergroup for a horizontal distance of about 8 kilometres, but also dislocated Malmani Subgroup rock as well as Timeball Hill quartzites.

The erosion of the Malmani dolomite by solution along structural planes of weakness resulted in the development of harsh karst-type topography in the dolomite and also in the creation of unstable residual materials, such as manganiferous wad. With the deposition of Karoo sedimentary rocks into the palaeo-karst dolomite topography, highly varied lithological profiles are created which add complexities to the promotion of ground instability.

The influence of the geohydrology, as a consequence of the changes of elevation adopted by the dolomitic water table in African and possible post-African erosion cycles, is also emphasised. Thus, the situation where vertical slots are eroded out of the dolomite in the vadose zone and horizontal caverns are developed in the phreatic zone, is duplicated. In the Far West Rand, therefore, it can be seen that the Malmani dolomite contains a complex system of vertical slots and horizontal caverns, each system having been evolved when the dolomite water table was positioned at a particular elevation for a prolonged period of time. The artificial lowering of the

/dolomite water ..

dolomite water, such as by dewatering activities of the gold mines, aggravated the instability of the cavern and slot systems, as witnessed at Driefontein and by the more dramatic and frequently tragic history of the Far West Rand.

The mechanisms responsible for the development of dolines and sinkholes, as proposed by numerous previous research workers, are described in detail. Acceptance of these theories, to explain surface and subsurface movement, accentuates the need to evolve logically sound procedures whereby meaningful interpretations of such movements can be made. Consequently, details are given of conventional procedures and the methodology required for precise measurements of surface levels and also the subsurface movements measured by telescopic bench marks. The principles of telescopic bench mark behaviour are elaborated upon as they enable diagnoses to be made on whether consolidation or progressive arch collapse over a void is occurring in the subsoils at depth. The relating of subsurface marker elevations changes to precise surface levels on a regular routine basis, with minimum required accuracies of 0,1mm and 1,0mm respectively, is an essential prerequisite for meaningful interpretations to be made of prevailing ground conditions. To interpret the historical behaviour of telescopic bench marks, the use of time/displacement graphs is recommended. However, to define the epicentres of unstable areas, the preparation of isopleth maps, showing the amounts of surface and subsurface

/movements ---

movement, which have occurred over a particular period of time, is advocated.

The study of the geological structure, lithostratigraphy and hydrology in the Driefontein area where Karoo sedimentary rocks infill slots and depressions weathered out of the dolomitic bedrock, show that complicated combinations of negative (downward) and positive (upward) surface and subsurface movements may occur. From several hundred correlation coefficient analyses, however, it has been established that the surface and subsurface movements are strongly related to cyclic elevation changes of complex ground water systems present in Karoo outliers. Negative ground movements are readily explained by the downward retreat of subsurface water through highly compactible soils mantling dolomitic bedrock beneath the Karoo sedimentary sequence. The intensity and prolonged history of consolidation is reflected by the pronounced slump structures occurring in the Rietvlei, Henley/Lawley and Driefontein outliers. Positive ground movements are, however, less readily explained as correlation coefficient analyses show a poor relationship between surface and subsurface behaviour and rainfall. Rather, the positive ground movements are promoted by rises in the elevation of subsurface water through Karoo sedimentary rocks containing expansive clay minerals. The distribution of expansive clay minerals in the Karoo sequence is, however, minor and indiscriminately disseminated rather than concentrated in well

/defined lithological ---

defined lithological units. Consequently, significantly greater upward migrations of moisture, over and above to those achieved by upward cyclic changes of subsurface water levels alone, are required to promote positive ground movements. Three mechanisms were considered, namely capillary action, the mineralogy of materials in the vadose zone and air-entrapment/atmospheric pressure effects. It has become apparent, however, that the upward migrations of moisture in the vadose zone cannot be effectively accomplished either by capillary action or the absorption ability of montmorillonite-bearing materials. Consequently, it must be concluded that the principal mechanism responsible for positive movement both at subsurface and ground level, are those of air-entrapment and atmospheric pressure effects.

All the conventional methods of interpreting surface and subsurface movements are retrospective in their approach. It is proposed, however, that by the application of further interpretive and statistical techniques to available data, predictions can be made as to the degree and intensity of future ground instability in Karoo outliers. Four techniques are proposed. Firstly, the conceptual evaluation of a potential instability risk hazard rating is presented. .Primarily such an evaluation requires that the physical or engineering characteristics of individual lithological units constituting a geological succession, be ranked according to their instability potential and that these potentials, in turn, are "weighted" on a basis of a

/units's apparent ---

unit's apparent thickness. It is considered that the instability potential of a geological material is a function of its compressibility, erodability and tensile weakness. By ranking the physical characteristics of infilling materials with numerical values to indicate degrees of instability and weighting these values in proportion to the thickness of each lithological unit, a potential instability value (Rf) may be obtained for a geological profile at a specific point. It is emphasised that cognisance must be made of the sequence with which the lithological units occur within the profile so that the Rf values can be modified if necessary. Once an Rf value has been obtained, hydrological and adjacent geological influences, such as the configuration of dolomitic bedrock and the percentage of cavities or voids present, must also be given numerical instability rankings and then applied as weighting factors so that an instability risk hazard rating (RH) may be obtained. Providing sufficient geological profile points, (e.g. boreholes), are available, an isopleth map can be prepared to which confidence limits, based on the density of the RH values, should be applied using geostatistical techniques. It is emphasised that the compilation of a meaningful potential instability risk rating necessitates that detailed geological hydrological and lithological data is collected, scrutinized and carefully evaluated by scientists or engineers experienced in dolomitic environments. Even then, the proposed concept of a potential

/instability ---

instability risk rating, which requires further research and refinement, should only be used in conjunction with other geotechnical evaluation techniques.

After interpreting and evaluating the surface and subsurface movements of several hundred telescopic bench marks, it becomes apparent that the rates of movement are more useful than the amounts of movement for diagnosing potential instability. Consequently, the second prediction technique proposed in this dissertation necessitates plotting and analysing velocity and acceleration/deceleration curve patterns. In the case of a developing doline for example, the subsidence of surface is characterised by a gradual, but steady increase in velocity without any erratic changes of either acceleration or deceleration. By contrast, the velocity and acceleration/deceleration patterns of movements in an area being subjected to sinkhole development are significantly different from that undergoing consolidation. Significant rates of movement in developing sinkhole situation are confined to the subsurface rather than the surface. Furthermore, the frequency of changes in either velocity, acceleration or deceleration patterns are widely erratic without any discernable trend. An example of actual rates of movement in a telescopic bench mark situated some 30m from a sinkhole shows that the velocity and acceleration/deceleration curves commenced fluctuating beyond 95 per cent confidence limits at least two months prior to actual collapse taking place.

/The third ---

The third proposed prediction technique involves plotting the means and standard deviations of surface and sub-surface movements over a selected number of measured cycles. Such mean and standard deviations isopleth maps, used in conjunction with normal time/displacement isopleth maps, enable existing epicentres of instability to be defined with considerable accuracy and enable future trends to be established. Furthermore, it is interesting to note that a close relationship appears to exist between standard deviation isopleths and crack development patterns. It is suggested, therefore, that the standard deviation isopleths may be used to predict areas where maximum distress may be imposed on either existing or proposed structures.

The cyclic recharging of aquifers constitutes the basis of the fourth prediction technique proposed in this dissertation. Research in the Driefontein area has shown that the amounts of movements occurring as a result of subsurface water migration are relative to the compaction and expansion capacities of infilling materials. Furthermore, because the subsurface water elevation changes are associated with the seasonal recharge of aquifers, these changes, as well as sympathetic movements in sub-soils and on the surface, can be predicted with reasonable accuracy. It must be noted, however, that these sympathetic cyclic movements in the subsoil and on surface are only measurable in millimetres and are over and above the total movements associated with deep-seated ground instability. Nevertheless, the importance of these relatively small cyclic movements cannot be over-emphasised as it is

/considered ---

considered they are the cause of differential movements. Since even small amounts of differential movement result in crack development and damage to surface structures, the ability to predict differential movement will be invaluable. Thus, the adequacy of existing foundations can be reassessed and, if necessary, modified, whereas the foundations for proposed structures can be designed to accommodate maximum cyclic movements. In conclusion, it must be stated that although the work presented in this dissertation has been reasonably comprehensive, it is realised that the complex subject of ground instability associated with Karoo outliers in a dolomitic environment has barely been penetrated and extensive avenues for research still exist.

- - - o O o - - -

ACKNOWLEDGEMENTS.

I wish to express my gratitude and indebtedness to all those persons who have assisted me with the preparation of this dissertation with particular reference to :

- * My promoter and co-promoter, Professor. A. Van Schalkwyk and Professor C.P. Snyman for their unstinting advice and guidance.
- * The Management of Tongaat Corogroup for permission to submit a great deal of the data used in this dissertation.
- * Mr. C.T. Dickinson and the staff of the Tongaat Corogroup Technical Department, particularly Mrs. Flottow and Miss G. Fourie for respectively typing the text and undertaking all the draughtsmanship.
- * The late Professor J.E. Jennings who was the inspiration for and the motivator of the research work undertaken in the Driefontein area.
- * My wife, not only for proof-reading the text but also for her moral support, forbearance and patience over the time it has taken to complete this research work.

- - - o 0 o - - -

LIST OF REFERENCES

- BEZUIDENHOUT, C.A. and ENSLIN, J.F. (1969). Surface subsidence and sinkholes in the dolomite area of the Far West Rand, Transvaal, Republic of South Africa. Int. Symp. on Land Subsidence. Tokyo.
- BIANCHI, W.C. and HASKELL, E.E. (1966). Air in the vadose zone as it affects water movement beneath a recharge basin. J. Water Research, Vol. 2, 315-322.
- BRAIN, C.K. (1958). The Transvaal ape man bearing cave deposits. Trans. Mus. Mem 11., Ph.D thesis, University of Cape Town.
- BRETZ, J.H. (1942). Vadose and phreatic features of limestone caverns. J. of Geol. Vol. 50 (6) Part II, 675-811.
- BRETZ, J.H. (1953). Genetic relations of caves to peneplains and big springs in the Ozarks. Amer. J. Sci., Vol. 251 (1), 1-24.
- BRINDLEY, G.W. (1951). X-ray identification and crystal structures of clay minerals. Mono. Miner. Soc. London, Chap. 2, 32-75.
- BRINK, A.B.A. (1979). Engineering Geology of southern Africa. Vol. 1. Building Publications, Pretoria.
- BRINK, A.B.A. (1983). Engineering Geology of southern Africa. Vol. 3. Building Publications, Pretoria.
- BRINK, A.B.A. and ERIKSSON, K.A. (1970). Geology of the Far West Rand dolomitic compartments with particular reference to the local area of the Driefontein Brickworks. Unpub. report to Brick. Corp. of S. Afr.

- BRINK, A.B.A. and PARTRIDGE, T.C. (1965). Transvaal karst: Some considerations of development and morphology, with special reference to sinkholes and subsidences on the Far West Rand. S. Afr. Geog. J. vol. 67, 11-34.
- BROCK, B.B. and PRETORIUS, D.A. (1964). Rand basin sedimentation and tectonics. In Houghton, S.H. The geology of some ore deposits in southern Africa. Trans. Geol. Soc. of S. Afr. vol. 1, 546-601.
- CLARK, I. (1979). Practical Geostatistics. Applied Science Publishers Ltd., London.
- CLEWS, F.H. (1969). Heavy clay technology. Academic Press, London.
- COON, R.F. and MERRITT, A.H. (1970). Predicting in-situ modulus of deformation using rock quality indexes. Amer. Std. Test. Materials. STP 477, 154-173.
- COUSENS, R.R.M. and GARRETT, W.S. (1969). The flooding at West Driefontein Mine, South Africa. J. of S. Afr. Inst. Min. and Metallurg. vol. 69 (8), 421-463.
- DAVIES, W.M. (1930). Origin of limestone caverns. Bull. Geol. Soc. of Amer. Vol. 41, (3), 475-628.
- DAY, P. (1981). Properties of wad. Proc. Seminar on the engineering geology of dolomite areas. University of Pretoria, 135-147.
- DE KOCK, W.P. (1964). The geology and economic significance of the West Wits Line. In Houghton, S.H. The geology of some ore deposits in southern Africa. Trans. Geol. Soc. of S. Afr., Vol. 1. 546-601.
- DOUCH, G.M. and WIID, B.L. (1982). Foundations investigation for a brick factory at BTL 11 property. Unpub. report Cl. 2972/1 submitted by Steffen Robertson and Kirsten (Civ) Inc., to Tongaat Corogroup, S. Afr.

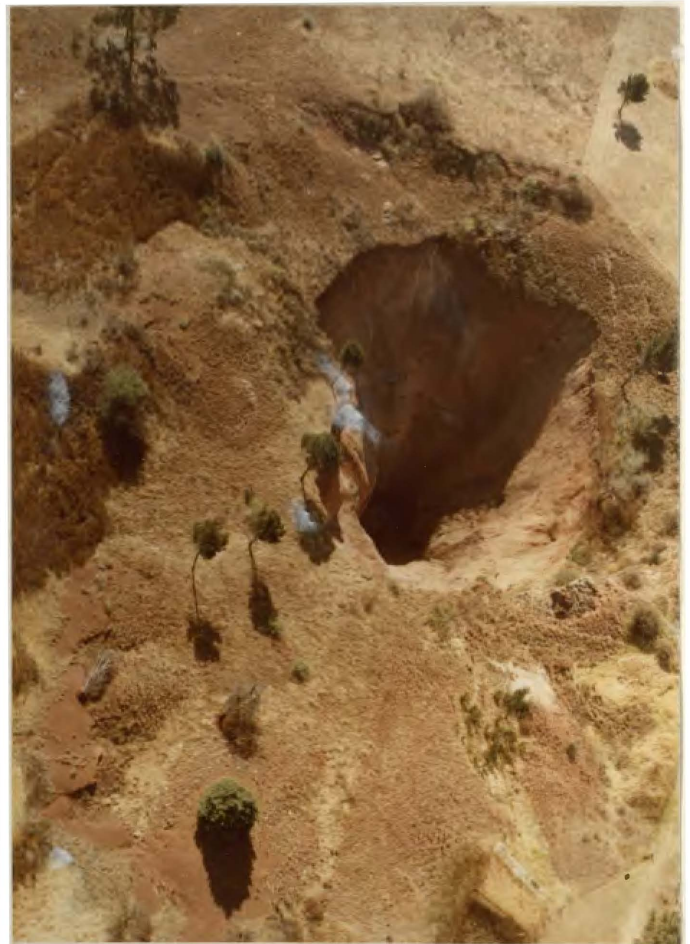
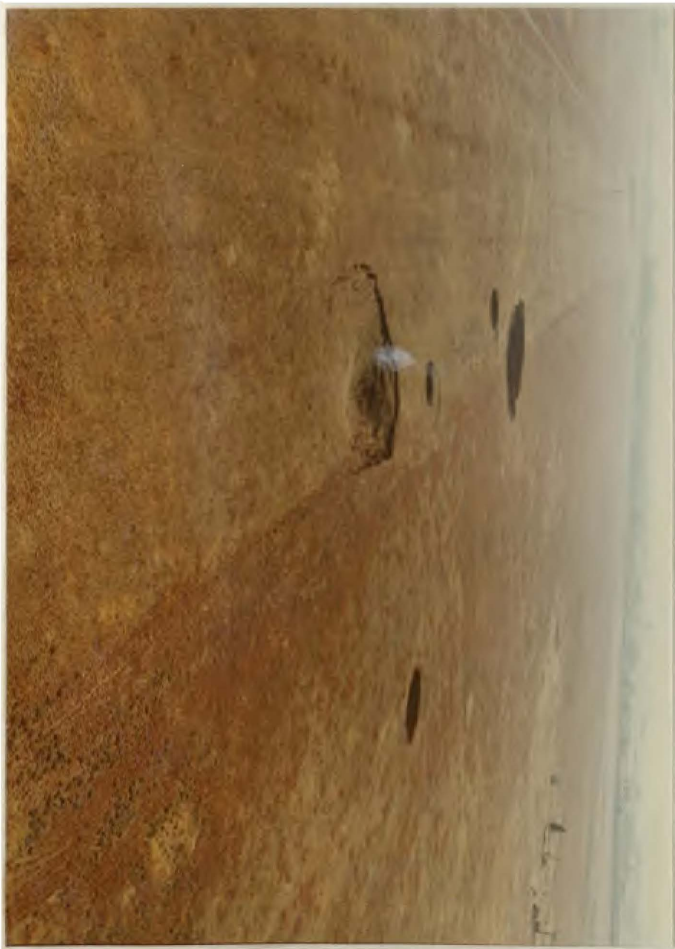
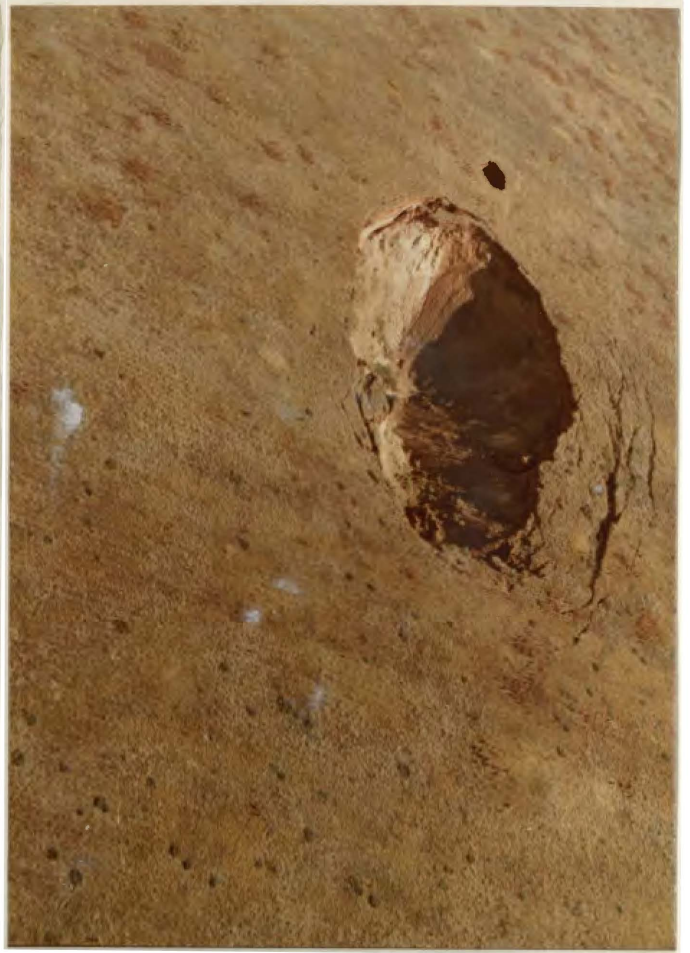
- DU TOIT, A.L. (1954). The Geology of southern Africa. Oliver and Boyd, London.
- ENSLIN, J.F. and SMIT, P.J. (1955). Geophysical surveys for foundations in South Africa with special reference to the sinkholes in the dolomite south of Pretoria. Proceedings of the First Regional Conference for Africa. Trans. S. Afr. Inst. of Civ. Engrs., Vol. 5 (9), 318-322.
- ERIKSON, K.A. (1970). A basin analysis of the Transvaal sequence in the Potchefstroom synclinorium, Transvaal and Orange Free State. M.Sc. thesis, Univ. of the Witwatersrand.
- ERIKSON, K.A., MCCARTHY, T.S. and TRUSWELL, J.F. (1975). Limestone formation and dolomitization in a Lower Proterozoic succession for South Africa. J. of Sediment Pet., Vol. 5 (3), 604-614.
- FLEISHER, J.N.E. (1979). Groundwater contaminations of a dolomite aquifer in the Zuurbekom area, southwestern Transvaal. Tech. Rep. GH 3110. Dept. of Water Affrs., Pretoria.
- FREEZE, R.A. and CHERRY, J.A. (1979). Groundwater. Prentice - Hall Inc., Englewood Cliffs, New Jersey.
- GARDNER, J.H. (1935). Origin and development of limestone caverns. Bull. Geol. Soc. of Amer. Vol. 46(8), 1255-1274.
- HOBBS, N.B. (1974). Factors affecting the prediction of settlement of structures on rock: With particular reference to the Chalk and Trias: Review paper Session IV, in Settlement of Structures. Pentech Pres. London, 579-610.
- HOLLAND, B.E. (1982). Economical housing foundation design on expansive soils. Paper presented at several locations under sponsorship of Natal Build. Soc.

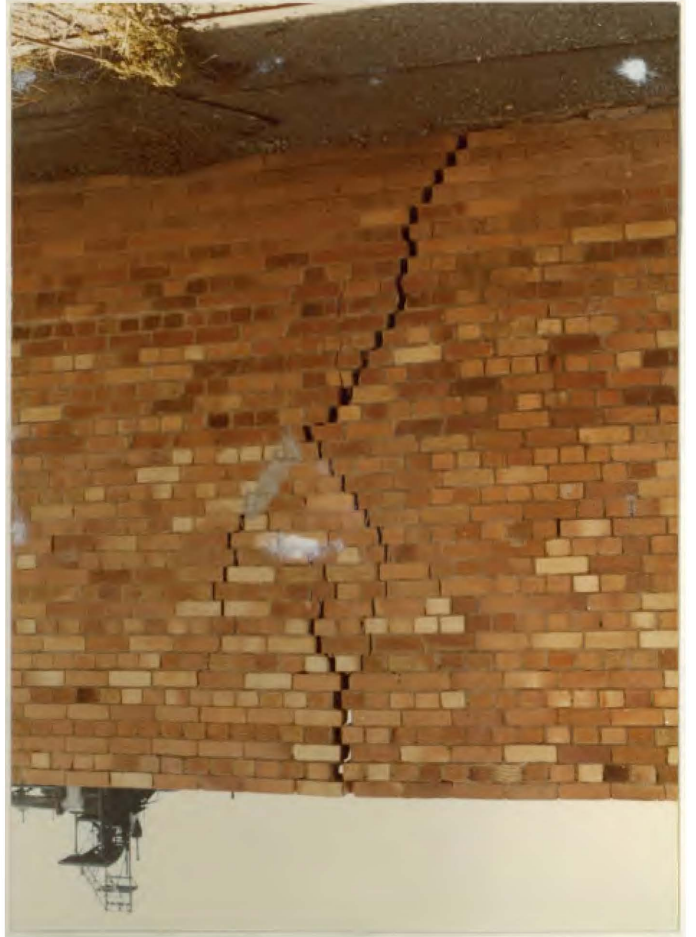
- JACOB, C.E. (1940). On the flow of water in an elastic artesian aquifer. Trans. Amer. Geophys. Union. Vol. 21, 574-586.
- JENNINGS, J.E. (1966). The mechanisms of collapse at a sub-surface void to form a sinkhole; full scale tests on the Pulik Caves at Venterspost. Unpub. report Tvl. and O.F.S. Chamb. of Mines. Research Proj., 212/64/10205.
- JENNINGS, J.E. (1971 a). The subsidence of the ground surface resulting from a lowering of the water table in a sub-soil which contains compressible soil strata. Unpub. report to Brick, Corp., of S.Afr.
- JENNINGS, J.E. (1971 b). The detection of potential sinkhole conditions in a dolomitic subsoil from observations of deformation of telescopic bench works. Unpub. report to Brick Corp., of S.Afr.
- JENNINGS, J.E., BRINK, A.B.A., LOUW, A. and GOWAN, G.D. (1965). Sinkholes and subsidences in the Transvaal dolomites of South Africa Proc., 6th Int. Conf. of Soil Mech. and Foundtn Engng., London Vol. 1, 316-319.
- MACLEOD, I.A. and ABU-EL-MAGD, S.A. (1980). The behaviour of brickwalls under conditions of settlement. Paper to Instn. of Struct. Engrs., London.
- McWHORTER, D.E. (1971). Infiltration affected by flow of air. Calif. State Univ. Hydrol. Paper 49.
- MIELENZ, R.C. and KING, M.E. (1955). Physical chemical properties and engineering performance of clays. Calif. Div. Mines., Bull. 167, 196-254.
- PAPENDORF, O.L. (1971). Strike frequency diagram of faults in the Far West Rand. In Brink, A.B.A., Engineering geology of southern Africa. Vol. 1. Building Publications, Pretoria.

- PARTRIDGE, T.C., HARRIS, C.H. and DIESEL, V.A. (1981).
Construction upon dolomites of the southwestern Transvaal Paper presented to Int., Engrng. Geol. Symp., Istanbul.
- PECK, A.J. (1960). The water table affected by atmospheric pressure. J. Geophys. Res. 2383-2388
- PIENAAR, F.L. (1971). The relationship between surface fractures and subsidence in the dolomite of the Far West Rand. M.Sc. thesis, Univ. of the Witwatersrand, Johannesburg.
- PIKE, D.R. (1971). Personal communication to A.B.A. Brink : In Engineering geology of southern Africa. Vol., 1. Building Publications, Pretoria.
- ROBINSON, T.W. (1939). Earth tides shown by fluctuations of water levels in wells in New Mexico and Iowa. Trans. Amer. Geophys. Union., Vol. 20, 656-666.
- SCHWARTZ, H.I. and MIDGLEY, D.C. (1975). Evaluations of geohydrologic constants on the Far West Rand. Trans. S. Afr. Instn. of Civ. Engrs. vol. 17, 31-36.
- STEFFEN, ROBERTSON and KIRSTEN (Civil) Inc. (1983). Geotechnical report for proposed brick factory at Rietvlei. Northern Transvaal. Unpub. report, Proj. No. PT. 3701, for Tongaat Corogroup, S. Afr.
- STEFFEN, ROBERTSON and KIRSTEN (Civil) Inc. (1984). Proposal for establishing and monitoring a geotechnical instrumentation system at Lawley I, Lawley II and Henley properties. Unpub. report, Proposal No. Cl 4051/1 to Tongaat Corogroup, S. Afr.
- TAUTE, A.H. and TRESS, P.W. (1971). Dewatering of the flooded mine workings in the Bank Compartment. S. Afr. Min. and Engng. J., Vol. 83 (4061), 23-45.

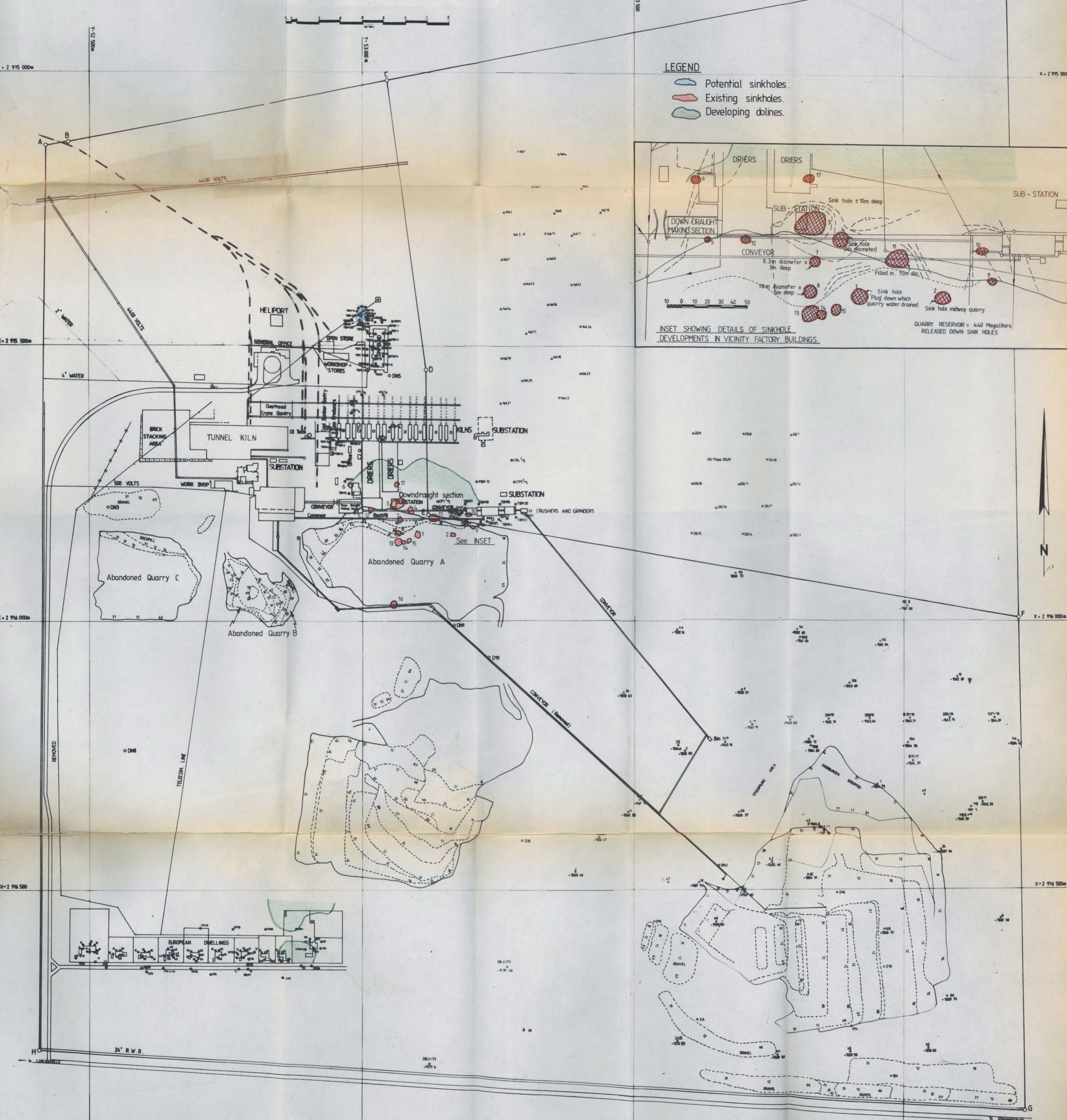
- TERZAGHI, K. (1925). Erdbaumechanik. F. Deutriche, Vienna.
- TODD, D.K. (1959). Groundwater hydrology. John Wiley and Sons Inc., New York.
- TRUSWELL, J.F. and ERICKSSON, K.A. (1972). Morphology of stromatolites from Transvaal dolomite. Trans. Geol. Soc. S. Afr. vol. 75 (2), 277-302.
- VENTER, I.S. (1981). Evaluasie van dolomietgebiede - 'n klassifikasiebenadering. Proc. Seminar on the engineering geology of dolomite areas. University of Pretoria 272-284.
- WATT, I. (1972). Driefontein Brick and Potteries : report on precise levelling June 1970 to October 1972. Unpub. report to Brick Corp. of S. Afr.
- WIID, B.L. (1981). Are Karoo outliers and similar geological bodies within dolomites completely stable? Proc. Seminar on the engineering geology of dolomitic areas. University of Pretoria, 261-271.
- WOLMARANS, J.F. (1976). Personal communication to A.B.A. Brink. In Engineering geology of southern Africa. Vol. 1 Building Publications, Pretoria.
- WOLMARANS, J.F. (1980). Results of drilling to select a suitable site for the establishment of kilns. Unpub. report submitted by Webb and Partners to Corobrik Transvaal.
- WRENCH, B.P. (1984). Plate tests for the measurement of modulus and bearing capacity of gravels. Draft of paper to be presented to S.A. Instn. of civ. Engrs.



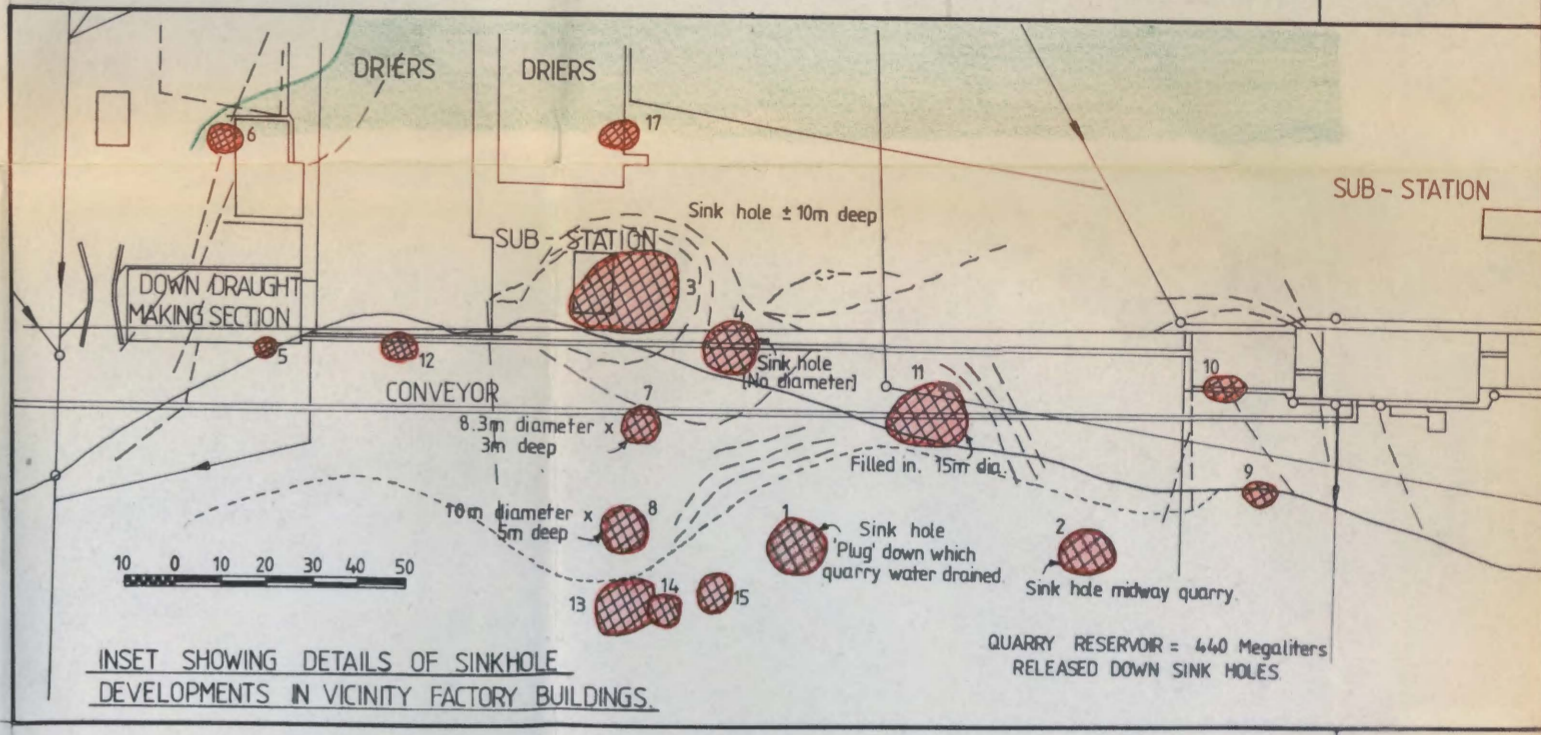




SCALE 1 : 4 000



- LEGEND**
- Potential sinkholes.
 - Existing sinkholes.
 - Developing dolines.

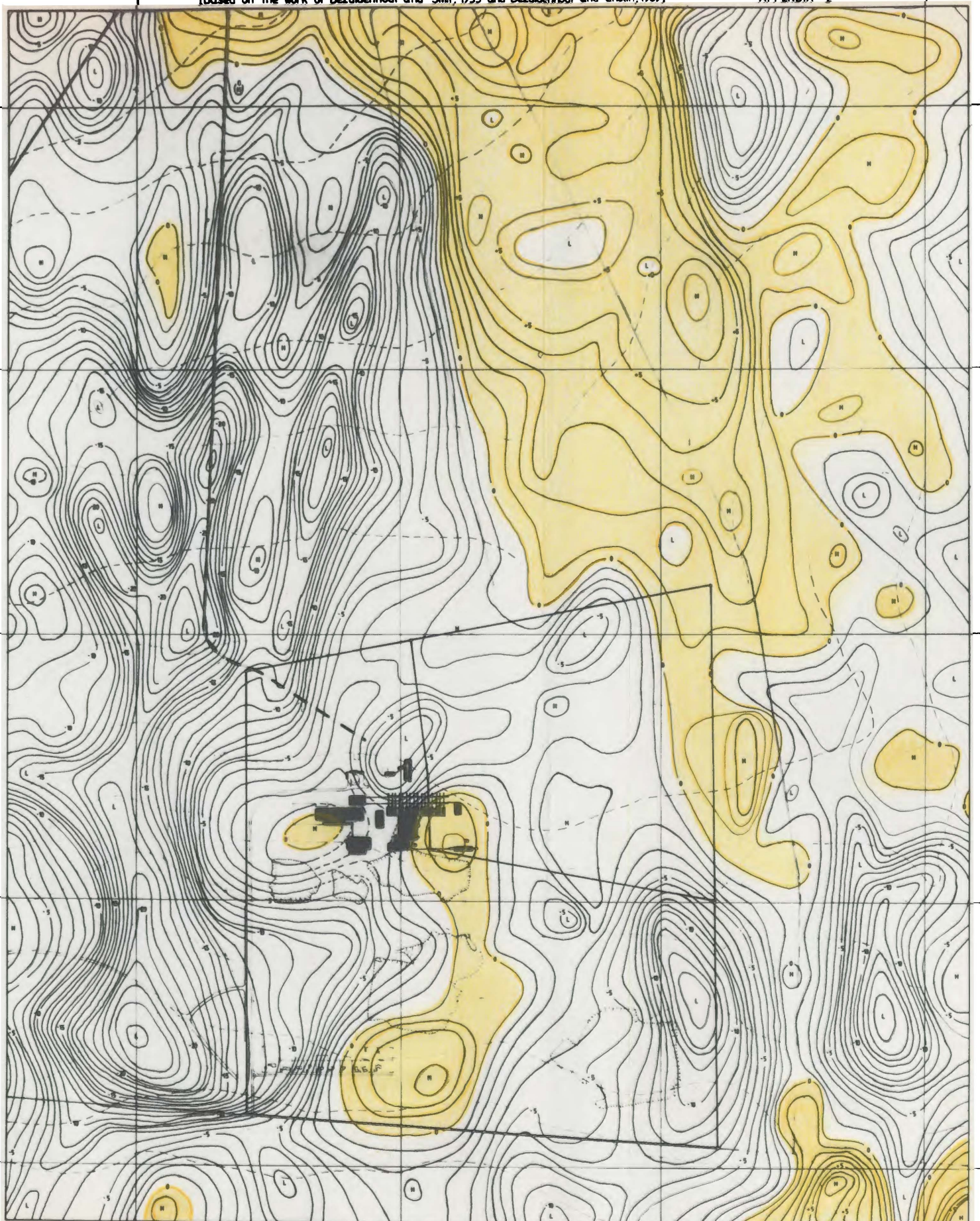


QUARRY RESERVOIR = 440 Megalitres
RELEASED DOWN SINK HOLES



Gravimetric Survey of the Drieruim area and environs.

[Based on the work of Bezuidenhout and Smit, 1955 and Bezuidenhout and Enslin, 1969]

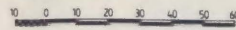


□ Areas shaded yellow depict where dolomitic bedrock was situated above the water table prior to dewatering.

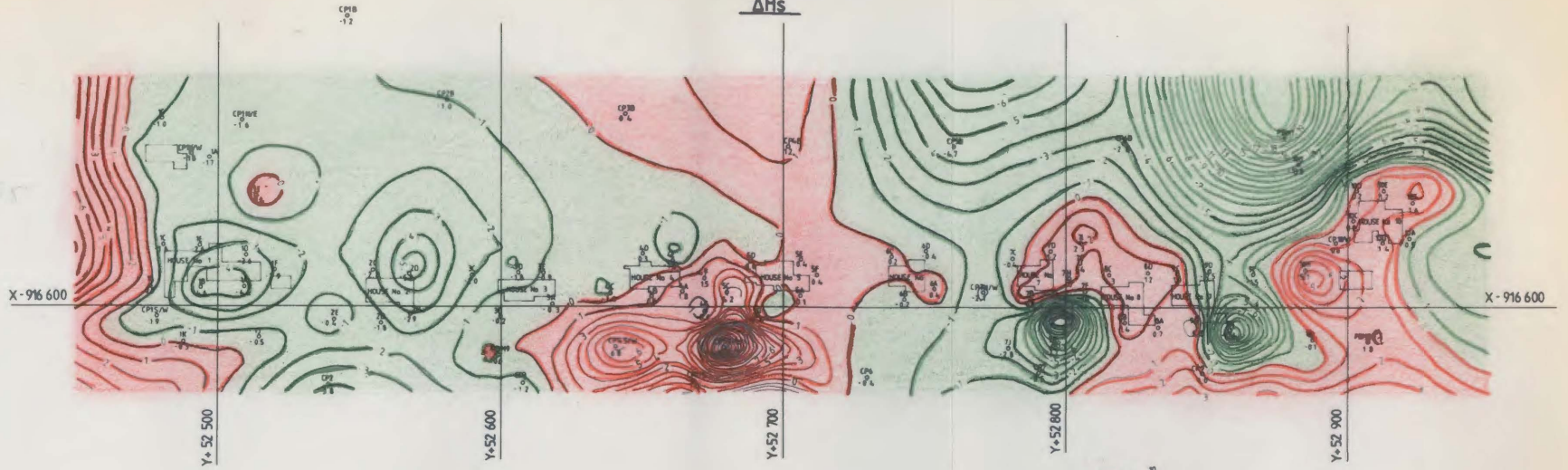
SCALE 1:10000

Isopleths showing Surface (ΔH_s), Upper Surface Marker (ΔH_u) and Lower Sub-Surface (ΔH_l) Elevation changes in the Housing area .

Scale 1:1000

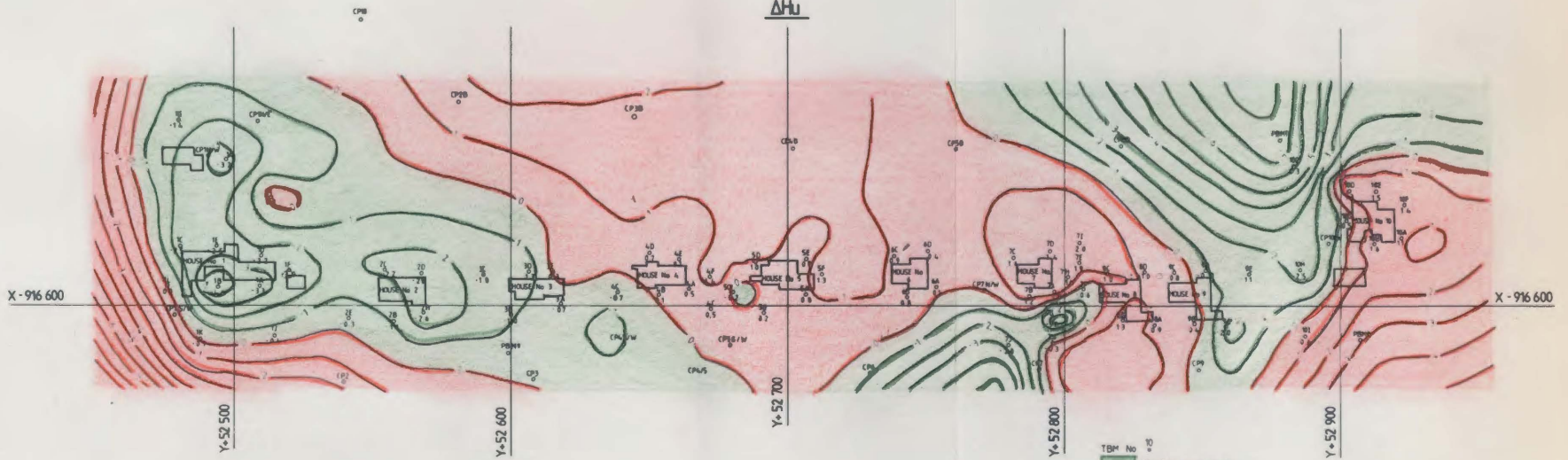


ΔH_s



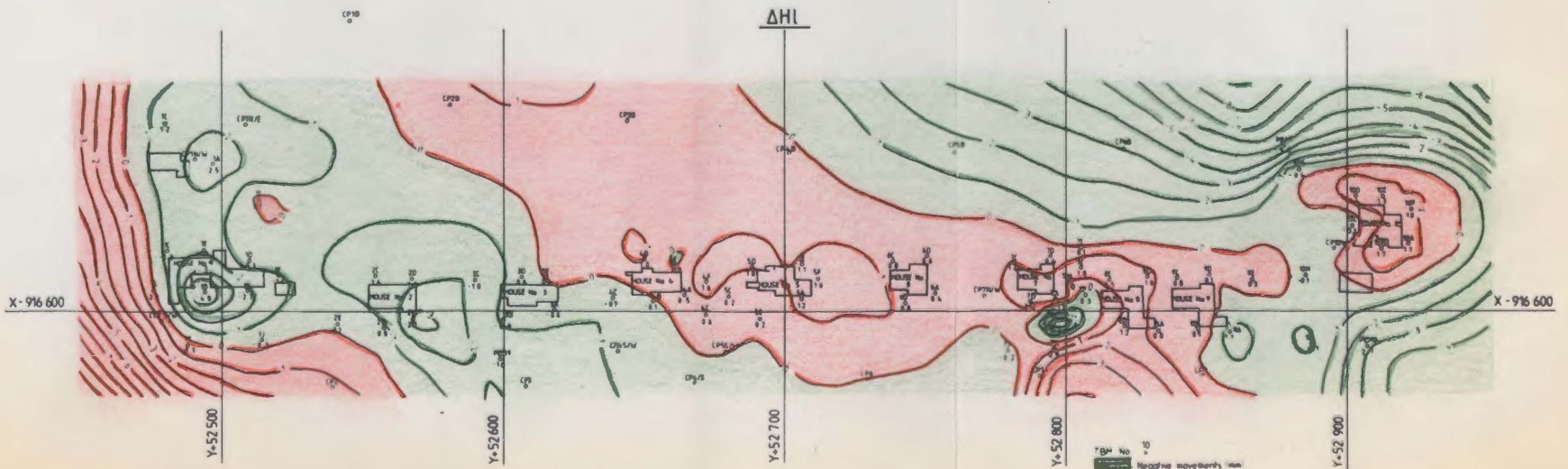
TBM No 10
█ Negative movements (mm)
█ Positive movements (mm)

ΔH_u



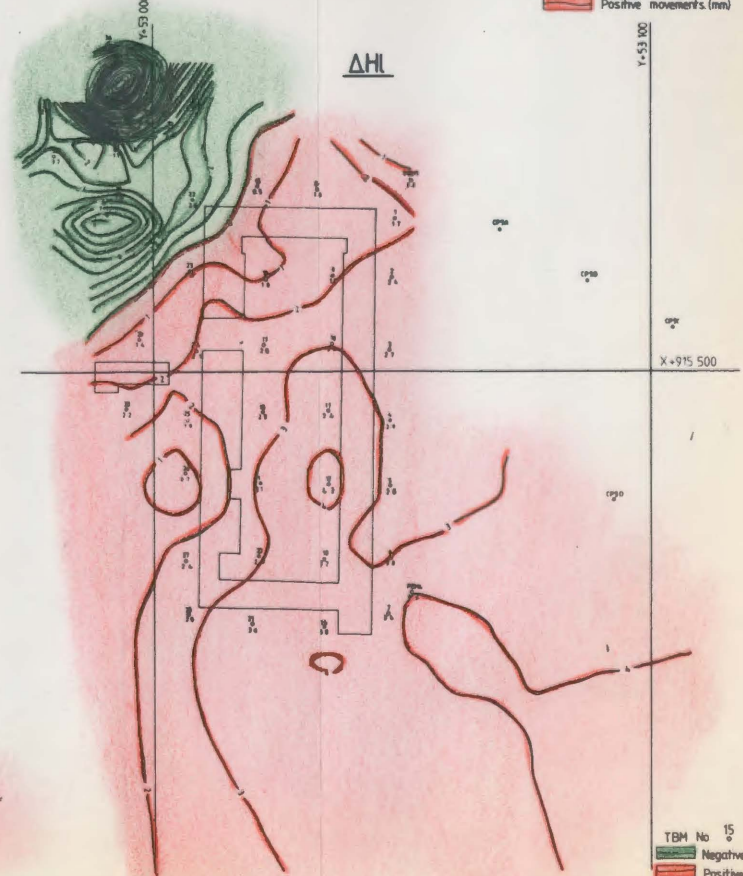
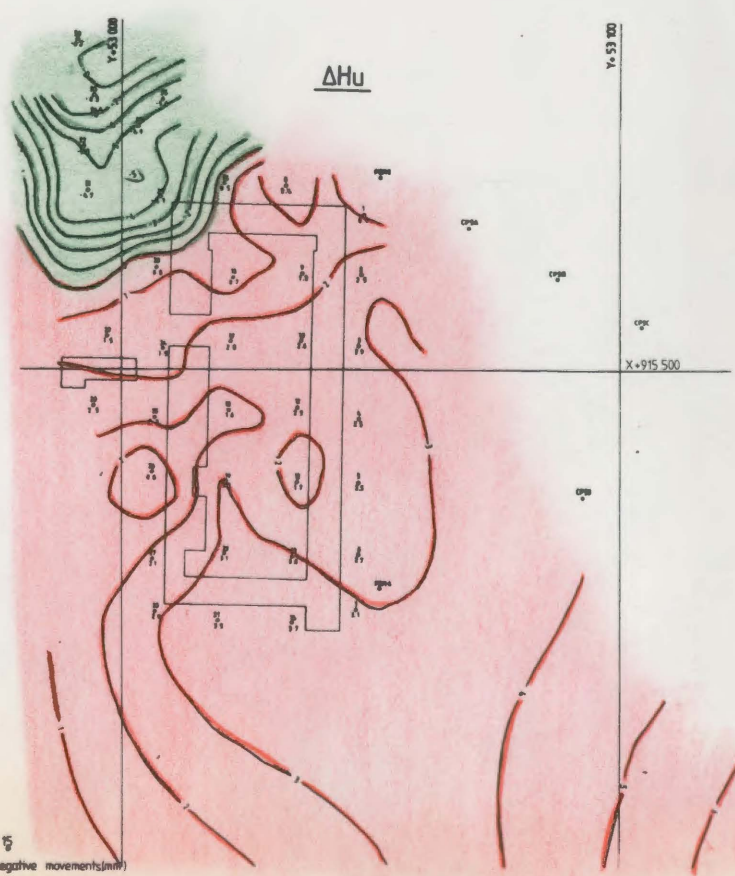
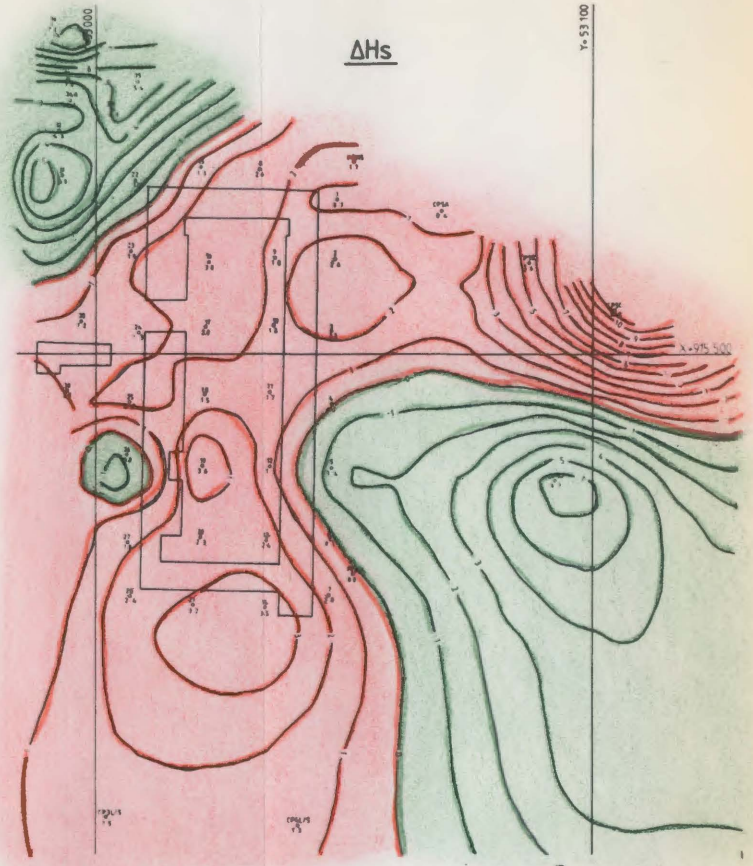
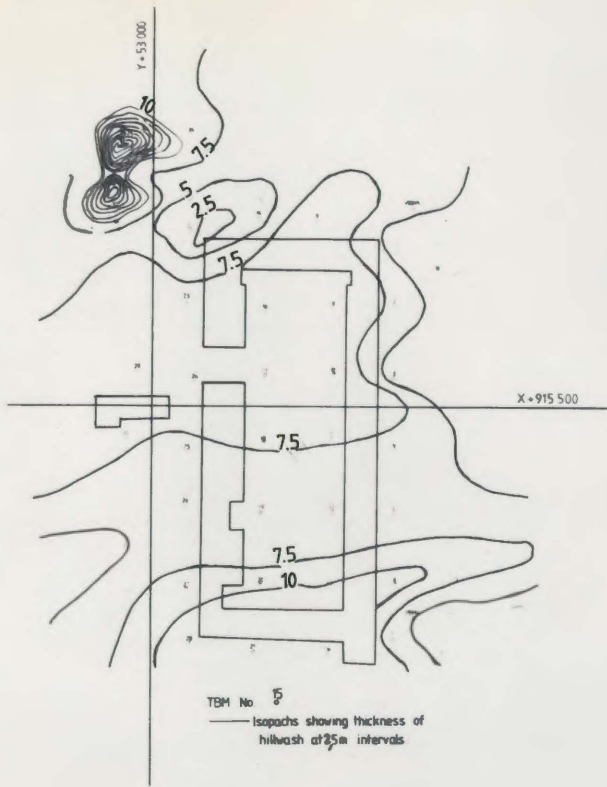
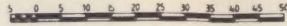
TBM No 10
█ Negative movements (mm)
█ Positive movements (mm)

ΔH_l



TBM No 10
█ Negative movements (mm)
█ Positive movements (mm)

Isopleths showing Surface (ΔH_s), Upper Surface Marker (ΔH_u) and Lower Subsurface (ΔH_l) elevation changes in the Compound area.



TBM No. 15
— Negative movements (mm)
— Positive movements (mm)

TBM No. 15
— Negative movements (mm)
— Positive movements (mm)

TBM No. 15
— Negative movements (mm)
— Positive movements (mm)

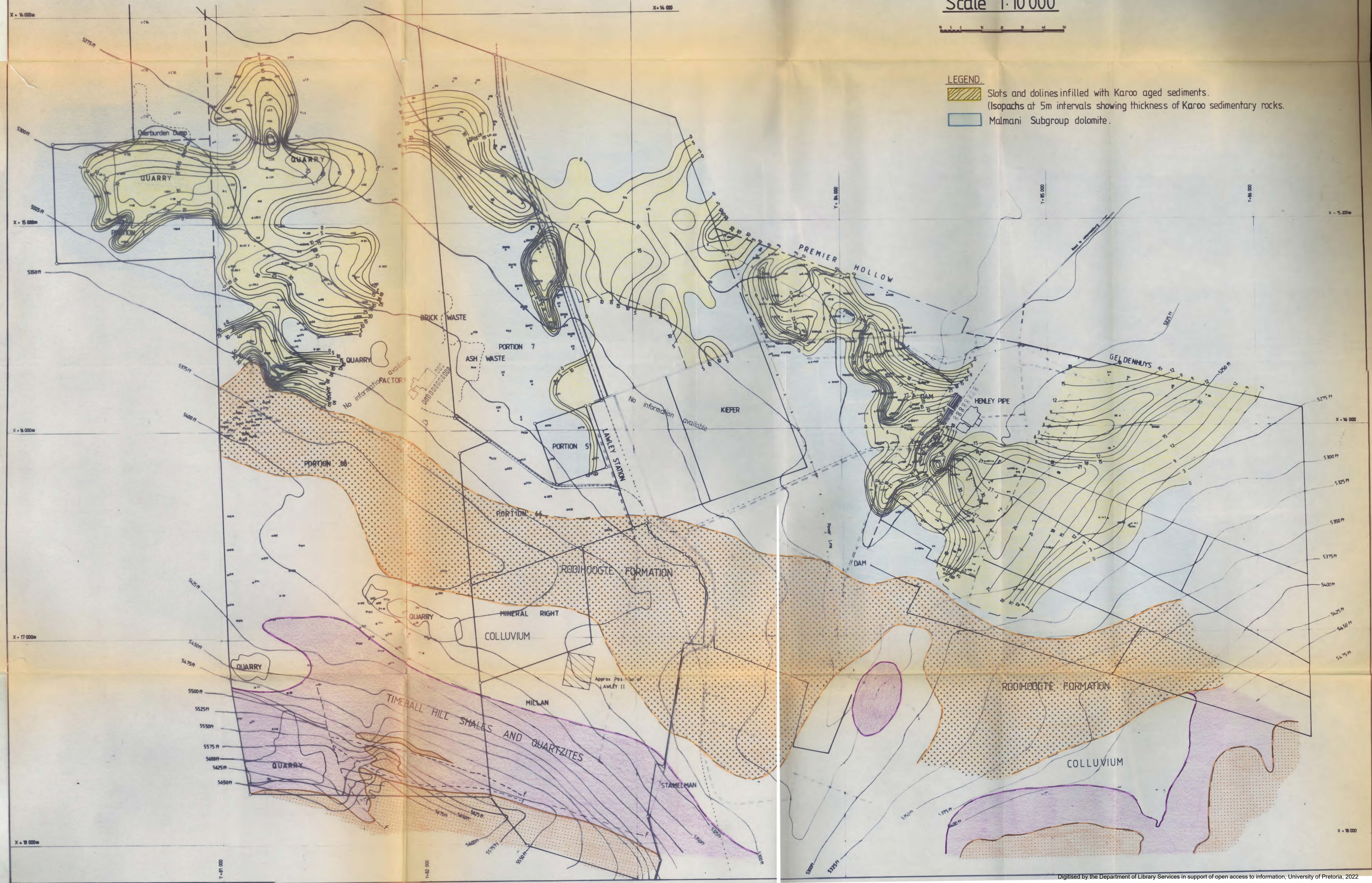
Slot configurations in the dolomite at Henley / Lawley outlier.

Scale 1:10 000



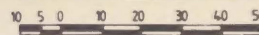
LEGEND

- Slots and dolines infilled with Karoo aged sediments. (Isopachs at 5m intervals showing thickness of Karoo sedimentary rocks.)
- Malmani Subgroup dolomite.



GEOLOGICAL PROFILES OF SLOTS IN THE VICINITY OF DRIEFONTEIN BRICKWORKS.

Scale 1 : 1000



PLEISTOCENE TO RECENT

Sandy soils with ferricrete gravels

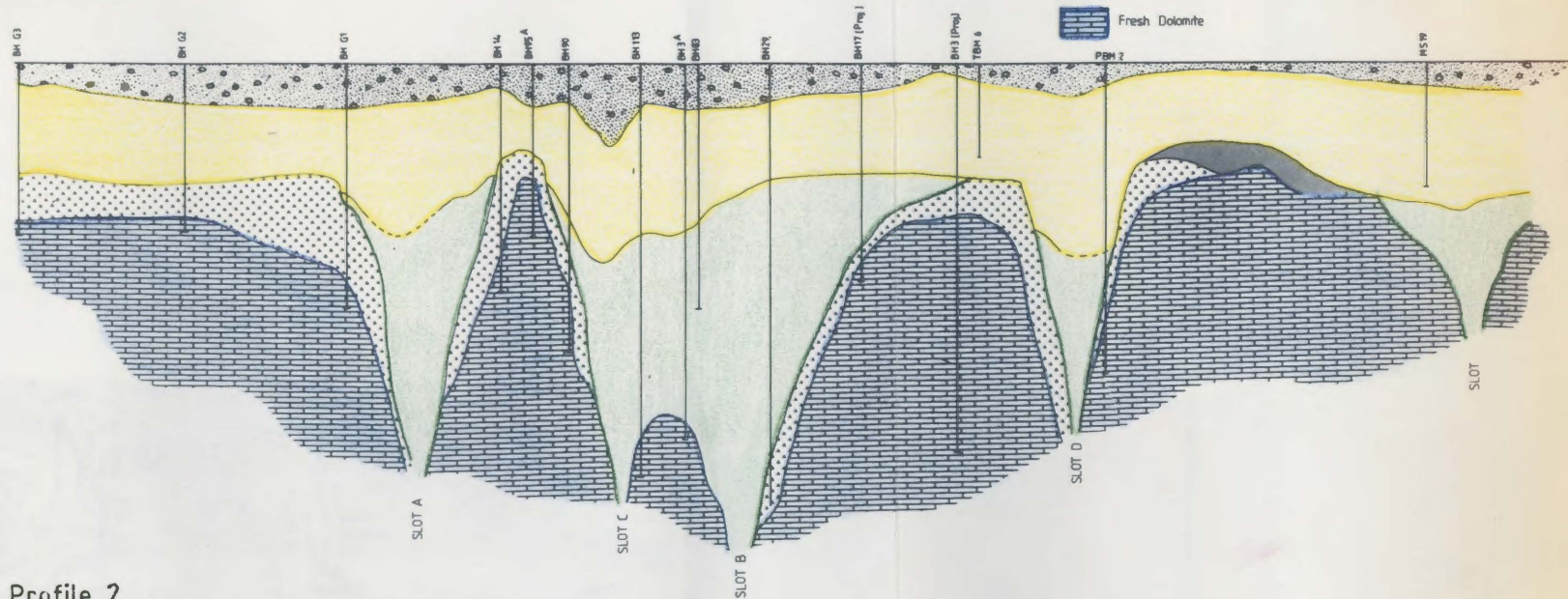
KAROO SUPERGROUP

Kaolinitic shales with occasional siltstone horizons
 Carbonaceous shales and mudstones with seams of low rank coal

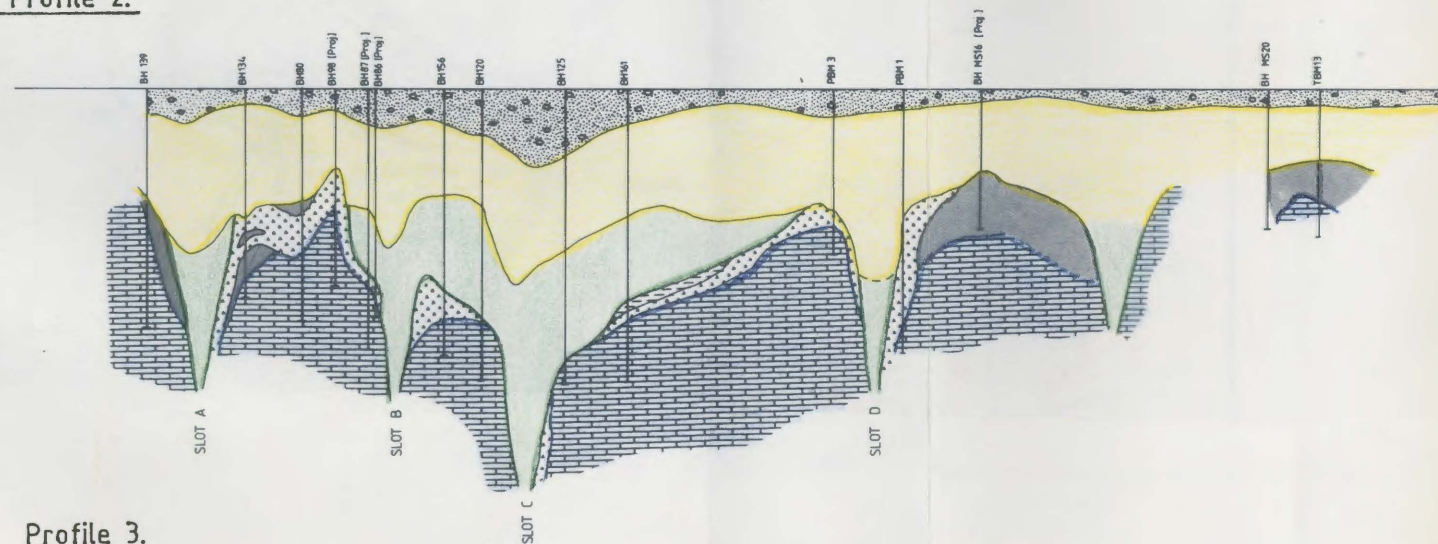
TRANSVAAL SUPERGROUP [MALMANI SUBGROUP]

Manganiferous wad
 Unctuous clays
 Pseudo brecciated chert and weathered dolomite with manganiferous wad
 Weathered dolomite and manganiferous wad
 Fresh Dolomite

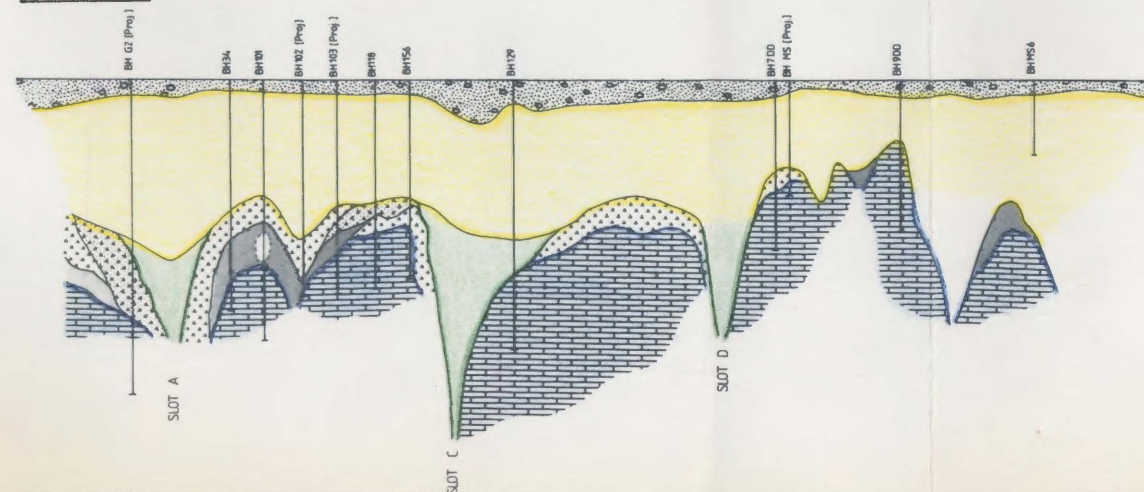
Profile 1.

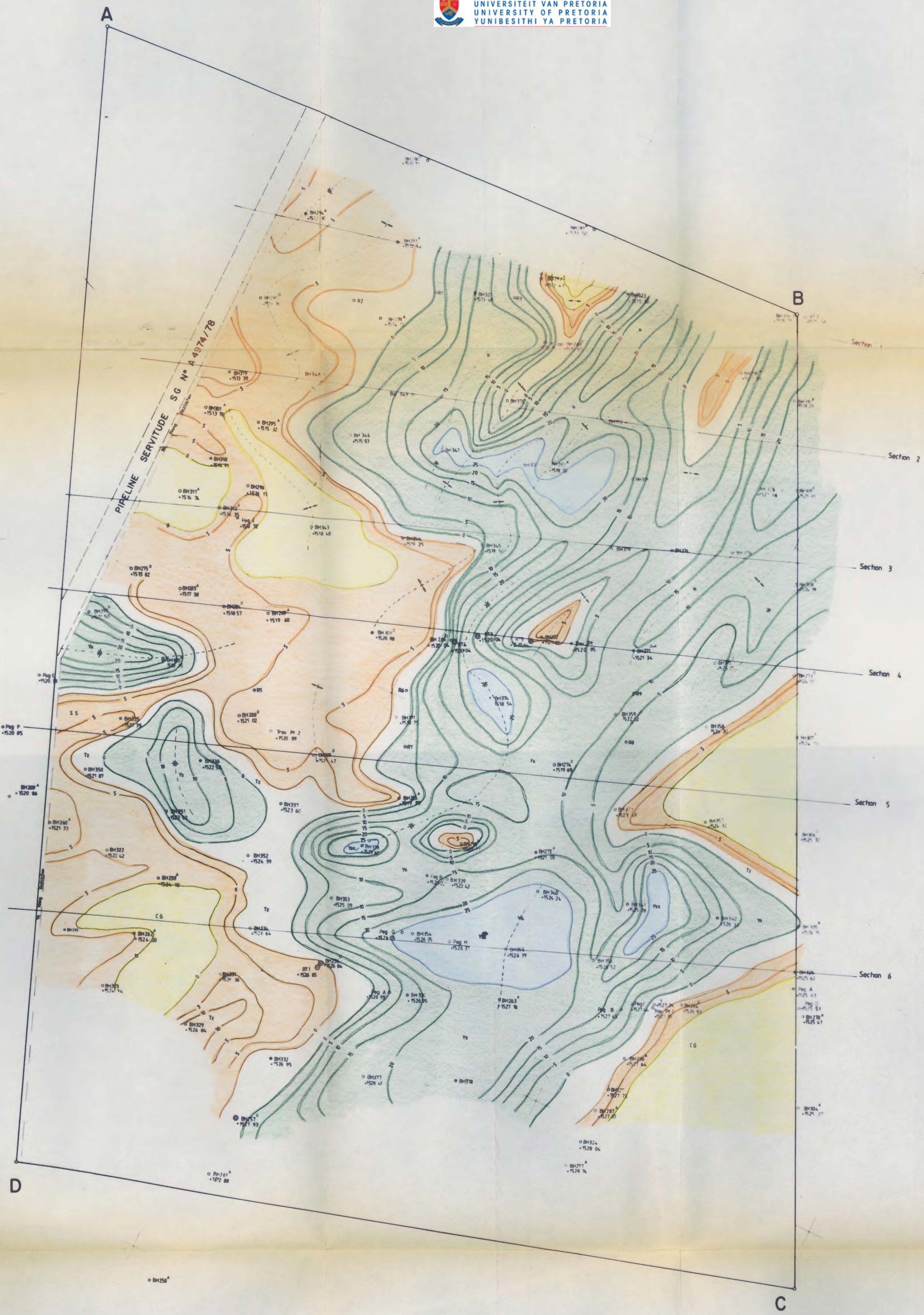


Profile 2.



Profile 3.





Geological Legend

10	Ys	Medium - coarse grained grt
20	Ys	Soft - moderately hard, yellow khaki slightly micaceous shale with grey phosps
30	Tz	Intercalated bands of plastic clay, cream shale, white sandstones and grits
40	SS	Soft brown shaly sandstone with thin, pale cream and purple ferruginous shale partings
50	CG	Soft crummy grey shale with yellow phase at base
	CG	Purple - brown - chocolate clay
	CG	Moderately hard, grey shale
	CG	Black carbonaceous shale with thin coal seams

STRUCTURAL FEATURES OF THE KAROO AGED SEDIMENTARY ROCKS IN THE RIETVLEI OUTLIER.

Isopachs at 5m intervals, showing thickness of the yellow khaki shale (Ys) and shaly sandstone (SS).

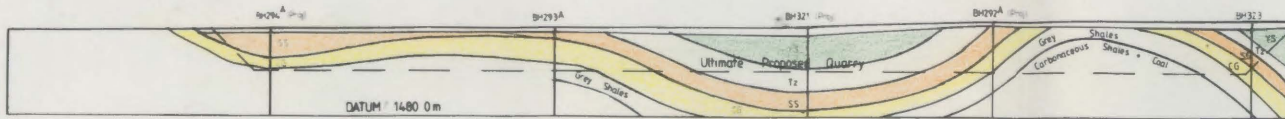
Scale 1 : 5 000

**GEOLOGICAL SECTIONS
RIETVLEI PROPERTY**

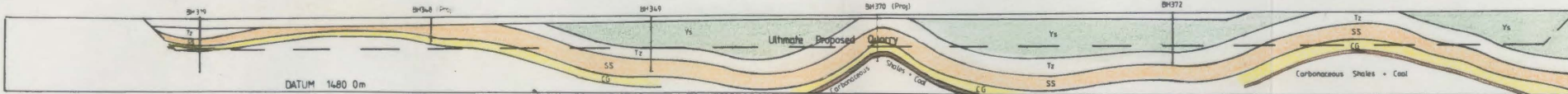
Scale:



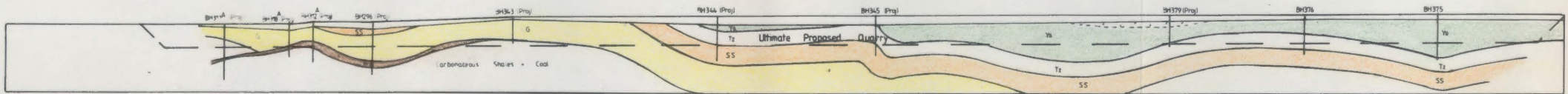
SECTION 1



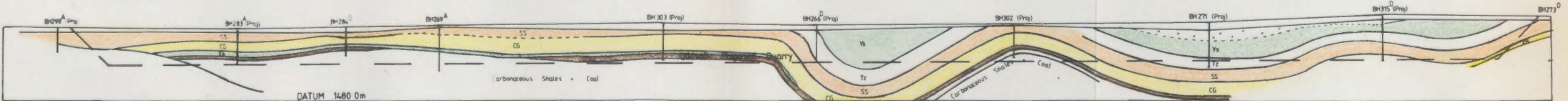
SECTION 2



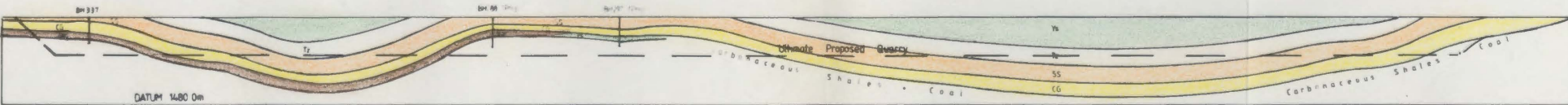
SECTION 3



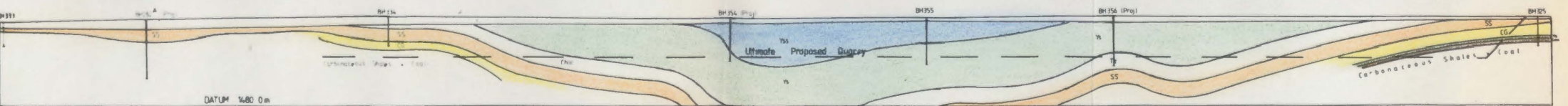
SECTION 4



SECTION 5

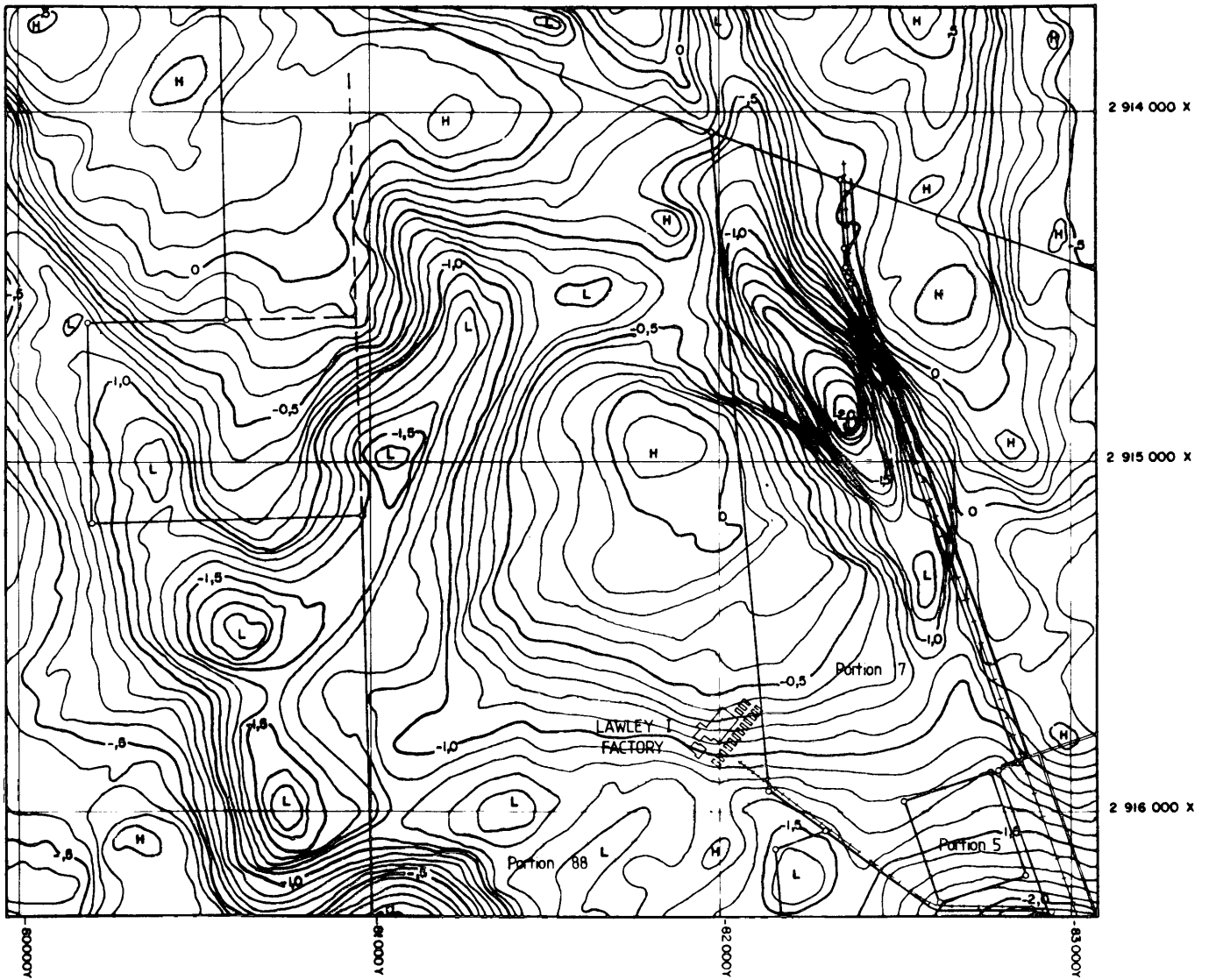


SECTION 6



GRAVIMETRIC SURVEY OVER PART OF THE LAWLEY OUTLIER.

100 0 100 200 300 400 500 meters

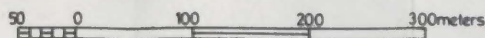


— RESIDUAL GRAVITY CONTOURS — GROUND CONTOURS

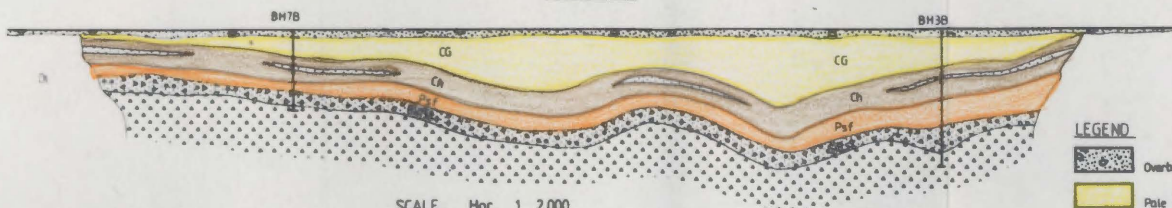
80239/ FIG 2

Structural features of the Karoo aged sedimentary rocks in a portion of Lawley outlier.

Contours (1m intervals) to interface between Pale Cream Shale and Carbonaceous mudstone.



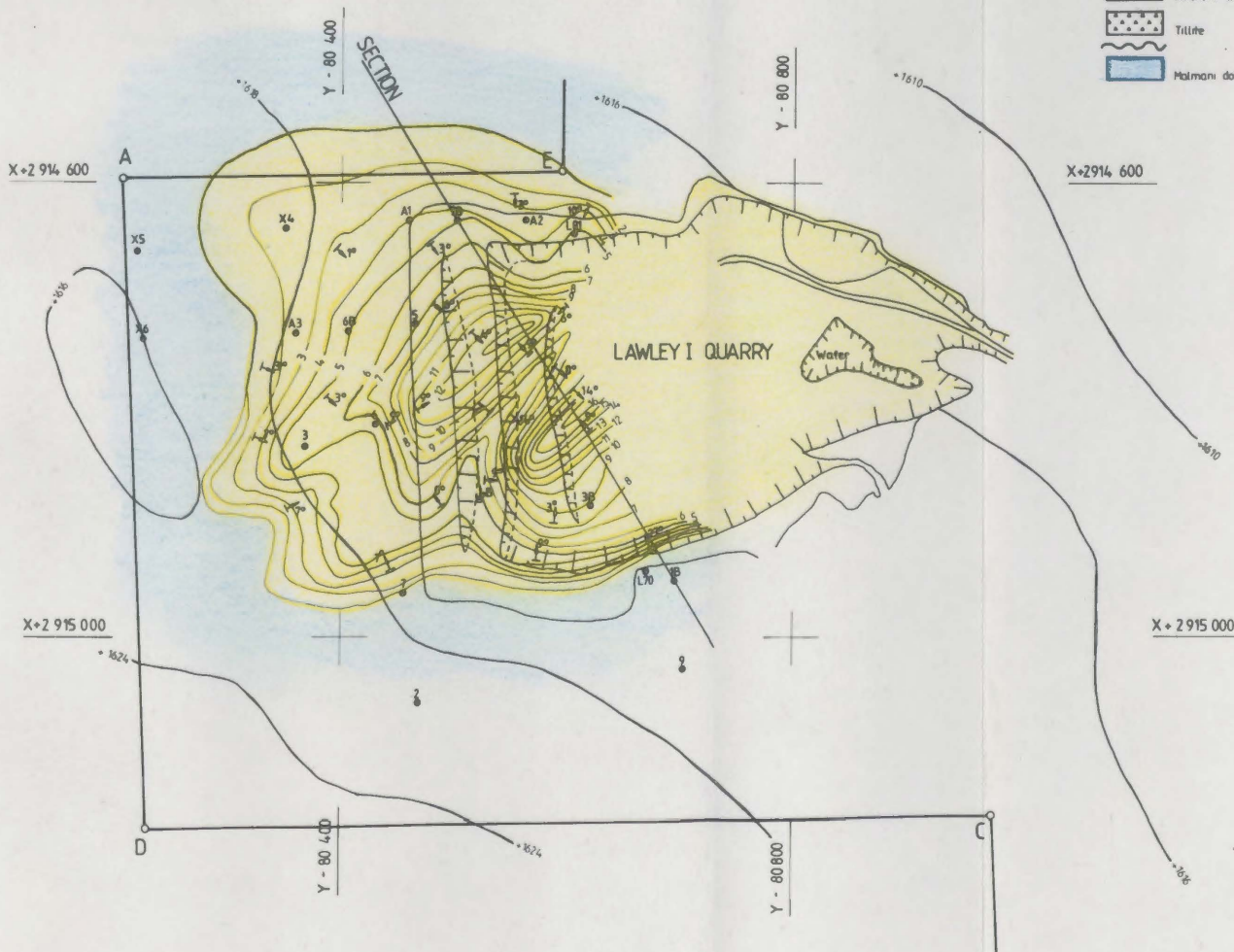
SECTION



SCALE Hor 1 2 000
Ver 1 1 000

LEGEND

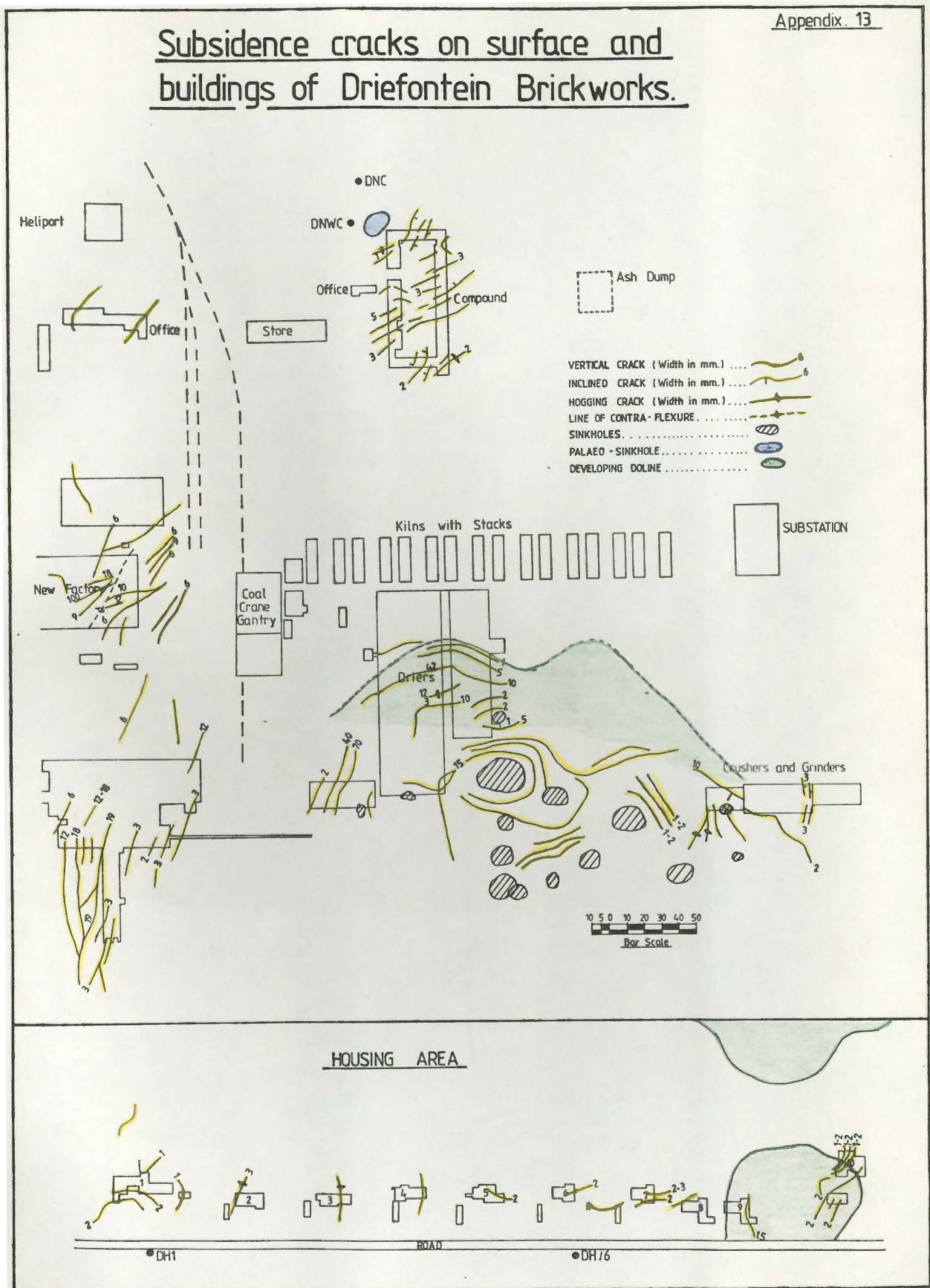
- Overburden
- Pale cream off white kaolinitic shale
- Brown + black carbonaceous mudstone with sporadic sandstone bands
- Pseudo flint clay
- Silstone with grit bands
- Tillite
- Malmani dolomite



Structural features in the Karoo carbonaceous shales
in the Driefontein Brickworks area.

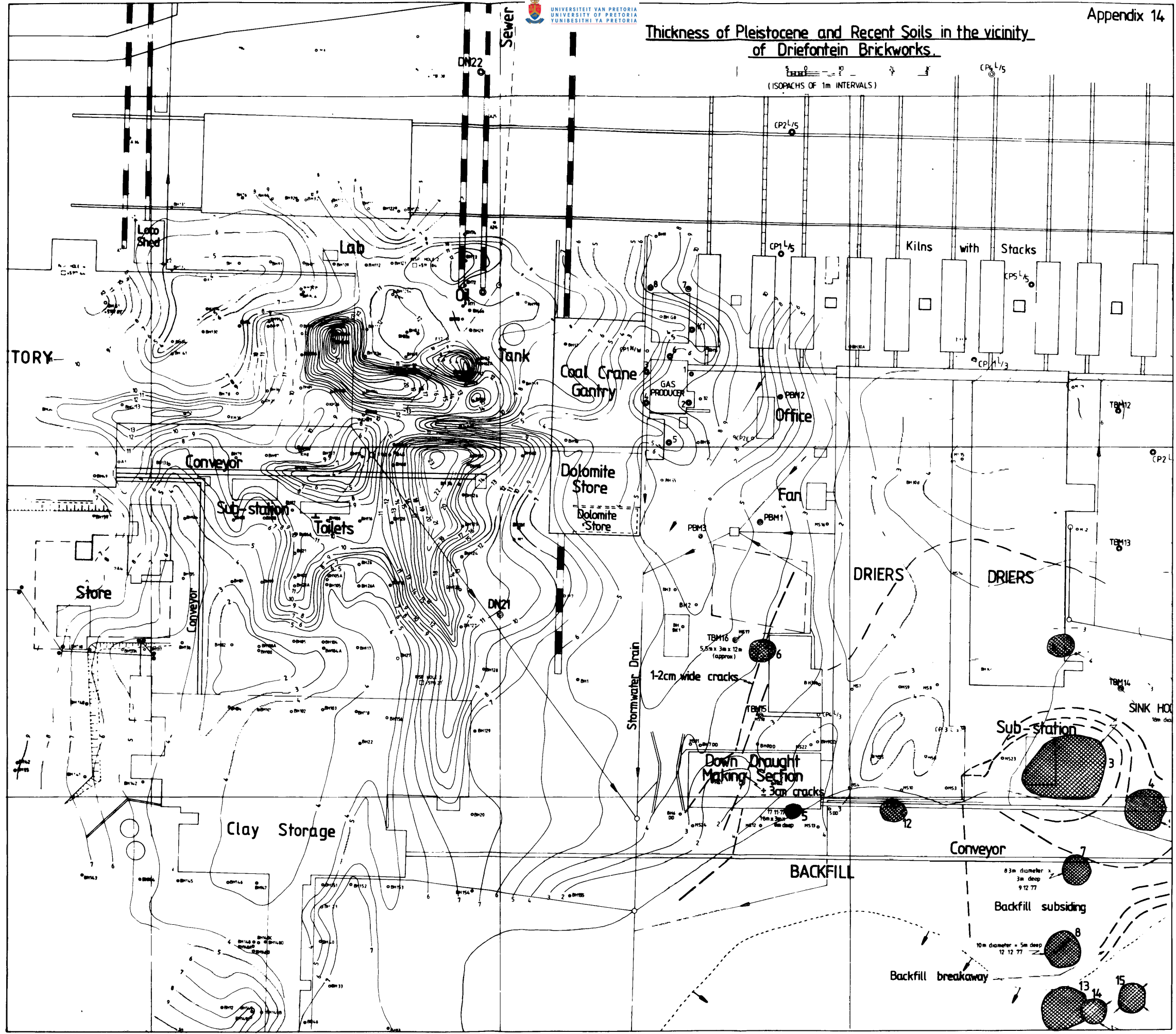


Subsidence cracks on surface and buildings of Driefontein Brickworks.



Thickness of Pleistocene and Recent Soils in the vicinity
of Driefontein Brickworks.

(ISOPACHS OF 1m INTERVALS)



Depths at which sub-surface water intersected in the Rietvlei outlier.
(Intersected water contour values in meters above mean sea - level)

Scale 1 : 5 000

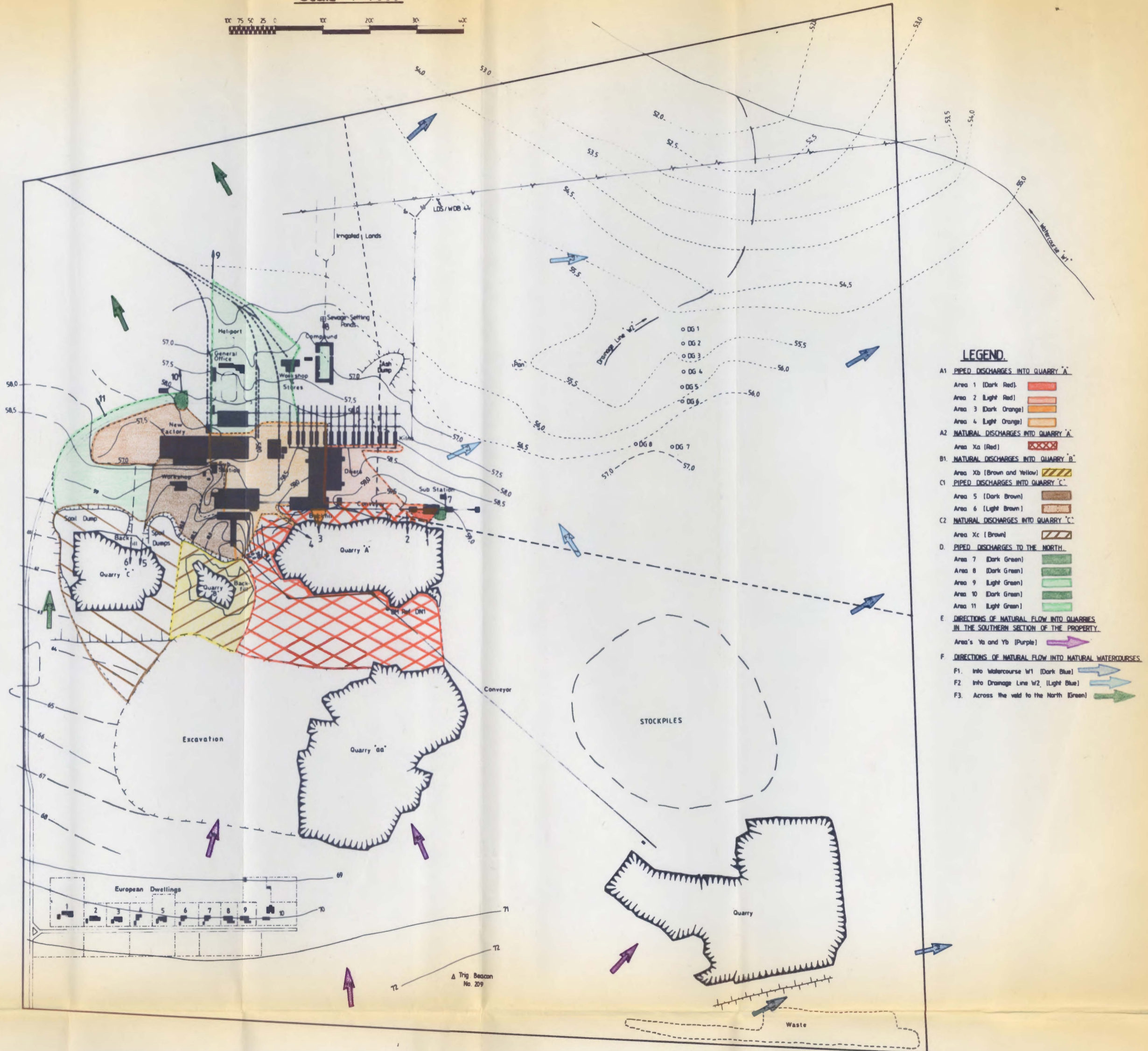
VAN RIEBEECK NATURE RESERVE



- Coordinates in the Factory Area have been tied to local system (Origin at Pag SS 1 Direction SS 1 to SS 10 (parallel to and 100mm south of the centre line of the northern gantry crane rail) equals 270°)
- Elevations generally are based on a value of 1562.171 above Mean Sea Level for the top of Bench Mark Ref. DN1 (A 12mm diam steel peg set in concrete with a brass surround fitted on the South side of the old quarry on the South side of the Factory area.)
- All elevations relate to ground, floor, pipe or drain invert levels. Their positions being of the decimal points or crosses marked on the plans. Add 1550.00 or 1500.00 as relevant to values shown to obtain heights above Mean Sea Level.

Pattern of surface run-off in the Driefontein outlier showing drainage systems prior and subsequent to October 1981.

Scale 1:4000



LEGEND

- A1 PIPED DISCHARGES INTO QUARRY 'A'**
 - Area 1 (Dark Red)
 - Area 2 (Light Red)
 - Area 3 (Dark Orange)
 - Area 4 (Light Orange)
- A2 NATURAL DISCHARGES INTO QUARRY 'A'**
 - Area Xa (Red)
- B1 NATURAL DISCHARGES INTO QUARRY 'B'**
 - Area Xb (Brown and Yellow)
- C1 PIPED DISCHARGES INTO QUARRY 'C'**
 - Area 5 (Dark Brown)
 - Area 6 (Light Brown)
- C2 NATURAL DISCHARGES INTO QUARRY 'C'**
 - Area Xc (Brown)
- D. PIPED DISCHARGES TO THE NORTH**
 - Area 7 (Dark Green)
 - Area 8 (Dark Green)
 - Area 9 (Light Green)
 - Area 10 (Dark Green)
 - Area 11 (Light Green)
- E. DIRECTIONS OF NATURAL FLOW INTO QUARRIES IN THE SOUTHERN SECTION OF THE PROPERTY**
 - Area's Ya and Yb (Purple)
- F. DIRECTIONS OF NATURAL FLOW INTO NATURAL WATERCOURSES**
 - F1. Into Watercourse W1 (Dark Blue)
 - F2. Into Drainage Line W2 (Light Blue)
 - F3. Across the veld to the North (Green)

CORRELATION COEFFICIENT DATA ON ΔH_s AND ΔH_l
MOVEMENTS IN TBM 34 RELATIVE TO SUB-SURFACE
WATER MOVEMENTS IN PIEZOMETER CLUSTER
NORTHWEST OF COMPOUND

(A) TIP 3 (Piezometer cluster NW Compound) : ΔH_s (TBM34)

LAG INTERVAL (CYCLES)	r^2 (100)	
	CYCLES 1- 10	CYCLES 17 - 26
0	37,37	82,67
1	60,13	70,60
2	14,45	24,18
3	1,83	0,18
4	6,74	6,90
5	17,00	25,57
6	37,01	40,05
7	5,03	50,65

(B) TIP 3 (Piezometer cluster NW Compound) : ΔH_l (TBM34)

LAG INTERVAL (CYCLES)	r^2 (100)	
	CYCLES 1 - 10	CYCLES 17 - 26
0	18,56	58,98
1	19,50	62,19
2	13,45	58,50
3	3,35	54,98
4	6,75	45,75
5	14,80	21,66
6	45,24	1,81
7	0,13	1,85

(C) TIP 1 (Piezometer cluster NW Compound) : ΔH_s (TBM34)

LAG INTERVAL (CYCLES)	r^2 (100)	
	CYCLES 1 - 10	CYCLES 17 - 26
0	34,10	58,00
1	0,71	69,02
2	49,31	58,33
3	75,07	55,07
4	80,73	45,58
5	69,42	21,19
6	42,91	1,96
7	37,46	1,52

 (D) TIP 1 (Piezometer cluster NW Compound) : ΔH_l (TBM34)

LAG INTERVAL (CYCLES)	r^2 (100)	
	CYCLES 1 - 10	CYCLES 17 - 26
0	65,28	0,85
1	45,78	7,17
2	22,37	18,56
3	0,35	31,59
4	7,55	48,88
5	5,26	79,38
6	0,01	84,99
7	0,33	72,84

Actual ΔH_s , ΔH_u and ΔH_l movements (mm) in TBM34 and subsurface water measurements (m) in piezometer cluster northwest of Driefontein Brickworks Compound.

CYCLE NO.	DATE	MEASUREMENTS - TBM 34 (mm)			MEASUREMENTS - PIEZOMETER CLUSTER N.W. COMPOUND (m)					
		ΔH_s	ΔH_u	ΔH_l	Tip 1	Tip 2	Tip 3	Tip 4	Tip 5	Tip 6
1	22-12-79	0,0	0,0	0,0	-0,02	-0,07	-0,04	0,00	+0,01	-0,01
2	2-02-79	-2,70	-2,80	-2,99	-0,13	-0,39	-0,01	0,00	-0,07	-0,36
3	20-03-79	-6,70	-6,90	-9,78	-0,23		-0,09	0,00	-0,14	-0,51
4	23-04-79	-7,70	-7,96	-16,21	-0,30		-0,37	-0,01	-0,20	-0,65
5	28-05-79	-8,70	-8,95	-17,21	-0,38		-0,47	0,00	-0,26	-0,71
6	28-07-79	-8,60	-9,02	-17,32	-0,50		-0,65	-0,65	-0,36	-1,04
7	10-09-79	-8,82	-9,10	-18,00	-0,61		-0,70	+0,01	-0,43	-1,25
8	15-11-79	-7,67	-8,14	-17,76	-0,77		-0,74	+0,01	-0,67	-1,26
9	18-12-79	-8,83	-9,23	-19,10	-0,85		-0,42	+0,01	-0,69	-0,93
10	13-02-80	-5,33	-5,77	-17,02	-0,91		+0,57	+0,01	-0,90	+0,14
11	21-03-80	-2,26	-2,82	-16,32	-0,86		+1,95	+0,01	-0,99	+1,54
12	6-05-80	-2,47	-2,96	-16,86	-0,83		+1,45	+0,01	-1,03	+1,08
13	13-06-80	-2,83	-3,38	-17,19	-0,80		+0,65	+0,01	-1,05	+0,03
14	29-07-80	-3,29	-3,74	-17,57	-0,86		+0,25	+0,02	-1,08	-0,10
15	9-09-80	-3,78	-4,31	-17,65	-0,87		-0,19	+0,04	-1,00	-0,50
16	28-10-80	-5,05	-5,58	-18,60	-0,93		-0,69	+0,01	-1,15	-0,94
17	19-12-80	-2,01	-2,55	-16,79	-0,96		+0,73	+0,02	-1,17	+0,20
18	13-02-80	+1,73	+1,12	-16,20	-0,98		+2,24	+0,02	-1,18	+1,85
19	2-04-81	+5,84	+5,14	-14,95	+0,01	-0,36	+3,84	+0,03	-1,18	+3,44
20	11-05-81	+5,25	+4,58	-15,46	+0,41	-0,12	+2,82	+0,02	-1,22	+2,47
21	29-06-81	+3,90	+3,23	-16,83	+0,46	+0,03	+1,52	+0,03	-1,24	+1,18
22	11-08-81	+1,61	+0,89	-19,14	+0,41	+0,06	+0,65	+0,03	-1,25	+0,30
23	16-09-81	+1,31	+0,66	-19,40	+0,32	-0,02	+0,33	+0,00	-1,28	-0,01
24	29-10-81	-3,48	-4,16	-24,28	+0,19	-0,14	-0,06	+0,01	-1,29	-0,36
25	24-11-81	-7,90	-8,48	-28,46	-0,11		+0,05	+0,03	-1,35	-0,58
26	27-01-82	-9,99	-10,68	-30,90	-0,03		-0,25	+0,03	-1,37	-0,63
27	5-03-82	-11,20	-11,84	-32,00	-0,07		-0,21	+0,02	-1,37	-0,65
28	8-04-82	-10,91	-11,54	-31,62	-0,11		-0,21	+0,03	-1,39	-0,81
29	2-06-82	-10,97	-11,39	-31,56	-0,15		+0,39	-0,18	-1,41	-0,81
30	9-07-82	-9,97	-10,57	-30,77	-0,23		+0,27	-0,36	-1,43	-1,11
31	19-08-82	-9,24	-9,92	-30,14	-0,28		+0,02	-0,37	-1,45	-1,29
32	12-10-82	-9,84	-10,57	-30,91	-0,35		-0,21	-0,41	-1,48	-1,54

Correlation coefficient data on ΔH_s and ΔH_l movements
in TBM10 relative to subsurface water movements in
piezometer cluster west of Gas Producer.

A. TIP 3 (Piezometer cluster West Gas Producer) : ΔH_s (TBM 10)

LAG INTERVAL (cycles)	r^2 (100)	
	Cycles 4 - 10	Cycles 20 - 26
0	97,99	72,36
1	73,52	58,02
2	26,95	74,19
3	2,45	74,90
4	0,24	87,12
5	26,98	83,20
6	58,67	82,87
7	91,73	84,27

B. TIP 3 (Piezometer cluster West Gas Producer) : ΔH_l (TBM 10)

LAG INTERVAL (cycles)	r^2 (100)	
	Cycles 4 - 10	Cycles 20 - 26
0	41,16	88,36
1	23,39	65,07
2	6,58	42,15
3	0,06	42,63
4	16,52	86,86
5	67,01	17,22
6	34,20	0,02
7	26,71	16,53

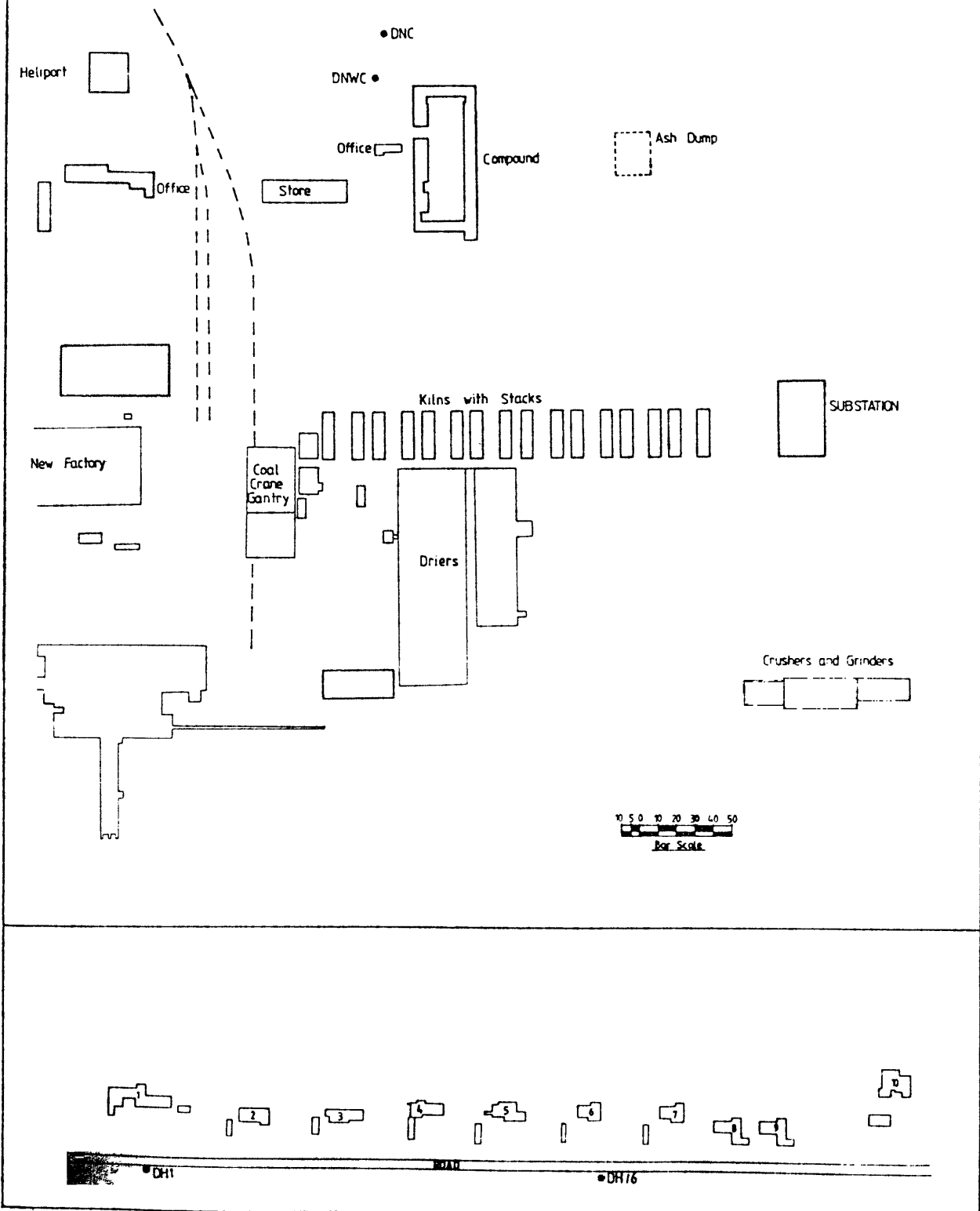
B. TIP 4 (Piezometer cluster West Gas Producer) : ΔH_s (TBM 10)

LAG INTERVAL (Cycles)	r^2 (100)	
	Cycles 4 - 10	Cycles 20 - 26
0	40,12	17,60
1	11,20	8,96
2	2,71	17,67
3	0,11	21,09
4	43,43	34,57
5	84,76	35,93
6	79,86	34,59
7	55,06	39,65

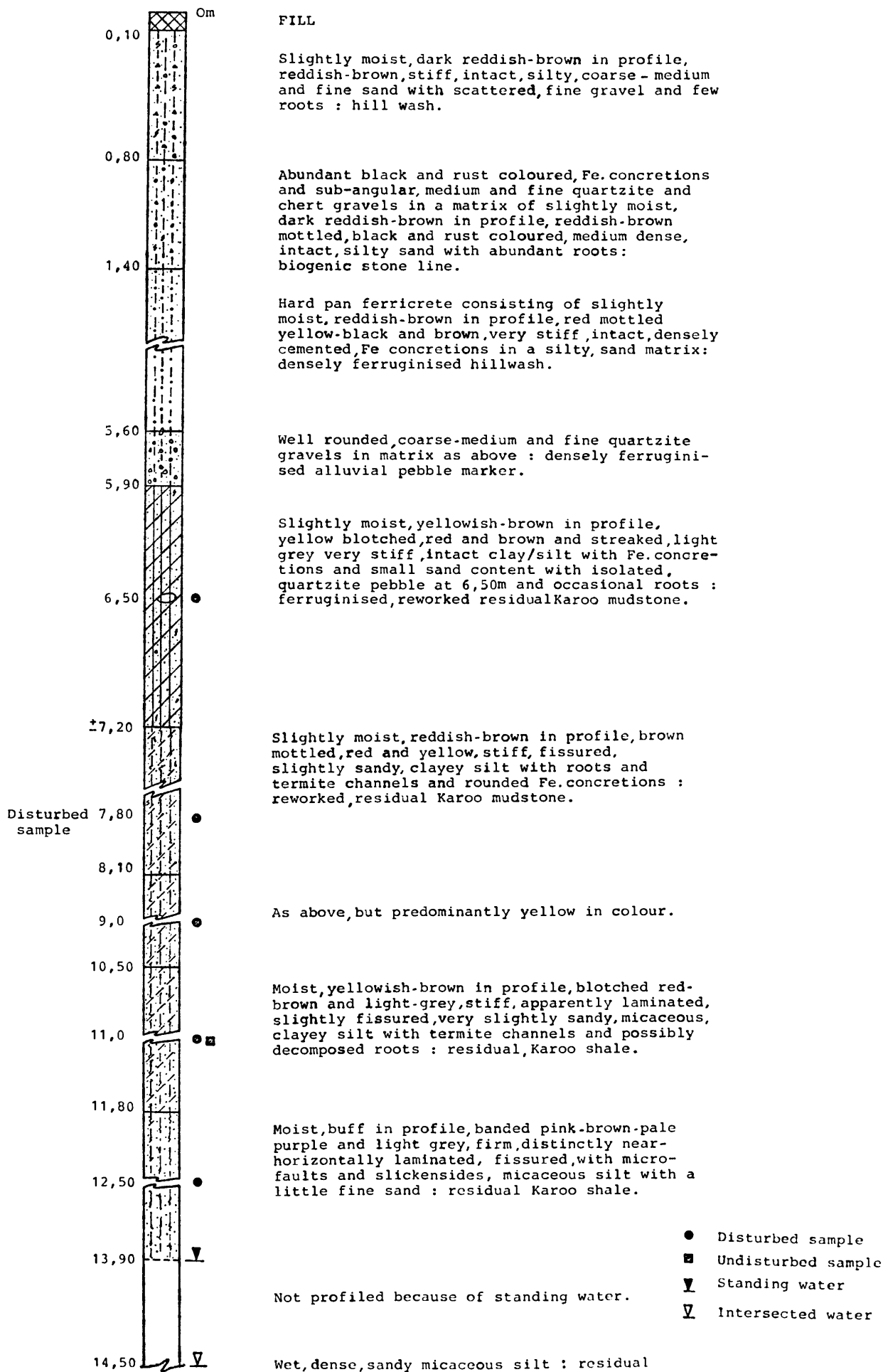
 D. TIP 4 (Piezometer cluster West Gas Producer) : ΔH_l (TBM 10)

LAG INTERVAL (Cycles)	r^2 (100)	
	Cycles 4 - 10	Cycles 20 - 26
0	95,40	34,34
1	5,08	16,29
2	12,85	55,27
3	15,58	2,00
4	12,51	17,58
5	13,11	64,10
6	4,29	13,15
7	0,93	0,13

Localities of 750mm diameter boreholes DNWC, DNC, DH1 and DH6.

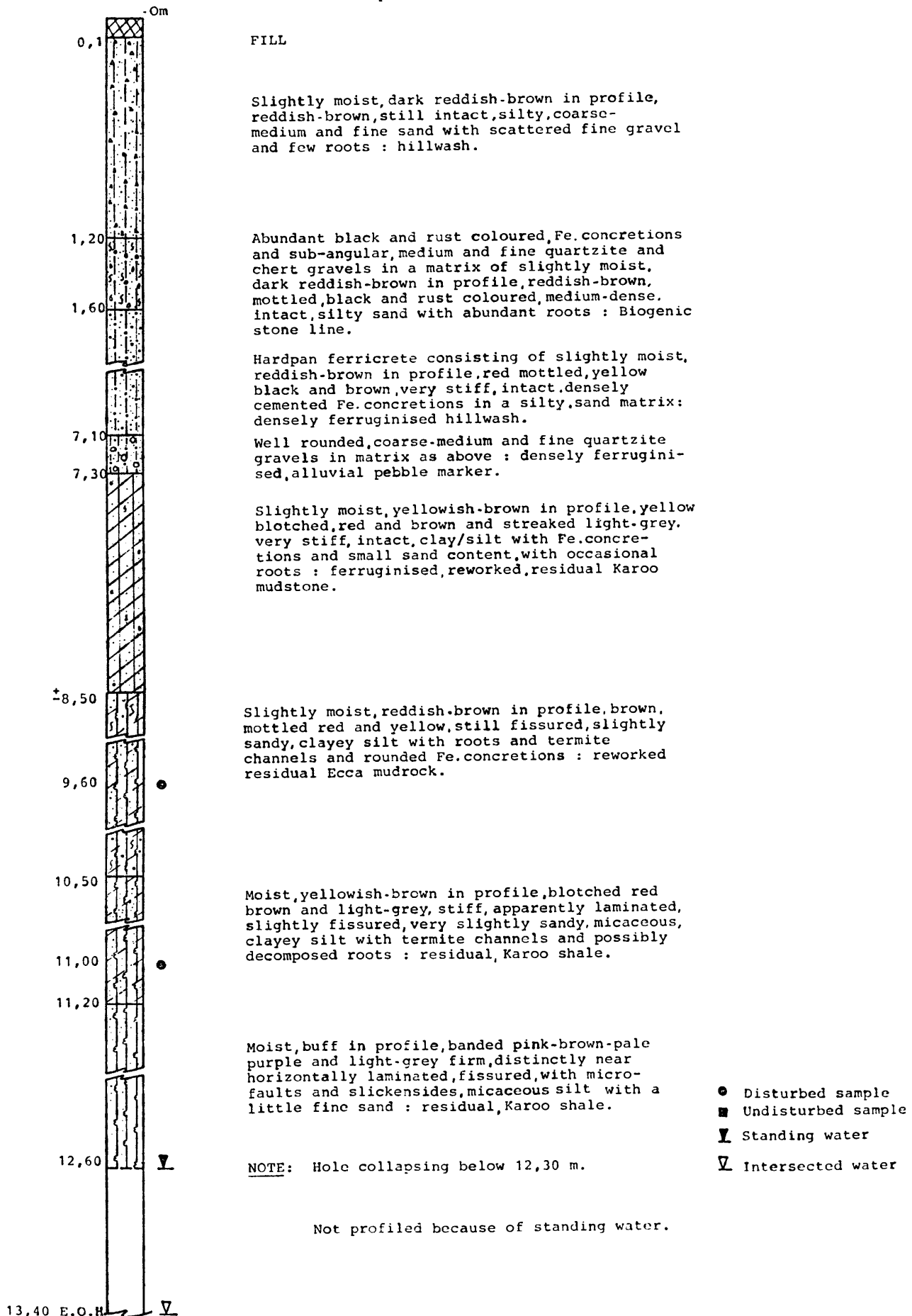


BH DNWC
(Depths in metres)

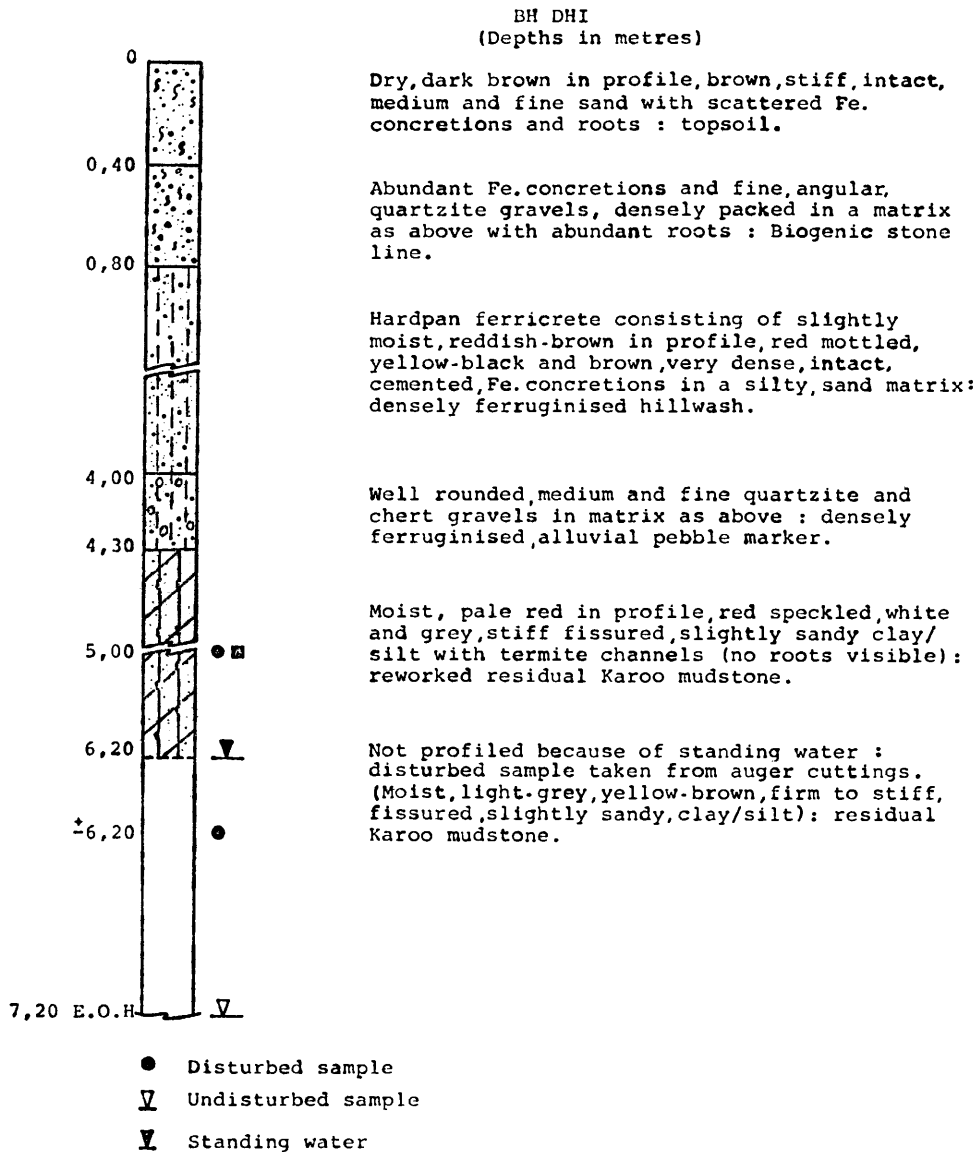


GEOLOGICAL PROFILE OF BOREHOLE DNC.

BH DNC
(Depths in metres)



GEOLOGICAL PROFILE OF BOREHOLE DH1.



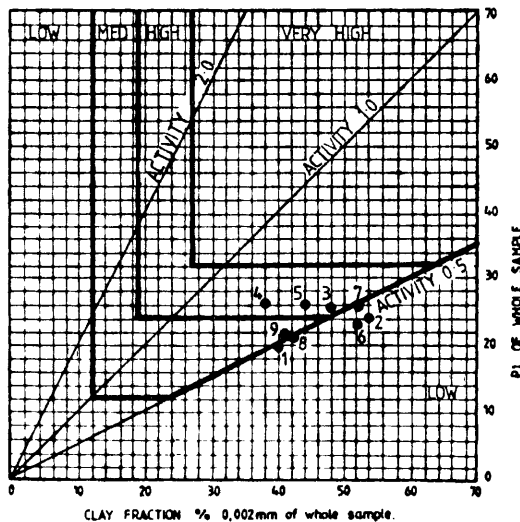
Results of Indicator Tests on samples from the Boreholes DNWC and DNC.

INDICATOR TEST

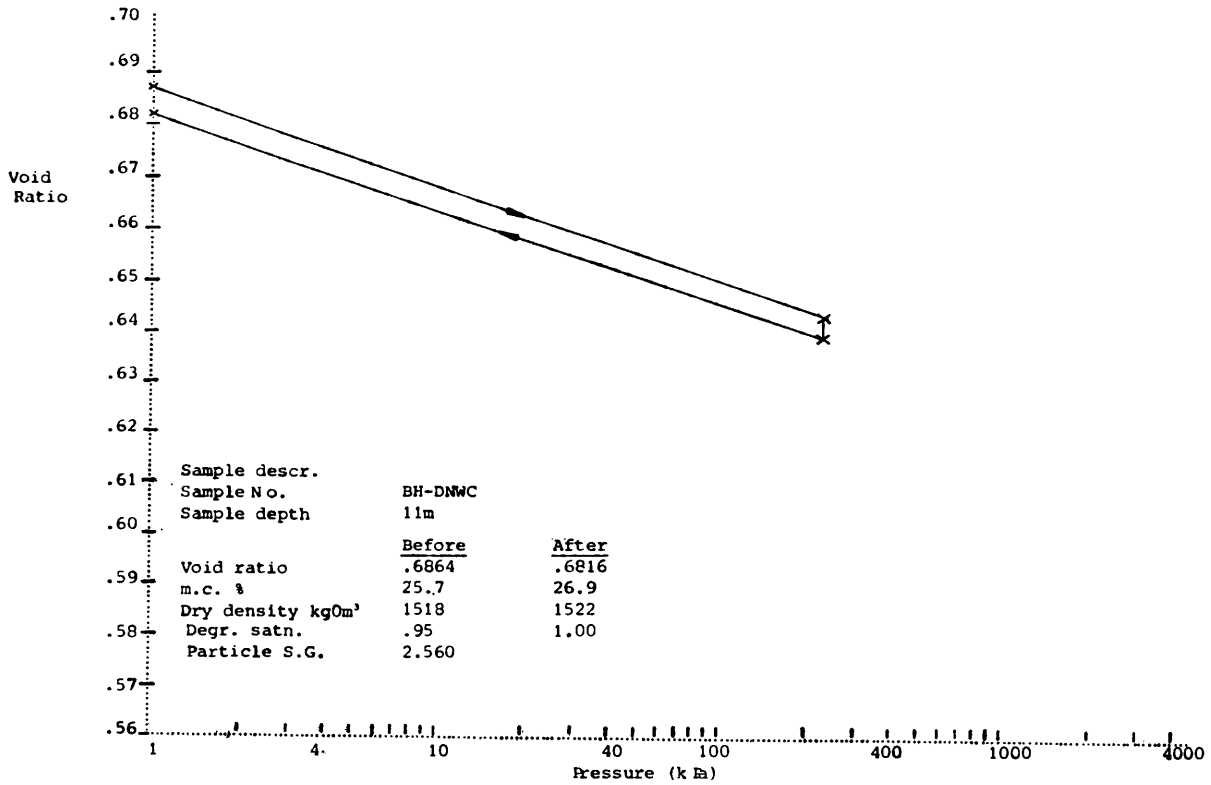
Location				Screen Analysis								Mechanical Analysis				Constants			
DRIEFONTEIN BRICKWORKS - Nw OF COMPOUND				Percentage Passing Screen (mm - ASTM, T - Tyler, B - British Standard.)								SAND < 2,0mm > .075mm		SILT < .075mm > .002mm	CLAY < .002mm		Liquid Limit	Plasticity Index	Lin. Shrinkage
Trial Hole No	Sample No.	Depth	Moisture Content	75mm No. 20 T	425mm No. 35 T	250mm No. 60 T	150mm No. 100 T	75mm No. 200 T	425mm No. 35 T	250mm No. 60 T	150mm No. 100 T	75mm No. 200 T	Coarse > 2,0 mm	FINE < 2,0 > .075 mm	Coarse > .075 > .002 mm	FINE < .075 > .002 mm			
DNWC	1	650	14,42	100	98	90	78	69	62,4	13	17	20	6	44	46	25	11,5		
	2	780	18,07		100	99	94	85	79,0	5	15	20	6	54	48	25	12,0		
	3	900	22,44				100	88	82,0	0	18	24	10	48	48	25	10,0		
	4	1 100	21,92				100	80	68,0	0	32	21	9	38	48	26	11,0		
	5	1 250	25,03				100	90	82,0	0	18	28	10	44	49	26	11,0		
DNC	6	800	17,60		100	95	91	82	76,4	4	15	20	5	56	45	25	10,5		
	7	950	21,68				100	90	84,0	0	16	24	8	52	47	26	10,5		
	8	1 100	24,27			100	98	88	84,3	2	14	23	11	50	42	21	9,0		
	9	1 200	23,77				100	98	88	80,4	2	18	22	5	53	41	21	9,0	

ACTIVITY DETERMINATION

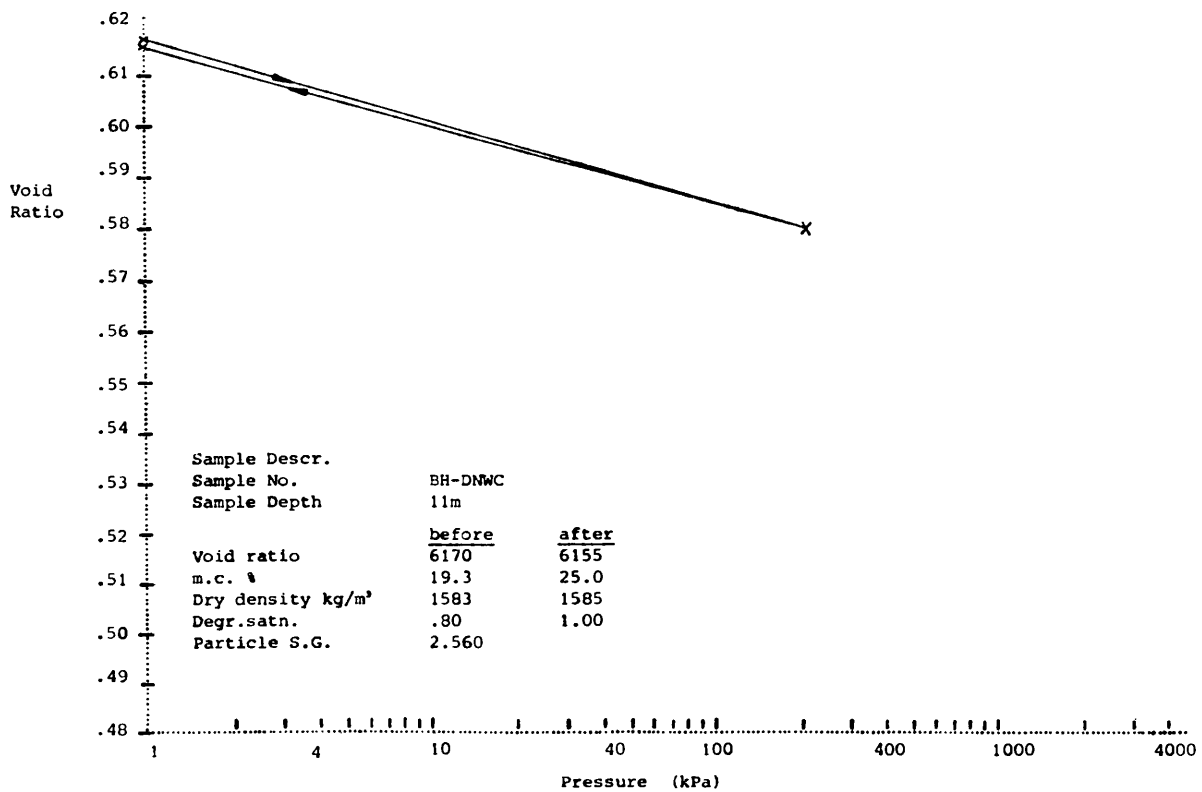
SAMPLE No.	Whole Sample		REMARKS
	CLAY 0,002 mm	PLASTICITY INDEX	
1	40	20	
2	54	24	
3	48	25	
4	38	26	
5	44	26	
6	53	23	
7	52	26	
8	42	21	
9	41	21	



Results of consolidometer tests on samples from
Borehole No. DNWC.



CONSOLIDOMETER TEST



CONSOLIDOMETER TEST